CHARACTERISATION OF TETRASPANINS TSPAN9 AND TSPAN33

by

ELIZABETH JAYNE HAINING

A thesis submitted to the University of Birmingham for the degree of DOCTOR OF PHILOSOPHY

School of Biosciences
College of Life and Environmental Sciences
University of Birmingham
September 2013

Abstract

The tetraspanins are a large superfamily of membrane proteins that contribute to the organisation of other cell surface proteins through homo- and heterogeneous lateral interactions. In platelets four of the 33 mammalian tetraspanins have been found to participate in mechanisms that regulate platelet sensitivity and activation. Tspan9 was recently discovered as a new platelet tetraspanin using an antibody and is highly expressed on platelets when compared to other tissues. Tspan33 was another new platelet tetraspanin identified by membrane proteomic approach. Neither tetraspanin had yet been functionally characterised on platelets and so their contribution to platelet biology was unknown. The aims of this thesis were to investigate the function of Tspan9 and Tspan33 in platelets using their respective knockout mice. The conclusion of this thesis was twofold. Firstly that Tspan33 is a member of the TspanC8 subfamily of tetraspanins that regulate the metalloprotease ADAM10, but is likely not expressed on mouse platelets. Secondly, Tspan9 promotes platelet activation through the collagen receptor GPVI by regulating its membrane dynamics. These novel regulatory mechanisms for ADAM10 and GPVI offer new avenues of research into therapy for diseases such as Alzheimer's disease and atherosclerosis in which ADAM10 and GPVI respectively play central roles.

Acknowledgements

This thesis could not have existed without the kind help and support of so many people. The first person I need to thank is my supervisor, Mike Tomlinson. Without his guidance, nurturing, support and encouragement (and excellent eye for typos) this thesis, and me as a scientist, would not exist. I also need to thank the other members of our lab, Jing and Beccy. Thank you Jing for taking me under your wing when I was new, answering all my (many) questions and then later putting up with all my bad habits in the lab - like when I steal Pasteur pipettes from your drawer and then forget to replace them! Thank you Beccy for being a great experiment partner for these past three years and smiling and laughing with me through all the crazy, like when I dropped our precious RNA samples down 8 flights of stairs. Also thanks to all the scientific nomads that have passed through our lab, especially to Stacey, Kab, Richard and Bill - if Carlsberg made masters students, they would have made you! I can wholeheartedly say that I have absolutely loved being part of this lab - I shall miss it dearly.

I also need to thank my second supervisor Steve Watson for his support right from the beginning through to the end, where his advice about the future was greatly appreciated. Also, I owe a great debt to all the members of the Watson Empire in the IBR and I'll miss being part of your lab. Lab meetings on a Monday morning always made me want to go away and be better at science so I could keep up - you're all brilliant! Thank you for answering my many many questions and for all your support and advice. Thank you Craig, Alice and Steve, for being my surrogate postdocs and never minding (outwardly) a tap on the shoulder when you were in the middle of something. Thanks also to Leyre, Alex, Jun, Brenda, Marie, Danai, Neil, Nat, Monica and Ale, you guys have always been there in my (many) times of scientific need and always took the time to show me something(s), give me reagents, and talk about science and more - it was really appreciated. Thanks also to Yotis for scaring me into being a more accurate scientist and also for advice and reagents. Thanks to Kate for biscuits and being reliable with favours, and to Sam, Stef, Jane, Osama and Gill for fun times at the aggregometer. And last but not least thanks to Gayle for making sure I get my blood money and Silke and Beata for again answering my questions, helping me out and being all round great people. If I've missed a bunch of people - please don't feel left out - I love you all (blame Steve, his lab is too big!) x

I must also thank Professor Bernhard Nieswandt for his generous support of the work in this thesis by supplying reagents, taking our mice for *in vivo* studies and suggesting great experiments. Also thanks to Dr. Schickwann Tsai for providing us with the Tspan33 knockout mice and thank you to Hanna Romanska for sectioning, staining and imaging mouse organs for this thesis.

I also need to thank all the other labs that have taken me in over the years. Thank you to Paloma for teaching me all things stem cells and to Jon for being up for collaboration. Also thanks to Mary, Lozan and Maelle for being nice and for welcoming me into your lab. Also thanks to Roger Bird, cell sorter extraordinaire. Thank you to Zubair for teaching me and Beccy all about retinas, definitely one of the coolest things I learnt during my PhD. Also thank you to Helen for teaching me SPT and spending hours with me on the microscope and guiding me through the analysis. You've made a big contribution to the final chapter of this thesis and to my understanding of the tiny world of the cell membrane. Never will I forget the day we turned away Chinese only to find the chippy was shut.... Also thanks the Kalia lab - literally the funniest bunch of people I have ever met. Thank you to Rob for good microscope times and all your help with electron microscopy. Thank you to the cell biology lab group - your interest in tetraspanins during our Friday lab meetings has led to some great discussion. Thank you in particular to John, Carina, Neil, Vicky and Helen for making great suggestions for improving my project.

Also thank you to Elena and Fedor for inviting us Tomlinsons to lab Christmas dinner every year and for great discussions about tetraspanins and beyond.

I have to thank the population of the 8th floor of Biosciences for putting up with me for the last 6 years. There have been some genius comedy moments and some great friendships made. I can only hope that out there in the real world there are places to work as great as this. To Josh, you found in me, the spark of a love for science and believed in it. For this I cannot thank you enough. To Kate and Linda, I miss you on the 8th and I can't wait 'til our next Las Iguanas/jagerbomb night, although I think my liver can. To Jen, thank you for sharing late nights in the lab and helping me wage war against the alarm that wouldn't stop beeping and also for being part of the best lunch time and more, friends ever. Your cakes = awesome, lunch time is not the same without you. To Rach and Yui and Yousra, other lunch time clubbers, thank you for all the laughter (there was a lot) and for helping to get me through the tough days. To Rich, the best mentor a girl could wish for, thank you for your advice and support since the beginning and for some awesome nights out. Sarah, if it wasn't for you I wouldn't have met Rich, Jen, Rach, Yui and Yousra. You took me in as a second year undergrad and introduced to the world of the lab and all your friends. I couldn't thank you enough for your mentorship, advice and friendship in these past 6 years.

To Laura, thank you for sorting me (and all of us) out and more importantly for becoming a great friend (and introducing me to SJA). Even looking past the great tomato explosion of 2013, where you took the collateral damage better than most would have. To Julie, I'm glad that in the short time you have been on the 8th we've become good friends, even if sometimes you can be a beach! It's great to have someone with a mean streak like me around to make me feel better about myself :)

To Eric, thanks for sharing the late working nights and for automating my life. To Phil and Jeremy, the other PSIBS boys, thank you for answering my microscope and maths questions, Phil, I'm sorry we got so drunk at your wedding. Actually I'm not, it was a great day and I'm so glad you shared it with us. To Jeni, we did it, we made it to the end of our tetraspanin journey! To Steve Pub and Klaus, thank you for our coffee room chats, your advice was always bang on the money.

To everyone in the BMSU thank you. In particular to Saiqa, Jenny, Ian and Sharon for always being helpful and friendly, even when you are crazy busy and I can't find my mice. Without the mice there would be no thesis, so I owe a lot to you! Thank you also to Alan and Graeme (and Ray) in the Stores and to all the staff in the downstairs office (esp. Holly).

To the University of Birmingham Rowing club, I can't say you've aided in the writing of this thesis but you've definitely helped keep me sane throughout. Special thanks to Alex Derby and the Henley eight of 2010 - special times. Also to University of Birmingham LINKS, I came late to being 'the difference' but am so glad I did.

Finally, thank you to my long suffering family. To Dad and Steph and little Fraser, thank you for your love and understanding. More frequent visits are planned now that this is done! To my mother, Judith, sister, Raisa, brother, Ashley and nephew Kai, thank you for understanding my annoying and bad habit of putting work first, and loving me anyway even if I'm the absent family member. Your support and love I feel with me always. To Heidi weasel, you kept me company when George was in another country and sat by me through the writing of this thesis, you are the best cat ever! To Gus, you arrived at the beginning and left at the end - my PhD angel - you will be missed. And finally to my boyfriend George, I literally don't know where I would be without you, all I do know is that I definitely wouldn't be sat here, writing the final part of this thesis, which I dedicate to you, with all my love.

Table of contents

List of figures

List of tables

List of abbreviations

ACD	Acid citrate dextrose
ADP	Adenosine diphosphate
ATP	Adenosine triphosphate
BFU-E	Blast forming unit erythroid
cAMP	Cyclic adenosine monophosphate
CFU-E	Colony forming unit erythroid
CFU-Eo	Colony forming unit eosinophil
CFU-GEMM	Colony forming unit granulocyte erythroid macrophage megakaryocyte
CFU-Meg	Colony forming unit megakaryocyte
cGK	cGMP-dependant protein kinase
cGMP	Cyclic guanosine monophosphate
EC1	Extracellular loop 1
EC2	Extracellular loop 2
ER	Endoplasmic reticulum
FBS	Foetal bovine serum
FITC	Fluorescein isothiocyanate
FRAP	Fluorescence recovery after photobleaching
FRET	Forster resonance energy transfer
GPCR	G protein coupled receptor
GPI	Glycophosphatidylinositol
IC	Interconnecting loop
ITAM	Immunoreceptor tyrosine-based activation motif
LTA	Light transmission aggregometry
MβCD	Methyl-β-cyclodextrin
PAR	Protease activated receptor
PBS	Phosphate buffered saline
PCR	Polymerase chain reaction
PI4K	Phosphatidyl inositol 4 kinase
PKA	Protein kinase A
PKC	Protein kinase C
PLC	Phospholipase
PLC 2	Phospholipase C 2
SAGE	Serial analysis of gene expression
SPTM	Single particle tracking microscopy
Syk	Spleen tyrosine kinase
TBS	Tris buffered saline
TBST	Tris buffered saline with Tween
TM	Transmembrane
vWF	von Willebrand factor

Publications arising from this thesis

Haining, E.J., Yang, J., Bailey, R.L., Khan, K., Collier, R., Tsai, S., Watson, S.P., Frampton, J., Garcia, P. and Tomlinson, M.G. (2012). The TspanC8 subgroup of tetraspanins interacts with A disintegrin and metalloprotease 10 (ADAM10) and regulates its maturation and cell surface expression. J Biol Chem, 287, 39753-65.

Haining, E.J., Yang, J. and Tomlinson, M.G. (2011). Tetraspanin microdomains: fine-tuning platelet function. Biochem Soc Trans, 39, 518-23.

CHAPTER I: INTRODUCTION

1.1 Tetraspanins

1.1.1 Tetraspanins overview

Tspan9 and Tspan33 (also called Penumbra) are members of the tetraspanin superfamily of transmembrane proteins of which there are 33 found in humans (Yáñez-Mó et al., 2009, Charrin et al., 2009). Only discovered around 20 years ago, tetraspanins have now been identified in organisms that represent nearly all of the major eukaryotic groups and are increasingly gaining more attention. Lacking obvious signalling machinery, catalytic domains and ligand binding sites, the tetraspanins are an enigmatic group of proteins. They have an intriguing ability to form heterogeneous clusters in cell membranes that coordinate other transmembrane proteins and have roles in processes as diverse as cell migration, cell adhesion and cell-cell fusion (Charrin et al., 2009, Yáñez-Mó et al., 2009, Hemler, 2005). Important tools such as antibodies are not available to most tetraspanins and consequently many known tetraspanins remain unstudied. However, as research in this field gathers momentum, mounting evidence highlights these proteins as important organisers of the cell surface.

1.1.2 Tetraspanin structure

As the name suggests tetraspanin proteins have four transmembrane (TM) domains that span the cell membranes in which they are found. They are set apart from other four TM proteins by the following general structure and several conserved 'tetraspanin signature' motifs. A diagram of this basic tetraspanin structure can be seen in Figure 1. Tetraspanins generally start with a short (less than 10 amino acids) intracellular N-terminal tail followed by the first TM domain called TM1. This TM region is connected to the next (TM2) by the first of two extracellular loop regions. This small extracellular loop (EC1) is overshadowed by the large extracellular loop (EC2) which is situated between the third and fourth TM domains (TM3 and TM4). Ending TM4 is the usually short (generally less than 20 amino acids) intracellular C-terminal tail. The entire extracellular portion of most tetraspanins extends only around 5 nm from the lipid membrane making tetraspanins dwarves of the cell surface in comparison to most other membrane proteins (Conley et al., 2012). Although there is currently only one crystal structure of a tetraspanin available, that of the EC2 of human CD81 (Kitadokoro et al., 2001b), other studies using techniques such as cryo-electron microscopy (Min et al., 2006), nuclear magnetic resonance spectroscopy (Rajesh et al., 2012), computational modelling (Seigneuret et al., 2001) and tetraspanin sequence analysis (Kovalenko et al., 2005) have allowed insight into the detail of tetraspanin structure. Figure 2 shows the most detailed structure of a full tetraspanin in the field which was derived from modelling studies by Seignueret based on the CD81 EC2 crystal structure (Seigneuret, 2006).

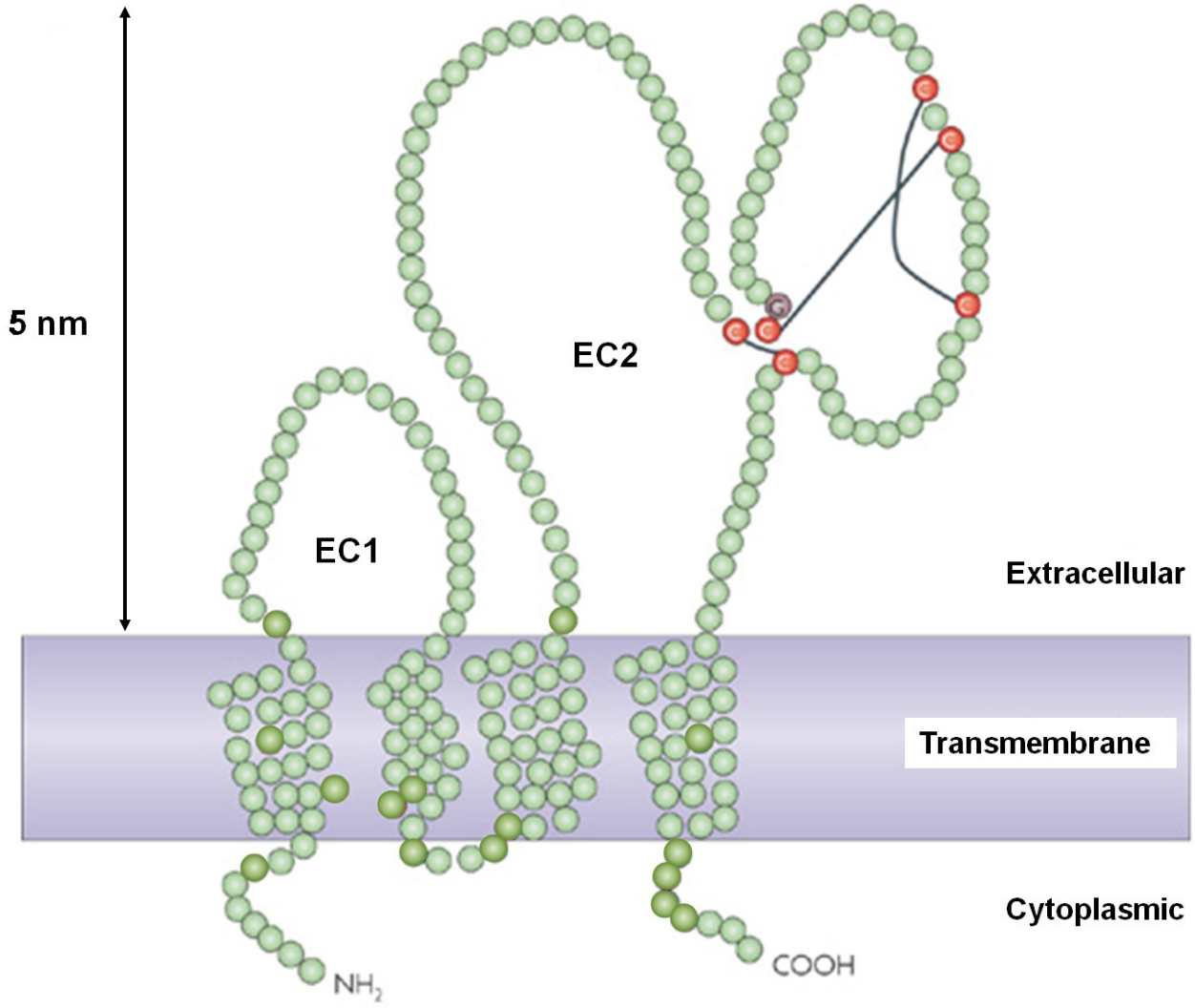

Figure 1. The basic structure of Tetraspanin superfamily proteins.

Tetraspanins are four transmembrane proteins that only extend 5 nm from the cell membrane. The four transmembrane proteins named 1 - 4 are delimited by two extracellular loops, one small termed EC1 and one large termed EC2. TM2 and TM3 are linked by a very short inter connecting or IC loop and the N and C-terminal tails are generally less than 10 and 20 amino acids respectively. Conserved cysteines that contribute to disulphide bridges in the variable region in the EC2 are shown in red with the bridges drawn in black. Modified from Zoller (2009).

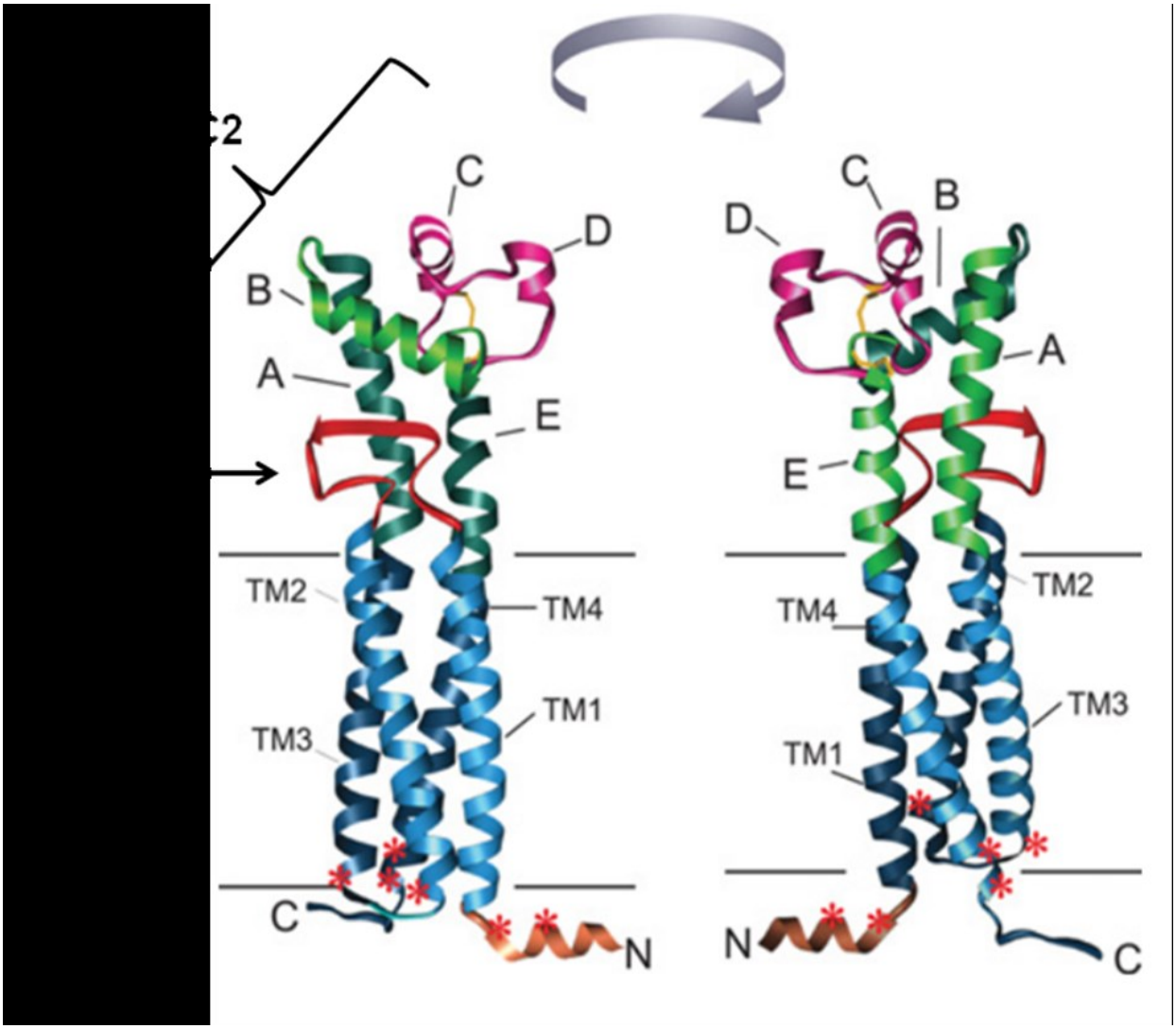

Figure 2. Model of tetraspanin CD81 by Seigneuret (2006).

This structure of computer modelled CD81 is currently the most detailed structure of a full tetraspanin in the field. Transmembrane domains are in blue, EC1 is in red, EC2 conserved domain is in green and the variable domain in purple. The disulphide bridges in the EC2 are in yellow. Sites that are probably palmitoylated are marked with a red star. Taken from (Charrin et al., 2009).

1.1.2.1 Tetraspanin transmembrane domains are tightly compact.

Tetraspanins appear to form very compact rod-like structures that do not extend far above or below the lipid bilayer. This compact structure is mainly created by the tight packing of the tetraspanin transmembrane domains into a left-handed coiled coil as seen in both computational modelling and cryo-electron microscopy (Seigneuret et al., 2001, Min et al., 2006). This left-handed coiled structure, which interestingly is more closely packed than a right-handed version, is created by conserved motifs and residues in each of the tetraspanin transmembrane domains. TM1, 2 and 3 all contain a heptad repeat pattern $(abcdefg)_n$ that is apparent in all coiled coil structures (Kovalenko et al., 2005, Seigneuret et al., 2001). Positions a and d are hydrophobic residues that face the inside of the coil and positions e and g are exposed external residues. These important heptad positions (a, d, e and g) all correspond to conserved residues in the tetraspanin superfamily (Seigneuret et al., 2001). Further supporting the close packing of the coiled coil is the size conservation of particular amino acid side chains in TM2 and TM3 that allow the transmembrane regions to fit closely together by 'knob into hole' packing and the very short connecting loop between TM2 and TM3 (Seigneuret et al., 2001, Kovalenko et al., 2005). The whole cylinder created by the transmembrane domain is further stabilised by van der Waals interactions and inter-coil hydrogen bonding, again maintained throughout the tetraspanin superfamily by conservation of key residues. It is predicted that residues involved in inter-helical contacts would be more conserved than those that face lipids as mutations in the former are more likely to cause destabilisation of protein structure. This indeed appears to be the case for the tetraspanin superfamily proteins

(Min et al., 2006, Kovalenko et al., 2005, Tachibana et al., 1997, Seigneuret et al., 2001).

Interestingly the transmembrane cylinder of tetraspanins does not appear to be a symmetrical structure. An accumulation of aromatic residues is seen in many tetraspanins around the TM1/2 side of the transmembrane region. These aromatic residues are hypothesised to be potential binding sites for cholesterol, as cholesterol binding sites in other proteins are aromatic residues (Kovalenko et al., 2005, Seigneuret et al., 2001). Whilst it is yet to be experimentally confirmed that the aromatic residues are cholesterol binding sites on tetraspanins, it is intriguing that some tetraspanins have such lateral asymmetry in a highly conserved part of their structure, especially when one considers the different types of interactions that a single tetraspanin is thought to be able to simultaneously coordinate. Additionally the overall hydrophobic nature of the transmembrane region may promote interactions with the particular membrane lipids with which they are known to associate (Seigneuret, 2006).

1.1.2.2 Tetraspanin extracellular domains

The extracellular regions of tetraspanins continue the compact nature of the transmembrane regions. The first of the extracellular loops, the EC1, is situated between TM1 and TM2 and is generally less than 30 amino acids in length (Seigneuret, 2006). The main feature known of this lesser studied extracellular loop is a generally conserved secondary structure of a β-strand at its centre. This central β-strand is enriched in hydrophobic residues (sequence ELLYLQ in CD81) and is predicted to come into close contact with a hydrophobic patch on the EC2

(Seigneuret, 2006). It has been suggested that this interaction may contribute to the stability of the large extracellular loop, however the folded EC2 has been produced in isolation, without EC1, and so this may not be the case (Rajesh et al., 2012, Kitadokoro et al., 2001a).

The large extracellular loop is a structurally and functionally interesting part of a tetraspanin containing both some of the most conserved and most variable parts of the protein, consequently it is the most studied aspect of tetraspanin structure. Different studies of this region, including the only tetraspanin crystal structure, all indicate that the EC2 is helical in nature and can be divided into two domains, one conserved and one variable (Kitadokoro et al., 2001b). The conserved region of the EC2 is made up of three α-helices termed A, B and E. These helices form a membrane proximal, structurally conserved, fold that, as previously discussed, may interact with the EC1 β-strand. The variable domain was thought to be comprised of a further two α-helices, namely C and D which were observed in the CD81 crystal structure (Kitadokoro et al., 2001b). However a more recent NMR study has suggested that actually it is more likely that the 'D helix' is a highly dynamic single turn helical loop and not an α-helix (Rajesh et al., 2012). In either case the 'D helix' is the most exposed part of the EC2 and it contains a hypervariable region that undergoes considerable insertions and deletions of sequence from tetraspanin to tetraspanin (Seigneuret, 2006). Interestingly this region in the CD81 crystal structure contains an exposed hydrophobic patch of amino acids that are conserved between different CD81 species, despite it being an energetically unfavourable formation due to its solvent exposed position (Kitadokoro et al., 2001b). It is suggested that regions of this type are important in protein-protein recognition and mutagenesis studies of

this region in several different tetraspanins support a protein interaction role for this area of tetraspanin EC2s (Kazarov et al., 2002). The structural integrity of the EC2 is in part maintained by disulphide bonds formed by conserved cysteine residues. All tetraspanins have at least 4 cysteine residues, which are contributed by tetraspanin signature motifs, the absolutely conserved CCG with another cysteine proximal to TM4 and a mostly conserved PXXC motif (Stipp et al., 2003). Many tetraspanins have an additional pair of cysteines to give 6 in total and the TspanC8 subgroup have 8 (Charrin et al., 2009, Stipp et al., 2003). These cysteine residues have been used to trace the evolutionary history of the tetraspanin superfamily (DeSalle et al., 2010).

1.1.2.3 Tetraspanin intracellular tails

The intracellular tails of tetraspanins are generally less than 20 amino acids long excluding those of Tspan10, Tspan12, Tspan15, Tspan32, RDS and ROM1. The C-terminus does not contain any conserved tetraspanin features but does contain other protein motifs. Some contain short PDZ binding motifs (such as CD63) and/or internalisation sequences such as the YXXΦ (where Φ represents an amino acid with a bulky side chain) found in CD151 (Liu et al., 2007a), and some carry an overall basic charge which is also shown to mediate protein-protein interactions. Both termini are thought to lie close to the intracellular membrane and are generally thought to be non-ordered. Interestingly tetraspanins have membrane proximal cysteine residues that are palmitoylated. This post-translational modification is thought to have an effect on the N-terminal tail, causing it to form an amphipathic helix along the underside of the plasma membrane (Seigneuret, 2006, Granseth et al., 2005). This is a common feature of transmembrane proteins and in tetraspanins that do not have a

membrane proximal cysteine available for palmitoylation in the N-terminal (such as CD53), there is instead a hydrophobic residue so that the amphipathic nature is retained (Seigneuret, 2006, Stipp et al., 2003). Whilst the C-terminal tail structure is thought to be mainly randomly ordered, the amino acid side chains are thought to also align along the membrane (Seigneuret et al., 2001).

As well as palmitoylation most tetraspanins also undergo N-linked glycosylation as a post-translational modification. The position and number of glycosylation sites are not conserved in the tetraspanin superfamily and so the function of this modification is a poorly understood aspect of tetraspanin structure (Stipp et al., 2003, Seigneuret, 2006). One recent study investigated the glycosylation of Tspan1 and found that this modification is important for the correct folding and progression of Tspan1 through the endoplasmic reticulum (ER) (Scholz et al., 2009b).

1.1.3 Tetraspanin microdomains

A major functional characteristic of tetraspanin proteins is that once in the cell membrane they self-associate, forming clusters called microdomains. As all cell types are thought to express many tetraspanins (for example more than 20 in endothelial cells (Bailey et al., 2011)) these microdomains contain several different tetraspanins and consequently several other surface membrane proteins. The current thought is that each protein found in a tetraspanin microdomain is there because of a specific association with a specific tetraspanin (Charrin et al., 2009). Studies of tetraspanin microdomains show that these structures are distinct from other lipid enriched microdomains such as lipid rafts. The current view of these microdomains is that they form from a series of interactions between different tetraspanins building a network

termed the tetraspanin web (Charrin et al., 2009). The mobile nature of tetraspanins and their multiple interactions suggests that the tetraspanin web is highly dynamic and this allows it to contribute to the regulation of specific proteins by influencing their position and movement in the cell membrane (Espenel et al., 2008).

1.1.3.1 Tetraspanin microdomains are formed by interactions between tetraspanins

Investigation into the different interactions within tetraspanin microdomains using detergents of differing properties has found that there are different strengths of protein-protein interactions found within the microdomain (Claas et al., 2001). The main building blocks of tetraspanin microdomains, the homo- and hetero- interactions between the tetraspanins, can only be maintained after cell lysis by using detergents such as Brij97. Lysis buffers containing Brij97 or other low stringency non-ionic surfactants appear unable to disrupt the interactions between tetraspanins and thus, though solubilised, tetraspanin microdomains are preserved after lysis. Interestingly this ability is augmented when the lysis buffer contains the divalent cations $CaCl_2$ and $MgCl_2$. This property has allowed the discovery and investigation of tetraspanin associated proteins which co-immunoprecipitate with tetraspanins in these lysis buffers. Cell lysis by more stringent detergents such as Triton X-100 does not preserve the interactions between tetraspanins thus disrupting tetraspanin microdomains. In these detergents however, tetraspanin-partner protein complexes are often maintained. This indicates a stronger interaction than that between tetraspanins themselves, which can be maintained where a more complete disruption

of the cell membrane occurs (Charrin et al., 2003b, Charrin et al., 2002, Hemler, 2001, Claas et al., 2001).

The difference between the interactions captured by these two different detergents can be clearly seen in Figure 3 (taken from Protty et al. (2009) where, in Brij97 lysis conditions, the 'barcode' of tetraspanin associated proteins can be seen in addition to the immunoprecipitated tetraspanin. This barcode pattern is similar no matter which tetraspanin is immunoprecipitated (from the same cell type) and is also seen when a tetraspanin partner protein is immunoprecipitated (α6). This barcode pattern is however not evident when a non tetraspanin-associated protein is immunoprecipitated (α2). When the same cells are lysed in Triton X-100, no barcode pattern is seen when microdomain resident proteins are immunoprecipitated and instead only the tetraspanin and, in some cases, its partner protein band can be detected (Figure 3).

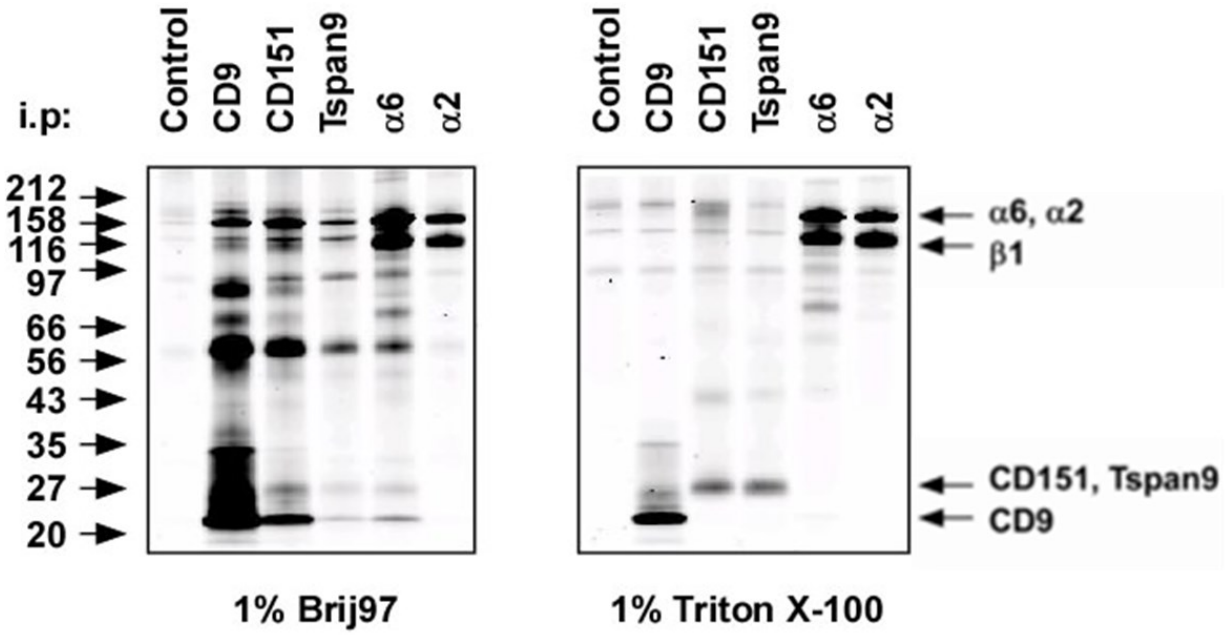

Figure 3. Tetraspanin-tetraspanin interactions are maintained in the weak detergent Brij97.

Surface biotinylated human platelets were lysed and immunoprecipitated with indicated detergents and antibodies. Western blotting with streptavidin identifies biotinylated proteins. The tetraspanin-tetraspanin interactions are only maintained in the less stringent lysis condition (1% Brij97) and are only seen when tetraspanin microdomain associated proteins are immunoprecipitated (CD9, CD151, Tspan9 and α6). These interactions are lost in more stringent detergents (1 % Triton X-100) leaving only the immunoprecipitated protein. Modified from Protty et al. (2009).

1.1.3.2 Tetraspanin microdomains are associated with certain lipids but are distinct from lipid rafts

As well as being enriched in tetraspanins and their partner proteins, tetraspanin microdomains are also enriched with specific lipids, in particular gangliosides and cholesterol. Cell line studies have demonstrated an interaction between CD9 and the ganglioside G_{M3} (Kawakami et al., 2002, Mitsuzuka et al., 2005). Other evidence for ganglioside involvement in tetraspanin microdomains include the reduction of tetraspanin-tetraspanin associations in cells where the glycosphingolipid biosynthetic pathway is inhibited or in which there is ectopic expression of a sialidase (Odintsova et al., 2006). As with tetraspanin partner protein interactions this association of tetraspanins and gangliosides is restricted to specific gangliosides, the two best characterised being G_{M3} and G_{MD1} (Hemler, 2005). Cholesterol is also enriched in tetraspanin microdomains as evidenced by the precipitation of tetraspanin microdomains by the saponin Digitonin (Charrin et al., 2003c), the fractionation of tetraspanin microdomains into low density fractions of sucrose gradients (Charrin et al., 2003b, Berditchevski et al., 2002, Claas et al., 2001, Delaguillaumie et al., 2004) and the interaction of tetraspanins with cholesterol analogues (Charrin et al., 2003c). How these lipids interact with tetraspanins and their functional consequence for tetraspanin microdomains is currently unknown. Current evidence from other multi-transmembrane proteins points to cholesterol binding by the palmitates attached to juxtamembrane cysteine residues found in all tetraspanins. Interestingly, whilst not required for initiating tetraspanin-tetraspanin interactions, palmitoylation is required to stabilise tetraspanin microdomains which, if they are responsible for tetraspanin cholesterol binding, could indicate a similar function for cholesterol (Charrin et al.,

2002). This hypothesis is however juxtaposed with the results of experiments using methyl-β-cyclodextrin (MβCD). Cholesterol depletion from cell membranes using MβCD, whilst attenuating tetraspanin mediated cell functions, does not disrupt tetraspanin microdomains (Claas et al., 2001, Charrin et al., 2003c). Another potential cholesterol binding site is the band of exposed aromatic residues found in many tetraspanins around transmembrane domains 1 and 2. These residues serve as binding sites in other transmembrane proteins too, however whilst present in many, they are not found in all tetraspanins (Seigneuret, 2006, Stipp et al., 2003).

The enrichment of tetraspanin microdomains with particular lipids and their separation into low density sucrose gradient fractions leads to their comparison with other membrane microdomains, in particular lipid rafts (Simons and Gerl, 2010). Whilst sharing these general similarities there are key differences between them which demonstrate that tetraspanin microdomains are clearly distinct from lipid rafts. As shown in Table 1, these differences are at the level of the biochemical characteristics that characterise many membrane microdomains and also in the repertoire of proteins found in each (Hemler, 2005). In addition to the experimental evidence provided in Table 1, lipid rafts and tetraspanin microdomains differ fundamentally in that tetraspanin microdomains are formed on the basis of protein-protein interactions whereas lipid rafts are formed through the interaction of lipid and protein (Hemler, 2005).

	Tetraspanin microdomain	Lipid raft
Temperature	Maintained at 37 °C	Disrupted at 37 °C
Cholesterol	Resistant to cholesterol depletion	Disrupted by cholesterol depletion
Non-ionic detergents	Mostly soluble in non-ionic detergents	Insoluble in non-ionic detergents
Resident proteins	Enriched in tetraspanins Do not contain GPI-linked proteins, caveolin and Src-family kinases	Do not contain tetraspanins Contain GPI-linked proteins, caveolin and Src-family kinases

Table 1. Comparison of tetraspanin microdomains and lipid rafts.

Despite being enriched in particular lipids and sometimes partitioning into low density membrane fractions, tetraspanin microdomains are distinct from the classical lipid raft microdomains. Some of the main differences are listed in this table. Abbreviations - Glycophosphatidylinositol (GPI). This table was modified from Hemler (2005).

1.1.3.3 Tetraspanin microdomains are dynamic structures

Discussion so far as focussed on the biochemical analysis of tetraspanin microdomains which, whilst highly informative of their composition and of the interactions that form them, gives little insight into how these microdomains may behave in the plasma membrane. Tetraspanins and their microdomains have also been studied using microscopy techniques that allow their analyses in live and fixed cell membranes. Initial studies used confocal microscopy to look at the distribution and size of tetraspanin microdomains by labelling CD9, CD81, CD82 and CD63 in HeLa cells. This study found them numerous and scattered across the cell surface with a size of ~200 nm (Nydegger et al., 2006). As this size is at the diffraction limit of light, more sophisticated techniques that overcome this limitation of light microscopy were used to look at these structures in more detail and at the movement of individual tetraspanins in the cell membrane. Förster resonance energy transfer (FRET) analysis showed that in addition to their microdomain forming interactions, tetraspanins also appeared to interact outside of tetraspanin microdomains (Barreiro et al., 2008). Single particle tracking microscopy (SPTM) allowed closer analysis of this and demonstrated that tetraspanins are highly mobile and undergo successive transient interactions (Espenel et al., 2008). These studies suggest that tetraspanins (and so the associated partner proteins), by their nature, are highly mobile and thus many microdomains may be highly dynamic, being formed transiently and successively many times. For tetraspanin microdomains that are longer lived (also seen in FRET and SPTM studies), it is predicted that a tetraspanin partner protein would be anchored to one position with many interactions becoming centred around this initial microdomain (Charrin et al., 2009).

1.1.3.4 Tetraspanin microdomains interact with cytosolic proteins

In addition to co-ordinating other transmembrane proteins there is evidence to suggest that proteins resident in the cytosol can also associate with tetraspanin microdomains. This promotes the idea that the tetraspanin microdomain and the tetraspanin web exists not only as a structure above the membrane, despite the short intracellular tails of tetraspanins. Several cytoplasmic effector proteins have been shown to associate with tetraspanin microdomains generally through interactions with tetraspanin C-terminal tails. These include PDZ domain containing proteins that act as molecular scaffolds (Pan et al., 2007, Bassani et al., 2012, Latysheva et al., 2006), actin-binding ezrin-radixin-moesin (ERM) family proteins (Sala-Valdés et al., 2006) and the signalling proteins phosphatidylinositol 4-kinases (PI4Ks) (Yauch and Hemler, 2000) and Rac GTPase (Tejera et al., 2013) and the classical PKC kinases PKCα and PKCβ (Zhang et al., 2001). It is thought that tetraspanins may act as linker molecules between these cellular effectors and the other transmembrane proteins present in the tetraspanin microdomains.

1.1.4 Tetraspanin regulation of partner proteins

Tetraspanins have been found to play roles in very diverse cellular functions, which is probably due to the diverse array of membrane proteins that interact with tetraspanins and the ubiquitous nature if tetraspanins throughout the body. The current view of tetraspanin microdomains as a tetraspanin web suggests that these structures influence the organisation of particular proteins in the plasma membrane and this regulates and facilitates efficiency of cell function (Charrin et al., 2009). Unfortunately, the detailed study of the function of tetraspanin microdomains as whole units has not yet been achieved. Instead studies have focussed on understanding the function of individual tetraspanins and the identification of their partner proteins.

There have been four main approaches to studying tetraspanins. Historically the effects of monoclonal antibodies against some tetraspanins on different cell types were the starting points of research into tetraspanin function (Levy et al., 1998, Higginbottom et al., 2000, Wu et al., 2001). The field is now dominated by silencing, mutagenesis and overexpression studies, whole organism knockout models including plants (Olmos et al., 2003), worms (Dunn et al., 2010), flies (Kopczynski et al., 1996) and mice (Maecker et al., 1998) and more recently discoveries of tetraspanin mutations in human diseases. In many of these approaches it can be difficult to ensure the observed effects of tetraspanin manipulation are specific to the targeted tetraspanin. This is due to the extensive interactions between tetraspanins and the influence of tetraspanin microdomain disruption on the many different proteins thought to be regulated by tetraspanins and the tetraspanin web (Charrin et al., 2003b, Charrin et al., 2009). An additional problem that is faced by knockdown

studies or knockout models is that cells express many tetraspanins, some of which may share partner proteins or similar functions. As such the loss of one tetraspanin may be compensated by another which can diminish or abrogate the effects caused by the loss of the targeted tetraspanin (Dornier et al., 2012, Haining et al., 2012). Despite this, and the wide ranging nature of tetraspanin partner proteins, three main areas of tetraspanin influence on their partner proteins have be identified: (a) regulation of biosynthetic transport and maturation, (b) regulation of trafficking, localisation and surface expression and (c) regulation of lateral mobility and clustering.

1.1.4.1 Tetraspanins regulate partner protein biosynthetic transport and maturation

Several tetraspanins have been shown to interact with their partner proteins in the ER. Furthermore, for a more select group of tetraspanins, this interaction early in protein synthesis is necessary for the progression of the partner proteins from the ER to the golgi and then forward to later cellular compartments (Charrin et al., 2009). Three key examples of this function of tetraspanins can be seen in studies of CD19 and CD81 (Tsitsikov et al., 1997, Shoham et al., 2003, van Zelm et al., 2010), the uroplakins and their partner proteins (Hu et al., 2005, Tu et al., 2006) and ADAM and the TspanC8 tetraspanins (Dornier et al., 2012, Haining et al., 2012, Prox et al., 2012). In each case the tetraspanin must be co-expressed for the partner protein to egress from the ER. This is clearly demonstrated by a patient that carried an insertion gene mutation in human CD81 which prevented CD81 expression. This patient had a severe immunodeficiency caused by the loss of CD19 (a subunit of the B cell antigen

receptor complex) from the surface of B cells (van Zelm et al., 2010). The mechanism by which these tetraspanins regulate the egress of their partner proteins from the ER is currently unknown, however masking of an ER retention motif or facilitation of partner protein glycosylation have both been suggested hypotheses (Haining et al., 2012, Scholz et al., 2009a).

1.1.4.2 Tetraspanins regulate partner protein cell surface expression

Other tetraspanins have been shown to regulate the cellular localisation and/or turnover of their partner proteins. CD63 is an interesting tetraspanin in this regard as it is found predominantly on intracellular compartments (Kobayashi et al., 2000). As such it is unsurprising that there are several examples of this tetraspanin regulating the targeting and/or retention of its partner proteins in intracellular compartments. Two partner proteins retained in intracellular compartments by CD63 expression are the chemokine receptor CXCR4 in MT-4 cells and the H^+/K^+ATPase in HEK 293T cells. In both cases, knockdown or mutation of CD63 caused an increased surface expression of these proteins as they were no longer trafficked to intracellular compartments (Yoshida et al., 2008, Duffield et al., 2003, Codina et al., 2005). The mechanism by which CD63 exerts this function is incompletely understood, however evidence suggests that association of these proteins with CD63 allows the cell to have a stimulus-regulated surface expression of these proteins. CD151 is also known to regulate the cellular localisation of some of its partner proteins, not by targeting them to a particular part of the cell but by influencing their turnover from the plasma membrane. Mutagenesis studies in a breast cancer cell line demonstrated that the internalisation motif ($YXX\Phi$) found in the C-terminal tail of CD151 not only regulated

the turnover of CD151 from the plasma membrane but also that of integrins α3β1 and α6β1, with which it associates (Liu et al., 2007b). Another example of this type of regulation was more recently discovered as a function of the tetraspanin Tspan1 in human intestinal cells. Expression of this tetraspanin in this cell type was shown to cause a doubling of the half life of the thiamine transporter with which it was found to associate (Nabokina et al., 2011).

1.1.4.3 Tetraspanins regulate partner protein membrane organisation

The final general theme of tetraspanin regulation of partner proteins is the regulation of how partner proteins are organised in the plasma membrane. Several tetraspanins have been shown to facilitate the clustering of their partner proteins into nano-platforms to facilitate efficient cell function. Key examples of this are the formation of adhesion platforms on endothelial cells by tetraspanins CD9 and CD151 (Barreiro et al., 2008) and the clustering of P-selectin and MHC class II molecules by CD63 and CD9 respectively (Doyle et al., 2011, Khandelwal and Roche, 2010). The formation of these clusters is thought to rely on the ability of tetraspanins to interact with one another as they move through the tetraspanin web. This is thought to contribute to efficient and rapid formation of homo- and heterogeneous clusters in response to stimuli. Linked to this function is the ability of tetraspanins to regulate the lateral mobility of their partner proteins in the plasma membrane. The modulation of the movement of α6 integrin by CD151 is one example of this aspect of tetraspanin function. In breast cancer epithelial cells α6 integrin was observed by single particle tracking microscopy to diffuse in a mostly confined manner in the cell membrane. After CD151 knockdown, however, this changed to a mostly directed diffusion (Yang

et al., 2012b). This discovery explained why CD151 knockdown in breast cancer lines affected $\alpha 6$ integrin clustering and functions without effecting integrin expression or activation (Lammerding et al., 2003, Yang et al., 2008). The diffusion of $\alpha 4$ integrin is also influenced by its tetraspanin partner. It was shown to be less mobile and in smaller clusters in CD37-deficient B cells when compared to wildtype as demonstrated by confocal, electron and fluorescence recovery after photobleaching (FRAP) microscopy (van Spriel et al., 2012). Other tetraspanins are predicted to influence their partner proteins lateral mobility but are yet to be studied in this way. Despite the mechanism of how tetraspanins regulate partner protein clustering and lateral mobility being incompletely understood, this final aspect of tetraspanin function provides the most clues as to the function of tetraspanin microdomains and the tetraspanin web.

1.1.5 Tetraspanin mutations cause human disease

Tetraspanins are reported to regulate a hugely diverse array of cellular functions. This diversity may be due to their likely expression in all mammalian cell types, the wide range of tetraspanin partner protein functions and, as just discussed, the different ways in which tetraspanins can regulate these proteins. The partner proteins for many tetraspanins are yet to be identified and so the mechanisms through which they exert their observed regulation of cell functions are unknown. Despite this, the importance of tetraspanins is clearly evidenced by the human diseases linked to mutations in tetraspanin genes. The following describes the known tetraspanin mutations linked to human diseases and, where known, how these mutations cause disruption of cellular processes.

Tspan7 was originally described due to its mutation in non-specific forms of X-linked mental retardation (Zemni et al., 2000). Subsequent research into its function resulted in a recently published study that demonstrated a role for this tetraspanin in the trafficking of the AMPA receptor (α-amino-3-hydroxy-5-methyl-4-isoxazolepropionic acid receptor) in hippocampal neurones (Bassani et al., 2012). Tspan7 appeared to regulate the turnover from the membrane of the GluA2 subunit of the AMPA receptor, not by direct association, but by competing for a mutually binding intracellular protein, PICK1. Through this regulation of AMPA levels the strength of synaptic signalling and synapse maturity in hippocampal neurones is regulated by Tspan7. This function in synapse maturity has been suggested as the link between the original observation of mutations in Tspan7 and X-linked mental retardation.

Mutations in the tetraspanin Tspan12 are one of the causes of the progressive retinal vascular disease familial exudative vitreoretinopathy (FEVR) (Yang et al., 2011). In this disease the vasculature of the retina is not maintained and its degeneration leads to blindness (Yang et al., 2011). Investigations of the Tspan12 knockout mouse revealed that Tspan12 is involved in the regulation of Norrin-induced Frizzed 4 signalling in retinal angiogenesis. Tspan12 appears to promote multimerisation of the Frizzed 4 receptor in newly forming blood vessels in the retina, which is important for Norrin-induced signalling and the development and maintenance of the retinal vasculature. Consequently Tspan12 knockout mice phenocopy defects seen in retinas from Norrin knockout mice and the human disease FEVR (Junge et al., 2009). Mutations in two other tetraspanins, ROM-1 and Peripherin/retinal degeneration slow (RDS), are also known to cause progressive degeneration in the eye. Peripherin/RDS is a tetraspanin found specifically in the membranes of the retinal cone and rod cell outer segments. It is essential for the correct organisation and maintenance of the outer segment discs required for the initiation of phototransduction in the retina (Goldberg et al., 2007). There have been 70 different mutations identified in the Peripherin/RDS gene, each contributing to one of several diseases collectively known as macular dystrophies (Goldberg, 2006). Retinitis pigmentosa, a subset of this group of diseases, has been found to involve another synergistic mutation in tetraspanin ROM1 (Loewen et al., 2003). This tetraspanin is also found in the outer membranes of the rod and cone cells and its loss or mutation also leads to disorganisation of the rod and cone cells disc stacks (Boesze-Battaglia et al., 2007).

Moving on from the eye, mutations in the tetraspanin CD151, that results in a truncated protein lacking its integrin binding region, causes end stage hereditary nephritis and a skin blistering disease known as pretibial epidermolysis bullosa (Karamatic Crew et al., 2004). These diseases are thought to be due to disruption in the organisation of basement membranes in which the laminin binding integrins, which are partner proteins for CD151, are found. Finally, a patient presenting with severe immunodeficiency was subsequently found to carry a mutation in CD81 that prevented its expression. As previously discussed this deletion of CD81 from B cells prevented the surface expression of CD19, a partner protein for CD81, essential for the function of the B cell antigen receptor thus resulting in immunodeficiency (van Zelm et al., 2010).

1.1.6 Tetraspanins and cancer

As well as having diverse roles in the normal functioning of many cells and processes, as detailed in the previous section, tetraspanins also appear to play a role in cancer. Many tetraspanins have been linked to various aspects of cancer initiation, progression and metastasis as they are often found up or down regulated in many different cancers from a variety of tissues. Two tetraspanins in particular, CD151 and CD82, have been shown to play roles specifically in cancer metastasis. CD82 has been termed a metastasis suppressor gene as it is frequently down regulated in many late stage epithelial cancers (Odintsova et al., 2000). Unlike other metastasis suppressor genes CD82 appears to suppress metastasis through several different mechanisms that ultimately lead to the inhibition of migration and invasiveness and the promotion of responses to external stimuli (Tsai and Weissman, 2011). Conversely CD151 is found to be upregulated in end stage cancers and is thought to be a metastasis promoter, promoting cell motility through its laminin binding integrin partner proteins (Haeuw et al., 2011). For other tetraspanins the exact consequences of the change in their expression for the cancer is poorly understood. Some tetraspanins are, however, advocated as biomarkers and prognostic markers of particular cancers which could impact cancer diagnosis and treatment (Hirano et al., 2009, Wang et al., 2013, Kwon et al., 2012). There is currently one tetraspanin targeted approach to cancer treatment in clinical trials. Antibodies against CD37 are currently in phase I clinical trials for use in the treatment of non-Hodgkin's lymphoma and chronic lymphocytic leukaemia, demonstrating the potential of targeting tetraspanins for cancer treatment (Robak et al., 2009).

1.1.7 Tetraspanins and infectious disease

Aside from the numerous reports of tetraspanin involvement in cancers there are more specific functions of tetraspanins known in human disease, in particular in the use of tetraspanins by infectious agents, especially by viruses. The most well studied and understood role of tetraspanins in infectious disease is the function of CD81 in the entry of hepatitis C virus into hepatocytes. CD81 is a co-receptor for the virus thought, with another protein called scavenger receptor class B member 1 **(**SRB-1), to be responsible for the initial attachment of the virus to the cells (Pileri et al., 1998, Reynolds et al., 2008). After attachment via CD81 the evidence suggests that the virus then utilises the particular movement of CD81 in the plasma membrane to promote its interaction with its other entry co-factors (claudin-1 and occludin) and its endocytosis into the target cell (Harris et al., 2013). As it plays such a key role in the infection of hepatocytes by hepatitis C virus, CD81 is the focus of much research as a potential drug target for this important human disease.

Another well documented example of viral targeting of tetraspanins is the molecular mimicry of Tspan4 by cytomegalovirus. Antibodies produced by many infected individuals against the cytomegalovirus protein UL94 cross-react with Tspan4 and due to the expression of Tspan4 on blood vessel endothelial cells and fibroblasts the anti-UL94 antibodies bind to these cells (Lunardi et al., 2000). The effects of anti-UL94 antibody binding are thought to be causative of the disease systemic scleroderma, that can occur after cytomegalovirus infection, and as such Tspan4 (also known as NAG-2) is also a potential drug target to prevent the development and progression of this disease (Traggiai et al., 2010). Other viruses, including human immunodeficiency virus 1 (Gordón-Alonso et al., 2006), influenza virus (Thali,

2011), human papillomavirus 16 (Scheffer et al., 2013) and herpes simplex virus 1 (Wang et al., 2010), are also known to require tetraspanins for their uptake into target cells, for replication and intracellular trafficking and/or for budding from host cells. However, the role of tetraspanins in the life cycle of these viruses is much less understood than the examples of hepatitis C and cytomegalovirus.

Other infectious agents also utilise tetraspanin expression on target cells, for example uropathogenic *E. coli* bacteria require the uroplakin tetraspanins to adhere to and invade the kidney urothelium (Zhou et al., 2001), and the protozoan *Plasmodium* (which is responsible for malaria) requires CD81 to invade hepatocytes in its sporozoite form, a step necessary for prolonged malaria infection (Silvie et al., 2003). The use of tetraspanins by infectious agents is the focus of research that aims to neutralise infections by targeting the tetraspanin-organism interaction using antibodies and recombinant proteins. Interestingly, as tetraspanins are discovered in more organisms, research has now also begun to target tetraspanin homologues expressed on some parasites to develop vaccines against important diseases such as schistosomiasis (Pearson et al., 2012).

1.1.8 Tetraspanins in lower eukaryotes

In addition to their clear roles in mammals, tetraspanins are also found in lower eukaryotes including flies, worms, fungi and plants. Knockout studies in these organisms, as in mice and humans, revealed diverse functions for tetraspanins. The following describes some of the key studies of tetraspanins in these lower eukaryotes. In *C. elegans* RNAi knockdown of tetraspanin Tsp-15 caused an abnormal morphology (Moribe et al., 2004). Consequent investigation demonstrated that Tsp-15 was required for the functioning of the dual oxidase pathway in the worm. This pathway, conserved through to mammals, generates reactive oxygen species required to crosslink the collagens that form the *C. elegans* exoskeleton (Moribe et al., 2012). Interestingly work in *C. elegans* has also discovered a role for the mammalian TspanC8 tetraspanin homologues Tsp-12 and Tsp-14 in the cleavage of the ADAM10 target protein Notch (Dunn et al., 2010). The conclusion of this work was that Tsp-12 and Tsp-14 may regulate γ-secretase activity, however in the light of three subsequent papers demonstrating the regulation of ADAM10 by the TspanC8 tetraspanin subfamily, it is possible that these *C. elegans* tetraspanins instead regulate Notch via ADAM10 (Haining et al., 2012, Prox et al., 2012, Dornier et al., 2012).

There are 37 tetraspanin proteins found in the fruit fly *D. melanogaster*. Three of these tetraspanin genes (late bloomer, Tsp42Ee and Tsp42Ej) are required for correct motor neurone synapse formation (Kopczynski et al., 1996, Fradkin et al., 2002). Tetraspanin Tsp42Ej is also called sunglasses due to the degeneration of photoreceptors in its null mutant fly. This fly tetraspanin is most closely related to CD63 and, like this mammalian tetraspanin, is predominantly found on intracellular

organelles, in this case lysosomes (Xu et al., 2004). Finally the tetraspanin Tsp68C has an as yet undetermined role in regulating the proliferation of fly hemocytes (Sinenko and Mathey-Prevot, 2004).

As previously mentioned, tetraspanins genes are also conserved in plants and have been found in rice, maize, wheat and moss. In the model organism *Arabidopsis thaliana* there are 17 different tetraspanins termed TET1 to TET17. Only TET1 has been studied by mutation. In two separate approaches mutations in this gene caused aberrant pattern formation and contortion of the plant organs. Whilst the mechanisms behind these phenotypes are incompletely understood, these mutants clearly demonstrate an important role for at least TET1 in plant development (Olmos et al., 2003, Cnops et al., 2006, Chiu et al., 2007).

Additional to these studies, tetraspanins have also been studied in fungi and in the parasitic worms that cause schistosomiasis and filariasis. In all three cases tetraspanin proteins are the focus of study to either reduce pathogenicity and infectivity, or are the targets of vaccines against disease (Gnanasekar et al., 2008, Tran et al., 2006, Lambou et al., 2008). In the case of schistosomiasis, vaccines against its surface expressed tetraspanin Tsp2 are currently being developed (Curti et al., 2013). This tetraspanin is known through knockout studies to be essential for the development and maintenance of the teguments that form the outer body of the parasite (Tran et al., 2010).

1.1.9 Tetraspanins are enriched in exosomes

One final aspect of tetraspanin function not yet discussed is their enrichment and function in the formation and targeting of exosomes. Exosomes are lipid vesicles that are released from the surface of multi vesicular bodies and are thought to target specific cells to deliver their contents, usually proteins or RNAs of varying sorts (Raposo and Stoorvogel, 2013). Tetraspanins are unusually enriched in exosomes and there is evidence to suggest that specific tetraspanins are recruited to particular exosomes destined for different target cells or containing differing cargo (Rana and Zöller, 2011). The mechanisms governing exosome formation and cell targeting are still incompletely understood, however tetraspanins are the focus of intense research in this area as they show potential in advancing current drug delivery strategies and in the development of non-invasive screening and follow-up programs (Rana and Zöller, 2011).

1.1.10 Platelet tetraspanins

Five tetraspanins have been identified on the platelet cell surface using antibodies, namely CD9, CD63, CD151, Tspan32 and Tspan9. CD9 is the most highly expressed tetraspanin in platelets and also is the second most highly expressed protein on the human platelet cell surface (roughly 50,000 copies per platelet), behind the very highly expressed αIIbβ3 integrin. The function of these tetraspanins on platelets, apart from Tspan9, has been investigated by generating the knockout mouse for each protein. A summary of the findings from these knockout mice can be seen in Table 2. Despite its high expression on platelets CD9-deficient platelets only displayed a mild defect in responses. This manifested in a mild hyper-responsive phenotype with increased activation of the αIIbβ3 integrin (Mangin et al., 2009). The CD63 knockout also shared a similar phenotype with mildly increased responses to a range of agonists (Schröder et al., 2009). Both of these phenotypes were attributed to augmented inside-out signalling leading to increased integrin activation, however no mechanism has been investigated to prove this hypothesis.

Conversely the CD151 and Tspan32 deficient platelets showed evidence of decreased activity of the integrin αIIbβ3. Additionally the phenotypes of both these knockout mice were more pronounced than the mild defects seen in the CD9 and CD63 knockouts. The CD151 knockout showed impairment of platelet responses in several assays including increased bleeding times and instances of re-bleeding (Wright et al., 2004), impaired spreading and clot retraction (Lau et al., 2004) and *in vivo* thrombus formation (Orlowski et al., 2009). These defects were shown to be platelet mediated as reconstitution experiments eliminated endothelial cell involvement (CD151 is also expressed in these cells). The Tspan32 (also known as TSSC6) knockout mice also had a similar phenotype with impaired spreading, clot

retraction and thrombus formation in *in vivo* experiments (Goschnick et al., 2006). Impaired signalling of the integrin into the platelets (outside-in signalling) was hypothesised as the cause of the defects in both these knockout mice as inside-out signalling as measured by integrin activation appeared normal. As for the CD9 and CD63 knockout mice, no clear mechanism was described to explain the effects of CD151 or Tspan32 knockout on αIIbβ3 integrin function.

Tspan9 was recently identified as the fifth platelet tetraspanin using an antibody but is yet to be functionally studied (Protty et al., 2009). Interestingly Tspan9 appears most highly expressed on platelets when compared to other mouse tissues in western blotting approaches potentially suggesting a key role for this protein in this cell type (Protty et al., 2009). Whilst the function of these tetraspanins in platelets has begun to be studied, several more have been identified as expressed by platelets by proteomics (Senis et al., 2007, Lewandrowski et al., 2009a). Tspan33 was the predicted to be the third most highly expressed platelet tetraspanin in human platelets behind CD9 and Tspan9 by Lewandrowski et al. and like Tspan9 has yet to be fuctionally studied in platelets.

Common name	Alternative name	Knockout mouse platelet phenotype	Attributed mechanism
CD9	Tspan29	Increased activated αIIbβ3 integrin after platelet activation Enhanced thrombus formation (Mangin *et al.* 2009)	Increased platelet inside-out signalling
CD63	Tspan30	Increased activated αIIbβ3 integrin after platelet activation Mildly increased aggregation responses (Schroder *et al.* 2009)	Increased platelet inside-out signalling
CD151	Tspan24	Increased tail bleeding time and re-bleeding after tail bleeding (Wright *et al.* 2004) Impaired platelet spreading on fibrinogen and clot retraction (Lau *et al.* 2004) Impaired in vivo thrombus formation (Orlowski *et al.* 2009)	Moderate outside-in αIIbβ3 integrin signalling defect
Tspan32	TSSC6, PHEMX	Increased tail bleeding time and re-bleeding after tail bleeding Impaired platelet spreading on fibrinogen and clot retraction Impaired thrombus formation in vivo (Goschnick *et al.* 2006)	Dysregulation of outside-in αIIbβ3 integrin signalling defect
Tspan9	NET-5	Not yet known	n/a

Table 2. Platelet tetraspanin knockout phenotypes

A table of the known platelet tetraspanins (demonstrated as expressed on platelets using antibodies) and the platelet phenotype from the associated knockout mouse. The exact mechanism of action of these tetraspanins in platelets is unknown however the conclusions of the papers that published the platelet phenotype in each case is provided.

Several surface transmembrane proteins found in platelets have been identified as associated with tetraspanin microdomains using tetraspanin immunoprecipitation in Brij97. This method isolates tetraspanin microdomains from platelets as cell lysis in Brij97 does not disrupt the interactions between tetraspanins which hold tetraspanin microdomains together. The major platelet proteins immunoprecipitated in tetraspanin microdomains and the known platelet tetraspanins are shown in Figure 4. These include GPVI (Protty *et al*. 2009), the laminin binding integrin $\alpha_6\beta_1$ (Miao et al., 2001), the metalloproteinase ADAM10, the choline transporter CD92 (Lewandrowski et al., 2009b) and CD36, the scavenger receptor notably binding oxidised low density lipoprotein (oxLDL) (Miao et al., 2001). The interactions of these platelet proteins with tetraspanins are yet to be studied in detail, with the exception of CD151 and $\alpha_6\beta_1$ integrin and ADAM10, and so their tetraspanin partners responsible for their inclusion in platelet tetraspanin microdomains remains unclear (Orlowski et al., 2009, Dornier et al., 2012, Haining et al., 2012).

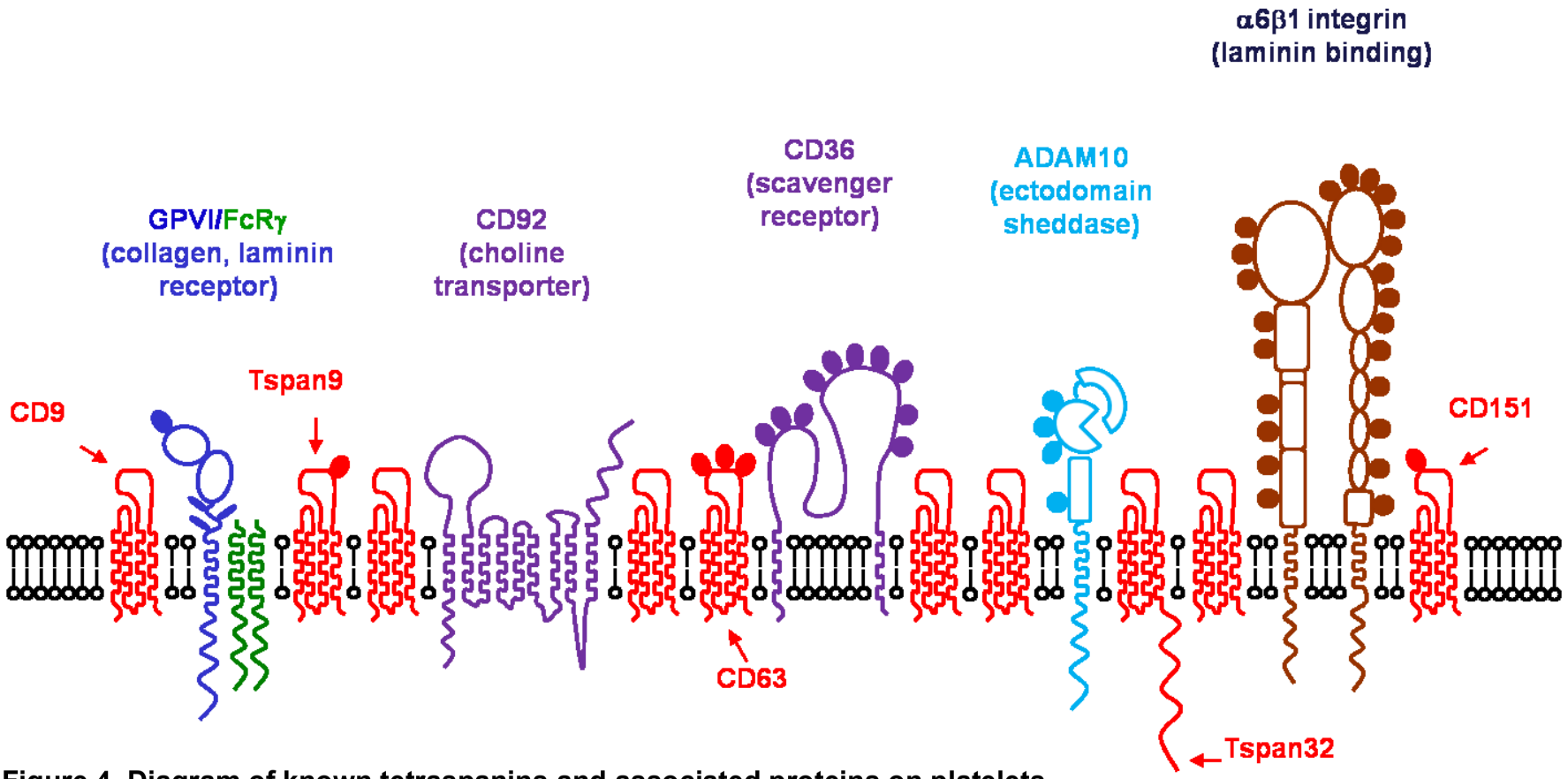

Figure 4. Diagram of known tetraspanins and associated proteins on platelets.

The tetraspanins (depicted in red) have all been shown on platelets using antibodies. All tetraspanins in the diagram are CD9 unless otherwise labelled. With the exception of GPVI (Protty et al. 2009), the tetraspanin associated proteins were detected using proteomics after CD9 immunoprecipitation in Brij97 (J. Yang, E.J. Haining and M.G. Tomlinson, unpublished data). Again with the exception of GPVI, all these proteins have been previously identified as tetraspanin associated in other cell types (Rubinstein, Charrin and Tomlinson, 2013 – The tetraspanin book).

1.2 Platelets

1.2.1 Overview

First described by Bizzozero in 1882, platelets are small anucleate blood cells that are only found in mammals. Generated by megakaryocyte cells in the bone marrow, platelets circulate in the blood at concentrations around 1.5 – 4 x 10^8 /ml, but due to their marginalisation by the flow of the much larger red blood cells are found at much higher concentrations near the blood vessel walls (Watts et al., 2013). Platelets are an important cell type in the body as they play a major role in haemostasis. Monitoring the integrity of the vasculature, their primary function is to bridge and plug any sites of damage in the vessel endothelium. The importance of this role is clearly seen in patients with thrombocytopenia where, without platelet transfusions, bleeding ranging from petechia in the skin to intracranial haemorrhage occurs (Hux and Martin, 2012). Unfortunately the response of platelets to vessel damage can also be activated by diseased endothelium or by atherosclerotic plaque rupture. This pathological activation of platelets often results in occlusive blood clots that cause myocardial infarction or stroke which, when taken together, are currently the biggest cause of death in the UK (Jennings, 2009, von Hundelshausen and Weber, 2007). More recently other roles have been uncovered for platelets including functions in the innate immune system (von Hundelshausen and Weber, 2007) and during development (Uhrin et al., 2010, Echtler et al., 2010). Additional to these new roles in normal mammalian biology, platelets also have emerging roles in several different human pathologies including atherosclerosis, cancer metastasis, and most recently in deep vein thrombosis and ischaemic stroke reperfusion injury (Nieswandt et al., 2011a, Fuchs et al., 2012, Lowe et al., 2012, Fuentes Q et al., 2012).

1.2.2 Platelet biogenesis

Platelets, like all other blood cells, are the product of haematopoiesis in the bone marrow. Platelets are generated by megakaryocyte cells that descend from committed myeloid progenitor cells (called colony forming unit granulocyte erythroid macrophage megakaryocyte cells [CFU-GEMM]) (Yu and Cantor, 2012) (Figure 5). As they mature, megakaryocytes migrate from the osteoblastic bone marrow niche to the vascular bone marrow niche where they become large (~50 μm across) polyploid cells under the regulation of the hormone thrombopoietin (Pitchford et al., 2012). Once matured, megakaryocytes form long cytoplasmic extensions from their cell body, called proplatelets, that extend into the blood vessels that supply the vascular niche. Platelets are shed from these proplatelet extensions into the bloodstream and in this way each megakaryocyte can produce 2000 - 3000 platelets in its lifetime (Patel et al., 2005, Yu and Cantor, 2012). The continual production of platelets by megakaryocytes is required as platelets only survive ~ 10 days in the circulation, after which they are cleared by splenic macrophages and Kupffer cells in the liver (Hoffmeister, 2011).

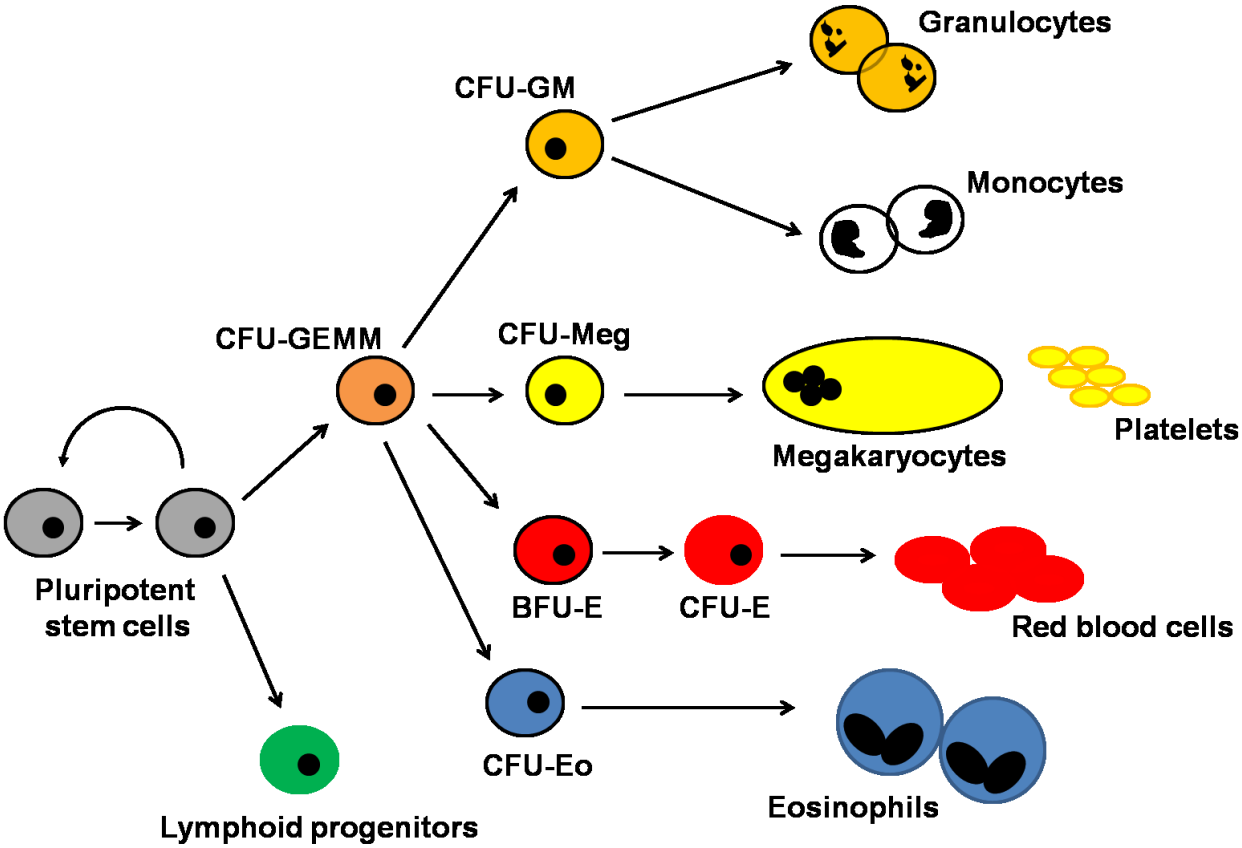

Figure 5. Megakaryocyte cells descend from myeloid progenitor cells in haematopoiesis.

This diagram is a much simplified diagram of the major later stages of haematopoiesis in the bone marrow. Megakaryocytes descend from the megakaryocyte committed progenitors colony-forming unit megakaryocyte cells (CFU-Meg cells). These cells descend from the committed myeloid progenitor cells colony-forming unit granulocyte erythroid macrophage megakaryocyte (CFU-GEMM). The differentiation process from CFU-Meg to megakaryocyte is regulated largely by the hormone thrombopoietin. All other blood cells are produced by haematopoiesis, those other than megakaryocytes which descend from CFU-GEMM cells are also depicted in this diagram.

1.2.3 Platelet function

The primary and best understood function of platelets is preventing blood loss from damaged blood vessels. On encountering a damaged vessel or ruptured atheroma platelets respond to the activatory signals embedded in the exposed subendothelial matrix that are usually shielded from the flowing blood by the intact endothelium. These platelet agonists include collagens and laminins and also others such as the glycoproteins von Willebrand factor (vWF) and fibrinogen which become adhered to the collagen in the exposed matrix or are converted to an active form at the damaged site. The agonists induce several physical and biochemical changes in recruited platelets in a process understood to have clearly defined steps which culminate in stable thrombus formation (Nieswandt et al., 2011b). A diagram of this process which is further discussed below can be seen in Figure 6.

Step 1 - platelet tethering to the damaged vessel wall

The platelet leucine rich repeat receptors GPIb, GPIX and GPV form a complex in the platelet membrane that is responsible for the recognition and binding of von Willebrand factor by platelets, after it has become immobilised on exposed sub-endothelial collagen. This step, known as platelet tethering, is responsible for the recruitment of platelets from the flowing blood (Li and Emsley, 2013). The importance of this step is highlighted by the rare autosomal recessive bleeding disorder Bernard-Soulier syndrome. Sufferers of this disorder carry mutations in the GPIb or GPIX genes, that result in significantly reduced levels of the protein complex on the platelet surface. Consequently Bernard-Soulier platelets can no longer recognise immobilised von Willebrand factor and the subsequent inability of their platelets to adhere to damaged vessels results in, what can be, a severe bleeding diathesis (Li and Emsley, 2013). In addition to the interaction between platelets and vWF proteins

upregulated on activated endothelial cells can also aid in platelet tethering to damaged vessels. These proteins include P-selectin which, through homotypic interactions, can tether activated platelets (which also express P-selectin) to endothelial cells.

Step 2 - Firm adhesion and activation

The second stage in platelet mediated thrombus formation is platelet activation and firm platelet adhesion. Though the interaction between the GPIb complex and von Willebrand factor can recruit platelets to a site of endothelial damage, the fast off-rate of this interaction results, not in the adhesion of platelets, but their rolling across the exposed matrix (Li and Emsley, 2013). This rolling and slowing of platelets is enough, however, to allow the low affinity immunoglobulin superfamily receptor GPVI to bind its ligand collagen. Constitutively associated with an Fc receptor γ-chain, this receptor recognises the frequent GPO repeats in collagen as a dimer. Despite its weak affinity for collagen, GPVI transduces powerful activatory signals into the platelet upon ligand engagement via the immunoreceptor tyrosine-based activation motif (ITAM) in its associated γ-chain. These signals activate platelets which leads to the activation of integrins such as the collagen binding α2β1 integrin and so the firm adhesion of the platelets to the damaged vessel wall (Nieswandt et al., 2011b).

Step 3 - Platelet spreading

Following firm adhesion the activated platelets change shape through cytoskeletal rearrangements that result in their spreading across the vessel wall. This spreading phase increases the amount of adhesion between the platelets and the vessel wall and also leads to the formation of actin stress fibres within the spread platelets, both of which are required for stable thrombus formation (Aslan and McCarty, 2013).

Step 4 - Platelet secretion

In addition to spreading, platelets also release the contents of specialised organelles called α granules and dense granules. α granules contain large proteins such as fibrinogen, vWF and P-selectin, proteins which provide a framework around which a thrombus can develop (Jackson et al., 2003). Dense granules contain smaller, often signalling, molecules many of which act as secondary mediators that act to positively reinforce platelet activation in both paracrine and autocrine fashions. One of the most important of these secondary mediators is ADP which binds to its receptors on platelets and synergises with other activatory signals. As well as the secreted ADP another important second secondary mediator of platelet activation, thromboxane A_2 is released by platelets. Not stored in the dense granules but generated in activated platelets from arachidonic acid in the cell membrane thromboxane A_2 also has a receptor on platelets and also synergises with other activatory signals including ADP.

Step 5 - Platelet aggregation and thrombus formation

More platelets are recruited to the damaged site via the vWF secreted by endothelial cells and bound platelets and are activated by the secreted agonists ADP and thromboxane A_2. This growing accumulation of activated platelets become linked together (or aggregated) by the binding of fibrinogen and vWF by the activated αIIbβ3 integrins (Stegner and Nieswandt, 2011). This function of αIIbβ3 is essential to haemostasis, as loss of this protein results in the rare disorder Glanzmann's thrombasthenia. Unable to bind fibrinogen or tightly bind vWF upon activation, the platelets of patients with Glanzmann's thrombasthenia are unable to aggregate and maintain a stable thrombus resulting in severe bleeding (Stegner and Nieswandt, 2011). The mass of aggregated platelets provides a pro-coagulant surface for the

coagulation cascade for thrombin generation. This procoagulent surface is generated by the flipping of negatively charged lipids from the inner leaflet of the platelet plasma membrane to the outer leaflet. Once flipped these lipids support the formation of the enzyme complex factor Xa and its subsequent cleavage of pro-thrombin to form activated thrombin. This step crucial to haemostasis as thrombin cleaves fibrinogen to form the fibrin mesh which stabilises the thrombus. Thrombin is also a powerful platelet agonist (Furie and Furie, 2006), as will be discussed later.

Step 6 - Clot retraction

The thrombus created by platelet aggregation and coagulation cascade activation is further stabilised by a processes called clot retraction. During this process actin stress fibres in the activated platelets contract, and as the αIIbβ3 integrins are attached to the actin cytoskeleton this puts tension through the fibrin mesh and causes the thrombus to shrink substantially (Stegner and Nieswandt, 2011). This process prevents the thrombus from being degraded or damaged by blood flow before the endothelium has had chance to repair the damaged vessel. In addition, secreted factors in the platelet releasate promote the repair of damaged vessels and also recruit leukocytes to areas of inflammation (Nurden, 2011).

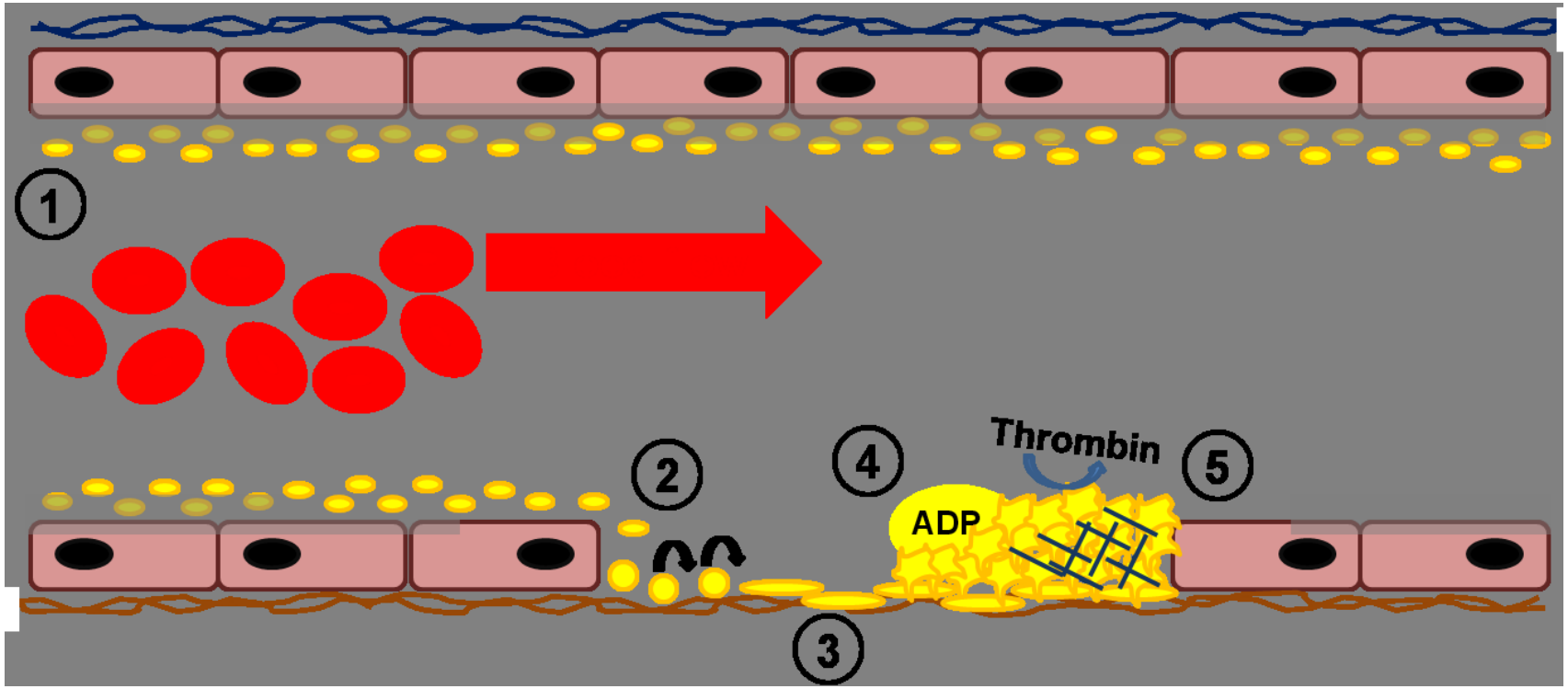

Red blood cell

Platelet

Endothelial cell

Sub endothelial matrix

Fibrin

Nitric oxide

Figure 6. Platelets play a crucial role in thrombus formation.

The primary role of platelets is in haemostasis. The diagram depicts the main phases of thrombus formation mediated by platelets.

1. Due to the size difference between platelets and red blood cells the platelets are marginalised and are concentrated at the vessel walls. Here they are continuously exposed to nitric oxide released from the intact endothelium. This keeps the platelets in a quiescent state.

2. In a phase of thrombus formation called platelet tethering platelets bind vWF factor immobilised on exposed collagen via GPIb. This interaction has a fast off rate resulting in the rolling of platelets across the damaged area of the vessel. This slows the recruited platelets down and allows an interaction between the low affinity collagen receptor GPVI and collagen. GPVI signalling causes platelet activation and the platelets become stably adhered to the matrix.

3. The activated platelets spread across the matrix and release the contents of their dense and alpha granules. Further platelets are recruited to the growing thrombus and are activated by the secreted ADP (and Thromboxane A_2).

4. The platelets become bridged or aggregated together via their activated αIIbβ3 integrin and the secreted fibrinogen. This growing thrombus provides a pro-coagulant surface for thrombin generation by the coagulation cascade. Thrombin both activates platelets and cleaves fibrinogen to form fibrin. The created fibrin mesh is bound by platelet αIIbβ3 integrin and aids thrombus stability.

5. To prevent the thrombus from breaking down before the endothelium has healed the thrombus is retracted by tension put through the fibrin mesh by the platelet cytoskeleton.

1.2.4 Platelet activatory signalling

The signalling events that take place during thrombus formation are generally well understood, with many of the major signalling receptors and their effector molecules already studied using knockout mouse models and tailored inhibitors. The major platelet activatory signalling pathways are discussed below.

1.2.4.1 GPVI

The immunoglobulin superfamily receptor GPVI is expressed on the platelet cell surface, at around 4000 - 6000 copies per platelet, constitutively associated with the FcR γ-chain. This receptor binds collagen (its physiological ligand) at its recurring GPO motifs as a dimer and, though a point for debate, is thought to exist on the platelet surface as a mixture of monomers and dimers (Clemetson, 2012). GPVI also binds the synthetic ligand collagen-related peptide (which is a series of GPO repeats) and the snake venom toxin convulxin. The ITAM motif YXXL/I$_{6\text{-}12}$YXXL/I, in the tail of the GPVI associated γ-chain, becomes phosphorylated by the Src-family kinases Lyn and Fyn upon ligand binding. This phosphorylation leads to the binding of spleen tyrosine kinase (Syk) to the ITAM via its SH2 domains. The recruitment of Syk to the receptor leads to the phosphorylation of a protein called LAT (as well as others) around which a number of adapter and effector proteins form a signalosome (Dutting et al., 2012). The formation of this signalosome ultimately leads to the activation of phospholipase C γ2 (PLCγ2) and the subsequent release of Ca^{2+} from the intracellular stores and the activation of protein kinase C (PKC). Both Ca^{2+} signalling and PKC lead to the inside-out activation of integrins, cytoskeletal rearrangements and granule secretion seen in platelet activation. This signalling cascade allows GPVI

to powerfully activate platelets despite being regarded as having low affinity for its ligand (Dutting et al., 2012).

Despite this clearly important role in platelet function, patients with a loss of GPVI due to autoantibodies or gene mutation only present with mild bleeding disorders (Arthur et al., 2007, Dumont et al., 2009, Hermans et al., 2009). This was also the case for GPVI knockout mouse models which only had moderate bleeding in tail bleeding assays (Kato et al., 2003, Lockyer et al., 2006, Bender et al., 2011, Nieswandt et al., 2000, Nieswandt et al., 2001). A more essential role emerged for GPVI when thrombus formation in arteries was assessed, using intravital microscopy in the various GPVI knockout mouse models, and in infarct size after reperfusion injury in the brain (Massberg et al., 2003, Kleinschnitz et al., 2007). As the loss of GPVI does not cause severe bleeding there is the potential that GPVI may be a good drug target in patients at high risk of heart attack or stroke.

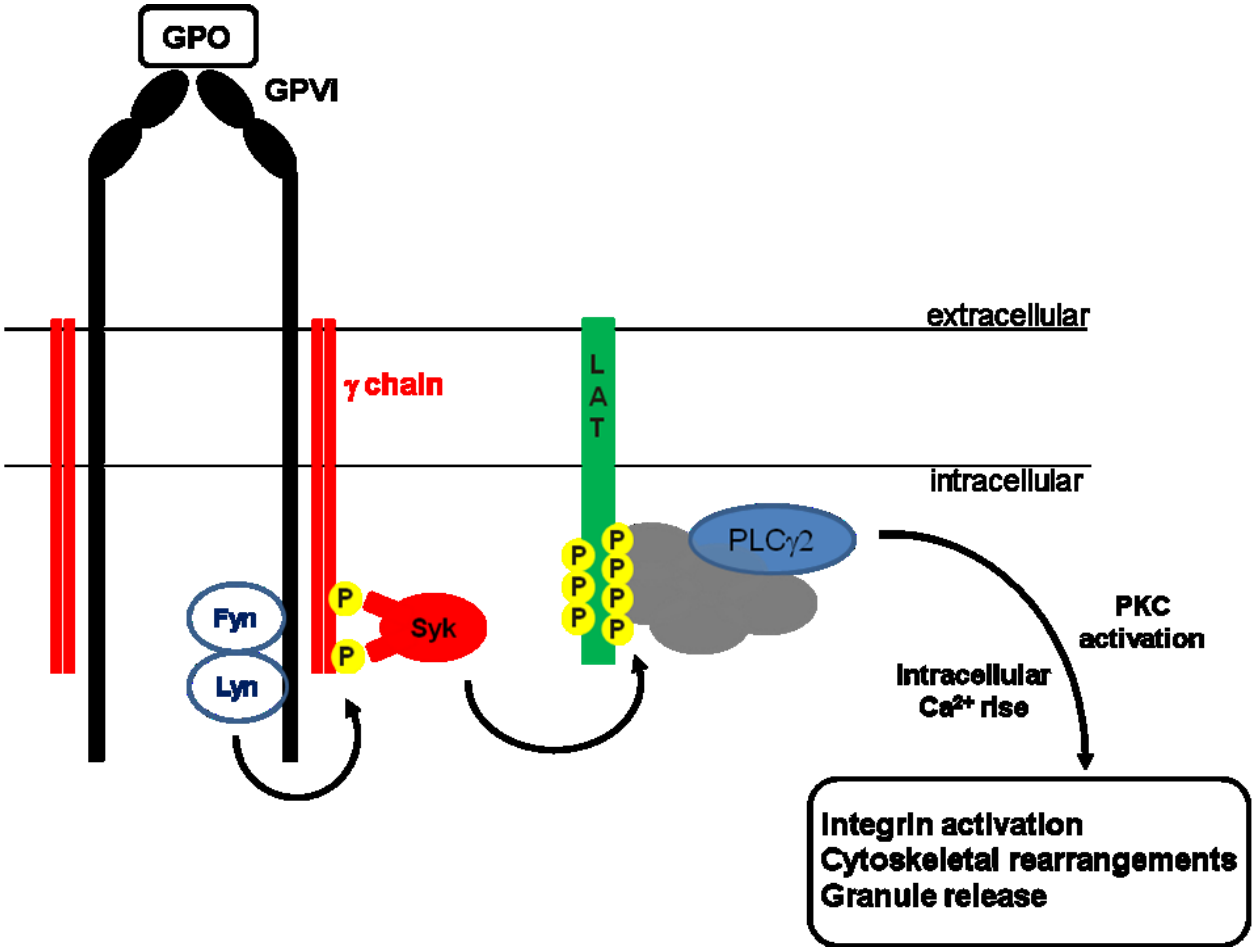

Figure 7. Simplified diagram of GPVI signalling and signalosome formation.

GPVI signalling is initiated by the binding of collagen by GPVI dimers at GPO motifs. This causes the phosphorylation of the associated γ-chain at its ITAM motif by the Src family kinases Fyn and Lyn. Syk binds the phosphorylated tyrosines in the ITAM motif via its tandem SH2 domains. The recruitment of Syk to GPVI leads to the formation of a downstream signalosome which contains a large number of adapter proteins and kinases centred around phosphorylated LAT. One outcome of signalosome formation is the activation of PLCγ2 and the subsequent increase in intracellular Ca^{2+} and PKC activation. This leads to integrin activation, cytoskeletal rearrangements and platelet granule release. This diagram shows a much simplified sequence of events and was modified from Dutting et al. (2012) .

1.2.4.2 αIIbβ3 integrins

The major platelet integrin αIIbβ3 is the most highly expressed platelet membrane protein; with ~ 80000 copies per platelet this protein is thought to make up 15 % of the molecules on the platelet cell surface. Once activated by inside-out signalling this integrin plays a major role in the physical aggregation of platelets and contributes to platelet activation and thrombus formation through outside-in signalling. Once bound to its ligands, fibrinogen or vWF forming the bridges that hold the platelets and the thrombus together, changes in the intracellular tail of the β_3 subunit leads to the activation of the Src family kinases with which it is associated (Stegner and Nieswandt, 2011). This conformational change in the integrin and the activation of Src family kinases was thought to lead to the recruitment of Syk to the integrin tail. Recent work from the Newman group has also suggested that $\alpha_{II}\beta_3$ activates Syk indirectly, though Syk binding to an ITAM within another platelet receptor FcγRIIA, which is proposed to interact with the integrin (Zhi et al., 2013). In either case similar to ITAM signalling this recruitment of Syk initiates a signalling cascade that finally converges on the activation of PKC isoforms and Ca^{2+} oscillations. Downstream of $\alpha_{II}\beta_3$ this signalling pathway results in the activation of myosin light chain which is key in platelet shape change and actin stress fibre formation (Versteeg et al., 2013).

1.2.4.3 ADP and Thromboxane A_2

ADP and thromboxane A_2 released during platelet activation bind to their G protein-coupled receptors in an autocrine (and paracrine) fashion. A diagram of a simplified signalling pathway downstream of these receptors can be seen in Figure 8. ADP binds to both $P2Y_1$ and $P2Y_{12}$ which synergise and produce a powerful activatory signal in platelets (Nieswandt et al., 2011b). These receptors couple to $G\alpha_q$ and $G\alpha_i$,

G proteins which activate PLCβ and inhibit cAMP formation, respectively. PLCβ leads to the formation of the secondary messengers diacylglycerol and IP_3 which lead to PKC activation and increases in intracellular Ca^{2+} respectively and subsequent decreases in inhibitory cAMP levels (Cunningham et al., 2013). The thromboxane receptor, TP, also couples to $G\alpha_q$ and additionally $G\alpha_{12/13}$ which activates Rho/Rho kinase signalling. Together these signalling pathways stimulate cytoskeletal rearrangements, actin stress fibre formation and feed into the other platelet signalling pathways that also converge on intracellular Ca^{2+} increases and PKC activation, thus creating a positive activatory feedback system (Smolenski, 2012). The importance of these two secondary mediators is evidenced by the efficacy of the antiplatelet drugs aspirin and clopidogrel in preventing thrombosis after stent placement in atherosclerosis patients. Aspirin prevents thromboxane A_2 production by platelets by irreversibly inhibiting cycloxygenase enzymes. Clopidogrel is also an irreversible inhibitor but it targets the ADP receptor $P2Y_{12}$ (Smolenski, 2012).

1.2.4.4 Thrombin

Thrombin (or Factor IIa) is generated by the coagulation cascade from prothrombin (or Factor II) and activates human platelets by the protease activated receptors (PAR) PAR1 and PAR4 (Versteeg et al., 2013). These receptors are activated by the cleavage of their extracellular N-terminal tail by thrombin, which exposes a tethered ligand in this domain. These G-protein coupled receptors also couple to the $G\alpha_q$ and $G\alpha_{12/13}$ proteins, like the TP receptor, and so signalling after receptor activation also feeds into the PKC activatory pathways (Figure 8). Thrombin is viewed as a highly potent platelet agonist which plays a key role in thrombus formation (Stegner and Nieswandt, 2011).

1.2.4.5 CLEC-2

CLEC-2 is a recently discovered single transmembrane activatory receptor in platelets and its role in thrombus formation currently remains unclear (Stegner and Nieswandt, 2011). It is the only so-called hemITAM receptor on platelets, with a YXXL motif in its intracellular tail, and intriguingly its only know endogenous ligand, podoplanin, is expressed on lymphatic endothelium, and not in the vasculature (Suzuki-Inoue et al., 2011). Knockout mouse models for this receptor display impairment in thrombus formation in arterial environments suggesting however that it does have some unknown role to play in haemostasis (Nieswandt et al., 2011b). Despite its unknown role on platelets in haemostasis the signalling downstream of this receptor has been revealed using clustering antibodies and the snake venom toxin rhodocytin which binds CLEC-2. Similar to GPVI, clustering of CLEC-2 causes phosphorylation of its hemITAM by Src family kinases and subsequent recruitment of Syk and signalosome formation (Stegner and Nieswandt, 2011). Knockout mice for

CLEC-2, and indeed Syk or podoplanin, result in a defect in the separation of the lymphatic and blood vessels. This defect has been shown to critically involve platelets in a previously unknown role in development (Suzuki-Inoue et al., 2011).

Recent work using the GPVI and CLEC-2 double knockout platelets and mice has highlighted a previously unappreciated functional redundancy between these two ITAM/hemITAM bearing receptors. Platelets deficient in both GPVI and CLEC-2 displayed much more profound defects in haemostasis than seen in the single knockouts for either of these proteins. The mechanism by which this redundancy occurs is currently unknown and represents a new emerging role of platelet ITAM signalling in haemostasis (Boulaftali et al., 2013, Bender et al., 2013).

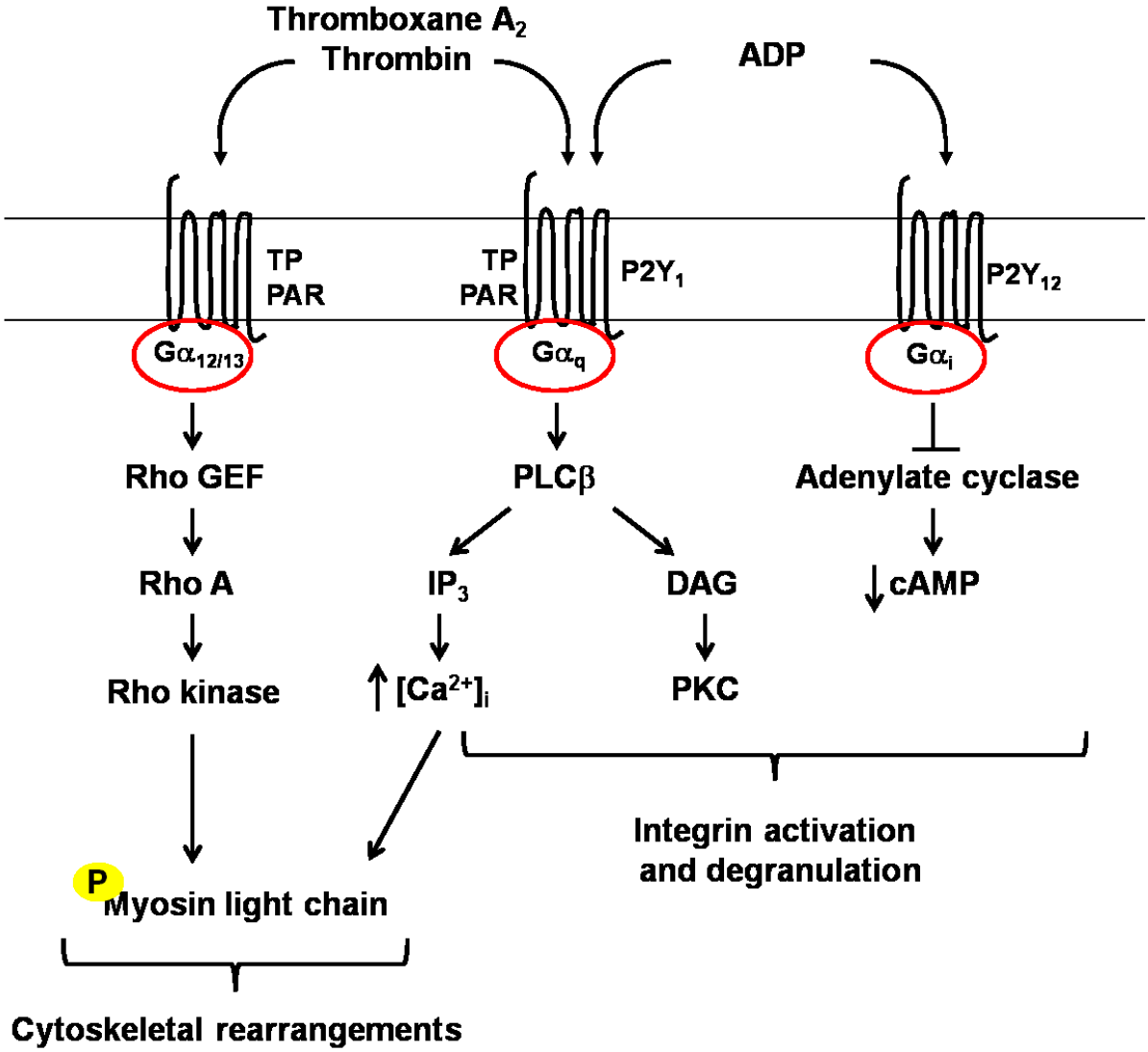

Figure 8. Simplified diagram of GPCR signalling in platelets.

This diagram shows the much simplified signalling cascades downstream of the platelet agonists ADP, thromboxane A_2 and thrombin. Signalling through their respective G protein-coupled receptors, these platelet agonists cause cytoskeletal rearrangements downstream of myosin light chain phosphorylation and the decrease of cAMP levels and PKC activation which leads to integrin activation and degranulation. In this way ADP and thromboxane A_2 positively feedback on platelet activation and thrombin powerfully activates platelets. This diagram was modified from Offermanns (2006).

1.2.5 Platelet inhibitory signalling

As demonstrated by the severe results of pathological platelet activation, it is essential that platelets are kept quiescent in healthy and undamaged vessels. The two best understood mechanisms for this are the release of nitric oxide and prostacyclin from the intact vessel endothelium. Nitric oxide, a membrane-permeable gas, is generated in endothelial cells by nitric oxide synthase (Busse and Mulsch, 1990). This gas activates guanylyl cyclase in platelets leading to the accumulation of cyclic guanosine monophosphate (cGMP). This accumulation of cGMP leads to the activation of cGMP-dependent protein kinase (cGK) type I which phosphorylates many targets that prevent the release of Ca^{2+} from intracellular stores, and inhibits integrin activation and cytoskeletal rearrangements. Additionally a rise in cGMP inhibits phosphdiesterase 3A which results in a rise in cAMP levels (Gresele et al., 2011). Prostacyclin is produced in endothelial cells by prostacyclin synthase and is bound by the IP receptor on platelets. This GPCR is coupled to $G\alpha_5$ which activates adenylate cyclase and leads to an accumulation of cyclic adenosine monophosphate (cAMP) inside platelets. Similar to the inhibitory mechanism of nitric oxide, this rise in cAMP levels activates a kinase (protein kinase A [PKA]), the targets of which inhibit integrin activation, cytoskeletal rearrangements, granule release and increase in intracellular Ca^{2+} levels (Smolenski, 2012).

1.3 Project background and aims

Both Tspan9 and Tspan33 have recently been identified on platelets but little is known about their function. Tspan9 was discovered by our group in a SAGE library of mouse megakaryocyte mRNA and a platelet proteomic study (Senis et al., 2007) and subsequently found to be relatively platelet specific in comparison to other mouse tissues (Protty et al., 2009). Tspan9 was also identified as the second most abundantly expressed tetraspanin after the highly expressed CD9 in another proteomic study of the platelet cell surface (Lewandrowski et al., 2009b). Since the publication of Tspan9 as a human and mouse platelet tetraspanin, our lab has generated a Tspan9 knockout mouse. Tspan33 was also identified as a probable platelet tetraspanin through its presence in the mouse megakaryocyte mRNA SAGE library and in human platelets by proteomics (Lewandrowski et al., 2009b, Senis et al., 2007). Tspan33 has already been identified as an important regulatory factor in erythropoiesis in a knockout mouse study and this mouse is available to us to study their platelets.

The aim of this project is to functionally characterise both Tspan9- and Tspan33-deficient platelets using their knockout mice and to identify their protein partners on the platelet cell surface. By analysing their knockout platelet phenotypes and identifying their partner proteins it is hoped that we may discover how these tetraspanins function on platelets and identify new regulatory mechanisms for important platelet proteins. This could lead to the identification of new anti-platelet drug targets.

CHAPTER II: MATERIALS AND METHODS

2.1 Antibodies and reagents

Agonists, antagonists and antibodies used are listed in Tables 3, 4 and 5, respectively. Antibodies were used at 1 μg per immunoprecipitation, 1 μg/ml for western blotting and 10 μg/ml for flow cytometry and microscopy unless otherwise indicated by the manufacturer's protocol. Cell culture reagents were from PAA laboratories (Somerset, UK) unless otherwise stated.

Table 3. Agonists

Agonist	Source
Thrombin	Sigma
PAR4 peptide (AYPGKF)	Dr. Richard Farndale (Cambridge University, UK)
Arachadonic acid	Cayman Chemical (Cambridge Bioscience Ltd., UK)
Collagen (HORM)	Nycomed Austria (Linz, Austria)
Collagen related peptide	Dr. Richard Farndale (Cambridge University, UK)
CLEC-2 antibody	Dr. Steve Watson (University of Birmingham, UK)
ADP	Sigma

Table 4. Antagonists

Antagonist		Source
Indomethacin		Sigma
Apyrase		Sigma
Prostacyclin		Sigma
Lotrafiban		Dr. Steve Watson

Table 5. Antibodies

Antibody	Host species	Source
mouse αIIb FITC	Rat	Emfret Analytics (Wurzburg, Germany)
mouse α2 FITC	Rat	Emfret Analytics
mouse α6 FITC	Rat	Emfret Analytics
mouse GPVI FITC	Rat	Emfret Analytics
mouse GPIb FITC	Rat	Emfret Analytics
mouse CD9 FITC	Rat	Emfret Analytics
mouse ADAM10 FITC	Rat	R&D Systems (Minnesota, USA)
mouse CLEC-2 FITC	Rat	Dr. Steve Watson
rat IgG_{2a} FITC	Rat	AbD Serotec (Oxford, UK)
mouse Gr-1 FITC	Rat	eBioscience (Hatfield, UK)
mouse B220 FITC	Rat	eBioscience
mouse Ter119 FITC	Rat	eBioscience
mouse c-kit FITC	Rat	eBioscience
mouse CD71 FITC	Rat	Becton Dickinson (California, USA)
mouse CD45 FITC	Rat	eBioscience
mouse CD16/32	Rat	BD Pharmingen (Oxford, UK)
mouse P-selectin FITC	Rat	BD Bioscience (Oxford, UK)
mouse IgG1 (MOPC)	Mouse	Sigma (Poole, UK)
human GPVI FITC (3J24)	Mouse	Dr. Jandrot-Perrus (Inserm U698, Paris, France)
human GPVI dimer FITC (9E18)	Mouse	Dr. Jandrot-Perrus
human/mouse Tspan9	Rabbit	Dr. Mike Tomlinson
human/mouse Tubulin (DM1A)	Mouse	Sigma
phosphotyrosine (4G10)	Mouse	Millipore
mouse CD9	Rat	Emfret Analytics
human GPVI (HY101)	Mouse	Dr. Pete Smethurst (Cambridge, UK)
mouse GPVI F(ab)[1]	Rat	Emfret Analytics
mouse CD9 F(ab)[1]	Rat	Emfret Analytics

2.2 Mice

Tspan9 knockout mice were generated from C57BL/6 mouse embryonic stem cells containing a genetrap vector (clone IST11668F5) between the first two exons of the Tspan9 gene at the Texas Institute for Genomic Medicine, Houston, Texas, USA. Rederivation of original mice onto clean BL/6 mice was performed at the Biomedical Services Unit at the University of Birmingham, UK and subsequent animals were produced through heterozygous x heterozygous mating to allow the use of litter matched control mice. The Tspan33 knockout mice were kindly provided by Dr. Schickwann Tsai (Salt Lake City, Utah) and are fully described in Heikens et al. (2007). These mice were also rederived onto clean BL/6 mice at the Biomedical Services Unit. GPVI knockout mice were kindly provided by Dr. Steve Watson (University of Birmingham, UK) and were originally described in Cheli et al. (2008a). GPVI heterozygote Tspan9 knockout ($GPVI^{+/-}$ $Tspan9^{-/-}$) mice were generated by crossing $Tspan9^{-/-}$ mice with $GPVI^{-/-}$ mice followed by a cross between the F1 generation of this cross with either $Tspan9^{+/+}$ or $Tspan9^{-/-}$ mice. Litter matched controls were not available for this strain. Mice were aged at least 8 weeks before use in experiments. All mice were bred and used in the Biomedical Services Unit, a designated site for animal use at the University of Birmingham, UK. All animal work was performed in accordance with the Animals (Scientific Procedures) Act 1986.

2.3 Platelet preparation

2.3.1 Human platelet preparation

Blood was drawn from the veins in the antecubital fossa using a 23 gauge butterfly needle and syringe. Blood was drawn into 10 % sodium citrate as anti-coagulant on the day of experiment. After collection, another anti-coagulant, 10 % acid citrate dextrose (ACD 120 mM sodium citrate, 110 mM glucose, 80 mM citric acid), was added to the blood. Platelet rich plasma (PRP) was collected after spinning anti-coagulated blood at 200 x g in a swing out centrifuge for 20 min. Platelets were sedimented by spinning platelet rich plasma at 1000 x g for 10 min in a swing out centrifuge after the addition of prostacyclin (10 μg/ml) to prevent platelet activation. Pelleted platelets were resuspended in modified Tyrode's buffer (134 mM NaCl, 0.34 mM Na_2HPO_4, 2.9 mM KCl, 12 mM $NaHCO_3$, 20mM HEPES, 5 mM glucose, 1 mM $MgCl_2$, pH 7.3) to a final concentration of 5 x 10^8 - 1 x 10^9 for biochemistry experiments. Platelets were allowed to rest for 30 min after resuspension before use. This method was previously described in McCarty et al. (2006).

2.3.2 Mouse platelet preparation

Blood was drawn from the exposed descending aorta of mice, terminally anaesthetised with isoflurane, using a 23 gauge needle and syringe. Blood was drawn into 10 % ACD for washed platelets (Séverin et al., 2012), 10 % sodium citrate for PRP or 40 μM D-phenylalanyl-L-prolyl-L-arginine chloromethyl ketone (PPACK) and 5 U/ml Heparin for *in vitro* flow studies (Auger et al., 2005) and then immediately mixed with 200 μl of modified Tyrode's buffer. Anti-coagulated blood was first spun for 5 min at 425 x g in a bench top microfuge and the plasma and top third of partially separated red blood cells collected. Collected pre-spun blood was then spun at 200 x

g for 6 min in a swing out centrifuge to better sediment red blood cells. Plasma collected after the second spin was set aside and the remaining sample spun again at 200 x g for 6 min. Remaining plasma and platelet layer were collected from the sedimented red blood cells and pooled forming the PRP. For washed platelets 10 μg/ml of prostacyclin was added to the PRP which was then spun for 6 min at 1000 x g. Extracted platelets were resuspend in modified Tyrode's buffer and concentration adjusted to 2 x 10^8/ml for aggregation, 2 x 10^7/ml for spreading assays, 5 x 10^8/ml for biotinylation and 5 x 10^8 - 1 x 10^9 for other biochemistry experiments. Washed platelets were allowed to rest for 30 min before use (Hughes et al., 2008).

2.4 Primary cell isolation

2.4.1 Megakaryocyte isolation from adult mouse bone marrow

Bone marrow was flushed from both femora and tibiae (previously stripped of all other tissue and sterilised with 70 % ethanol) of adult mice using approximately 10 ml of ice cold Dulbecco's modified eagle medium (DMEM) complete with 10 % foetal bovine serum (FBS), glutamine (20 mM) and the antibiotics penicillin (100 U/ml) and streptomycin (100 μg/ml) and a 25 gauge needle. Collected bone marrow was spun for 5 min at 300 x g in a swing out centrifuge and the pellet resuspended in 6 ml of ammonium-chloride-potassium (ACK) buffer (0.15 M NH_4Cl, 1 mM $KHCO_3$, 0.1 mM Na_2EDTA, pH 7.3) and left to incubate at room temperature for 5 min to allow red blood cell lysis. The ACK cell suspension was filtered through a sterile 70 μm nylon mesh filter and spun at 300 x g for 5 min at 4 °C in a swing out centrifuge. The cell pellet was resuspended in 1 ml complete DMEM media and incubated with the following antibodies for 30 min on ice: anti-Gr1, anti-B220 and anti-CD16/32. After incubation 1 ml of complete DMEM was added to the cells which were then spun down at 300 x g for 5 min at 4 °C. The cell pellet was resuspended in 1 ml complete DMEM containing 2 x 10^7 anti-rat magnetic Dynal beads (Dynabeads, Invitrogen, UK), which had been previously washed 3 times in complete DMEM. Antibody stained cells containing the anti-rat magnetic beads were spun down at 300 x g for 5 min at 4 °C and then resuspended without a change in media. This step was repeated and then a magnet used to pull down the Dynal beads. After the bead pull down step the supernatant was removed into a fresh tube. The pulled-down beads were then resuspended in 500 μl of complete DMEM then again pulled down using the magnet. Remaining supernatant was pooled with previous and the beads

discarded. The supernatants were spun down at 300 x g for 5 min at 22 °C. The cell pellet was resuspended in 1.5 ml complete StemPro media (StemPro-34 serum free media plus provided nutrient supplement (Invitrogen), 20 mM glutamine and the antibiotics penicillin (100 U/ml) and streptomycin (100 μg/ml)) containing 20 ng/ml of mouse stem cell factor (PeproTech, London, UK). Cells were incubated for 48 hr at 37 °C with 5 % CO_2. After this time cells remaining in suspension were collected and spun at 300 x g for 5 min at 22 °C and cell pellets were resuspended in 1.5 ml complete StemPro media containing 20 ng/ml stem cell factor and 50 ng/ml mouse thrombopoietin (PeproTech). After a further 3 - 4 days incubation at 37 °C with 5 % CO_2 cells were separated over a BSA gradient (4 ml of 3 % BSA with 4 ml 1.5 % BSA on top) for 45 min. Cells still in the top 8 - 10 ml after 45 min were spun down at 300 x g for 5 min at 22 °C and resuspended in 1.5 ml complete StemPro media containing 20 ng/ml stem cell factor and 50 ng/ml mouse thrombopoietin to continue differentiation. Cells collected in the bottom 2 ml were an enriched population of mature megakaryocytes and ready for further experiments. This method was taken from the method previously published in Dumon et al. (2006).

2.4.2 Erythroblast isolation from adult mouse bone marrow and spleen

This method was taken from Vegiopoulos et al. (2006). Bone marrow wash flushed from the hind legs of adult wildtype and Tspan33 knockout mice in the same way as for megakaryocyte isolation and then collected bone marrow was spun for 5 min at 300 x g in a swing out centrifuge. Cells were resuspended in 100 μl of complete DMEM media and were then ready to undergo antibody staining for flow cytometry and cell sorting. Spleens from adult wildtype and Tspan33 knockout mice were cleaned of any contaminating soft or connective tissue and then placed in 1 ml of

complete DMEM in dishes on ice. Cells were released from the whole spleens by pecking at the tissue using fine tipped curved tweezers. Media around the 'pecked' spleen was collected and spun for 5 min at 300 x g in a swing out centrifuge. Cells were resuspended in 100 μl of complete media and were then ready to undergo antibody staining for flow cytometry.

2.4.3 Erythroblast *in vitro* differentiation and maturation from foetal liver cells

This method was taken from Dolznig et al. (2001). Tspan33 heterozygous mice were timed mated and resulting pregnant females schedule 1 culled by cervical dislocation at estimated day 14.5 gestation. The womb was dissected from the females and placed in a sterile tissue culture hood. Embryos were dissected out of the womb and tail tips taken for genotyping. Livers were dissected from the embryos into 1 ml of sterile PBS. Single cell suspensions were created by pipetting up and down. Cells were spun down at 200 x g for 5 min in a swing out centrifuge and cell pellets resuspended in ACK buffer to lyse red blood cells. After red cell lysis 1 ml of PBS was added to the cells which were then spun down at 200 x g for 5 min. Cells were resuspended in 1 ml complete erythro-StemPro-34 media (StemPro-34 serum free media plus provided nutrient supplement, 2 mM L-glutamine, 50 U/ml penicillin, 50 ng/ml streptomycin, 100 ng/ml murine stem cell factor, 1 μM dexamethasone (Sigma) and 2 U/ml human recombinant erythropoietin (Roche, West Sussex, UK)) in 12 well tissue culture plates. After 1 day incubation at 37 °C with 5 % CO_2 an additional 1 ml of StemPro-34 media was added to each well. On Day 2 of culture, without disturbing the cell layer in the bottom of the well, the top 1 ml of media was removed from each well, the cells were then resuspended in the remaining 1 ml of media and transferred into a 6-well tissue culture plate and an additional 2 ml of media added to each well.

Cells were fed with 1.5 ml complete erythro-StemPro-34 media (after removal of top 1.5 ml media in each well) for 8 days. On day 9 cells were resuspended in the 3 ml of media in the well and spun down at 200 x g for 5 min in a swing out centrifuge, resuspended in 3 ml sterile PBS then spun down again. The washed cell pellet was resuspended in 2 ml of sterile PBS and layered on top of 2 ml of Ficoll-Paque PLUS (GE Healthcare, Buckinghamshire, UK). Layered cells were spun at 1100 x g for 5 min at room temperature in a swing out centrifuge. The PBS cell layer and the Ficoll layer were collected from on top of the cell pellet and re-layered, Ficoll then cells. The re-layered cells were then spun at 200 x g for 5 min at 4 °C . The pelleted cells were resuspended in 1 ml PBS then spun down at 200 x g for 5 min. The cells were resuspended to a final concentration of 2 - 3 x 10^6/ml in complete erythro-StemPro-34 media and were ready for cell sorting after 2 further days at 37 °C with 5 % CO_2.

2.5 Platelet function testing

2.5.1 Whole blood counting

60 µl of anti-coagulated mouse whole blood was run through a Pentra 60 whole blood counting machine from ABX Diagnostics (London, UK), which had been previously calibrated for mouse blood. All cell count readings were normalised for the added volume of ACD and modified Tyrode's buffer to the blood.

2.5.2 Tail bleeding

Mice aged between 8 and 12 weeks were anaesthetised with isoflurane and administered 0.05 mg/kg of the analgesic buprenorphine by subcutaneous injection. Whilst under continued isoflurane anaesthesia 2 mm or 3 mm of tail tip was removed using a razor blade. Resulting blood drops were collected into pre-weighed Eppendorf tubes. Each drop of blood was estimated to be 30 µl. The mice were allowed to bleed for either 20 min, until maximum blood loss (15 %, as estimated by weight) was reached or until bleeding ceased (judged as no blood fall for 5 min). Cauterisation of the wound ended the procedure. Collected blood was weighed to assess blood loss in mg and was normalised for animal weight variations. This method was taken from the method previously published in Mazharian et al. (2012).

2.5.3 Light transmission lumi-aggregometry

Aggregation of mouse platelets was measured in a Born lumi-aggregometer (model 460VS; Chronolog, Labmedics, Manchester, UK). Samples were warmed to 37 °C for 1 min with no stirring, then stirred at 37 °C for a further min before agonist addition. Light transmission through the platelet sample was measured against a sample of modified Tyrode's buffer and concomitantly recorded on a chart recorder (Chronolog,

Labmedics, Manchester, UK). Platelet responses were measured for at least 4 min after agonist addition (Suzuki-Inoue et al., 2003, Dawood et al., 2007).

2.5.4 ATP secretion measurement

Adenosine triphosphate (ATP) secretion was assessed at the same time as platelet aggregation in the aggregometer and recorded using the same chart recorder as for the aggregation responses. During the 1 min 37 °C incubation with no stirring a premix of luciferin and luciferase was added to the platelet sample (Chronolog, Labmedics, Manchester, UK). This allowed ATP secreted from activated platelets to be measured indirectly by the release of light from the reaction catalysed by the luciferase enzyme. Each test was calibrated by the addition of 2 nmol of ATP at the end of each aggregation. Maximal ATP released from the platelets was measured (Dawood et al., 2007, Suzuki-Inoue et al., 2003)

2.5.5 P-selectin exposure and fibrinogen binding

Whole blood samples that had been collected into ACD were diluted 1:10 with modified Tyrode's buffer. Diluted blood was incubated at 37 °C in a water bath for 5 min and were then stimulated for 5 min with either 10 μg/ml of collagen-related peptide or 500 μM PAR4 peptide. Stimulated samples were incubated with either anti-mouse P-selectin antibody or fibrinogen, both conjugated to FITC, for 30 min. After staining samples were diluted 1:10 with modified Tyrode's buffer and then analysed using a FACScalibur flow cytometer (BD Biosciences, Oxford, UK), with platelet specific staining being isolated by gating on size. Geometric mean fluorescent intensities were used to measure P-selectin surface expression or the amount of FITC-fibrinogen bound by the platelets. Method taken from Manne et al. (2013).

2.5.6 Platelet stimulations to generate samples for biochemical analyses

For stimulation experiments mouse platelets at 5 x 10^8/ml were incubated for 5 min at 37 °C with 10 μM lotrafiban, to prevent platelet aggregation, and indomethacin (10 μM) and apyrase (2 U/ml) to block signalling caused by Thromboxane A2 and ADP. After inhibitor incubation platelets were stimulated with 10 μg/ml of CRP and samples taken at 10, 20, 30, 60 and 300 s after stimulation. Time course samples were directly lysed in an equal volume of 2x reducing Laemmli buffer (20 % glycerol, 10 % β-mercaptoethanol, 4 % SDS, 50 mM Tris, 0.004 % Brilliant Blue R). Method described previously in Hughes et al. (2008).

2.5.7 *In vitro* flow adhesion

The Bioflux 200 microfluidic flow system (Labtech, Sussex, UK) was used to perfuse whole blood through collagen coated microcapillaries. Microcappillaries in 0 – 200 dyne glass bottomed 24 well plates were coated with collagen (30 μg/ml) (5 dyne for ~ 30 s followed by gravity flow) overnight at 4 °C. After washing with Tyrode's buffer the coated capillaries were blocked with 5 mg/ml of denatured and filtered fatty acid free bovine serum albumin (10 dyne for 5 min followed by gravity flow) for 1 hr at room temperature. After blocking, capillaries were again washed with Tyrode's buffer and kept in Tyrode's until use. Whole blood was incubated with 0.2 μM $DiOC_6$ membrane dye (Molecular Probes, Oregen, US) for 5 min at 37 °C then flowed over the prepared capillaries at 300 or 1000 s^{-1} for 4 and 8 min respectively. The flow experiment was imaged using fluorescence video microscopy using a 40X Plan APO 1.4 NA oil immersion DIC objective with a TE2000 (Nikon) microscope with Digital Sight DS-Qi1MC camera (Nikon) using NIS elements AR software (Nikon). Images were taken every 2 s. Images were analysed using the thresholding function of

ImageJ software to allow automated detection of the surface area covered by platelet aggregates in each field of view. This method was developed with support from LabTech.

2.6 Protein biochemistry

2.6.1 Biotinylation and immunoprecipitation of blood cells

Washed platelets at 5 x 10^8 – 1 x 10^9/ml and red blood cells at 5 x 10^8/ml washed in Tyrode's buffer were incubated with 1 mg/ml of EZ link Sulpho NHS LC Biotin (Thermo Fisher Scientific, IL, USA) for 30 min at room temperature with gentle rocking to ensure good mixing. The reaction was quenched with 100 mM glycine. Biotinylated cells were then spun down at 1000 x g for 6 min in a swing out centrifuge (10 μg/ml prostacyclin was added to platelets) and then resuspended in either 1 % Brij97 lysis buffer (1 % Brij97, 10 mM Tris pH 7.5, 150 mM NaCl, 1 mM $CaCl_2$, 1 mM $MgCl_2$, 0.01 % NaN_3), 1 % Triton X-100 lysis buffer (1 % Triton X-100, 10 mM Tris pH 7.5, 150 mM NaCl, 1 mM EDTA, 0.01 % NaN_3) or 1 % Digitonin lysis buffer (1 % Digitonin (dissolved in methanol 10 % w/v), 10 mM Tris pH 7.4, 150 mM NaCl, 0.01 % NaN_3). Depending on the experiment some cells were resuspended in PBS before lysis and then lysed in an equal volume of 2x lysis buffer. Cells were lysed on ice for 30 min then spun down for 10 min at 4 °C at 20 817 x g in a bench top microfuge. The supernatant was rotated with protein G sepharose beads for 1 hr at 4 °C after a sample was taken for whole cell lysate controls. The precleared lysates were spun down at 2655 x g in a bench top microfuge for 20 s at 4 °C and the supernatant transferred onto protein G sepharaose beads that had been pre-coupled with the relevant antibody (1 μg per IP). After rotation at 4 °C for either 90 min or overnight beads were spun down at 2655 x g for 20 sec in a bench top microfuge and lysate aspirated. Beads were then washed four times with 1 ml of the lysis buffer that the cells were lysed in. Beads were then stored in Laemmli's buffer, reducing or non-

reducing as appropriate. This method was previously published in Ellison et al. (2010), Serru et al. (1999) and Senis et al. (2009).

2.6.2 Western blotting

Protein samples denatured by incubating at 100 °C for 5 min were separated on varying % polyacrylamide gels. Gels with a single polyacrylamide concentration were prepared and set in house, gradient gels (4 - 12 %) were from Invitrogen, Paisley, UK. Samples were run through the gels with 125 V for 2 hr or until the dye front reached the end of the gel. Separated proteins were then transferred onto methanol activated Immobilon FL transfer membrane (Merck Millipore, Billerica, MA) by wet transfer for 90 min with 30 V. The membrane was blocked for 1 hr or overnight with either 5 % Milk in TBS or 3 % BSA in TBS (Tris-buffered saline 20 mM Tris, 137 mM NaCl, pH 7.6) then incubated with primary antibody in 3 % BSA/TBST (Tris-buffered saline with 0.1 % Tween-100) overnight. After washing 3 x 10 min with TBST-high salt (TBST with 500 mM NaCl) the membrane was incubated with secondary antibodies conjugated to infra red dye (IR dye) 800 CW or 680 (LI-COR biosciences, Cambridge, UK) for 2 hr. The stained membrane was then washed 5 x 5 min with TBST high salt followed by a final wash in TBS to remove any Tween, then imaged using the Odyssey Infrared scanner (LI-COR biosciences, Cambridge, UK).

2.7 Real time PCR

2.7.1 RNA extraction from primary cells

RNA was extracted from cultured megakaryocytes and sorted erythroblast cells using an extraction kit from Norgen BioTek (Ontario, Canada). Cell pellets that had been frozen at - 80 °C were directly lysed with 350 μl lysis solution and vortexed for 15 s. The amount of starting material varied for each experiment due to the nature in which the cells were obtained. Once lysed 200 μl of 100 % ethanol was added to the cells which were then vortexed for 10 s. This lysate was added to an equilibrated resin column and spun at 20 817 x g for 1 min in a bench top microfuge to bring the lysate into the resin bed. The resin was washed with wash solution three times and then eluted with 50 μl elution solution by spinning at 425 x g for 2 min then 20 817 x g for 1 min. RNA quality was assessed by running 1 μg of RNA on a 1 % agarose gel (100 V for ~ 15 min). RNA yield was assessed using a Nanodrop spectrophotometer (Nanodrop, Delaware, USA).

2.7.2 cDNA reverse transcription

To generate the template required for real time PCR experiments cDNA was generated from the purified RNA using an Invitrogen High Capacity cDNA Reverse Transcriptase kit. For each reaction the following was required : 2 μl of 10 x reverse transcription buffer, 0.8 μl of 25 x deoxyribonucleotide triphosphates (dNTPs), 2 μl 10 x random decamer primers, 1 μl reverse transcriptase enzyme and 14.2 μl of RNA (neat from the extraction prep). For all erythroblast samples the reaction volume was increased to 60 μl due to some of the low concentrations of RNA recovered. cDNA was generated with the following PCR cycle program: 10 min at 25 °C, 120 min 37 °C, 5 min 85 °C with a final hold at 4 °C. cDNA was stored at - 20 °C until use.

2.7.3 Real time PCR

The real time PCR approach used FAM-TAMRA TaqMan hydrolysis probes (Applied Biosystems) with one internal control gene (GAPDH) for megakaryocyte analysis and two internal control genes for erythroblast samples (GAPDH and 18 S). The additional control gene for the erythroblast samples was to provide a control for initial cDNA loading. For each gene of interest, and a water only control, 10 μl of master mix buffer and enzyme was mixed with 1 μl of TaqMan primer and aliquoted into a half skirted 96 well real time PCR reaction plate. Each gene was assessed in duplicate. 9 μl of cDNA (megakaryocyte samples diluted 1:30 and erythroblast samples diluted 1:3 in water) was added to each well and mixed by pipetting up and down. The plate was covered with an optical quality plastic cover and the samples analysed on an ABI Prism 7000 Sequence Detection system (Applied Biosystems) using the following PCR cycle program: 2 min at 50 °C, 10 min at 95 °C followed by 44 cycles of 15 s at 95 °C then 1 min at 60 °C. Standard curves were generated with serial 2 fold dilutions of cDNA and PCR efficiencies calculated. Efficiencies were required to be within 10 % of the house keeping gene for valid experiments. Primers were tested on an equal mix of cDNAs previously generated from each of the following mouse whole organs, brain, heart, kidney, liver, lung, muscle and thymus.

2.7.4 Analysis

To generate relative values for the different TspanC8 tetraspanins the cycle threshold (ct) values for the house keeping gene GAPDH were subtracted from the ct values of each TspanC8 gene. This, now delta ct, value was used to compare the expression of the genes with the data being presented as percentage expression of the most highly expressed gene. For the analysis of the erythroblast cells an additional step

was used of normalising the initial ct values for each gene for differences in the ct values of the 18 S gene between the different erythroblast populations tested on the same plate. This allowed for any differences in cDNA concentrations between different erythroblast samples.

2.8 Single particle tracking

2.8.1 Antibody labelling

50 μg of each Fab fragment (JAQ1, CD9 or IgG) was mixed with 0.5 μg Attofluor 647N or 565 in PBS pH 7.4 (no calcium or magnesium) and incubated with rotation for 2 hr at room temperature. The reaction was quenched with Tris pH 7.5 at a final concentration of 10 mM. The antibody and fluor mix was added to an equilibrated desalting column (PD-10, Amersham, UK) and allowed to soak into the resin bed. 10 μl of PBS was added on top of the antibody soaked resin which was then spun at 106 x g for 2 min at room temperature. The eluate from the spin was retained and the column then spun again after the addition of another 10 μl of PBS. This fraction was also collected. The eluate fractions containing the antibodies were coloured slightly and these were aliquoted and stored at - 20 °C until use. When higher concentrations of antibodies are labelled, the labelling efficiency can be measured using a spectrophotometer and the Beer-Lambert Law $A = \varepsilon b c$ where A is absorbance at 280, ε is the extinction coefficient ($Lmol^{-1}cm^{-1}$), b is path length (cm) and c is the concentration of species (M, $molL^{-1}$). The final concentration of labelled antibody was 0.5 μg/ml.

2.8.2 Coverslip preparation

25 mm round glass coverslips were rinsed in acetone, then methanol, then ultrapure water. These rinsed coverslips were then submerged in 1 M potassium hydroxide and sonicated for 20 min. After sonication the coverslips were washed 10 times in ultrapure water. After washing, the coverslips were submerged in fresh ultrapure water and sonicated again for 5 min. The twice sonicated coverslips were then washed 15 times in ultrapure water. The prepared coverslips were completely dried

by passing quickly through a flame before being stored individually in 6 well plates. Extra caution was taken to prevent dust from gaining access to the prepared coverslips.

2.8.3 Microscope and imaging set up

500 μl of washed mouse platelets at 2 x 10^7/ml were allowed to spread on a prepared glass coverslip held in a coverslip holder (Attofluor cell chamber, Invitrogen, UK) for 35 min at 37 °C. After spreading non-adhered platelets were removed from the coverslip by gentle washing, twice with Tyrode's. The relevant antibodies were incubated for 10 min at 37 °C with the platelets in a volume of 500 μl of Tyrode's at a final concentration of 10 ng/ml for JAQ1, 5 ng/ml for CD9 and 50 ng/ml for IgG controls. After incubation unbound antibody was removed by gentle washing with Tyrode's buffer three times. At this point the platelets were ready for imaging for a window of 1 hr. The platelets were imaged using an Olympus IX81-ZDC dual TIRF microscope with a Hamamatsu EM-CCD digital camera using an Olympus 150x UAPO N 1.45 NA immersion oil TIRF objective with Violet Diode 400-405nm, Argon-Ion 457-514nm, Green Diode 561nm lasers. Videos were a sequence of 500 images captured every 100 ms. Laser power was kept to a minimum to avoid untimely bleaching of the fluors and camera gain was set to maximum. At least 15 different fields of view were imaged in ensemble labelled conditions and at least 30 for single particle labelled conditions.

2.8.4 Analysis

Single particle tracking videos were analysed using the purpose made software PaTrack (Espenel et al., 2008). Briefly the software was used to identify individual particles and track their movements based on preset parameters that defined

allowable individual point spread function limits. The tracked particles were then manually checked for software errors. Once the true tracks had been identified different aspects of the trajectories of each particle were extracted from the software, including motion type and diffusion speeds. Bootstrap Monte Carlo sampling was used to determine the sample sizes required for a true reflection of all types of trajectories displayed by a population. This was found to be 100 trajectories for both GPVI and CD9. The software, experimental and analysis approach was previously determined and discussed in Espenel et al. (2008).

2.9 Cell culture

2.9.1 Cells

Human embryonic kidney (HEK) 293T cells were cultured in DMEM medium containing 10 % FBS, 20 mM glutamine and the antibiotics penicillin (100 U/ml) and streptomycin (100 μg/ml).

2.9.2 HEK 293T cell transfection

24 hr before transfection cells were plated out such that on the day of transfection ~ 80 % confluencey was achieved (See Table 6) in DMEM media that did not contain antibiotics. On the day of transfection the appropriate amount of DNA and polyethylenimine (PEI, Sigma) (see table below) was added to Opti-MEM (Invitrogen), gently vortexed and allowed to incubate for 10 min. This mixture was added drop wise onto the cells which were used 48 hr later (Ehrhardt et al., 2006).

Table 6. PEI transfection of HEK 293T cells guide

Plate size	Cells plated	DNA	PEI
6-well	5×10^5	1 μg	4 μl
6 cm	1×10^6	2 μg	8 μl
10 cm	3×10^6	9 μg	36 μl

2.10 Flow cytometry

2.10.1 Measuring megakaryocyte ploidy

Megakaryocyte cells matured in culture were spun down at 300 x g for 10 min then resuspended in 0.5 ml PBS and fixed with an equal volume of 1 % paraformaldehyde for 30 min on ice. Cells were washed free of fixative with 5 ml of PBS and spun down at 300 x g for 10 min. Washed cells were resuspended in 1 ml of DNA staining solution (PBS containing 2 mM $MgCl_2$, 0.05 % saponin, 0.01 mg/ml of propidium iodide and 10 U/ml of RNAse) and stained overnight at 4 °C. Stained cells were diluted with 1 ml of FACS buffer (0.2 % BSA, 0.02 % NaN_3 in PBS) and analysed with a FACScalibur flow cytometer (BD Biosciences). Megakaryocytes were identified and gated on by size. The percentage of cells in each peak in a ploidy profile, generated by a histogram of propidium iodide (Sigma) intensity against cell count, was measured.

2.10.2 Erythropoiesis analysis and erythroblast cell sorting

Erythroblast cells isolated from adult bone marrow, adult spleen or cultured from foetal liver cells were spun down at 300 x g for 5 min at 4 °C in a swing out centrifuge and resuspended in 100 μl of 5 % ice cold FBS in PBS and transferred into a V-bottomed 96 well plate. Cells were incubated with anti-CD16 antibody for 5 min to block the Fc receptors and then stained with fluorescein isothiocyanate-conjugated anti-Ter119, phycoerythrin-conjugated anti-CD71 and allophycocyanin-conjugated anti-CD45 in the dark for 1 hr. In addition to the multi stained cell samples single colour and unstained controls were included in the experiment to allow compensation adjustments. After staining 100 μl of 5 % ice cold FBS in PBS was added to the cells which were then spun down at 300 x g for 5 min at 4 °C and resuspended in 500 μl of

5 % ice cold FBS/PBS. Cells going forward into real time PCR assays were passed through a 70 μm mesh filter before being sorted using a Beckman Coulter MoFlo high speed cell sorter. Proerythroblasts were isolated by their double positive staining with anti-Ter119 and anti-CD71 and CFU-E cells isolated by their anti-CD71 low and anti-Ter119 negative staining. Cells used to investigate erythropoiesis in the Tsapn33 knockout mice were analysed using a Cyan flow cytometer and cell populations analysed by their Ter119/CD71 expression or their CD45/CD71 expression. Fluorescence crosstalk and bleed through was addressed with post acquisition compensation using the single colour control cells. Analysis and compensation was done using DAKO summit flow cytometry software. This method was previously published in Vegiopoulos et al. (2006).

2.10.3 Analysis of blood cell surface proteins

5 μl of whole blood per condition was diluted with 45 μl modified Tyrode's buffer. The diluted blood was stained for 30 min at room temperature with 10 μg/ml of relevant anti-mouse antibody (including negative control antibodies). 1 ml of modified Tyrode's buffer was added and a FACScalibur flow cytometer was used to analyse stained samples. Platelet and red blood cells were gated by size. Fluorescence in the gate was measured and geometric mean fluorescence intensity used to assess the surface expression of each protein.

CHAPTER III: FUNCTIONAL STUDIES OF TSPAN33-DEFICIENT PLATELETS

3.1 Introduction

Tspan33 (or Penumbra) is a 283 aa tetraspanin that was first identified as a candidate mouse platelet tetraspanin in 2007 by its presence in a mouse megakaryocyte serial analysis of gene expression (SAGE) library (Senis et al., 2007). This study also identified Tspan33 in human platelets, a result which was replicated in another proteomic study of human platelet cell surface proteins in 2009 (Lewandrowski et al., 2009a). Prior to these two findings Tspan33 had been identified as an important regulatory factor in erythropoiesis in a study that generated the Tspan33 knockout mouse (Heikens et al., 2007). At the time of this project this was the only published study of Tspan33 and it observed defects in erythropoiesis in Tspan33 knockout mice. Abnormal red blood cells termed basophilic and macrocytic, occurred in blood smears of 30 % of knockout animals. These abnormal red blood cells increased as the animals aged and developed a subsequent anaemia. *In vitro* work with an erythroblast cell line generated from the knockout mice indicated that Tspan33 was required for the survival of erythropoietin responsive erythroid progenitors *in vitro* however the mechanism for this remained unknown. No other tissues in the Tspan33 knockout mouse have been studied though it is clear that Tspan33 is expressed in other cell types (Heikens et al., 2007). As such the indication that Tspan33 may be a yet unstudied platelet tetraspanin was the foundation of a project that aimed to use the Tspan33 knockout mouse to discover the function of Tspan33 in platelets.

3.2 Results

3.2.1 The platelet count and other blood parameters of Tspan33 knockout mice were normal in comparison to wildtype.

Before beginning detailed analysis of the platelet function in the Tspan33 knockout mouse whole blood counts were used assess the levels and normality of all the major blood cell types. The platelet count and other blood cell counts in the Tspan33 knockout mouse appeared normal when compared to wildtype and other blood cell parameters also fell within the normal ranges (Table 7). The only statistically different parameter was the mean platelet volume which was significantly larger in the Tspan33 knockout mice by 0.2 μm^3, though still within the accepted normal range for platelet size (4 - 7 μm^3). Whilst a minor change, this small increase in platelet size appeared valid as it was accompanied by the trend for reduced platelet counts following the known inverse correlation between platelet size and platelet count (Levin and Bessman, 1983). As the increase in Tspan33-deficient platelet size was only small, the lack of significance in the decrease of the more variable parameter, platelet count, was unsurprising.

Blood parameter	Wildtype	Knockout	P value
Platelet count ($10^3/mm^3$)	907.90 +/- 118.06	878.46 +/- 167.16	0.46
Mean platelet volume (μm^3)	5.22 +/- 0.14	5.4 +/- 0.21	0.006
Plateletcrit (%)	0.29 +/- 0.05	0.29 +/- 0.05	0.88
White blood cell count ($10^3/mm^3$)	7.26 +/- 4.54	7.48 +/- 4.14	0.89
Red blood cell count ($10^6/mm^3$)	10.31 +/- 0.69	10.16 +/- 0.72	0.54
Haemoglobin concentration (g/dl)	9.73 +/- 0.70	9.43 +/- 0.89	0.28
Haematocrit (%)	30.8 +/- 2.35	29.5 +/- 2.79	0.15
Red blood cell distribution width (%)	13.26 +/- 1.07	13.71 +/- 0.92	0.19
Mean corpuscular volume (μm^3)	47.59 +/- 1.37	46.5 +/- 2.15	0.09
Mean corpuscular haemoglobin (pg)	15.0 +/- 0.50	14.88 +/- 0.57	0.53
White cell percentages:			
-Lymphocyte	84.15 +/- 10.44	82.93 +/- 8.66	0.92
-Monocyte	5.14 +/- 2.22	6.58 +/- 4.14	0.21
-Neutrophil	7.12 +/- 5.20	9.17 +/- 5.06	0.25
-Eosinophil	1.28 +/- 2.16	0.96 +/- 1.36	0.6
-Basophil	0.44 +/- 0.60	0.36 +/- 0.50	0.69

Table 7. Global haematopoiesis in Tspan33 knockout mice appears normal.
All of the blood parameters assessed in the whole blood count, with the exception of mean platelet volume, were not significantly different between wildtype and knockout blood samples. n = 17 of mice aged 9 - 29 weeks, +/- values represent standard deviation around the mean. p value determined by an unpaired Students t-test.

3.2.2 Tspan33 deficient megakaryocytes mature normally *ex vivo.*

The significant increase in mean platelet volume in the Tspan33 knockout mouse indicated that there may have been a defect in platelet production. To assess this megakaryocytes were harvested and purified from adult mouse bone marrow and allowed to mature *ex vivo*. This well defined approach (Shivdasani and Schulze, 2005) assesses megakaryocyte maturity as an increase in cell ploidy using flow cytometry analysis after staining with the DNA intercalating agent propidium iodide. In this controlled *ex vivo* environment Tspan33-deficient megakaryocytes developed normally and there were no significant differences between wildtype and knockout ploidy profiles (Figure 9). This suggested that Tspan33 was dispensable for megakaryocyte maturation.

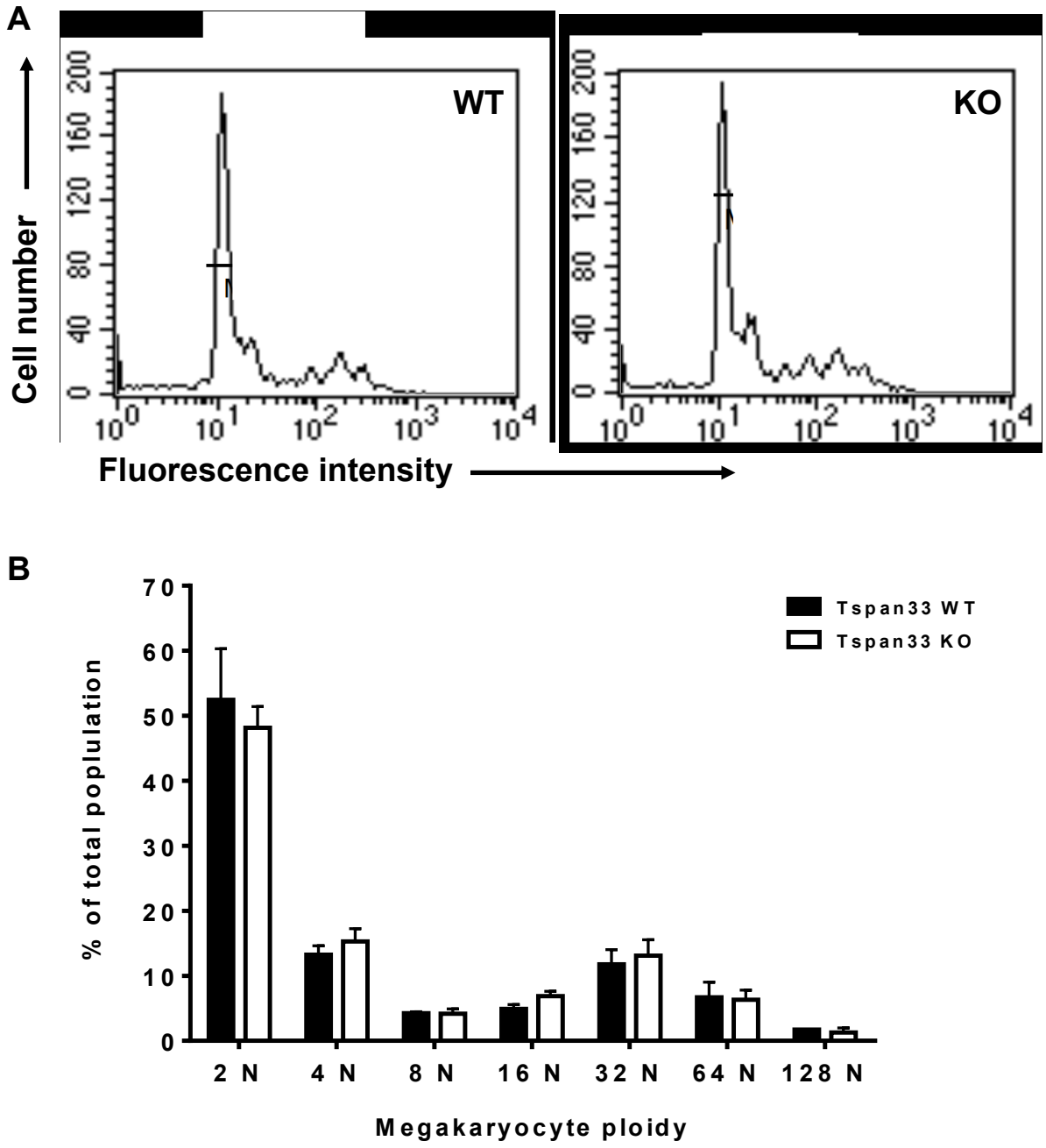

Figure 9. Tspan33-deficient megakaryocytes develop normally *ex vivo.*
Megakaryocytes from wildtype and knockout mouse adult bone marrow were matured *ex vivo*. Megakaryocyte specific propidium iodide (PI) staining was isolated by gating on megakaryocytes by size. A. Representative ploidy profiles for wildtype and Tspan33-deficient megakaryocytes. B. % of total megakarocyte population in each peak of the PI histogram was measured. No clear differences were observed between wildtype and knockout cultures. n = 2 +/- represent standard error of the mean.

3.2.3 Tspan33-deficent platelets had normal levels of major surface proteins.

After the general assessment of haematopoiesis in the Tspan33 knockout mouse the platelets themselves became the focus of the investigation. Some tetraspanins have been found to influence partner protein trafficking to the cell surface (Shoham et al., 2003, Haining et al., 2012, Berditchevski and Odintsova, 2007), therefore it was important to check the surface levels of the major platelet proteins in the Tspan33-deficient platelets. Whole blood was stained with FITC conjugated antibodies against the following major platelet surface proteins αIIbβ3, α2β1, α6β1, GPVI, GPIb, CD9, ADAM10 and CLEC-2. Flow cytometry allowed platelet specific staining to be isolated by gating on platelets by size and geometric mean fluorescence intensity was used to assess the protein surface levels (Figure 10A). All of the proteins measured were present in Tspan33-deficient platelets at levels that were not significantly different from those measured in wildtype platelets (Figure 10B). This data indicated that Tspan33 was not required for the surface expression of any of the listed platelet surface proteins.

A

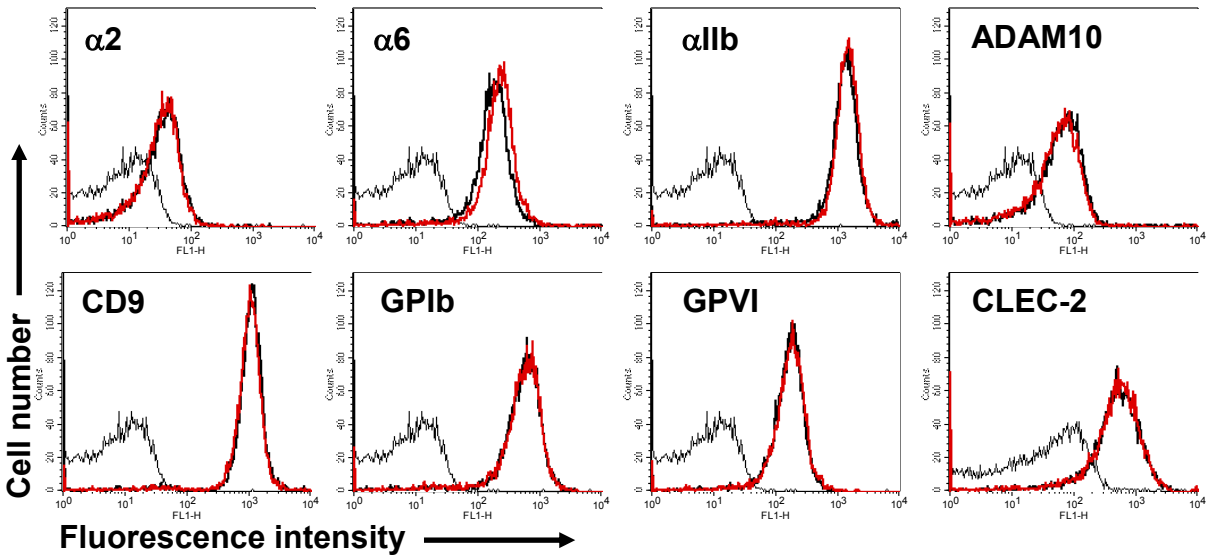

B

Surface protein	Wildtype	Knockout	p value
Alpha 2	17.36 +/- 3.61	17.66 +/- 3.51	0.92
Alpha 6	150.23 +/- 9.02	167.64 +/- 15.86	0.17
Alpha IIb	1085.71 +/- 64.79	1047.69 +/- 125.88	0.67
ADAM10	38.91 +/- 3.33	39.21 +/- 1.15	0.83
CD9	785.61 +/- 54.62	761.80 +/- 32.85	0.56
GPIb	427.25 +/- 3.02	430.14 +/- 23.69	0.84
GPVI	137.21+/- 7.13	146.91 +/- 4.76	0.12
Clec-2	392.64 +/- 25.25	384.15 +/- 79.15	0.87

Figure 10. Tspan33-deficient platelets express normal levels of the major platelet surface glycoproteins.
Whole blood drawn into acid citrate dextrose was incubated with the relevant anti-mouse antibody conjugated to FITC. Platelet specific staining was isolated by gating on platelets by size. A. Representative FACS plots for each indicated protein. Wildtype in black and Tspan33-deficient in red. For simplicity only the control trace from wildtype staining is shown as it overlays the Tpsan33-deficient trace. B. Geometric mean intensity used to assess surface receptor levels. n = 3 - 6 +/- represents standard deviation around the mean. p value determined by an unpaired Student's t-test.

3.2.4 Tspan33 knockout mice do not have a bleeding phenotype.

The initial assessment of haemostasis in the Tspan33 knockout mice was the tail bleeding assay, a test analogous to the human bleeding time test used in the clinic (Marshall et al., 1997, Hughes et al., 2008). In this assay the tail tip is cut from the mice and subsequent blood loss in a set time-frame is recorded. Tail bleeding is well documented to detect gross defects in haemostasis. However, due to its inherent inclusion of several haemostatic responses and its variability, it is viewed as unreliable in identifying more subtle bleeding tendencies in which only one aspect of haemostasis, such as platelet function, may be only mildly affected (Greene et al., 2010). In this initial screen of haemostasis blood loss from the Tspan33 knockout mice was not significantly different from wildtype and thus these mice were not judged to have a bleeding defect (Figure 11).

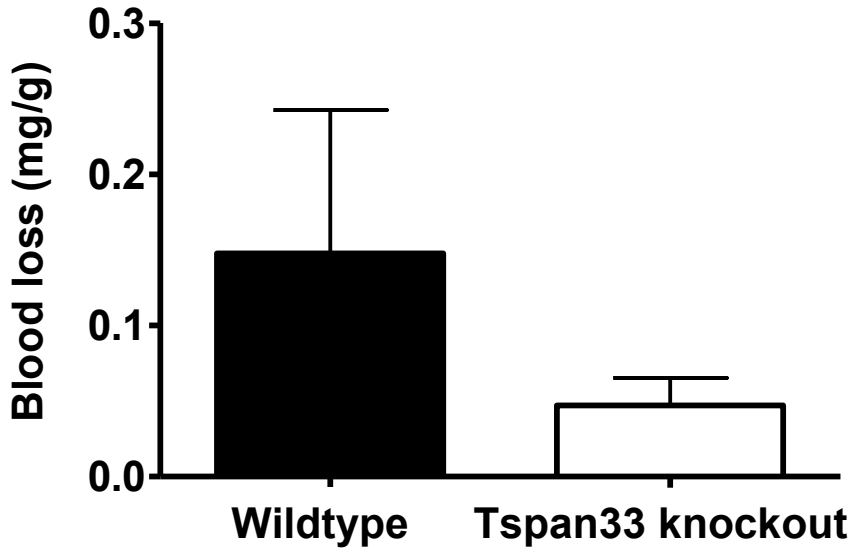

Figure 11. Tspan33 knockout mice do not have a bleeding defect as measured by the tail bleeding assay.
Blood loss after tail tip excision is presented as a factor of mouse weight so as to normalise blood loss from mice of different sizes. No significant difference was found between the blood loss (mg/g) of wildtype and Tspan33 knockout mice using an unpaired Students t-test ($p = 0.2861$). All mice were aged between 8 - 12 weeks and between 2 - 3 mm of tail tip removed. $n = 20$ and error bars represent standard error of the mean.

3.2.5 Tspan33-deficient platelets display normal responses to collagen-related peptide and thrombin in light transmission aggregometry.

As previously stated the tail bleeding assay only allows an assessment of the functioning of haemostasis as a whole. To begin to focus more specifically on platelet function, light transmission lumi-aggregometry (LTA) was used assess platelet aggregation responses to different agonists. LTA is the gold standard in platelet function testing (Lordkipanidze et al., 2009), it captures platelet aggregation responses over time, including the very initial shape change and subsequent granule release allowing detailed analysis of specific platelet signalling pathways. Two agonists that stimulate two major platelet activatory pathways were used to investigate the functionality of Tspan33-deficient platelets; collagen-related peptide, which binds and activates the collagen receptor GPVI and thrombin which cleaves and activates the PAR G protein-coupled receptors. Aggregation experiments used washed platelet samples without added fibrinogen. Responses to both these agonists were normal and not significantly different to wildtype responses (Figure 12A, B, C and D). ATP secretion, which is a measurement of dense granule release, was also normal in the Tspan33-deficient platelets and not significantly different from wildtype in response to the two agonists (Figure 12E and F).

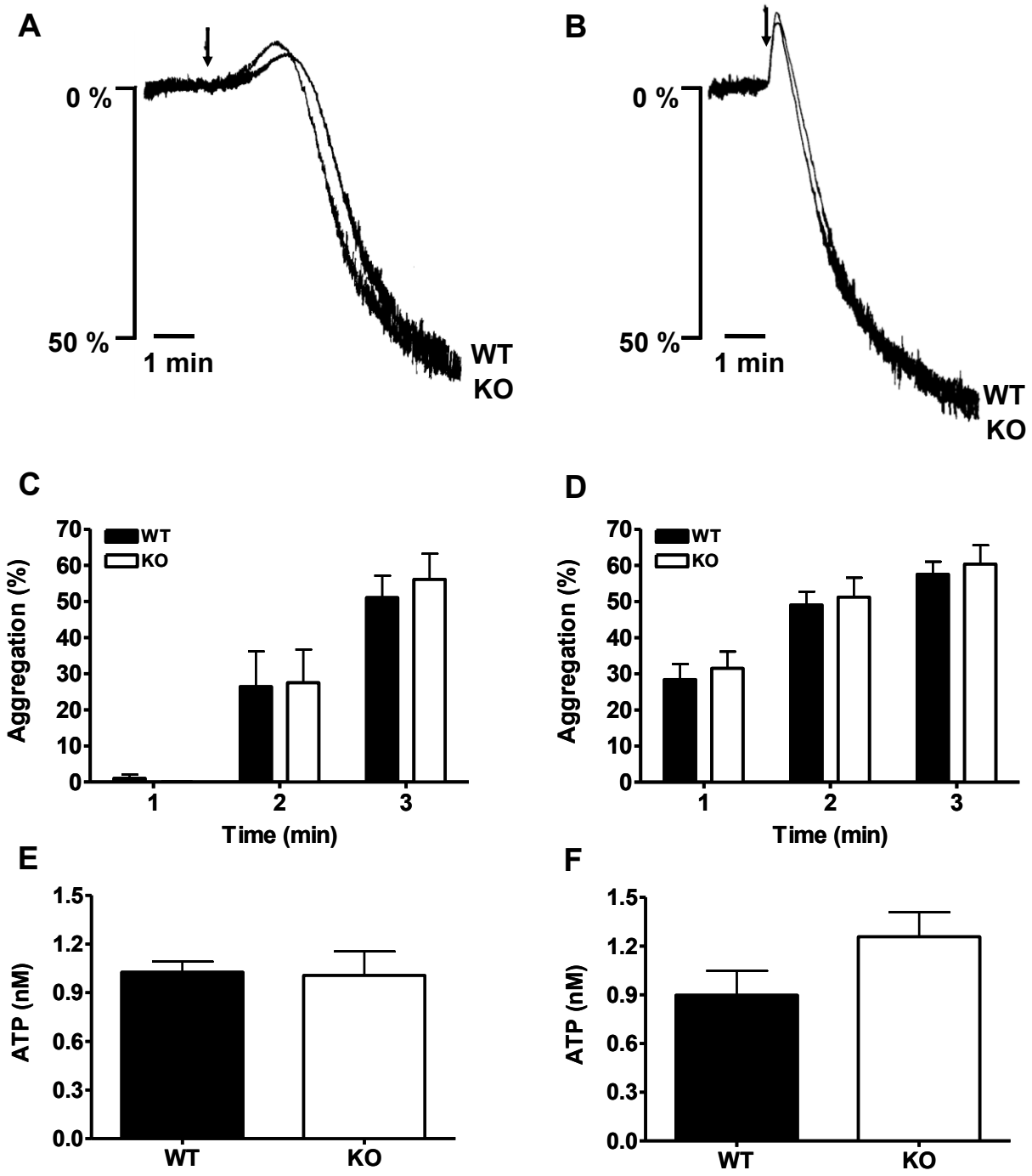

Figure 12. Tspan33-deficient platelets display normal responses to the agonists collagen-related peptide and thrombin.
Tspan33 wildtype and deficient washed platelets were stimulated with collagen-related peptide (0.3 μg/ml) or thrombin (0.06 U/ml) and responses measured with lumi-aggregometry. No significant differences were seen in the aggregation traces (A, collagen-related peptide and B, Thrombin), percentage aggregation over time (C, collagen-related peptide, p = 0.84 and D, thrombin p = 0.69) or in the amount of ATP secretion (E, collagen-related peptide p = 0.91 and F, thrombin p = 0.17). n = 3 and error bars represent standard error. Statistical test used in C/D was a two-way ANOVA and in E/F an unpaired Student's t-test.

3.2.6 Tetraspanin microdomains immunoprecipitated from Tspan33-deficient platelets have the normal complement of tetraspanin associated proteins.

As all investigations had found that Tspan33-deficient platelets were no different in their functional responses from wildtype platelets a different approach that assessed the platelet tetraspanin microdomains themselves was the next step. An immunoprecipitation and western blotting approach that had been previously validated was used as a method of isolating and probing tetraspanin microdomains (Protty et al., 2009). The aim of this experiment was to compare the tetraspanin microdomains from wildtype and Tspan33-deficient platelets. To immunoprecipitate the highest amount of material possible CD9, the most highly expressed platelet tetraspanin, was immunoprecipitated from washed mouse platelets that had been surface biotinylated. These precipitates were separated on 4 - 12 % polyacrylamide gradient gels and the co-immunoprecipitated biotinylated surface proteins detected by western blotting with neutravidin.

As it is thought that each tetraspanin is responsible for the inclusion of its partner protein in tetraspanin microdomains any proteins missing from the western blot of Tspan33-deficient samples could be potential partner proteins for Tspan33 (Charrin et al., 2003b). Thus informing a more directed approach to the further analysis of the Tspan33-deficient platelets. However, there was no significant differences between wildtype and Tspan33 deficient western blots (Figure 13). All the major bands in the microdomain pattern caused by neutravidin blotting in wildtype immunoprecipitates were also found at the same intensity in the Tspan33-deficient samples. Interestingly there appeared to be no clear band for Tspan33 which we would expect to see in the

wildtype but not in the knockout, however there were also no clear bands for any tetraspanin other than CD9.

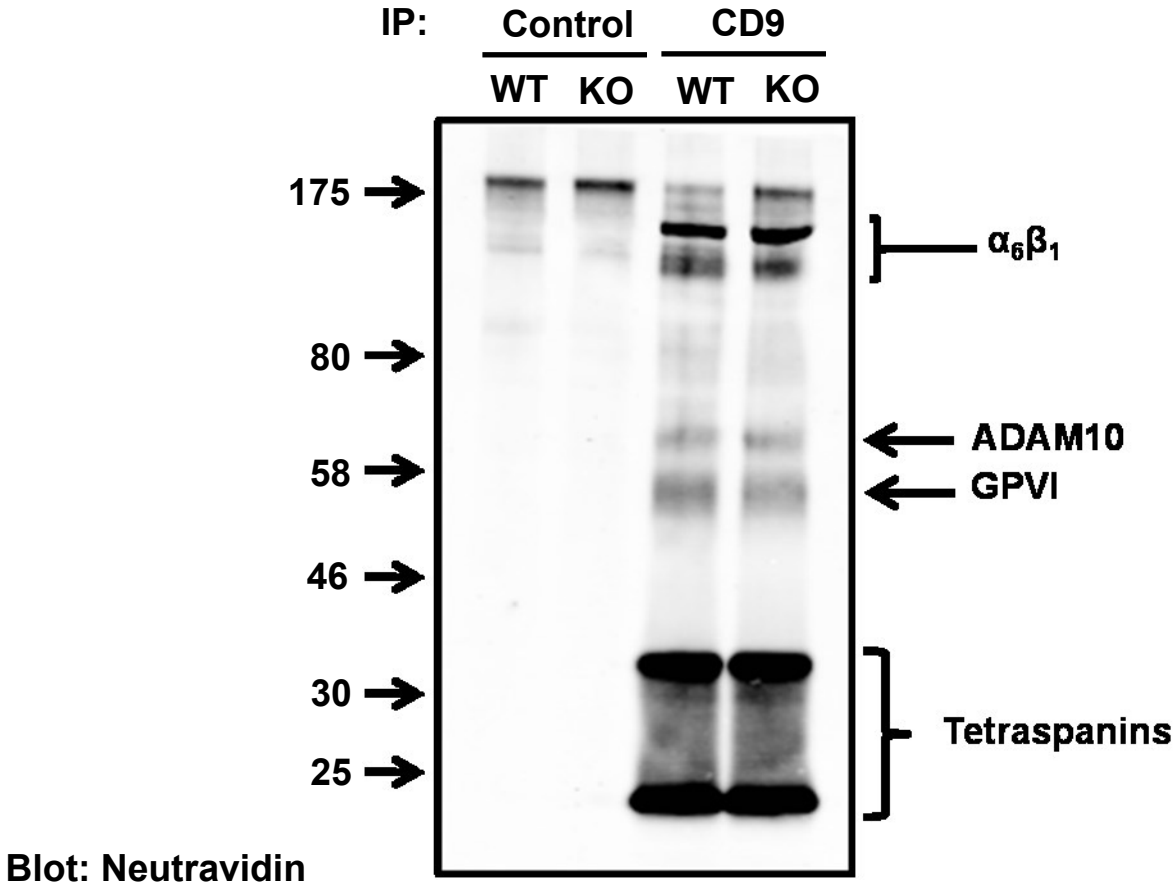

Figure 13. Tspan33-deficient tetraspanin microdomains have a similar complement of membrane proteins as wildtype.
5 x 10^8 washed platelets per condition were surface biotinylated using EZ-link sulpho NHS LC Biotin (1 mg/ml) for 30 min. After biotinylation the platelets were lysed in 1 % Brij97 lysis buffer for 1 hour whilst rotating with unconjugated protein G sepharose beads. After this preclear step lysates were incubated with beads that been pre-coupled to either IgG control or anti-CD9 antibody for an additional hour. Samples were washed and separated on 4 - 12 % polyacrylamide gradient gels. Separated proteins were western blotted with neutravidin to detect biotinylated proteins from the platelet cell surface. No difference was found between wildtype and Tspan33-deficient samples.

3.2.7 Tspan33 mRNA is highly expressed in human platelets but minimal in mouse platelets.

Following the analyses of Tspan33-deficient platelets a new platelet transcriptomics study was published (Rowley et al., 2011). This study used paired-end next generation RNA sequencing to detect the levels of all the polyadenylated RNA transcripts in human and mouse platelets. It was the first study of its kind that focussed on solely platelets. The published lists of detected RNAs and their respective levels were mined for all the known mammalian tetraspanins (Figure 14). Tspan33 was the most highly expressed tetraspanin in human platelets at the mRNA level. In mouse platelets however the level of Tspan33 transcript detected was 1000 times less than that detected in human platelets. Interestingly Tspan33 was not only differentially expressed tetraspanin between human and mouse platelets. It is possible that such a low level of mRNA would indicate that mouse platelets express no Tspan33 protein, or at best minimal levels in comparison to other tetraspanins. A lack of expression on mouse platelets would be consistent with the lack of platelet phenotype in the Tspan33 knockout mouse.

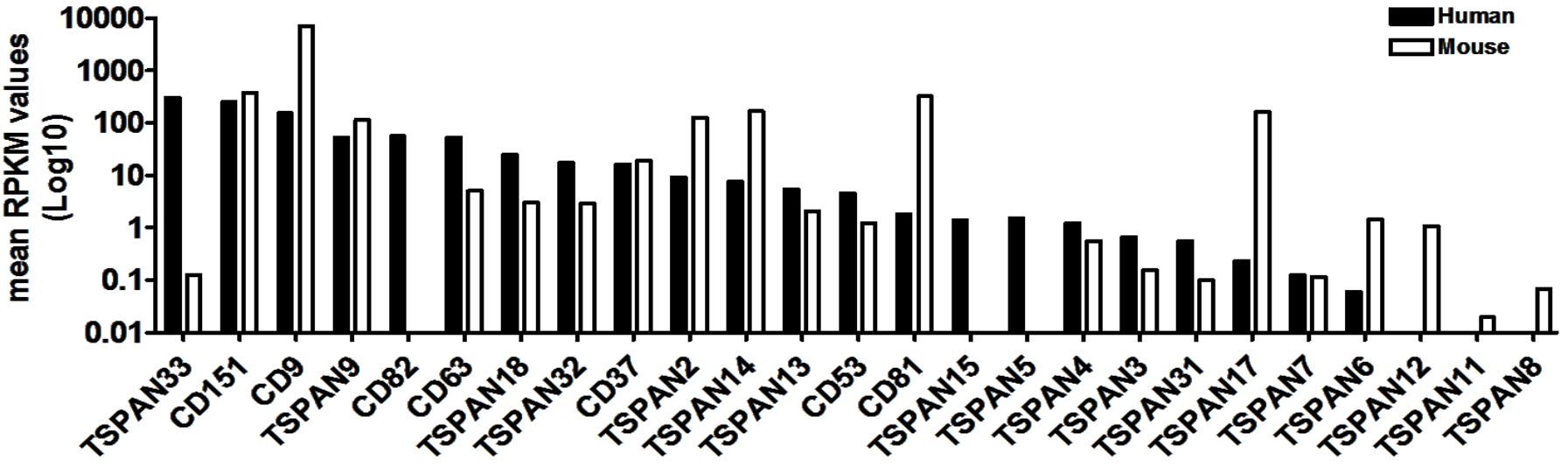

Figure 14. Tspan33 may be differentially expressed between human and mouse platelets.
RNA Seq data published by Rowley *et al.* of polyadenylated RNA transcripts found in human or mouse platelets was mined for all known mammalian tetraspanins. RPKM represents reads per kilobase per million reads, defined by the authors as abundance.

3.3 Discussion

Presented here is a short investigation into the function of Tspan33 on platelets. The initial hypothesis for the project was that Tspan33 is a novel platelet tetraspanin and that it contributes to platelet function by regulating another platelet transmembrane protein. The aim of the project was to use the Tspan33 knockout mouse and Tspan33-deficient megakaryocytes and platelets to investigate the initial hypothesis. The final conclusion of this project was that Tspan33 does not play an important part in platelet generation, haemostasis or platelet activation downstream of the PAR receptors or GPVI. Additionally whilst highly expressed on human platelets Tspan33 is minimally or not expressed on mouse platelets. This latter finding may potentially explain the results of the experiments using platelets from the Tspan33 knockout mouse and suggests that this knockout mouse is no longer a useful tool for further study of the function of this protein on platelets.

The only significant difference found between wildtype and Tspan33-deficient platelets in this study was the larger mean platelet volume (by 0.2 μm^3) of Tspan33-deficient platelets. The cause of this small change in platelet size was not discovered in this investigation and taken into context with the rest of the study such a small change may be insignificant in terms of understanding Tspan33 function in platelets. Further experiments including assessment of proplatelet generation and, taking into account the erythropoiesis defect, details of associated other bone marrow cell populations are required before this difference in the Tspan33 knockout mouse can be fully understood and its significance appreciated.

Additional to the lack of a platelet function defect in the Tspan33 knockout mice the main evidence for concluding that Tspan33 is a human platelet tetraspanin but likely

not expressed on mouse platelets came from data mined from a transcriptomics paper that was published during the study. After extracting expression levels for all known mammalian tetraspanins from this study a striking difference in the RNA levels for Tspan33 became clear between human and mouse platelets. This 1000 fold difference mirrored albeit to a greater extent the differences in detection of Tspan33 in the two original papers that were used as the premise for this study, with the human proteomics (Lewandrowski et al., 2009a, Senis et al., 2007) ranking Tspan33 as a much more highly expressed tetraspanin than the mouse megakaryocyte SAGE library (Senis et al., 2007) (Table 4). One caveat to this data is however that one can never assume that RNA levels directly correlate with final protein levels (Greenbaum et al., 2003). Interestingly whilst the top ten expressed tetraspanins identified by Rowley *et al.* correlate well with the human platelet proteomics published by Lewandrowski *et al.* 2009, there is less agreement between the mouse megakaryocyte SAGE library and the Rowley transcriptomics study in terms of tetraspanins detected and their relative amounts (Table 8). As all three studies identified the known platelet tetraspanins - CD9, CD63, CD151, Tspan9 and Tspan32 (demonstrating the validity of each approach) the differences between the megakaryocyte SAGE library and the platelet transcriptomics may be a reflection of true differences between the two cell types.

As well as discovering that Tspan33 is most likely not expressed on mouse platelets this investigation has highlighted some interesting questions in terms of the study of platelet tetraspanins. In particular the big difference in expression of Tspan33 between human and mouse. Human and mouse Tspan33 protein have 97 % identity (Heikens et al., 2007); why would two virtually identical proteins have such different

expression levels? This would not be the first example of differentially expressed proteins between human and mouse platelets (Kahn et al., 1998, Maruoka et al., 2004) and interestingly it does not appear to be the only differentially expressed tetraspanin as CD82, CD81 and Tspan17 also appear to have differential expression according to the mined data from Rowley *et al.* Finally the question remains of what the function of Tspan33 is and understanding this became the focus of the work presented in the following chapter.

	Human		Mouse	
Rank	Lewandrowski (A)	Rowley (B)	Senis (C)	Rowley (B)
1	CD9	Tspan33	CD63	CD9
2	Tspan9	CD151	CD9	CD151
3	Tspan33	CD9	CD151	CD81
4	CD151	Tspan9	Tspan4	Tspan17
5	CD63	CD82	CD37	Tspan14
6	CD82	CD63	Tspan32	Tspan 2
7	Tspan14	Tspan18	CD81	Tspan9
8	Tspan32	Tspan32	Tspan9/Tspan13/Tspan31	CD37
9	Tspan15	CD37	Tspan14	CD63
10	Tspan4	Tspan2	Tspan33	Tspan18/Tspan32

Table 8. Comparison of the 10 most highly abundant tetraspanins detected in Lewandrowski *et al.* 2009, Senis *et al.* 2007 and Rowley *et al.* 2011.
Data on the ten most highly detected tetraspanins from each study (A) Lewandrowski *et al.*2009 (B) Rowley *et al.* 2011 (C) Senis *et al.*2007 has been aligned to allow clear comparison of the different complement of tetraspanins detected by each method. Rank indicates the relative amount of each tetraspanin with 1 donating the most highly detected. To aid in comparisons tetraspanins that appear in the top five of the Lewandrowski study are colour-coded with the same colour across the whole table.

CHAPTER IV: TSPAN33 IS A MEMBER OF THE TSPANC8 TETRASPANIN SUBFAMILY WHICH REGULATES THE PROTEASE ADAM10

4.1 Introduction

Whilst assessing the levels of the major platelet surface proteins on Tspan33-deficient platelets by flow cytometry it was noticed that the levels of the transmembrane metalloprotease ADAM10 on red blood cells appeared reduced. The aim of the work in this chapter was to characterise and understand this loss of ADAM10 from Tspan33-deficient red blood cells. ADAM10 is one of the best known tetraspanin associated proteins in the field (Charrin et al., 2009). However its tetraspanin partner is unknown. A report identifying Tspan12 as a direct ADAM10-interacting tetraspanin was not definitive because other tetraspanins could have been bridging the Tspan12-ADAM10 interaction under the immunoprecipitation conditions used (Xu et al., 2009). Moreover, Tspan12 has a relatively restricted expression profile (Junge et al., 2009), unlike the ubiquitous ADAM10. ADAM10 cleaves other transmembrane proteins in a process termed ectodomain shedding. This 'sheddase' action of ADAM10 results in the loss of the extracellular domains of its transmembrane target proteins from the cell surface. This can result in the release of transmembrane chemokines and growth factors such as heparin-bound epidermal growth factor (HB-EGF), the initiation of trans-cellular signal transduction such as that through the Notch receptors, the reduction in cell-cell adhesion through shedding of cadherins (Lichtenthaler, 2011, Saftig and Reiss, 2011, Vincent and Govitrapong, 2011, Endres and Fahrenholz, 2010), and the down regulation of ligand binding signalling receptors such as GPVI (Gardiner et al., 2007, Bender et al., 2010). The importance of the function of ADAM10 is demonstrated by the embryonic lethality of

the ADAM10 knockout mouse which dies around E9.5 due to dysregulation of Notch signalling (Hartmann et al., 2002). ADAM10 is responsible for the initial cleavage of Notch, following ligand binding, that leads to intracellular cleavage by γ-secretase and translocation of the intracellular domain of Notch to the nucleus, where it functions as a transcription factor to drive cell fate decisions (Greenwald and Kovall, 2013). ADAM10 is known to have over 40 targets and as such is involved in the activation, regulation and termination of a diverse array of cellular signalling (Deuss et al., 2008, Vincent and Checler, 2012). Much research has focussed on ADAM10 as several of its targets play central roles in the development and progression of human diseases. An important example of this is the amyloid precursor protein, which gives rise to the beta amyloid peptide that forms amyloid plaques in Alzheimer's disease. ADAM10 cleavage of amyloid precursor protein prevents beta amyloid production and so is protective against development and progression of the disease (Postina et al., 2004). ADAM10 is also upregulated on some cancers where its cleavage of epidermal growth factor can promote tumour invasiveness and the epithelial to mesenchymal transition necessary for metastasis.(Crawford et al., 2009). However, attempts to target ADAM10 in human diseases such as Alzheimer's disease are hampered by the ubiquitous nature of the protein, which would likely result in severe side-effects, and a lack of clear understanding of its regulation (Lichtenthaler, 2011, Saftig and Reiss, 2011, Vincent and Govitrapong, 2011, Endres and Fahrenholz, 2010). As such, determining which tetraspanin(s) interact with ADAM10, and how they regulate this metalloprotease, could have important implications for the progression of research into some significant human diseases.

4.2 Results

4.2.1 ADAM10 surface levels are reduced on Tspan33-deficient red blood cells.

The initial observation for this project came from a flow cytometry experiment that used whole blood samples to test for surface expression levels of several different proteins on Tspan33-deficient platelets (Figure 10). By gating on the red blood cell population instead of the platelet population (which are clearly separated by forward scatter and side scatter) the surface levels of the chosen proteins could also be detected on red blood cells (Figure 15A). Of the chosen panel of platelet proteins only ADAM10 and CD36 were shared between platelets and red blood cells. The surface levels of ADAM10 were significantly reduced in Tspan33-deficient cells by ~ 90 % (Figure 15 B). This reduction may be specific to ADAM10 as the CD36 levels on Tspan33-deficient red blood cells were normal.

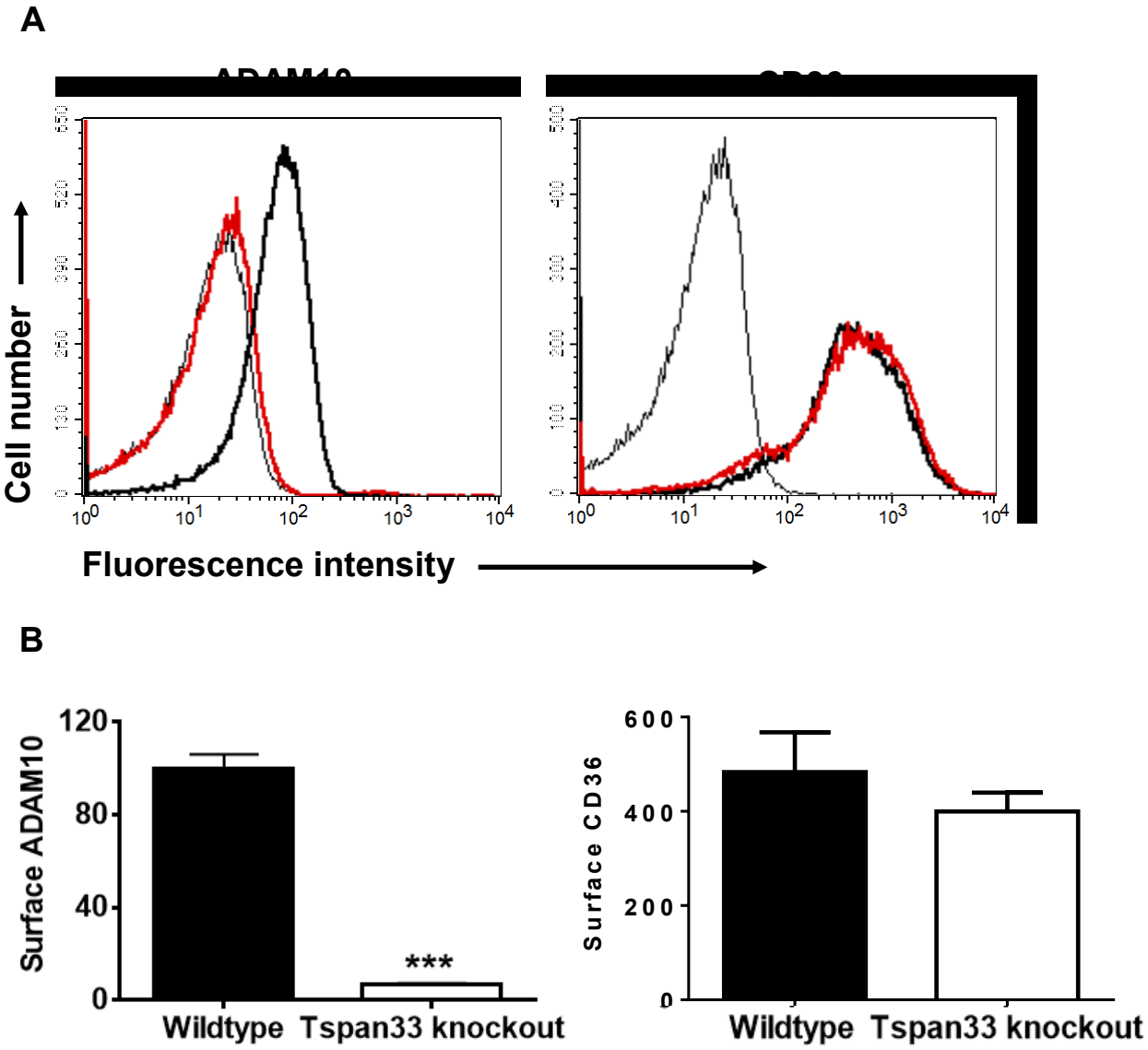

Figure 15. ADAM10 surface levels are reduced on Tspan33-deficient red blood cells.

Whole blood drawn into acid citrate dextrose was incubated with the relevant anti-mouse antibody conjugated to FITC. Red blood cell specific staining was isolated by gating on red blood cells by size. A. Representative FACS plots for each indicated protein, with wildtype in black and Tspan33-deficient in red. For simplicity only the negative control trace from the wildtype staining is shown as it superimposes with the Tspan33-deficient control. B. Geometric mean fluorescence intensity was used to assess receptor levels. n = 4, error bars represent standard error of the mean. Significant difference was determined by an unpaired Student's t-test. *** is $p < 0.0001$.

4.2.2 ADAM10 total cell levels are reduced on Tspan33-deficient red blood cells.

To follow up the observed difference between surface levels of ADAM10 on Tspan33-deficient and wildtype red blood cells, an experiment was designed to specifically isolate and detect both the surface and total red blood cell ADAM10 levels. An immunoprecipitation approach after biotinylation was selected. This allowed the detection of surface ADAM10 levels after immunoprecipitation by western blotting with neutravidin and total cell levels of ADAM10 by western blotting with an anti-ADAM10 antibody. There was a clear decrease in the both the surface level of biotinylated ADAM10 detected and the total levels of ADAM10 in Tspan33-deficient samples (Figure 16). This correlated with the significant decrease seen in the analysis of ADAM10 surface levels by FACS analysis. In addition this result indicated that the reduction in ADAM10 at the cell surface is not due to defective transport of the protein to the cell surface and actually reflects a loss of protein from the cell.

In addition to this experiment assessing the levels of ADAM10, it also allowed an initial assessment of the tetraspanin microdomains on mouse red blood cells. Three major proteins appeared to co-immunoprecipitate with ADAM10 using this Brij97 lysis buffer approach, and their sizes were ~44, 48 and approximately 100 kDa. The identity of these is unknown, but they are likely to be tetraspanin microdomain-associated proteins on the red blood cell surface.

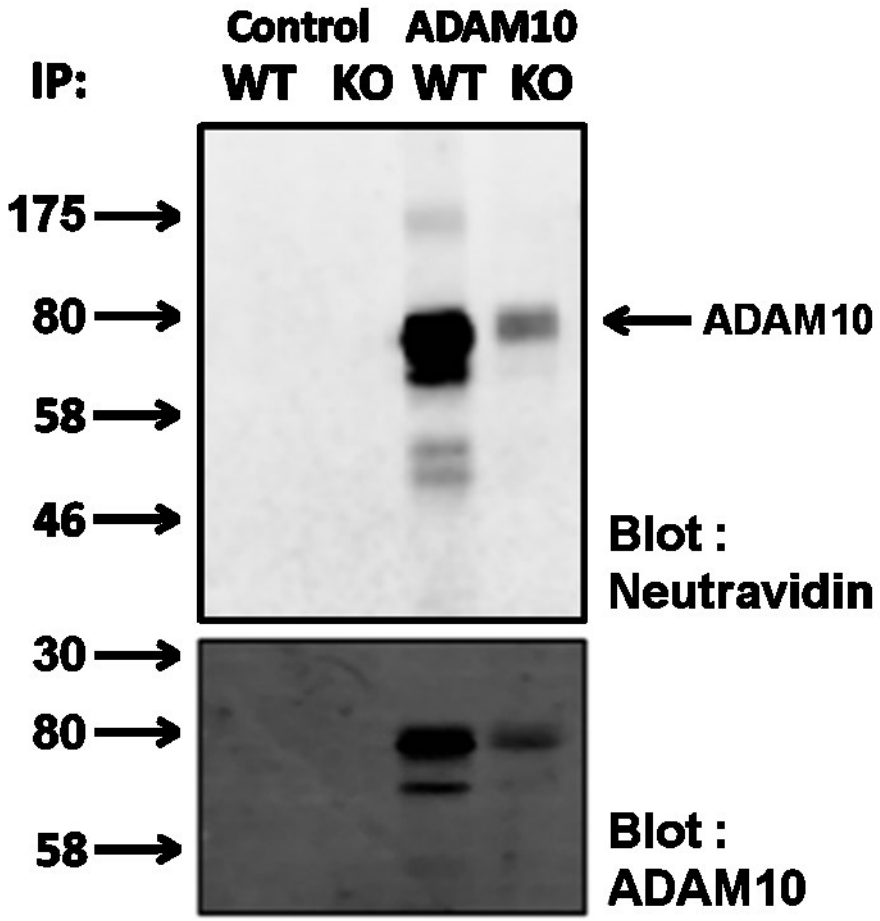

Figure 16. Total ADAM10 protein levels are reduced on Tspan33-deficient red blood cells.

Washed red blood cells at 5 x 10^8/ml (per ip) were surface biotinylated using EZ-link sulpho NHS LC Biotin (1 mg/ml) for 30 min. After biotinylation the red blood cells were lysed for 30 min on ice in 1 % Brij97 lysis buffer, pre-cleared for 1 hour using protein G sepharose beads, then rotated with protein G sepharose beads that had been pre-coupled to IgG control or anti-ADAM10 antibody. Samples were washed and separated on a 4 - 12 % polyacrylamide gradient gel. Separated proteins were western blotted with neutravidin to detect biotinylated proteins from the cell surface and anti-ADAM10 antibody to detect all the ADAM10 immunoprecipitated from the cell.

4.2.3 ADAM10 mRNA levels are not reduced in Tspan33-deficient proerythroblasts.

One explanation for the lower levels of ADAM10 protein seen in Tspan33-deficient red blood cells was that ADAM10 mRNA was expressed at lower levels in Tspan33-deficient proerythroblasts, the precursors to red blood cells, which themselves, have minimal mRNA. To investigate this hypothesis, ADAM10 mRNA levels were measured by real time PCR in proerythroblasts sorted from *ex vivo* differentiated Tspan33 wildtype and knockout foetal liver. Red blood cells are the anucleate result of the final step in erythropoiesis, their complement of proteins determined by the biosynthesis of proteins in the preceding stages (Testa, 2004). Therefore to investigate protein expression levels, ADAM10 mRNA needed to be assessed in the proerythroblasts. Using this approach no difference was found in the ADAM10 mRNA levels between wildtype and Tspan33-deficient proerythroblasts (Figure 17). This result suggested that ADAM10 protein is likely to be produced in Tspan33-deficient proerythroblasts but that it was unable to be packaged into subsequent reticulocytes and red blood cells.

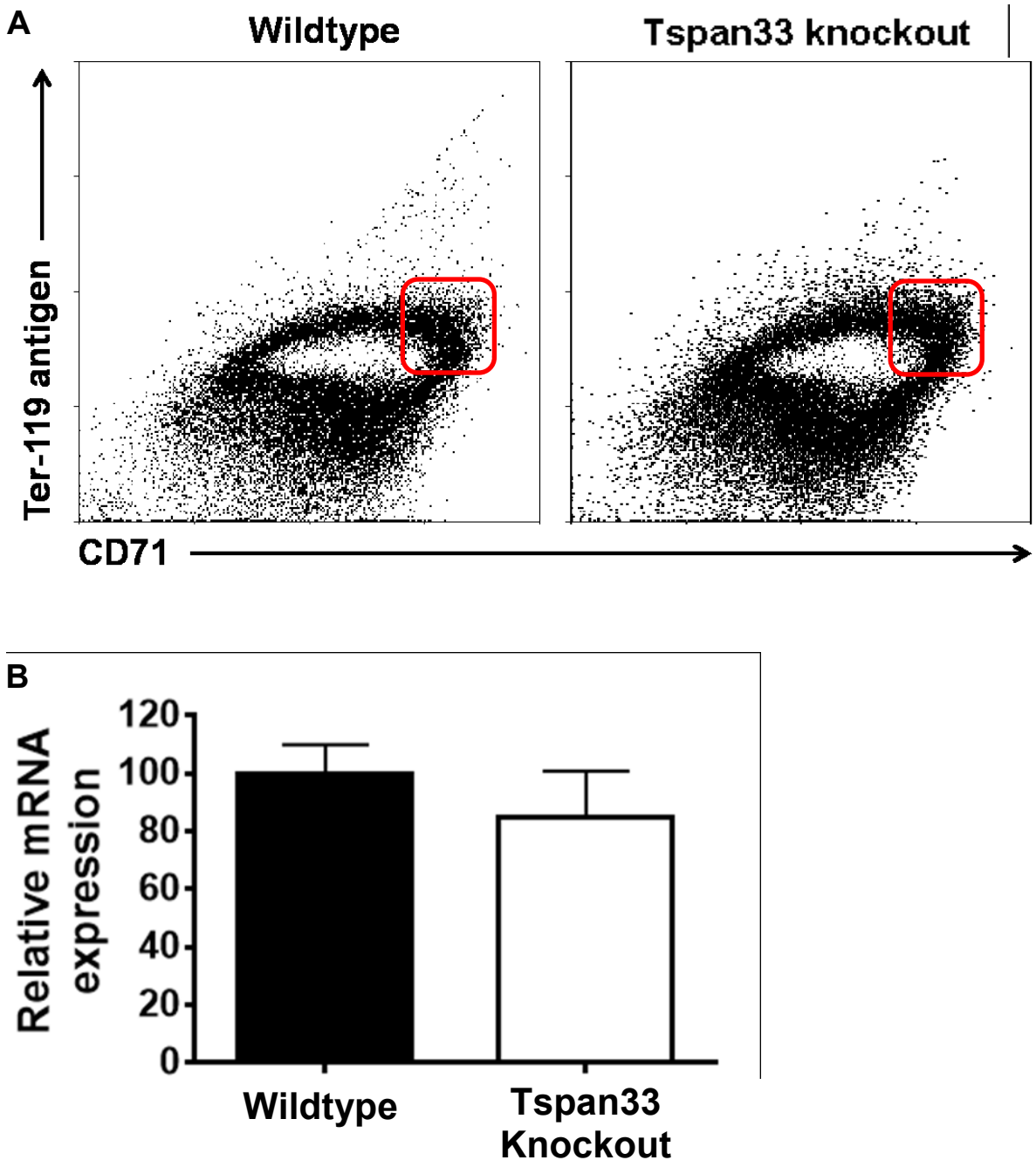

Figure 17. ADAM10 mRNA levels in Tspan33-deficient proerythroblasts are not significantly different from wildtype.

Foetal livers from E14.5 Tspan33 wildtype or knockout embryos were cultured *ex vivo* in medium that promoted erythroid differentiation. (A) Proerythroblast cells were sorted by their high Ter119 antigen and CD71 expression. The red boxes show the sorted population. (B) ADAM10 mRNA relative expression was assessed by real time PCR using Taqman fluorogenic probes. GAPDH was used to normalise results for loading and 18S used as a housekeeping reference gene. Real time PCR results were analysed using the delta CT method and shown as relative expression as a percentage of wildtype. n = 3, error bars represent the standard error of the mean.

4.2.4 Characterisation of ADAM10 levels during erythropoiesis.

As ADAM10 mRNA was expressed in Tspan33-deficient proerythroblast cells at similar levels to wildtype, it was important to check the cell surface levels of ADAM10 before and after this stage to ascertain at which point ADAM10 was lost from the Tspan33-deficient erythrocytes. To do this, bone marrow was flushed from wildtype and Tspan33 knockout mice and erythroblasts resolved by their expression of the transferrin receptor (CD71) and Ter-119 antigen (Figure 18 A). Three stages of erythropoiesis were gated, CFU-E cells (early), proerythroblasts (mid) and reticulocytes/red blood cells (late) and surface ADAM10 levels were analysed in each gate (Figure 18 B). There was no significant difference in ADAM10 surface levels between wildtype and Tspan33-deficient CFU-E cells but a significant decrease in Tspan33-deficient proerythroblasts and red blood cells (Figure 18 C). Interestingly ADAM10 surface levels in wildtype cells decreased dramatically between CFU-E and proerythroblasts suggesting that ADAM10 is naturally lost from cells during the progression of erythropoiesis. There is currently no known function of ADAM10 in erythropoiesis and so the cause and nature of this decrease in expression is unknown. This result, in combination with Figure 15 and Figure 16, suggests that ADAM10 may be a partner protein for Tspan33. Other tetraspanins, such as CD81 (which partners CD19), are required for the surface expression of their partner proteins and so when they are no longer expressed their partner protein does not reach the cell surface (Shoham et al., 2003).

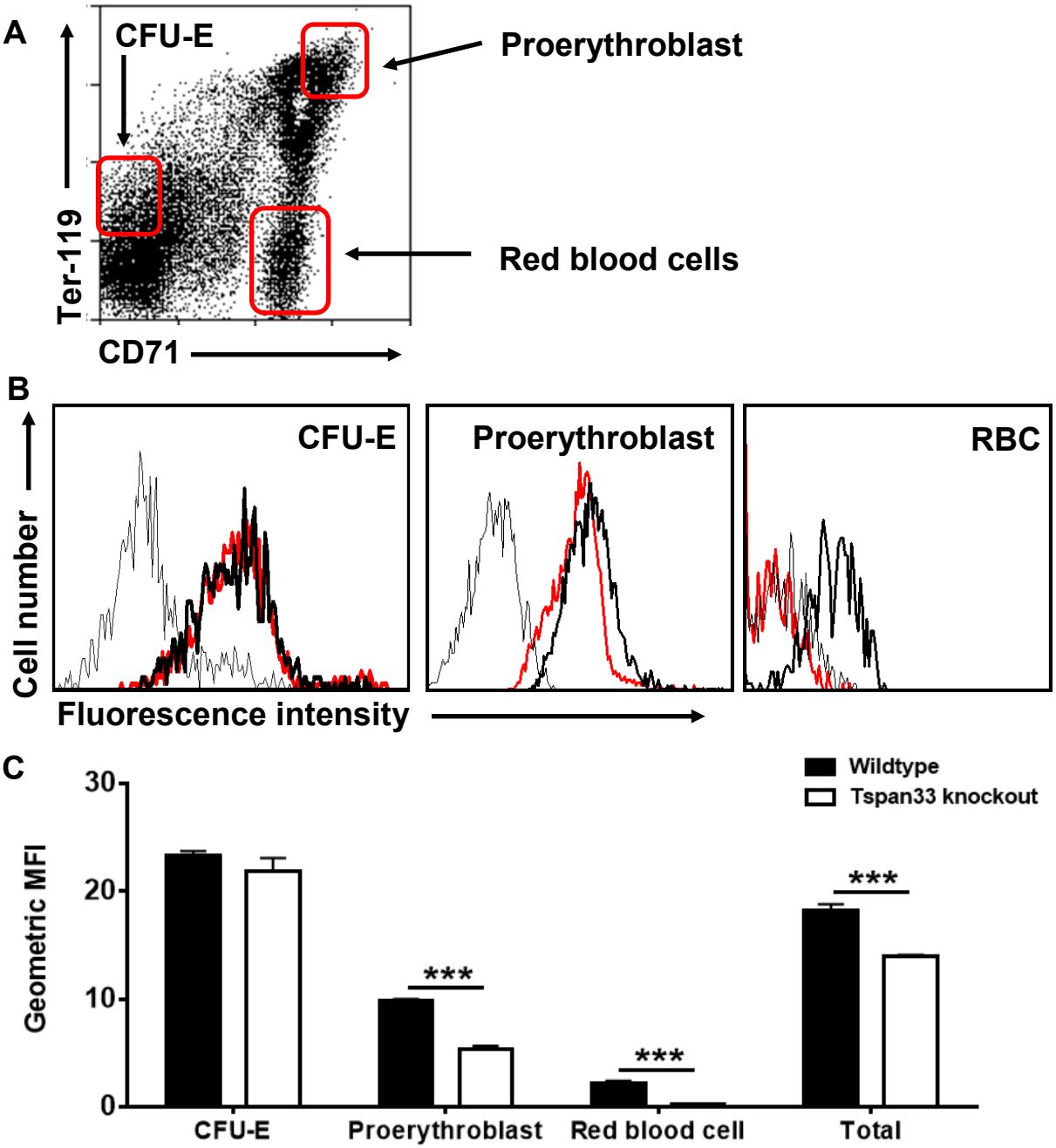

Figure 18. Characterisation of ADAM10 levels during erythropoiesis.

Bone marrow was flushed from the hind legs of adult mice and erythroblasts were visualised by flow cytometry. A. Staining specific to the different stages of erythropoiesis were isolated by the well characterised expression of Ter-119 antigen and CD71 (the transferrin receptor). B. Representative FACS plots of ADAM10 expression for each identified erythroblast stage indicated show wildtype in black and knockout in red. For simplicity only the control trace from wildtype staining is shown as the knockout control superimposed on the wildtype trace. C. ADAM10 levels on the cells in each gate were determined by geometric mean fluorescence intensity. n = 3 error bars represent standard error of the mean, significance determined by one way ANOVA followed by Tukey's post test.

4.2.5 Tspan33 is a member of the TspanC8 subfamily of tetraspanins.

A sequence alignment analysis comparing Tspan33 with all the other known mammalian tetraspanins highlighted that Tspan33 falls in a cluster with five other related tetraspanins (Figure 19). This cluster of tetraspanins, containing Tspan33, Tspan17, Tspan15, Tspan14, Tspan10 and Tspan5, are distinct from all the other mammalian tetraspanins in that they all contain 8 cysteines in their EC2 domain. Subsequently termed the TspanC8 tetraspanins, these tetraspanins were a relatively unstudied group. Apart from Tspan33 (Heikens et al., 2007), none of the other TspanC8 tetraspanins had been studied when this work started.

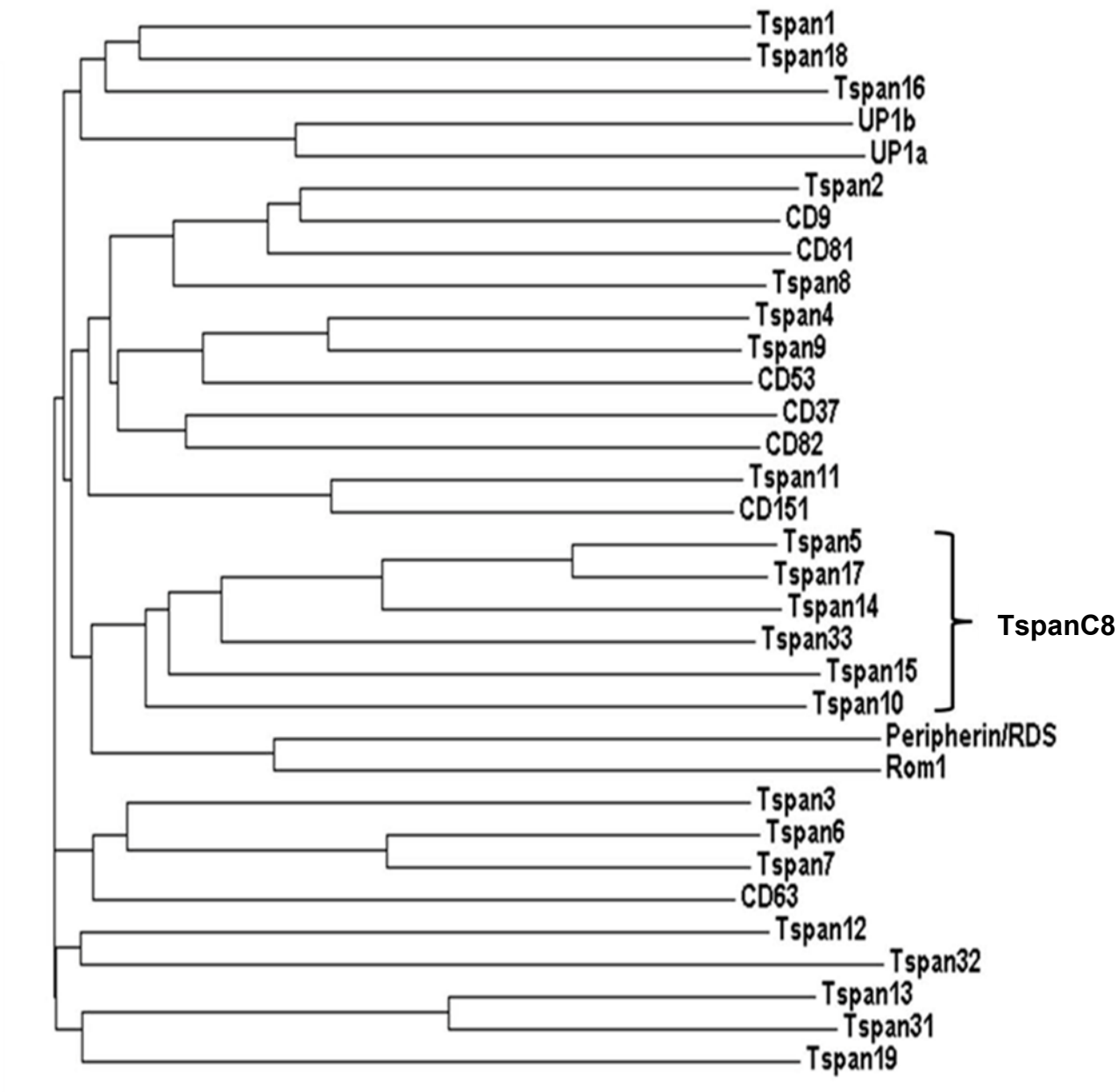

Figure 19. Tspan33 is part of the TspanC8 subfamily of tetraspanins.

The protein sequence of Tspan33 was compared to all the other mammalian tetraspanins by sequence alignment using Clustal Omega software. This program produced a dendrogram that places Tspan33 in a subfamily of tetraspanins that all contained 8 cysteines in their EC2 domains. Only the tetraspanins in this subfamily have this many cysteines. This figure was taken from Haining et al. (2012).

4.2.6 The TspanC8 subfamily of tetraspanins all associate with ADAM10.

Alongside this investigation of Tspan33 and ADAM10 in red blood cells, a cell line based assay, set up and carried out by another Tomlinson lab member, Dr Jing Yang, demonstrated an interaction between all six TspanC8 tetraspanins and ADAM10 (Appendix Figures 1 A). Furthermore this interaction appeared to promote the maturation of ADAM10 as evidenced by the increased amount of ADAM10 without its pro-domain in TspanC8 co-transfected cells (Appendix Figure 1 B). ADAM10 is produced in the cell as an immature pro-protease that requires a cleavage step, mediated by the furin proteases in the Golgi, to remove its inhibitory pro domain thus forming the mature protein. Immature ADAM10 has an apparent molecular weight of ~ 80kDa and mature ADAM10 has an apparent molecular weight of ~ 60 kDa. The other related tetraspanins that are known to share partner proteins are CD9 and CD81, which both associate with EWI-2 and EWI-F (Montpellier et al., 2011, Stipp et al., 2001, He et al., 2009). These results, in conjunction with two complementary publications, lead to a model in which the TspanC8 tetraspanins associate with ADAM10 in the ER, and this association promotes the trafficking of ADAM10 to the cell surface (Haining et al., 2012, Dornier et al., 2012, Prox et al., 2012).

4.2.7 The TspanC8 subfamily of tetraspanins have differential expression between red blood cells and platelets.

The next step in the investigation was to understand why the surface expression of ADAM10 was normal on Tspan33-deficient platelets and substantially reduced on red blood cells. As with most tetraspanins there is a lack of antibodies available for the TspanC8 tetraspanins, so the expression profiles of these proteins were assessed by real time PCR. As both platelets and red blood cells are anucleate cells, with very low mRNA levels, the TspanC8 expression profile was assessed in the progenitor cells: megakaryocytes for platelets and CFU-E and proerythroblast cells for red blood cells. Megakaryocytes, differentiated from adult mouse bone marrow, and proerythroblasts and CFU-E cells, sorted from mouse bone marrow, were lysed and all RNA extracted. cDNA was generated from extracted RNA and real time PCR used to assess relative levels of mRNA for each of the TspanC8 tetraspanins.

In proerythroblasts, Tspan33 was the most highly expressed TspanC8 tetraspanin with very little or no expression of the other tetraspanins (Figure 20 A). It is important to note that Tspan33 mRNA was detected in the knockout sample because the real time PCR probe does not distinguish between the mRNA products from wildtype and gene-targeted Tspan33 loci. Therefore in Tspan33-deficient proerythroblasts, that have minimal expression of any TspanC8 tetraspanins, ADAM10 cannot egress from the ER thus explaining the loss of ADAM10 from Tspan33-deficient red blood cells. In megakaryocytes, however, Tspan14 was the most highly expressed TspanC8 tetraspanin and Tspan33 was comparably expressed at very low levels (Figure 20 B). This supports the conclusion from the first chapter of this thesis that proposes that Tspan33 is not expressed in mouse platelets. In addition it suggests that ADAM10

surface expression is normal in Tspan33-deficient platelets because the megakaryocytes have their normal complement of TspanC8 tetraspanins. Finally, in CFU-E cells, Tspan33 and Tspan14 were expressed with the additional expression of Tspan5 (Figure 20 C). This result likely explains the normal surface expression of ADAM10 in this cell type (as shown in Figure 18), assuming that the remaining Tspan14 and Tspan5 can compensate for the loss of Tspan33, and additionally is reflective of the shared myeloid lineage of red blood cells and platelets.

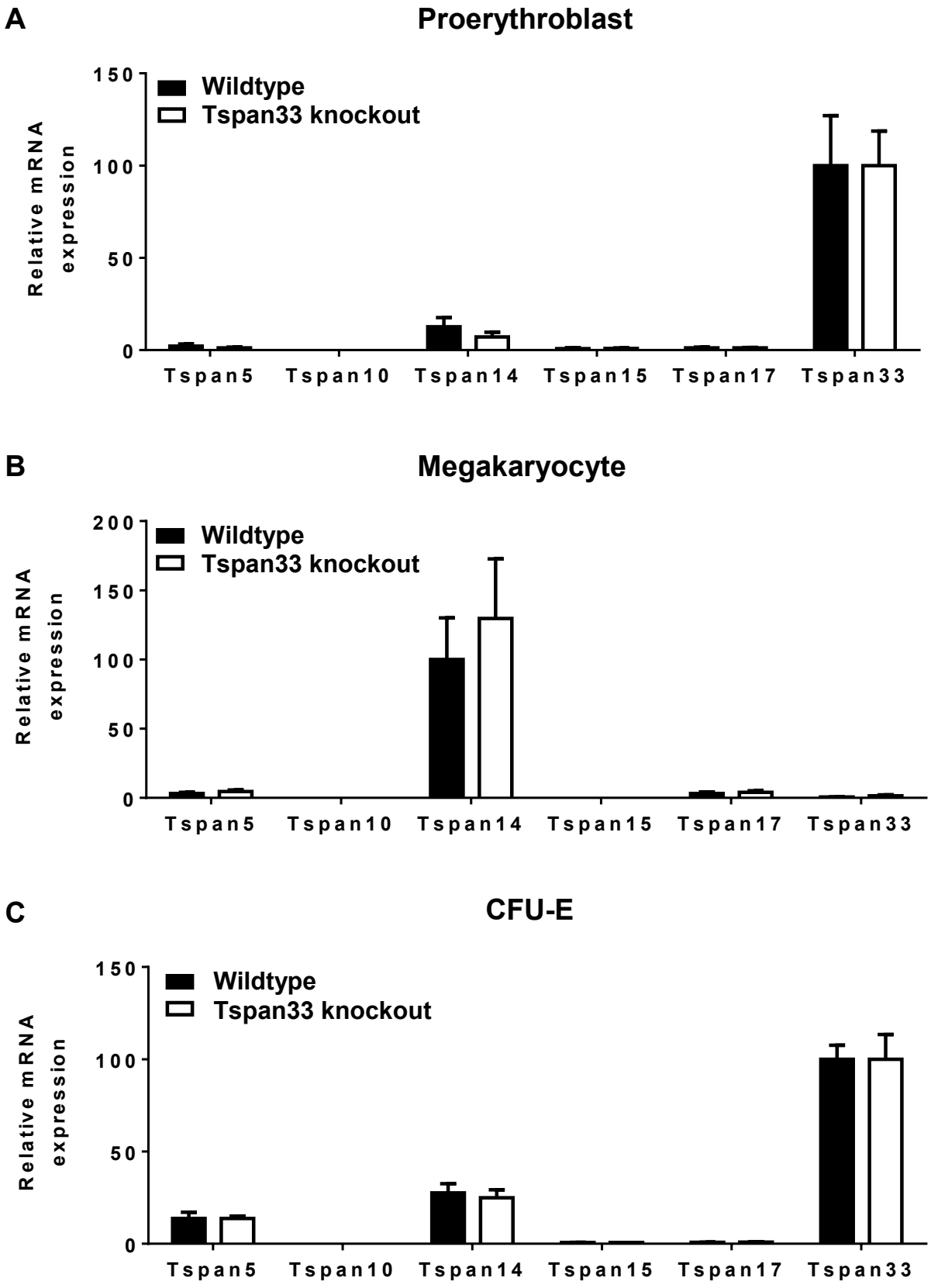
A
Proerythroblast
Wildtype
Tspan33 knockout
Relative mRNA expression
150
100
50
0
Tspan5
Tspan10
Tspan14
Tspan15
Tspan17
Tspan33
B
Megakaryocyte
Wildtype
Tspan33 knockout
Relative mRNA expression
200
150
100
50
0
Tspan5
Tspan10
Tspan14
Tspan15
Tspan17
Tspan33
C
CFU-E
Wildtype
Tspan33 knockout
Relative mRNA expression
150
100
50
0
Tspan5
Tspan10
Tspan14
Tspan15
Tspan17
Tspan33

Figure 20

Figure 20. Tspan33 in not expressed in megakaryocytes but is highly expressed in proerythroblasts.

Wildtype and Tspan33-deficient megakaryocytes were differentiated *in vitro* from progenitors collected from adult bone marrow. Wildtype and Tspan33-deficient CFU-E and proerythroblast cells were sorted from adult bone marrow with cells from three mice pooled for each experiment. A. Megakaryocytes. B. Proerythroblasts. C. CFU-E cells. cDNA, generated from extracted RNA from each cell type, was used as the template for real time PCR studies that used TaqMan fluorogenic probes for each of the TspanC8 tetraspanins. GAPDH was used to normalise results for loading and 18S used as a housekeeping reference gene. Real time PCR results were analysed using the delta CT method and shown as relative expression as a percentage of the most highly expressed tetraspanin in each cell type. n = 3 - 4, error bars represent the standard error of the mean.

4.2.8 Characterisation of erythropoiesis in Tspan33 knockout mice.

As previously reported, the Tspan33 knockout mouse have a red blood cell phenotype of basophilic macrocytic anaemia in aged animals (Heikens et al., 2007). The cause of this phenotype appeared to be due to defective responses of erythroid progenitors to erythropoietin. Analysis of the progression of erythropoiesis *in vivo* in the Tspan33 knockout mouse was not published in the paper in which the anaemia was reported. Interestingly, despite the appearance of basophilic red blood cells only being reported in 30 % of 12 week old mice (Heikens et al., 2007), the decrease in ADAM10 detected by flow cytometry was found in 100 % of knockout animals screened. The next step in this investigation was to analyse *in vivo* erythropoiesis by flow cytometry with the aim of assessing the sizes of the different erythroid cell populations. Should a particular compartment be enriched or diminished, this would indicate a stage of erythropoiesis to focus on to discover a role, if any, for ADAM10. Mice aged 12 weeks and mice aged 24 were both assessed to ensure any progressive defect was detected.

Erythropoiesis was assessed in directly extracted cells from the bone marrow (Figure 21) and the spleen (Figure 22), and in neither tissue were abnormalities found. No significant changes in the proportions of the different erythroid cell types were found in cells from the bone marrow (Figure 21 B, C and E) or the spleen (Figure 22 B, C and E). Furthermore, no difference was found between the two age groups of mice, so their results were grouped and displayed together. This failure to detect a defect in erythropoiesis suggests that the reported phenotype, which was observed in only 30 % of mice (Heikens et al., 2007), may have been largely lost during the re-derivation and colony expansion that was carried out before the mice were analysed in our lab.

This theory is also consistent with the loss of phenotype on some genetic backgrounds (Schickwann Tsai, personal communication).

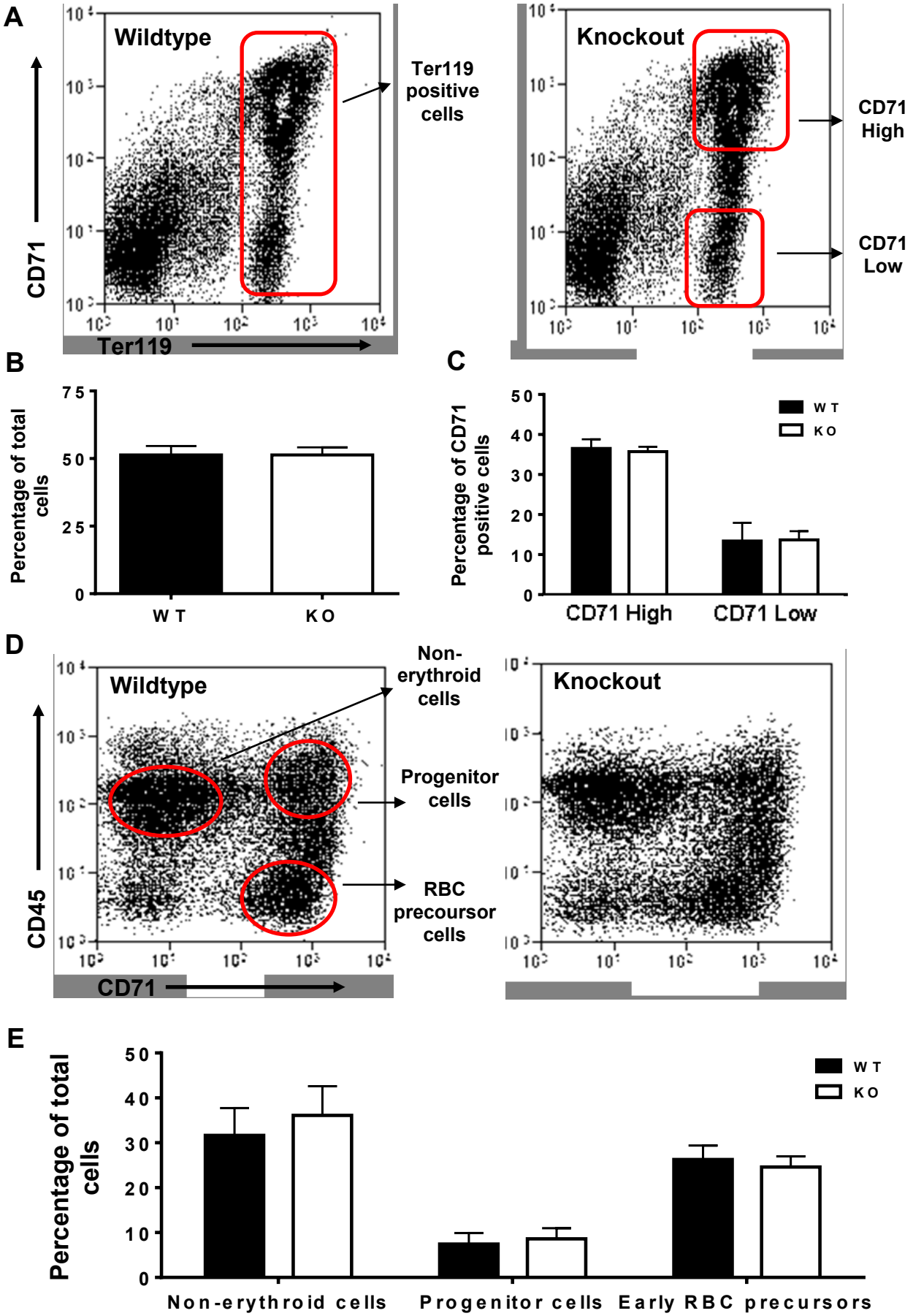
A
Wildtype
Ter119 positive cells
CD71
Ter119
Knockout
CD71 High
CD71 Low
B
Percentage of total cells
75
50
25
0
WT
KO
C
Percentage of CD71 positive cells
50
40
30
20
10
0
WT
KO
CD71 High
CD71 Low
D
Wildtype
Non-erythroid cells
Progenitor cells
RBC precoursor cells
CD45
CD71
Knockout
E
Percentage of total cells
50
40
30
20
10
0
WT
KO
Non-erythroid cells
Progenitor cells
Early RBC precursors

Figure 21

Figure 21. Erythroid cell populations appear normal in Tspan33-deficient bone marrow.

Bone marrow cells were flushed from wildtype and Tspan33 knockout mice into 10 % FCS in PBS. Cells were blocked with anti-CD16 antibody for 5 min, then stained with an erythroid antibody cocktail (including single colour controls) for 30 min on ice in the dark. Erythroid cells were isolated by flow cytometry after colour compensation A. Representative flow cytometry plots of CD71 and Ter119 stained erythroid committed cells from either wildtype or Tspan33 knockout mice B. percentage of Ter119 positive cells present in the CD71 and Ter119 flow cytometry plots. C. Percentage of cells expressing Ter119 that have high or low CD71 expression D. Representative flow cytometry plots of CD45 and CD71 stained progenitor cell populations from either wildtype or Tspan33 knockout mice E. Progenitor cell populations in the bone marrow identified using CD71 and CD45 staining. n = 3, error bars represent standard error of the mean. Statistical significance in B and C judged by an unpaired Student's t-test and in E by two way ANOVA followed by Bonferroni post test. Erythroid cocktail: Ter119-FITC, CD71-PE, cKit-PECy5 and CD45 APC.

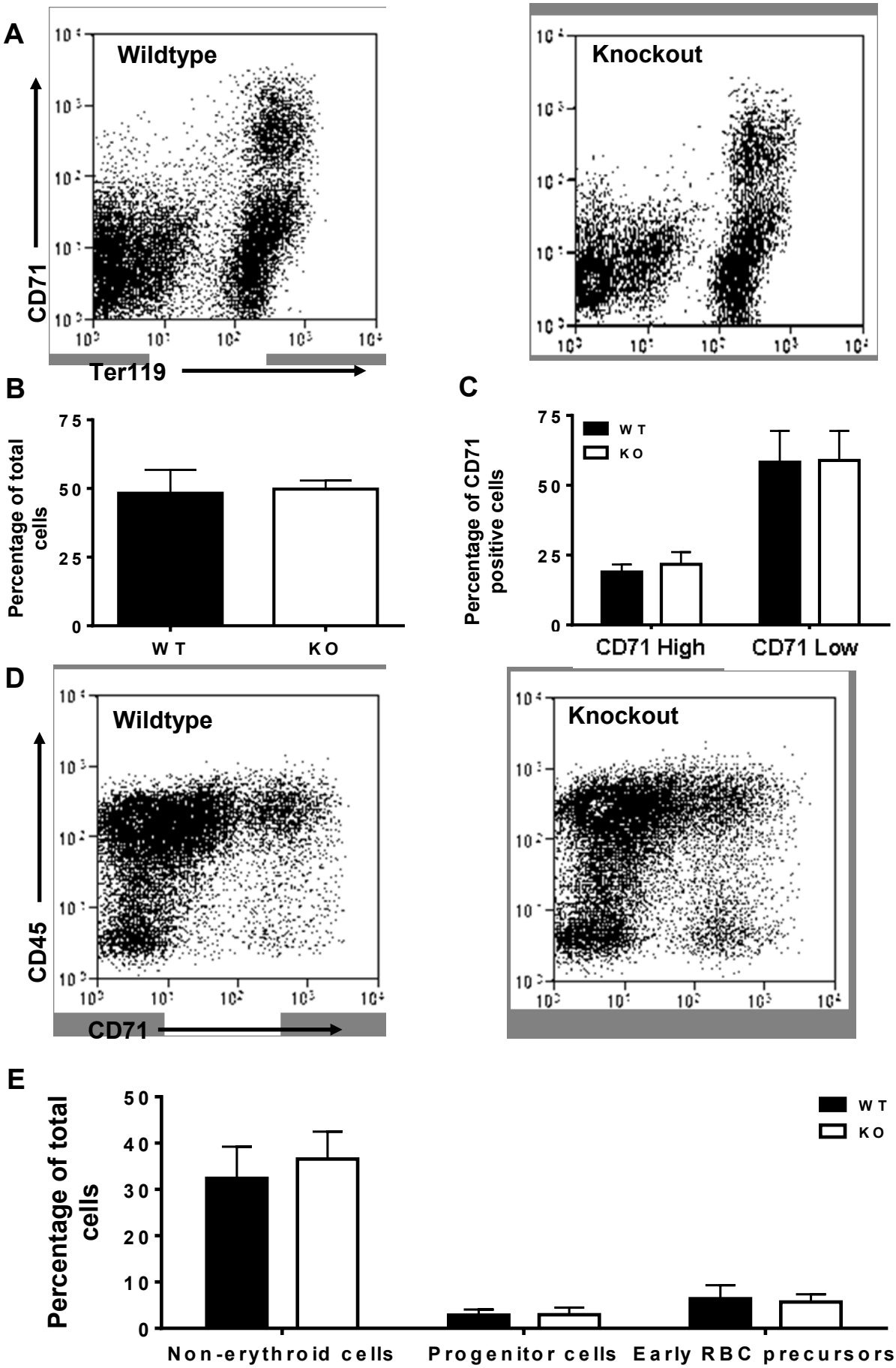
A
Wildtype
Knockout
CD71
Ter119
B
Percentage of total cells
75
50
25
0
WT
KO
C
Percentage of CD71 positive cells
WT
KO
CD71 High
CD71 Low
D
Wildtype
Knockout
CD45
CD71
E
Percentage of total cells
50
40
30
20
10
0
WT
KO
Non-erythroid cells
Progenitor cells
Early RBC precursors

Figure 22

Figure 22. Erythroid cell populations appear normal in Tspan33-deficient spleen.

Spleen cells were taken from wildtype and Tspan33 knockout mice into 10 % FCS in PBS. Cells were blocked with anti-CD16 antibody for 5 min, then stained with an erythroid antibody cocktail (including single colour controls) for 30 min on ice in the dark. Erythroid cells were isolated by flow cytometry after colour compensation A. Representative flow cytometry plots of CD71 and Ter119 stained erythroid committed cells from either wildtype or Tspan33 knockout mice B. percentage of Ter119 positive cells present in the CD71 and Ter119 flow cytometry plots. C. Percentage of cells expressing Ter119 that have high or low CD71 expression D. Representative flow cytometry plots of CD45 and CD71 stained progenitor cell populations from either wildtype or Tspan33 knockout mice E. Progenitor cell populations in the spleen identified using CD71 and CD45 staining. n = 3, error bars represent standard error of the mean. Statistical significance in B and C judged by an unpaired Student's t-test and in E by two way ANOVA followed by Bonferroni post test. Erythroid cocktail: Ter119-FITC, CD71-PE, cKit-PECy5 and CD45 APC.

4.3 Discussion

Presented here is an investigation into the loss of ADAM10 from Tspan33-deficient red blood cells. The initial observation of this project was that the surface levels of the sheddase ADAM10 were reduced on Tspan33-deficient red blood cells and the aim of this project was to further characterise and understand this loss of ADAM10. The final conclusion of this project was that the reduction in ADAM10 at the cells surface of red blood cells can be seen in the Tspan33-deficient proerythroblast precursor cells despite their normal production ADAM10 mRNA. In addition Tspan33 was found to be part of a novel subfamily of tetraspanins termed the TspanC8 tetraspanins. Work published by our lab and others demonstrated that all the members of this subfamily interact with and promote the trafficking and maturation of ADAM10 (Haining et al., 2012, Prox et al., 2012, Dornier et al., 2012). Finally erythropoiesis was assessed in the Tspan33 knockout mouse but no clear defect could be seen in the approach used.

The discovery that Tspan33 was part of a subfamily of related tetraspanins, all of which share the same partner protein, was not a new concept in tetraspanin biology as both CD9 and CD81 interact with the Ig superfamily proteins EWI-2 and EWI-F (Stipp et al., 2001). Additionally, CD9 and CD81 are able to compensate for each other, with CD81 partially rescuing the fusion defect in CD9 null oocytes (Kaji et al., 2002), and lymphatic defects and defects in macrophage migration and protease production in the lung only being revealed upon knockout of both genes in mice (Iwasaki et al., 2013, Takeda et al., 2008). The existence of the structurally defined TspanC8 subfamily has implications for research into the function of other tetraspanins. Other subfamilies of related tetraspanins were evident from the

dendrogram of mammalian tetraspanins and therefore these tetraspanins may too share partner proteins. As such there may be significant compensation between these tetraspanins in model systems thus masking any phenotype in knockout/knockdown experiments.

In terms of ADAM10 research, the TspanC8 subfamily represents a previously unknown aspect of ADAM10 regulation and opens exciting new avenues in ADAM10 research. For example the development of therapeutics targeted to ADAM10 have been hindered by the ubiquitous nature of the protein and the likely toxic side effects of targeting ADAM10 on every cell in the body (Saftig and Reiss, 2011). The TspanC8 tetraspanins, however, appear to have differential expression, and so targeting of a specific TspanC8/ADAM10 complex could confer increased tissue specificity for any treatment. The question of why one protein has six tetraspanins with which it associates remains unanswered. The current hypothesis to explain this phenomenon is that the association of ADAM10 with the TspanC8 tetraspanins can influence the substrate specificity of ADAM10 by regulating its cellular localisation and potentially further localisation in the cell membrane. Evidence from Dornier at al. (2012) suggests that Tspan10 is largely expressed on intracellular compartments and so could target ADAM10 away from the cell surface. Additionally this paper also presents evidence that Tspan5 and Tspan14 can promote the cleavage of the ADAM10 target protein Notch more effectively than Tspan15. Further research is required before the purpose of the association between TspanC8 tetraspanins and ADAM10 can be fully understood and their full therapeutic impact appreciated.

Another question raised by this project is what, if any, is the function of ADAM10 in erythropoiesis. There are currently no published studies of ADAM10 in erythropoiesis

and there is also no published data on an erythroid specific ADAM10 knockout mouse. ADAM10 expression appeared to sharply reduce during wildtype erythropoiesis which would suggest that it may have no function in mid to late erythropoiesis. It is interesting, however, that Tspan33 knockout mice were published to have a defect in erythropoiesis and that the red blood cells were found to have a defect in ADAM10 expression. As the Tspan33 knockout mouse is a full knockout and erythropoiesis is supported and regulated by the surrounding bone marrow microenvironment (Chasis and Mohandas, 2008), the Tspan33-deficient stromal cells and erythroid associated macrophages could be the cell type in which ADAM10 function is critically defective for erythropoiesis. Further research would be required to understand the function of this protein in erythropoiesis and thus if its loss could be the cause of the anaemia published in the Tspan33 knockout mouse.

CHAPTER V: FUNCTIONAL STUDIES OF THE TSPAN9 KNOCKOUT MOUSE AND TSPAN9-DEFICIENT PLATELETS

5.1 Introduction

Tspan9 is a 239 amino acid tetraspanin that was first identified as a platelet tetraspanin in 2007 by its presence in a mouse megakaryocyte SAGE library and in a proteomic analysis of human platelet transmembrane proteins (Senis et al., 2007, Lewandrowski et al., 2009a). Tspan9 was confirmed at the protein level as expressed in both mouse and human platelets using an antibody made by our group in 2009 (Protty et al., 2009) that recognises the C-terminal tail. As well as confirming the expression of Tspan9 on megakaryocytes and platelets, this publication also quantified the relative amount of Tspan9 on human platelets. Tspan9 was found to be expressed at 6 % of the levels of the highly expressed platelet tetraspanin CD9 giving it a copy number of around 2800 (Protty et al., 2009). Prior to this publication Tspan9 was an unstudied tetraspanin. It appeared to be an interesting tetraspanin in terms of platelet biology as it was relatively specific to platelets, in comparison to other mouse tissues. Additionally, the availability of an antibody against Tspan9 was an advantage as many tetraspanins do not have antibodies available for their study (Protty et al., 2009).

The aim of this project was to extend the work of Protty et al. and functionally characterise Tspan9 on platelets using the Tspan9 knockout mouse. This unpublished knockout had been generated by Texas A and M Institute for Genomic Medicine prior to the start of the project.

5.2 Results

5.2.1 Confirmation of the generation of Tspan9 knockout mice

The Tspan9 knockout mouse was generated using gene trapping technology at the Texas A and M Institute for Genomic Medicine. The gene trapping method prevents full transcription of the targeted gene by forcing a splicing event early in transcription between endogenous exon mRNA and the mRNA of the gene trap cassette. Thus transcription of any downstream exons is prevented. In this case the commonly used β-geo gene trap cassette was introduced into C57BL/6 ES cells by retroviral infection. Infection is the favoured method over electroporation of plasmid DNA as it significantly reduces the possibility of multiple insertions of the gene trap cassette and favours the incorporation of the cassette into the 5' end of targeted genes (Wiles et al., 2000, Skarnes, 2000). The β-geo gene trap cassette consists of (from the 5' end) a splice acceptor site followed by a β-galactosidase and neomycin phosphotransferase gene fusion transcript and a polyadenylation sequence (Friedrich and Soriano, 1991).

In the ES cells used to generate the Tspan9 knockout mouse, this cassette had inserted between the first two exons of the gene, upstream of the other eight Tspan9 exons and in the 5' untranslated region of the gene (the translation start site is found in the third exon). The consequent fusion transcript generated from 'trapped' Tspan9 genes contained just the mRNA of the first exon and the β-geo gene trap cassette. A diagram of the insertion site and genotyping strategy can be seen in Figure 23.

Whilst gene trapping is a highly successful knockout mouse generation method, it is possible that the transcription machinery could bypass the splice acceptor site

introduced by the gene trap cassette (Forrai and Robb, 2005). Therefore it was important to check the Tspan9 protein levels in knockout animals. Western blotting of platelet and lung (where Tspan9 is also expressed) lysates from the mice confirmed the lack of Tspan9 protein in knockout animals and showed reduced protein levels in the heterozygote in comparison to wildtype animals (Figure 24).

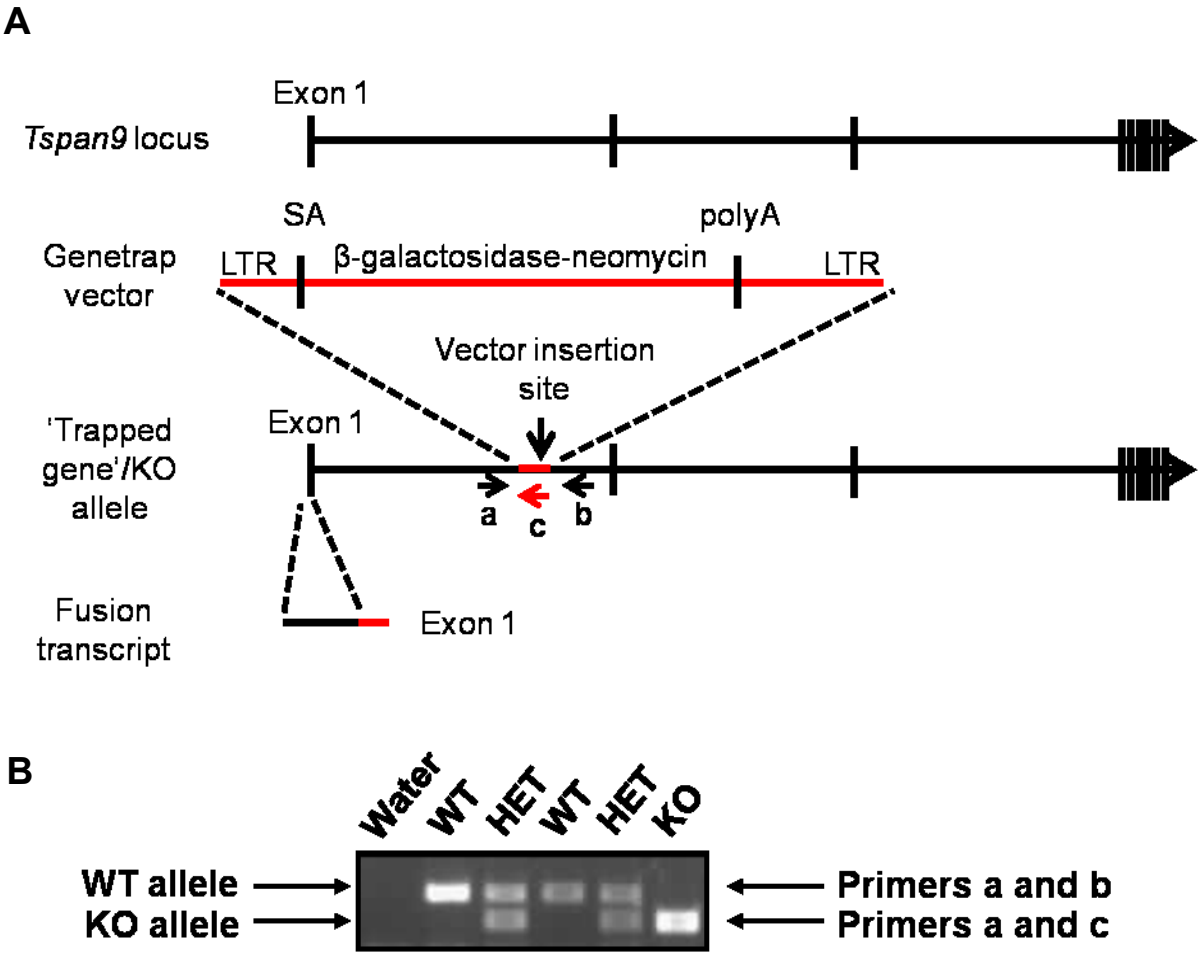

Figure 23. Gene trap technology was utilised to generate the Tspan9 knockout mouse.

A. The common gene trap cassette β-geo was randomly incorporated into the Tspan9 gene between the first two exons using retroviral infection of C57BL/6 ES cells. The splice acceptor site in the cassette and the subsequent poly A tail causes termination of transcription before any of the coding region of the Tspan9 gene is transcribed. B. PCR was the approach selected for genotyping Tspan9 knockout animals. Two primers (denoted a and b in Figure.1A) specific for the Tspan9 gene either side of the cassette insertion site were used to amplify WT transcripts. The Tspan9 forward primer (a) in conjunction with a reverse primer specific for the β-geo cassette (c) were used to amplify gene trapped transcripts. Abbreviations: LTR – long terminal repeat, SA – splice acceptor site, Poly-A – polyadenylation sequence,.

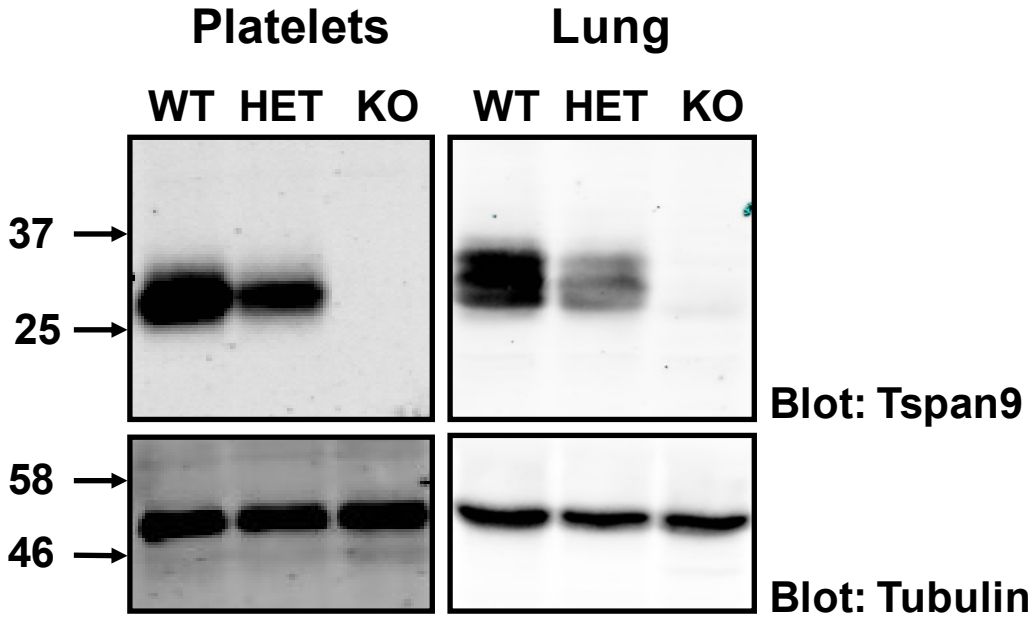

Figure 24. Confirmation that Tspan9 knockout mice do not express Tspan9 protein.

Lysates of 1 x 10^7 platelets or 1 mg of lung tissue per lane were separated on a 12 % polyacrylamide gel and western blotted with rabbit anti-Tspan9 antibody and mouse anti-tubulin.

5.2.2 Tspan9 knockout mice are born at expected frequencies.

The health and development of some knockout mice can be affected by the loss of their targeted protein, as is the case for the tetraspanin CD151, the knockout mouse for which develops spontaneous nephritis (Sachs et al., 2006). This however was not the case for the Tspan9 knockout mice. These mice were indistinguishable from their wildtype littermates in size (as measured by weight, Figure 25) and health. Tspan9 knockout pups were born at Mendelian frequencies from heterozygote/heterozygote breeding pairs (Table 9). The average litter size for heterozygote crosses was 7 and this was also the case for knockout/knockout breeding pairs which had a litter size range of 4 - 10 across 5 litters (data not shown). The apparent normality of the Tspan9 knockout mice continued throughout the aging process with Tspan9 knockouts surviving to 52 weeks without the development of any obvious ill health.

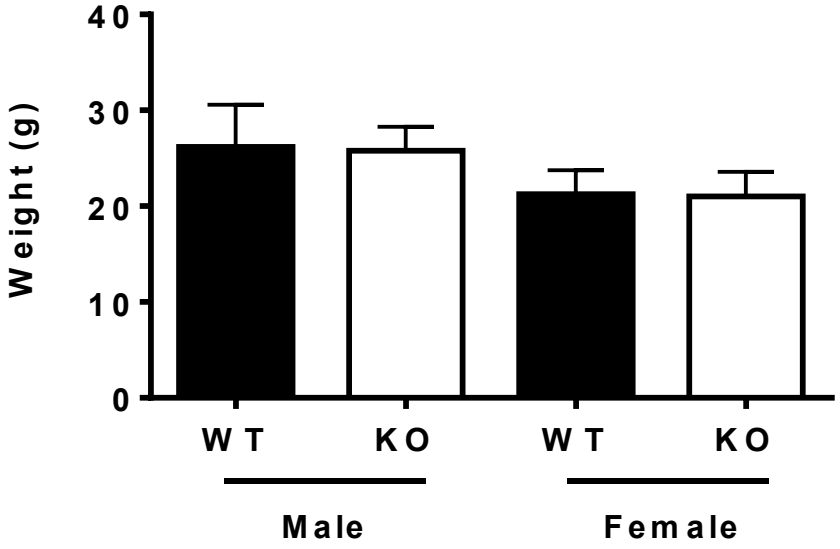

Figure 25. Tspan9 knockout mice have similar weights to their wildtype littermates.

Adult mice between the ages of 8 - 16 weeks were weighed and knockout animals were compared to wildtype littermates of the same sex (males n = 10, females n = 9). No significant difference was seen between either group as judged by a paired Student's t-test. Error bars represent standard error of the mean.

Genotype	Number	Observed ratio	Expected ratio
Wildtype	116	0.29	0.25
Heterozygote	196	0.49	0.5
Knockout	85	0.21	0.25
Total	**397**	**1**	**1**

Table 9. Tspan9 knockout mice are born at expected Mendelian frequencies.

Total numbers of mice of each genotype produced from heterozygote/heterozygote breeding pairs were counted. These numbers represent 65 different litters from 20 different breeding pairs. A Chi^2 test found no significant difference between observed and expected numbers of each genotype.

5.2.3 Tspan9 knockout mice do not have any gross morphological defects in their kidneys, liver or lungs.

Aside from a high expression in platelets, Tspan9 was also detected in the lungs, liver and kidney (and other organs but to a lesser extent) in mice by western blot (Protty et al., 2009). As the function of the protein was unknown, it was possible that it was required for the proper development and/or maintenance of the architecture of the organs in which it was found. To check this, paraffin embedded sections of formalin fixed kidney, lung and liver were stained with haematoxylin and eosin to allow an assessment of the gross and finer structures of each organ. The sections were prepared, stained and analysed by pathologist Hanna Romanska, and no differences were found between the organs of wildtype and knockout animals (Figure 26 and Figure 27).

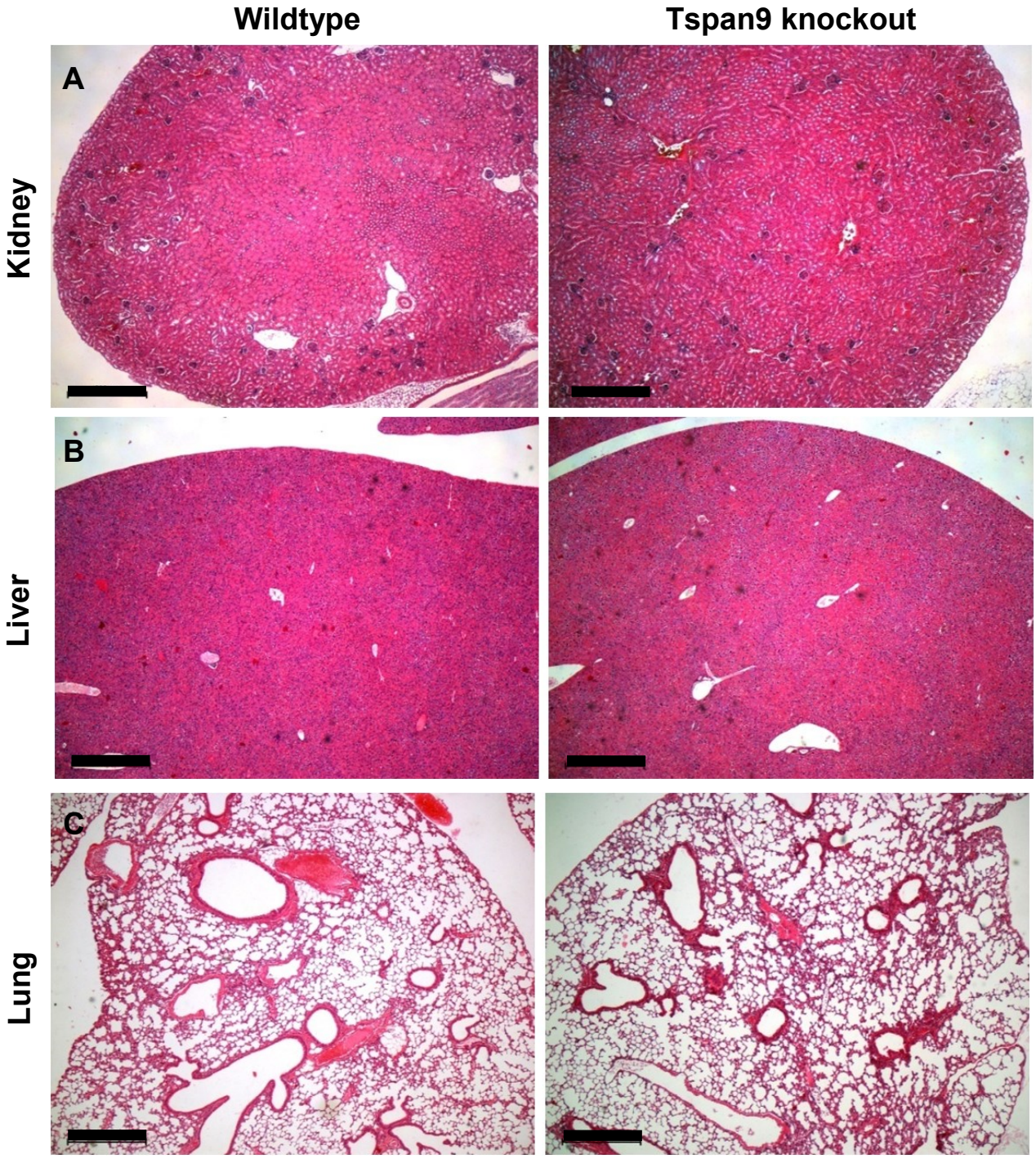

Figure 26. The gross morphology of the kidney, liver and lung remains normal in Tspan9 knockout mice.

Whole organs (A. Kidney, B. Liver, C. Lung) fixed in Formalin were paraffin embedded, sectioned and stained with Haematolyxin and Eosin stain. Scale bar represents 500 μm, images are representative of n = 3. Sections prepared and imaged by Hanna Romanska.

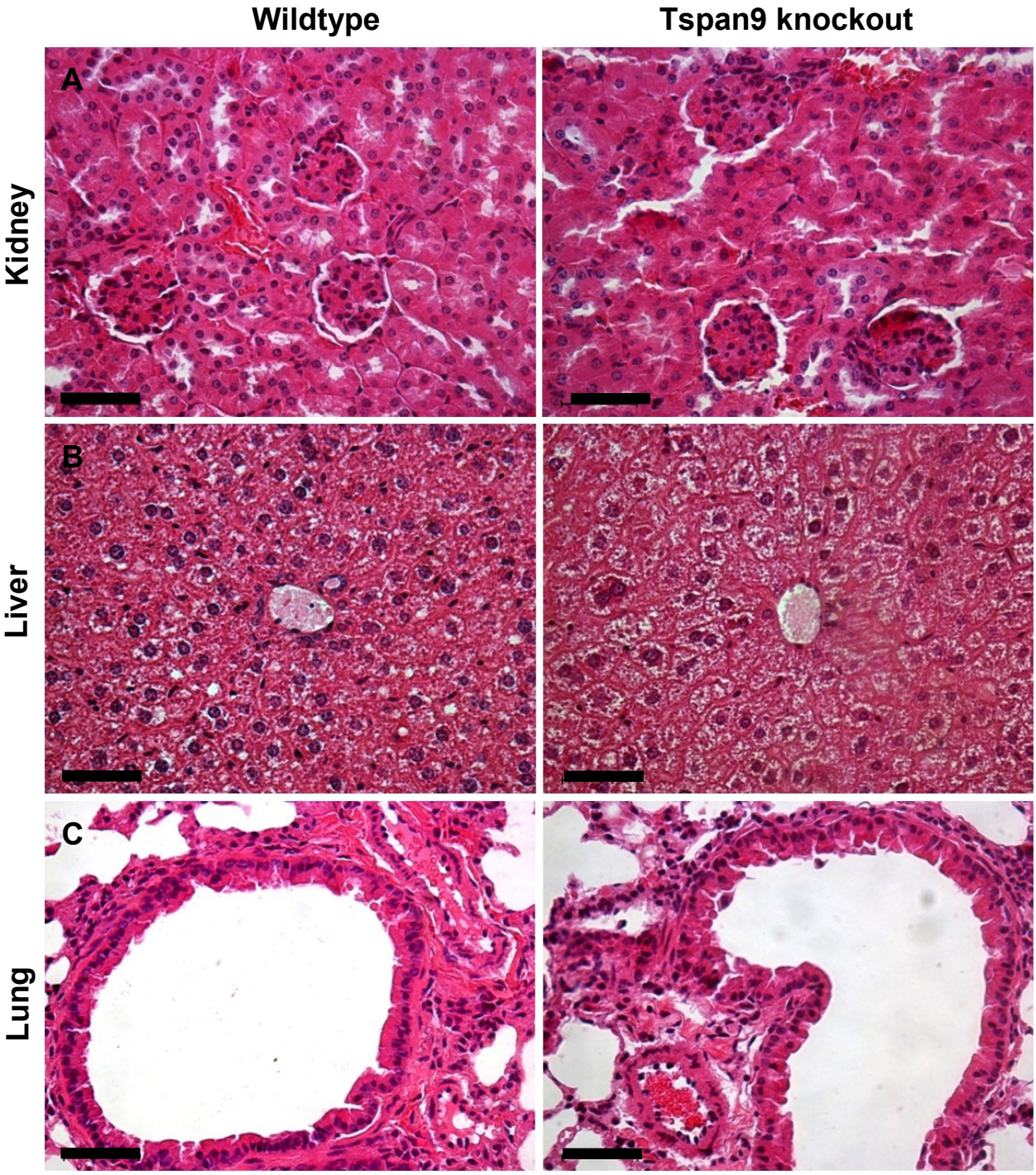

Figure 27. The general structure of the kidney, liver and lung remains normal in Tspan9 knockout mice.

This figure shows representative images of the tissue sections in Figure 26 imaged at higher magnification. A. Kidney cortex B. Liver around a lobule central vein C. Lung around the bronchus. The higher magnification allowed closer inspection of the finer structure of each organ. Scale bar represents 50 μm. Images representative of n = 3. Sections prepared and imaged by Hanna Romanska.

5.2.4 Tspan9 knockout mice have a significant reduction in heart to body weight ratio.

In addition to analysing the structure of the kidneys, liver and lung in the Tspan9 knockout mice, tissue sections from wildtype mice were stained with Tspan9 antibody and the Tspan9 knockout tissues as a control. Staining of Tspan9 in wildtype heart demonstrated Tspan9 expression in the small vessels and capillaries in the tissue (Figure 28 A), despite Tspan9 not appearing highly expressed in the heart by western blot. To assess the maintenance of the heart tissue without Tspan9 the 'dry' weight (not containing any exogenous blood) of whole hearts from Tspan9 wildtype and Tspan9 knockout mice was measured. In this measure Tspan9 knockout mice had a small but significant decrease of 7 % in their heart to body weight ratio (Figure 28 B). The cause of this decrease or indeed its effect on heart function is unknown, although a potential hypothesis is that the small vessels in which Tspan9 is expressed are in some way defective in Tspan9 knockout mice. A more detailed analysis of Tspan9 knockout hearts are required to understand this defect further, but fall outside the remit of this project. Additional sections of brain, lung, spleen, liver, skin and bone marrow stained with Tspan9 antibody can be seen in Appendix Figure 2. Organ sectioning and staining was done by Hanna Romanska.

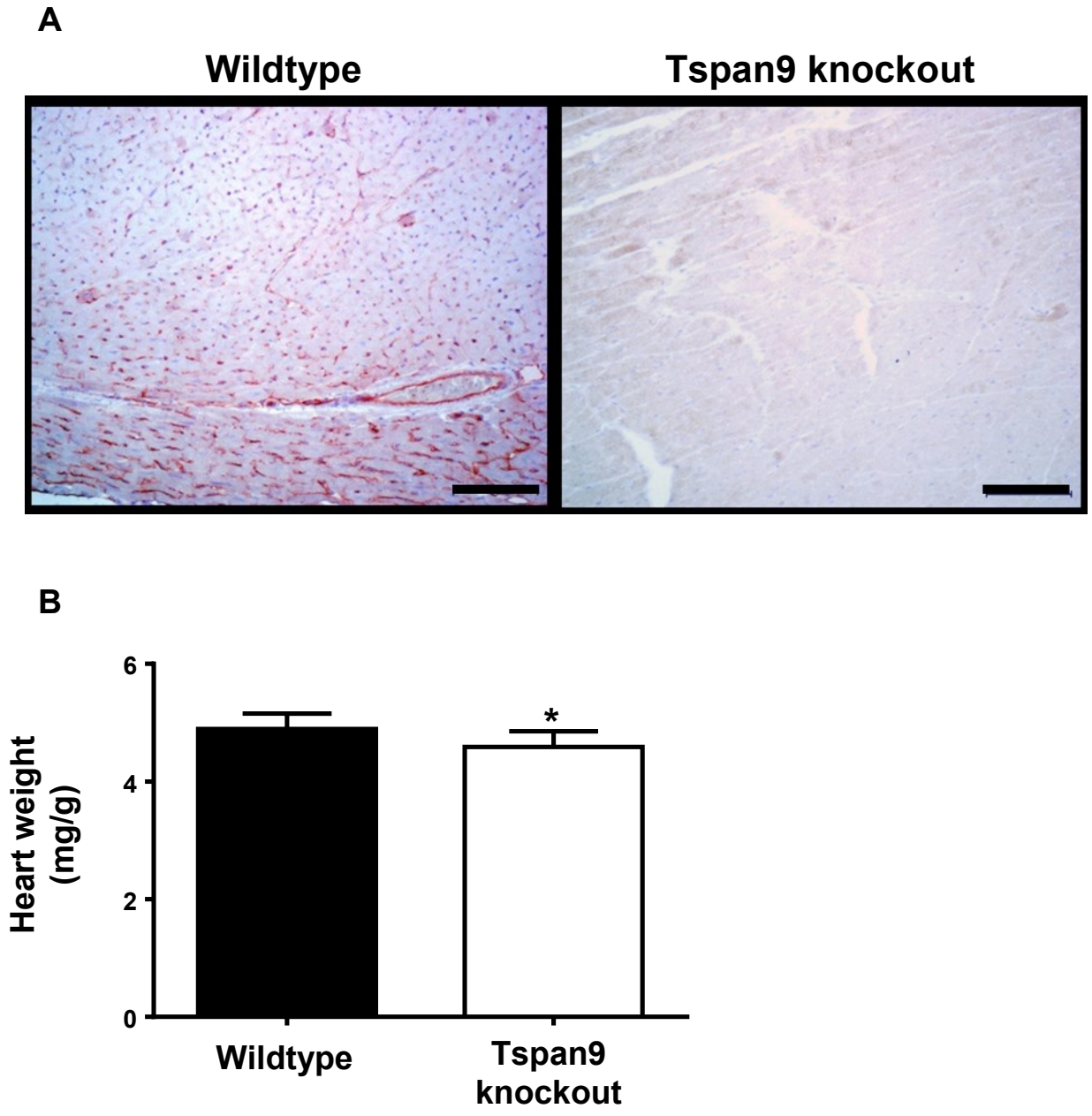

Figure 28. Tspan9 knockout mice have a significant reduction in heart to body weight ratio.

A. Formalin fixed whole hearts were sectioned and stained with Tspan9 antibody by Hanna Romanska. Scale bar represents 100 μm. B. Tspan9 knockout mice had a significant reduction in heart weight, shown as heart weight in mg per g of whole mouse weight. n = 9 and error bars represent the standard error of the mean. Statistical significance was judged by an unpaired Student's t-test.

5.2.5 The platelet count and other whole blood parameters of Tspan9 knockout mice were normal in comparison to wildtype.

Before beginning the focussed analysis of Tspan9-deficient platelets a gross assessment of the different blood cell groups was made using whole blood counts from wildtype and Tspan9 knockout mice. Tspan9 knockout mice had normal platelet counts and normal platelet size. In addition, other blood cells also appeared unaffected by Tspan9 deletion as all other assessed blood parameters from Tspan9 knockout mice fell within the normal ranges and were not significantly different from wildtype (Table 10).

Blood parameter	Wildtype	Knockout	p value
Platelet count ($10^3/mm^3$)	891.97 +/- 158.97	923.78 +/- 280.78	0.69
Platelet volume (μm^3)	5.36 +/- 0.25	5.35 +/- 0.27	0.84
Plateletcrit (%)	0.29 +/- 0.07	0.29 +/- 0.07	0.83
White blood cell count ($10^3/mm^3$)	8.24 +/- 3.94	8.3 +/- 4.04	0.96
Red blood cell count ($10^6/mm^3$)	10.29 +/- 1.12	10.08 +/- 0.73	0.46
Haemoglobin concentration (g/dl)	9.145 +/- 0.61	9.34 +/- 0.64	0.32
Haematocrit (%)	29.37 +/- 2.39	30.68 +/- 5.06	0.33
Red blood cell distribution width (%)	12.75 +/- 0.78	12.84 +/- 0.54	0.69
Mean corpuscular volume (μm^3)	47.89 +/- 1.33	48.29 +/- 1.27	0.35
Mean corpuscular haemoglobin (pg)	15.06 +/- 0.51	16.85 +/- 7.91	0.36
White cell percentages:			
- Lymphocyte	86.19 +/- 6.88	85.14 +/- 7.39	0.66
- Monocyte	4.18 +/- 1.97	4.90 +/- 2.48	0.34
- Neutrophil	7.69 +/- 4.24	8.29 +/- 4.35	0.68
- Eosinophil	1.17 +/- 1.41	0.97 +/- 1.37	0.66
- Basophil	0.76 +/- 0.9	0.65 +/- 1.02	0.72

Table 10. Counts of the major blood cell groups in Tspan9 knockout mice appear normal.
All of the blood parameters assessed in the whole blood count were not significantly different between wildtype and knockout blood samples. n = 18 - 20 +/- values represent standard deviation around the mean. p value determined by an unpaired Student's t-test.

5.2.6 Tspan9-deficient platelets had normal levels of several platelet surface proteins.

The investigation into the function of Tspan9 on platelets began with an analysis of surface levels for several platelet proteins in Tspan9-deficient platelets. As previously discussed in the analysis of Tspan33-deficient platelets, some tetraspanins have been found to influence partner protein trafficking to the cell surface (Shoham et al., 2003, Haining et al., 2012, Berditchevski and Odintsova, 2007), thus it was again important to check this aspect of Tspan9-deficient platelets. Using the same method as set out in Figure 10 (Chapter 3), the surface levels of αIIbβ3, α2β1, α6β1, GPVI, GPIb, CD9, ADAM10 and CLEC-2 were assessed (Figure 29 A). All of the proteins measured were present on Tspan9-deficient platelets at levels that were not significantly different from those measured in wildtype platelets (Figure 29 B).

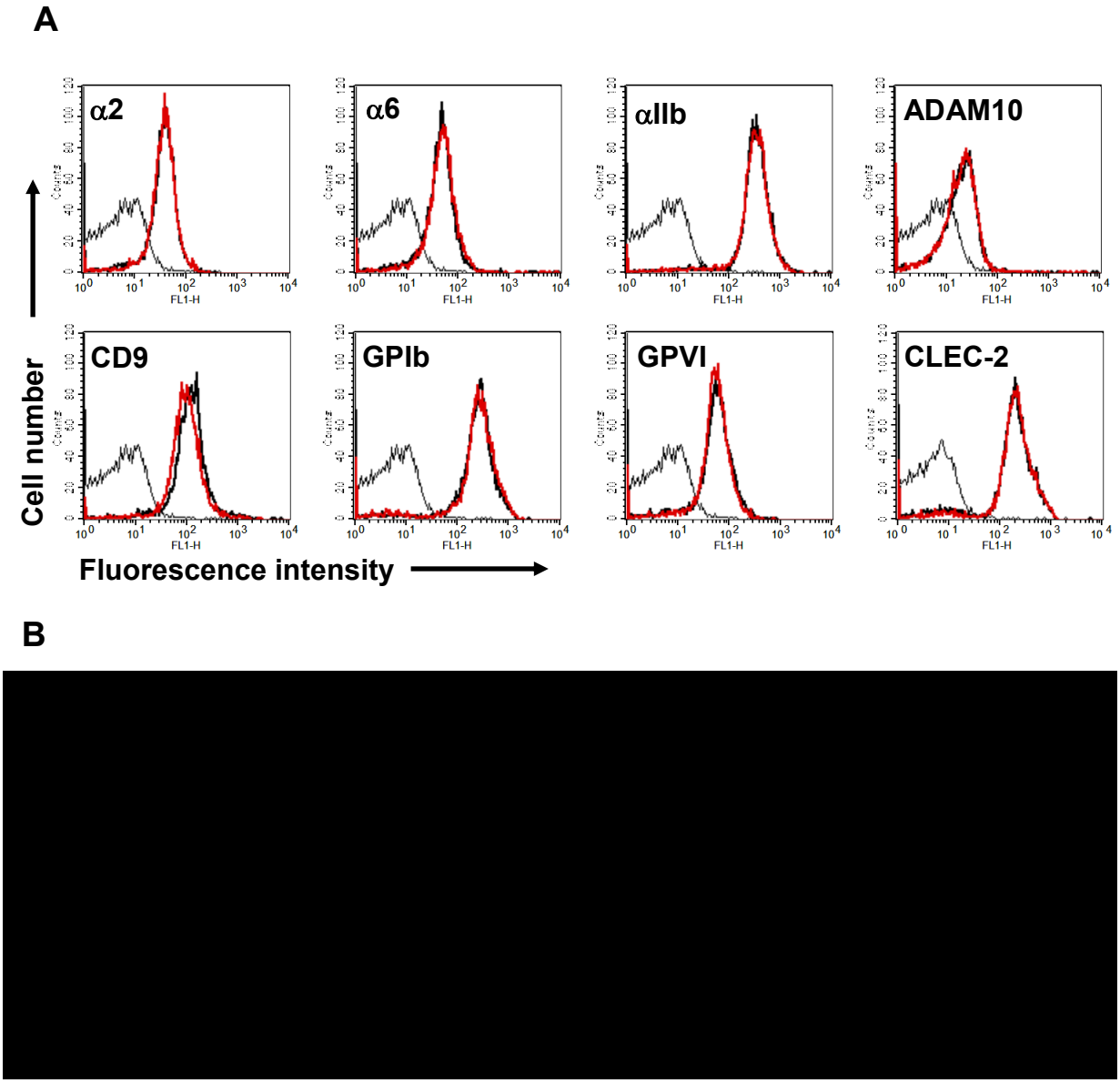

Figure 29. Tspan9 knockout platelets express normal levels of the major platelet surface glycoproteins.

Whole blood drawn into acid citrate dextrose was incubated with the relevant anti-mouse antibody conjugated to FITC. Platelet specific staining was isolated by gating on platelets by size A. Representative FACS plots for each indicated protein. Wildtype in black and Tspan9-deficient in red. For simplicity only the control trace from wildtype staining is shown. B. Geometric mean fluorescence intensity used to assess surface receptor levels. n = 5 - 8 +/- values represent standard deviation around the mean and p value determined by an unpaired Student's t-test.

5.2.7 Tspan9 knockout mice do not have a bleeding phenotype.

To begin to focus on platelet function in the Tspan9 knockout the next step in the analysis was to challenge haemostasis using the tail bleeding assay. This procedure, done in the same manner as for the Tspan33 knockout mice (Figure 11, Chapter 3) records blood loss in a set time-frame after tail tip excision. The blood loss from Tspan9 knockout mice was not significantly different from wildtype, as such these mice were not judged to have a bleeding phenotype (Figure 30).

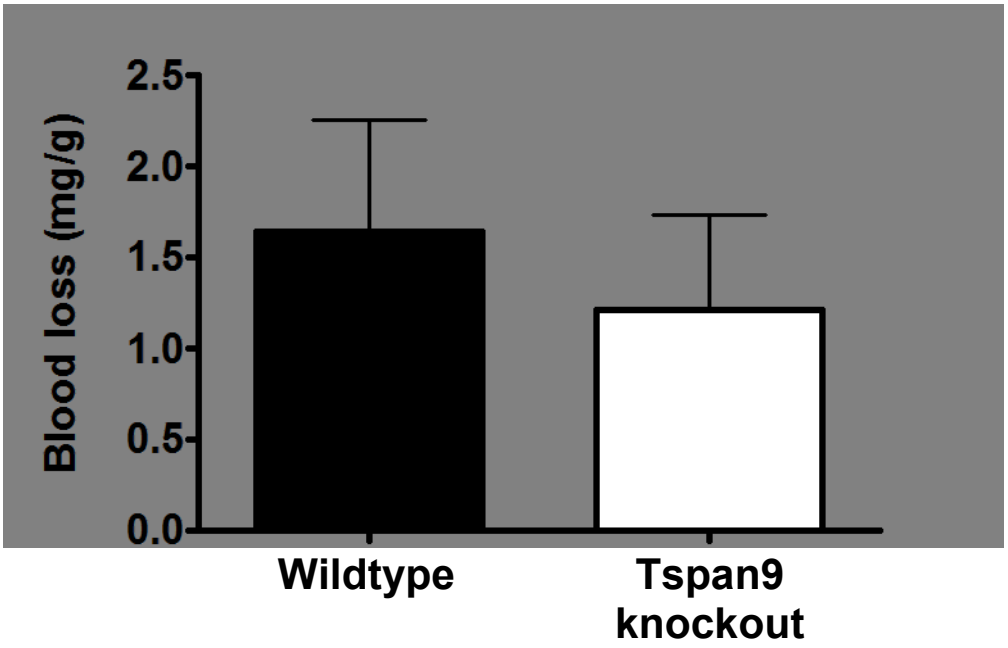

Figure 30. Tspan9 knockout mice do not have a bleeding defect.

Blood loss after tail tip excision is presented as a factor of mouse weight so as to normalise for mice of different sizes. No significant difference was found between the blood loss (mg/g) of wildtype and Tspan9 knockout mice using an unpaired Student's t-test. All mice were aged between 8 - 12 weeks and between 2 - 3 mm of tip removed. n = 20 and error bars represent standard error of the mean

5.2.8 Tspan9 knockout platelets display aggregation defects in response to collagen-related peptide in light transmission aggregometry assays.

After assessment of the functioning of haemostasis as a whole using the tail bleeding assay, the next step in the investigation was to focus specifically on the functioning of Tspan9-deficient platelets. The approach taken assessed platelets that had been washed free of any other blood components (washed platelets) and platelets in plasma (platelet rich plasma). Washed platelets were tested with thrombin, collagen-related peptide, collagen and CLEC-2 antibody, and the platelet rich plasma with PAR4 peptide, collagen-related peptide, collagen, ADP and arachidonic acid. Washed platelets are not in the presence of any fibrinogen and so any aggregation in response to agonist relies on functional platelet activation and secretion of fibrinogen from the platelet alpha granules. The platelet rich plasma aggregation assesses the platelet responses in the more physiological environment of the plasma. The four agonists chosen for the Washed platelets target four important platelet receptors (PAR3 and PAR4, GPVI and CLEC-2) and, as CLEC-2 and GPVI share similar signalling molecules, two signalling pathways that powerfully activate platelets. PAR4 peptide replaces thrombin in the platelet rich plasma conditions to prevent a mesh of fibrin forming in the aggregation tube. In addition to measuring aggregation as a readout for platelet activation, platelet secretion was directly measured by the addition of a luciferin/luciferase mix to the platelets.

In platelet rich plasma conditions the responses of Tspan9-deficient platelets to intermediate doses of collagen-related peptide were almost abolished (Figure 31 B). Interestingly this defect could be overcome by increasing the dose of this agonist (Figure 31 C). However, responses to collagen (which also initially binds the same

receptor, GPVI) were not significantly different from wildtype at doses of 3 μg/ml (Figure 31 D) and 10 μg/ml (Figure 31 E). The responses to PAR4 peptide (250 μM), ADP (10 μM) and arachidonic acid (0.15 mM) were normal, suggesting a defect specifically in response to collagen-related peptide (Figure 31 A, F and G respectively). This result indicated that Tspan9 may be important in the function of GPVI, a platelet receptor that was recently published to be tetraspanin associated (Protty et al., 2009). Figure 31 shows representative aggregation traces in response to all the agonists just discussed, and Figure 32 shows quantitation of these traces as percentage aggregation over time. The defect in Tspan9-deficient platelet responses to intermediate doses of collagen-related peptide was also reflected in the amount of secretion detected, where total ATP secreted was significantly less than wildtype platelets (Figure 33 B). Secretion in response to all other agonists was normal (not measured in response to ADP), apart from in response to PAR4 peptide which had a small but significantly reduced secretion response (Figure 33). This result was unexpected as no defect was seen in the aggregation responses to this agonist.

In Washed platelets the defect seen in Tspan9-deficient platelets in response to intermediate doses of collagen-related peptide was diminished such that there was no longer a significant difference between wildtype and Tspan9-deficient responses, however, a reproducible extension in the shape change phase could be noted (Figure 34 B). The responses of Tspan9-deficient washed platelets to all the agonists tested were not significantly different from wildtype (Figure 34 A - E representative traces, Figure 35 A - E quantitation of aggregation and Figure 36 A - E quantitation of secretion).

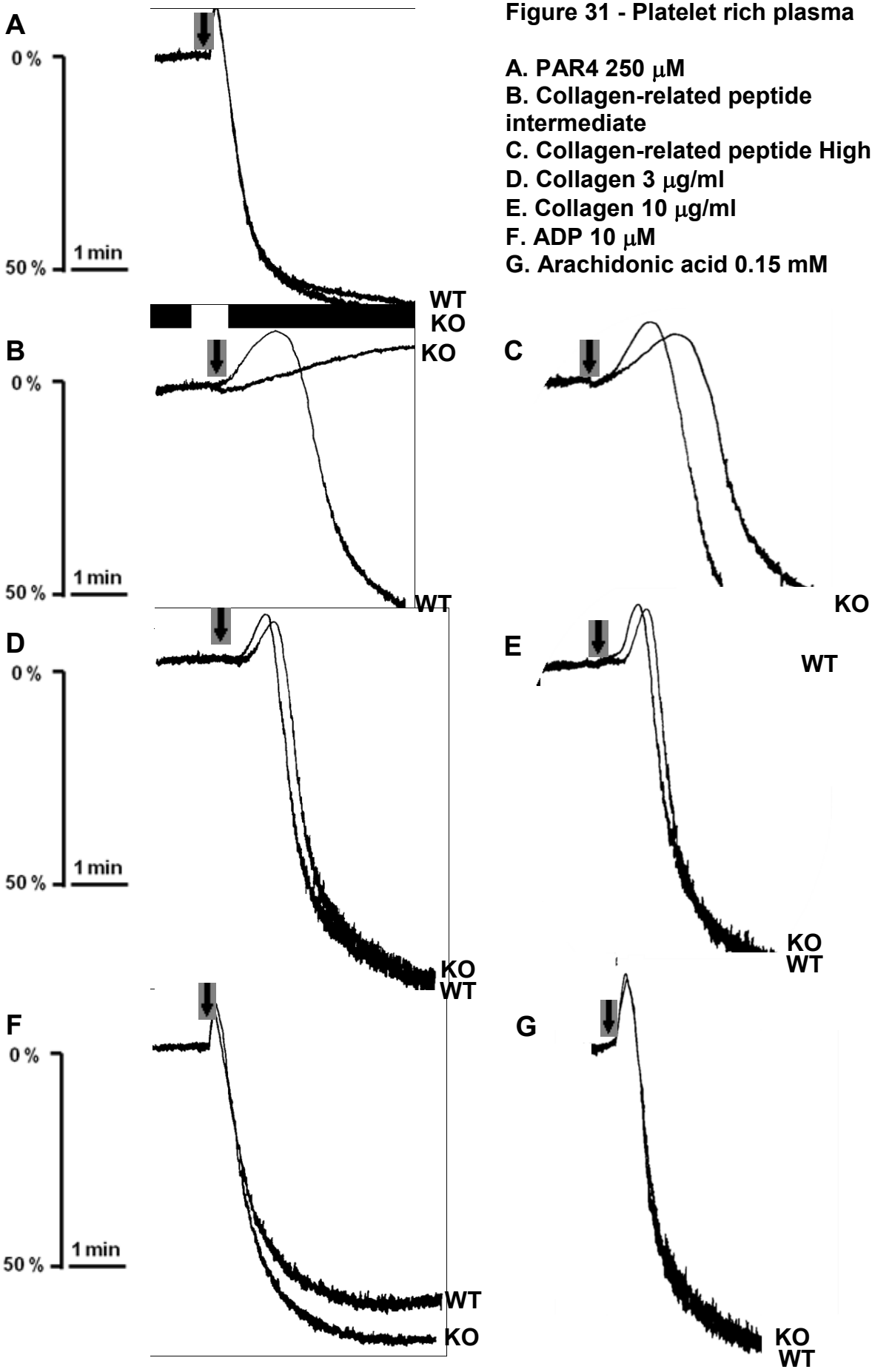

Figure 31 - Platelet rich plasma

A. PAR4 250 μM
B. Collagen-related peptide intermediate
C. Collagen-related peptide High
D. Collagen 3 μg/ml
E. Collagen 10 μg/ml
F. ADP 10 μM
G. Arachidonic acid 0.15 mM

Figure 32 - Platelet rich plasma

A. PAR4 250 μM
B. Collagen-related peptide intermediate
C. Collagen-related peptide High
D. Collagen 3 μg/ml
E. Collagen 10 μg/ml
F. ADP 10 μM
G. Arachidonic acid 0.15 mM

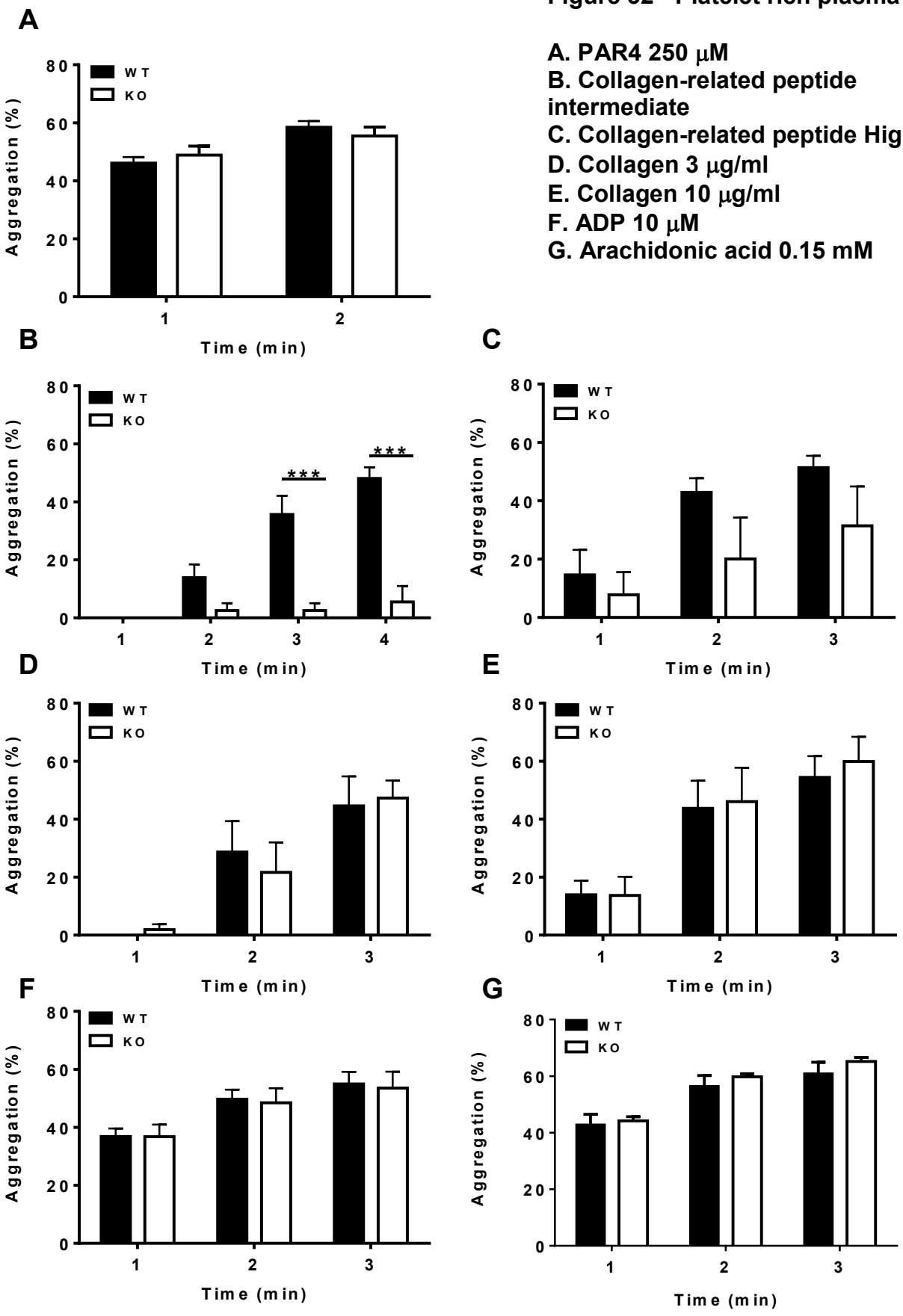

Figure 33 - Platelet rich plasma

A. PAR4 250 μM
B. Collagen-related peptide intermediate
C. Collagen-related peptide High
D. Collagen 3 μg/ml
E. Collagen 10 μg/ml
F. Arachiadonic acid 0.15 mM

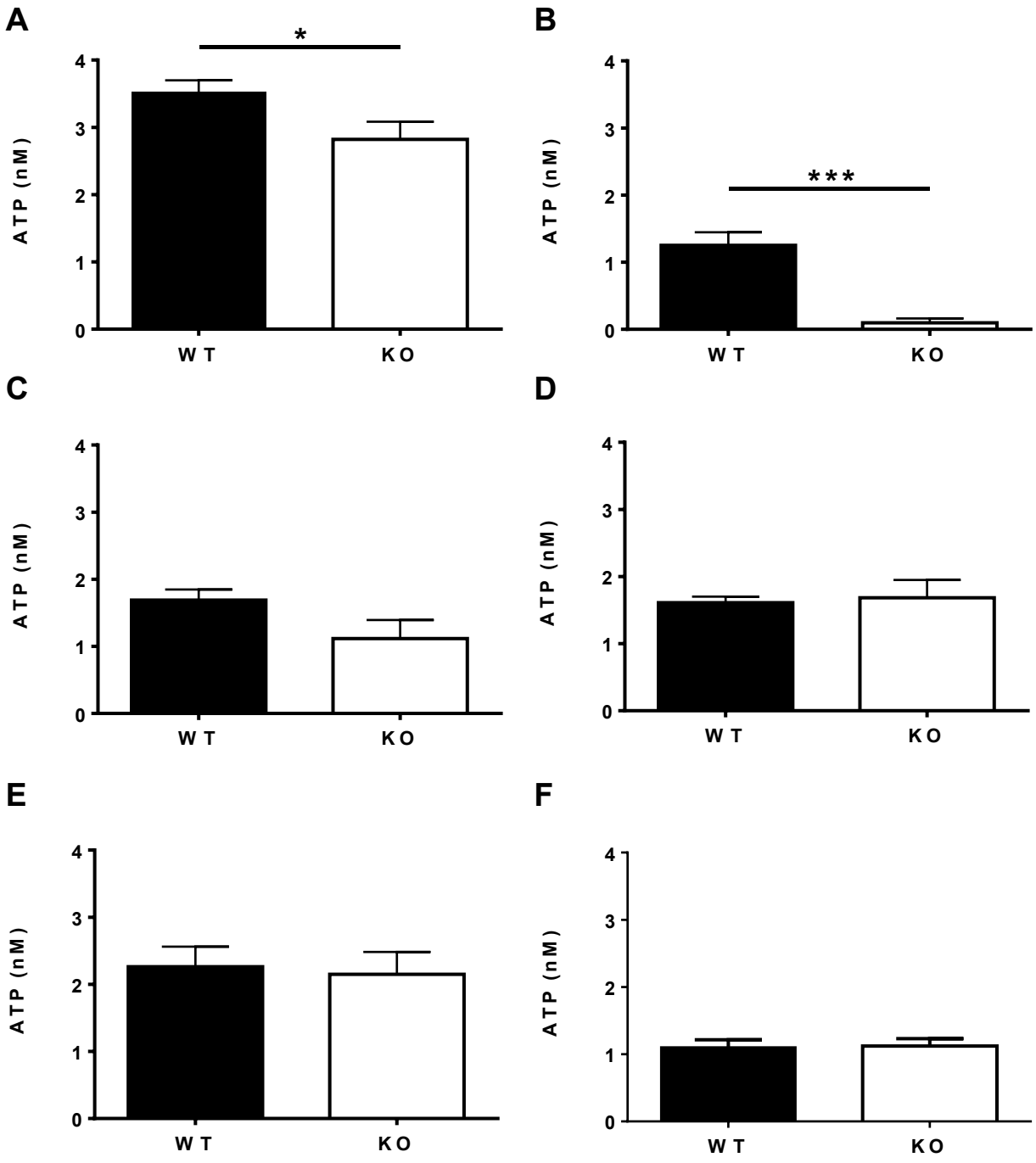

Figure 31. Tspan9-deficient platelets in plasma display aggregation defects in response to collagen-related peptide.

Tspan9 wildtype and deficient platelets in plasma at 2 x 10^8/ml were stimulated with the following agonists A. PAR4 peptide 250 μM B. Collagen-related peptide intermediate dose C. Collagen-related peptide high dose D. Collagen 3 μg/ml E. Collagen 10 μg/ml F. ADP 10 μM G. Arachidonic acid 0.15 mM. Responses were measured by lumi-aggregometery. Only in response to collagen-related peptide at intermediate doses did Tspan9-deficient platelet traces appear different from wildtype. Representative traces of each experiment shown. n = 3 - 9

Figure 32. Tspan9-deficient platelets in plasma display a significant defect in response to intermediate doses of collagen-related peptide.

Aggregation traces from the experiments listed in Figure 30 were analysed by measuring the percentage aggregation reached at minute intervals after agonist addition. A. PAR4 peptide 250 μM B. Collagen-related peptide intermediate dose C. Collagen-related peptide high dose D. Collagen 3 μg/ml E. Collagen 10 μg/ml F. ADP 10 μM G. Arachidonic acid 0.15 mM. A significant reduction in response was seen in Tspan9-deficient platelets in response to collagen-related peptide at intermediate doses. The responses to all other agonists appeared normal and were not significantly different from wildtype. n = 3 - 9, error bars represent standard error of the mean. Significance assessed by two way ANOVA followed by a Bonferroni post test.

Figure 33. Tspan9-deficient platelets in plasma display a significant defect in ATP secretion in response to intermediate doses of collagen-related peptide and PAR4 peptide.

Tspan9 wildtype and deficient platelets in plasma at 2 x 10^8/ml were stimulated with the following A. PAR4 peptide 250 μM B. Collagen-related peptide intermediate dose C. Collagen-related peptide high dose D. Collagen 3 μg/ml E. Collagen 10 μg/ml F. Arachidonic acid 0.15 mM and responses were measured by lumi-aggregometery. A significant decrease in secretion was seen in response to intermediate doses of collagen-related peptide and, to a lesser extent, PAR4 peptide. n = 3 - 9, error bars represent standard error of the mean. Significance assessed by unpaired Student's t-tests.

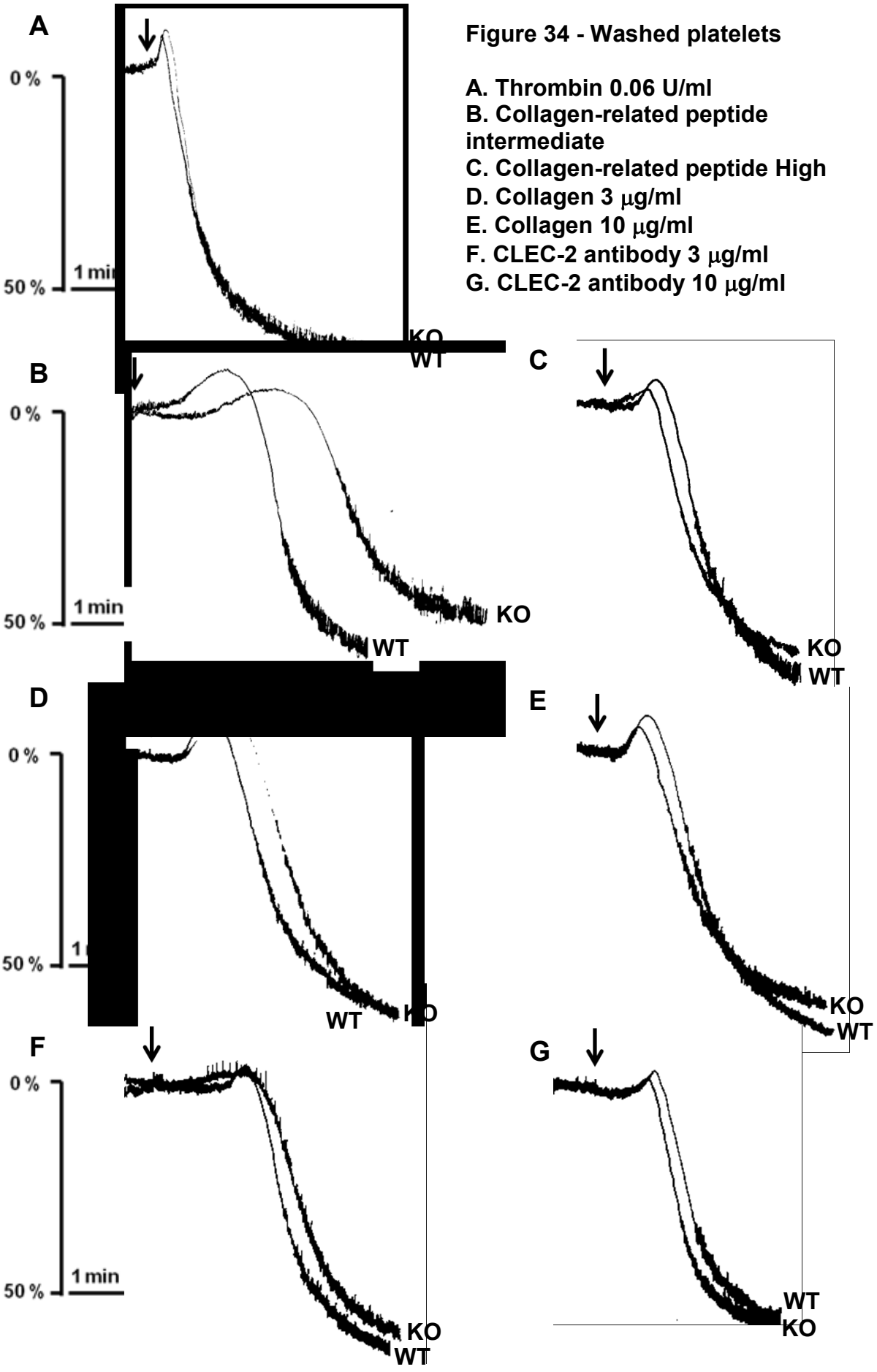

Figure 34 - Washed platelets

A. Thrombin 0.06 U/ml
B. Collagen-related peptide intermediate
C. Collagen-related peptide High
D. Collagen 3 μg/ml
E. Collagen 10 μg/ml
F. CLEC-2 antibody 3 μg/ml
G. CLEC-2 antibody 10 μg/ml

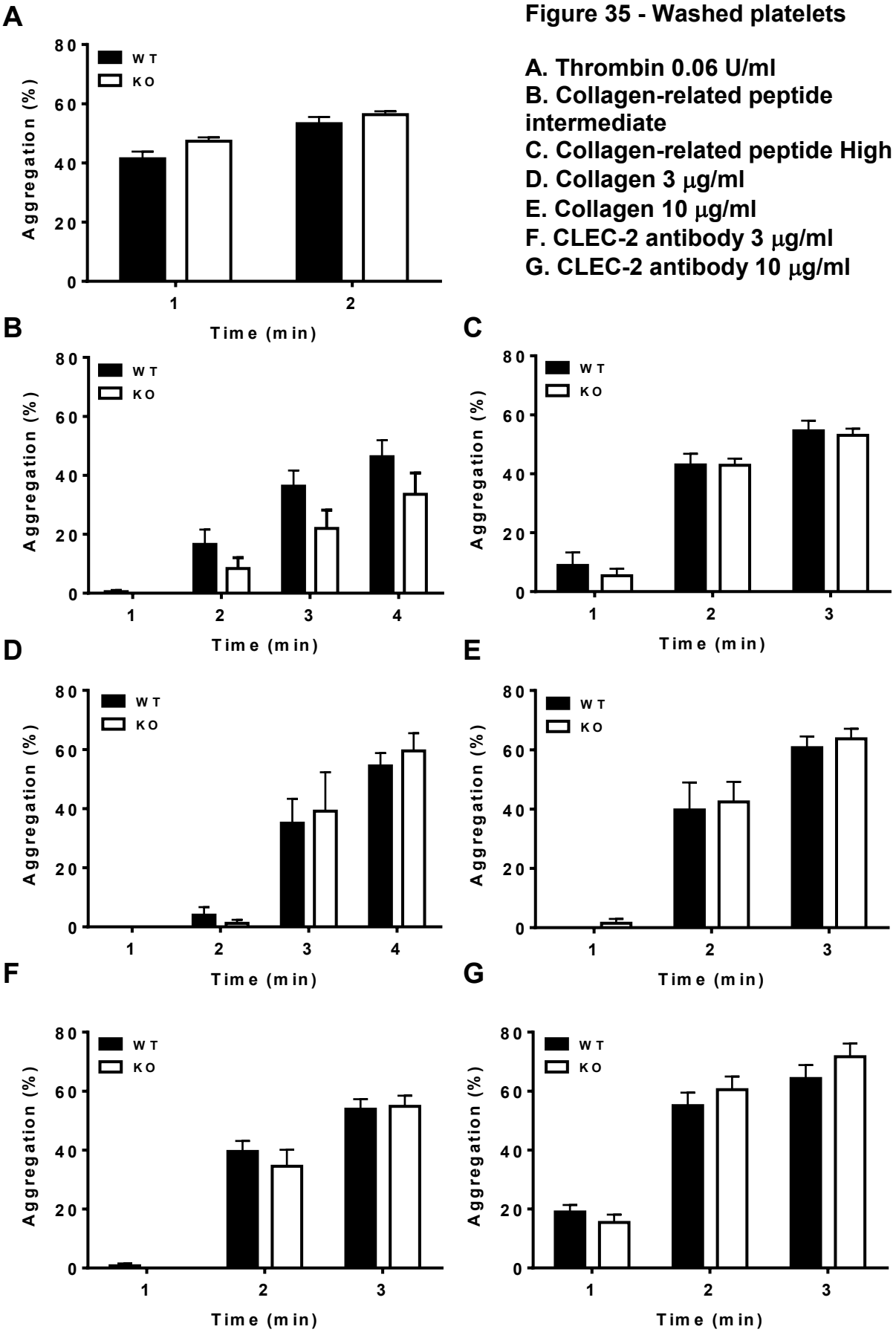

Figure 35 - Washed platelets

A. Thrombin 0.06 U/ml
B. Collagen-related peptide intermediate
C. Collagen-related peptide High
D. Collagen 3 μg/ml
E. Collagen 10 μg/ml
F. CLEC-2 antibody 3 μg/ml
G. CLEC-2 antibody 10 μg/ml

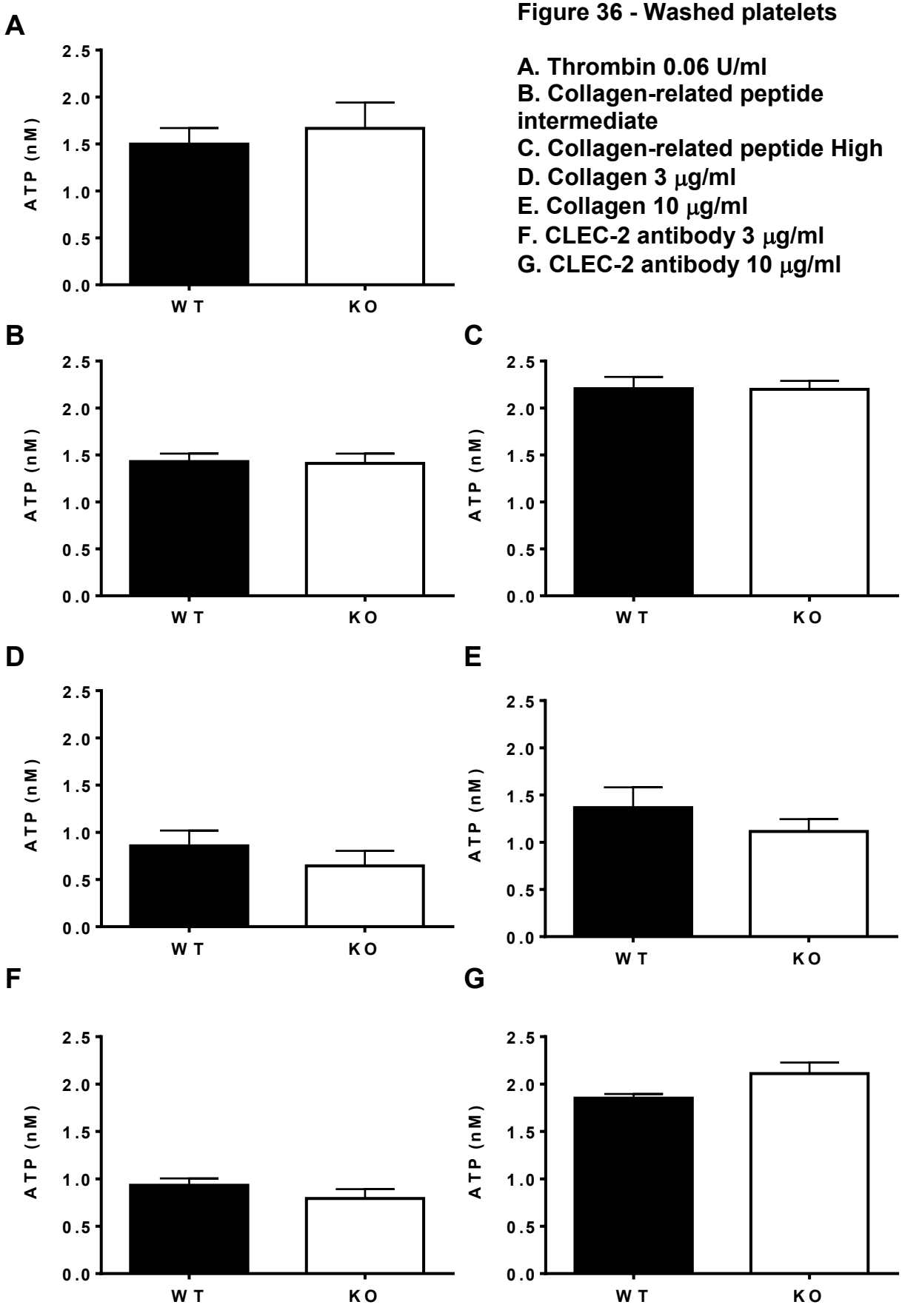

Figure 36 - Washed platelets

A. Thrombin 0.06 U/ml
B. Collagen-related peptide intermediate
C. Collagen-related peptide High
D. Collagen 3 μg/ml
E. Collagen 10 μg/ml
F. CLEC-2 antibody 3 μg/ml
G. CLEC-2 antibody 10 μg/ml

Figure 34. Aggregation traces of wildtype versus Tspan9-deficient washed platelets.

Tspan9 wildtype and deficient washed platelets at 2 x 10^8/ml were stimulated with the following agonists A. Thrombin 0.06 U/ml B. Collagen-related peptide intermediate dose C. Collagen-related peptide high dose D. Collagen 3 μg/ml E. Collagen 10 μg/ml F. CLEC-2 antibody 3 μg/ml G. CLEC-2 antibody 10 μg/ml. Responses were measured by lumi-aggregometery. Representative traces of each experiment shown. n = 4 - 13

Figure 35. Tspan9-deficient washed platelets display no significant defect in aggregation responses.

Aggregation traces from the aggregation experiments listed in Figure 35 were analysed by measuring the percentage aggregation reached at minute intervals after agonist addition. A. Thrombin 0.06 U/ml B. Collagen-related peptide intermediate dose C. Collagen-related peptide high dose D. Collagen 3 μg/ml E. Collagen 10 μg/ml F. CLEC-2 antibody 3 μg/ml G. CLEC-2 antibody 10 μg/ml. n = 4 - 13, error bars represent standard error of the mean. Significance assessed by two way ANOVA followed by a Bonferroni post test.

Figure 36. Tspan9-deficient platelets have normal secretion responses to a range of agonists.

Tspan9 wildtype and deficient washed platelets at 2 x 10^8/ml were stimulated with the following agonists A. Thrombin 0.06 U/ml B. Collagen-related peptide intermediate dose C. Collagen-related peptide high dose D. Collagen 3 μg/ml E. Collagen 10 μg/ml F. CLEC-2 antibody 3 μg/ml G. CLEC-2 antibody 10 μg/ml and responses were measured by lumi-aggregometery. No significant differences were seen between wildtype and Tspan9-deficient platelets in total amount of ATP released after stimulation by any agonist. n = 4 - 13, error bars represent standard error of the mean. Significance assessed by unpaired Student's t-tests.

5.2.10 Signalling downstream of GPVI is reduced in response to collagen-related peptide in Tspan9-deficient platelets.

The defect seen in the aggregation responses of Tspan9-deficient platelets to collagen-related peptide was similar to the defects in aggregation seen in the responses of the GADS knockout mouse (Hughes et al., 2008). GADS is an adapter molecule that is part of the signalosome complex that forms downstream of GPVI after ligand binding. Correct formation of this complex is essential for functional and efficient signal transduction from GPVI (Watson et al., 2001). As such, the defect in Tspan9-deficent platelets could have been due to defects in the recruitment of GADS or another protein in the GPVI signalling pathway. To assess the signalling downstream of GPVI, tyrosine phosphorylation in Tspan9-deficient platelets after collagen-related peptide stimulation was visualised using western blotting. Washed Tspan9-deficient or wildtype platelets were stimulated with high dose collagen-related peptide in the presence of apyrase and indomethacin to prevent signalling from secondary mediators and lotrafiban to prevent platelet aggregation and αIIbβ3 signalling. At 10 s, 30 s, 60 s and 5 min after activation, samples were taken and subsequently western blotted for tyrosine phosphorylation (Figure 37). Tspan9-deficient platelets did respond to the stimulation over the time course, however the response was weaker than that of the wildtype, consistent with the responses seen in aggregation experiments. Interestingly, no individual protein appeared affected in the Tspan9-deficient platelets suggesting that the defect that caused the reduction in response to collagen-related peptide may be upstream of signalosome formation.

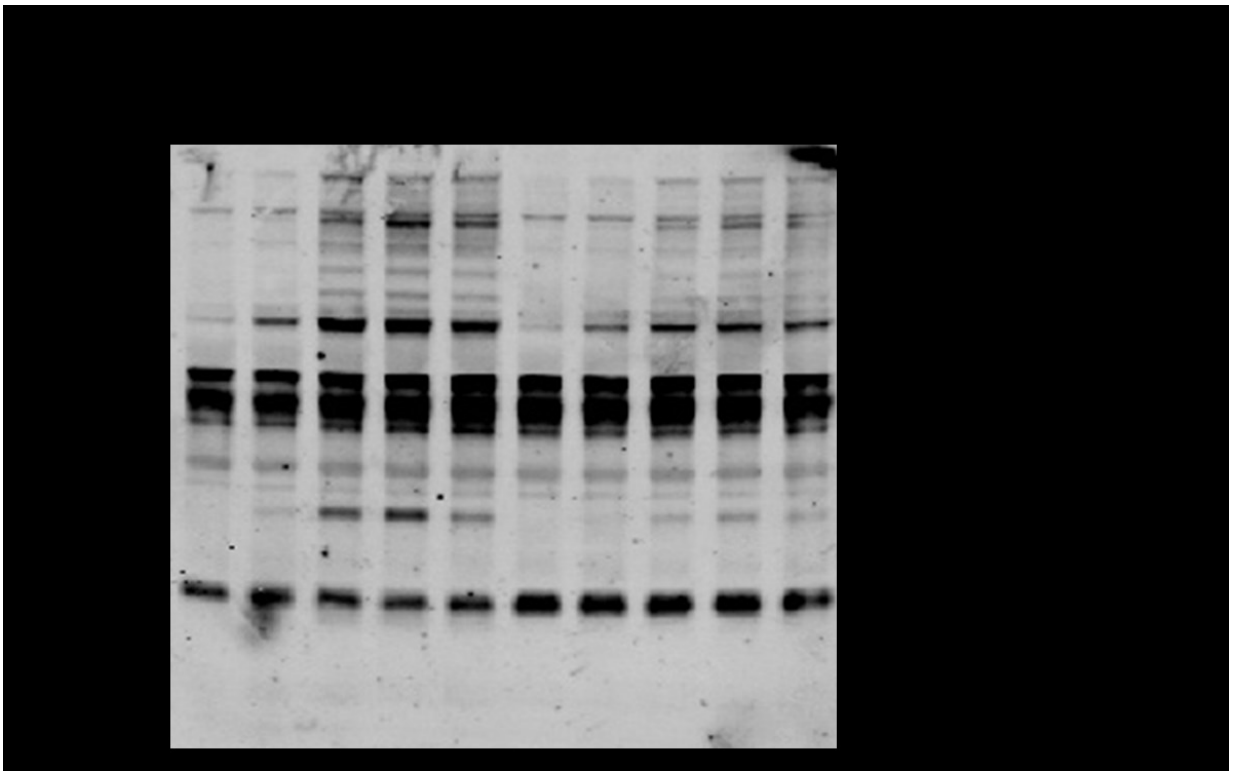

Figure 37. Tspan9-deficient platelets have reduced signalling responses to collagen-related peptide.

Washed platelets at 5 x 10^8/ml were incubated at 37 °C with apyrase (500 U/ml), indomethacin (10 mM) and lotrafiban (1 mM) for 5 min. Platelets were then stimulated with 10 μg/ml collagen-related peptide and samples taken at 10 s, 30 s, 60 s and 5 min. Samples were lysed directly in 2 x reducing sample buffer and separated on 4 - 12 % gradient polyacrylamide gels. Western blotting with the anti-phosphotyrosine antibody 4G10 revealed tyrosine phosphorylated proteins. Representative of n = 3.

5.2.11 Tspan9-deficient platelets adhere normally to collagen under flow.

Analysis of the behaviour of Tspan9-deficient platelets by aggregation and spreading assays allows a clear dissection of individual signalling pathways within the platelets. However, these assays do not allow assessment of platelet behaviour under the conditions that occur *in vivo*. It is well documented that physiological conditions such as shear forces affect the behaviour of platelets by modulating the action of several surface proteins, including GPVI (Auger et al., 2005, Moroi et al., 1996, Best et al., 2003b). An assay that recapitulates some of the conditions that platelets experience in the vascular system is whole blood flow adhesion. In this assay whole blood is flowed at controlled rates across a glass capillary that can be coated with several different platelet agonists such as collagen and fibrinogen. Responses of the platelets to the coated capillary are recorded by fluorescence video microscopy so that platelet aggregate formation can be assessed in real time. Tspan9-deficient platelets were exposed to collagen in this assay at two different flow rates 1000 s^{-1} (high, equivalent to arterial shear) and 300 s^{-1} (low, equivalent to venous shear) (Figure 38). There was no significant difference between the surface area coverage of aggregates formed by wildtype or Tspan9-deficient platelets (Figure 39).

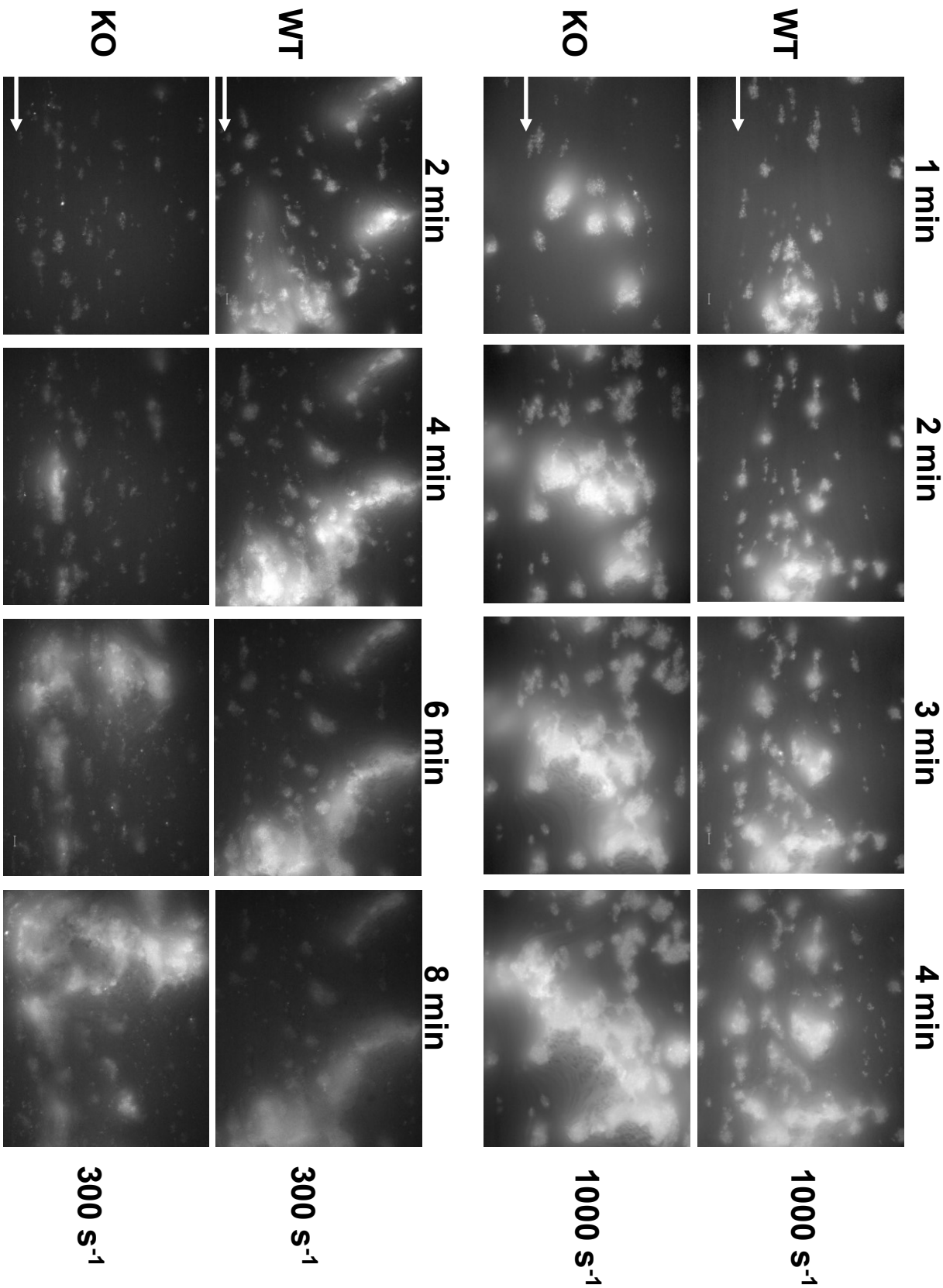
WT
KO
1 min
2 min
3 min
4 min
1000 s-1
WT
KO
2 min
4 min
6 min
8 min
300 s-1

Figure 38

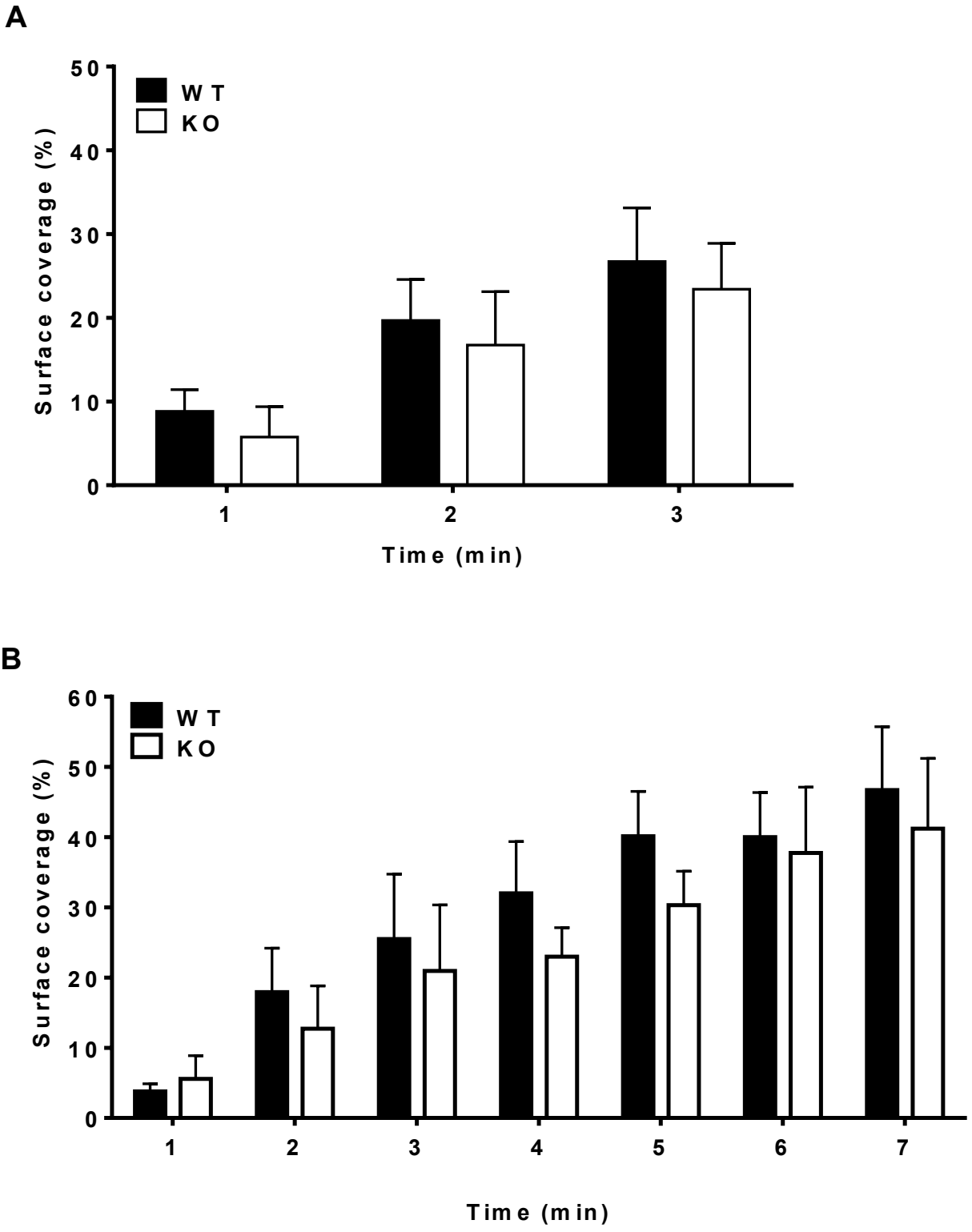
A
WT
KO
Surface coverage (%)
0
10
20
30
40
50
1
2
3
Time (min)
B
WT
KO
Surface coverage (%)
0
10
20
30
40
50
60
1
2
3
4
5
6
7
Time (min)

Figure 39

Figure 38. Representative images of Tspan9 wildtype and deficient whole blood flowing over collagen.

Representative images of Tspan9 wildtype and deficient platelets flowing over collagen coated capillaries at speeds of 1000 or 300 s^{s-}. Fluorescence microscopy images were taken every 2 s with a 40 x oil objective. These images are representative of n = 3. The arrows denote the direction of flow.

Figure 39. Tspan9-deficient platelets adhere normally to collagen under flow.

Stills from each video at the noted time points were assessed for surface area coverage of platelets in the field of using imageJ software. A. At 1000 s^{-1} surface area coverage of Tspan9-defcient platelets over time was not significantly different from wildtype. B. At 300 s^{-1} surface area coverage of Tspan9-deficient platelets over time was not significantly different from wildtype. Error bars represent standard error of the mean and statistical significance determined by two way ANOVA.

5.3 Discussion

Presented here is an investigation into the function of Tspan9 on platelets. The initial hypothesis for the project was that the tetraspanin Tspan9 was important for the function of platelets through its regulation of another platelet surface protein. The aim of this investigation was to use the newly generated and unpublished Tspan9 knockout mouse and Tspan9-deficient platelets to investigate the initial hypothesis. The final conclusion of this project was that Tspan9 is required for normal GPVI-induced platelet activation, but the defect is subtle and only observed in certain assays, most notably platelet aggregation in plasma to collagen-related peptide.

The Tspan9 knockout mouse had never previously been studied and so initial investigations assessed its normality. No obvious differences were found between Tspan9 wildtype and knockout mice that could have indicated the function of Tspan9 or any potential Tspan9 partner proteins. The only difference found was that Tspan9 knockout mice had a 7 % reduction in their heart to body weight ratio. This result was initially surprising as Tspan9 was much more highly expressed in the other organs assessed and found to be normal in structure. However tissue sections of heart stained with the Tspan9 antibody highlighted a specific staining for Tspan9 on the small vessels and capillaries that permeate through the heart tissue. It could be possible that a defect in this vessel network could lead to decrease in heart mass as the muscles in the heart could be less oxygenated than in wildtype. Further investigations directly focussed on the heart would be required to understand this phenotype and to test this hypothesis.

The production of Tspan9-deficient platelets appeared normal as there was no difference between wildtype and Tspan9-deficient platelet counts, platelet size or

expression of platelet surface proteins. There was, however, a significant defect in the responses of Tspan9-deficient platelets to the GPVI agonist collagen-related peptide in aggregation studies. This defect was seen as an extension of the shape change phase of activation before aggregation, and was so marked in platelet rich plasma that Tspan9-deficient platelets rarely aggregated in the same time frame as wildtype platelets. The result indicated that the Tspan9-deficient platelets were less sensitive to collagen-related peptide, however this effect appeared mild as it could be overcome by increasing the dose of the agonist.

The cause of this defect appeared to be at the level of the receptor as the signalling proteins downstream of ligand binding appeared to be phosphorylated in the same manner as wildtype, but to a lesser extent despite being stimulated with the same dose of collagen-related peptide. Additionally many of the proteins that are involved in the GPVI signalling cascade are shared by the signalling pathway downstream of the platelet podoplanin receptor CLEC-2, which appeared to be functioning normally in aggregation experiments using Tspan9-deficient platelets. As GPVI was expressed at normal levels on Tspan9-deficient platelets, the cause of the defect in response to collagen-related peptide may be in the regulation of receptor clustering. As discussed in the introduction, the minimal signalling unit for GPVI is a dimer and further clustering of GPVI dimers are proposed to cause more powerful signal transduction into the platelet (Nieswandt and Watson, 2003). Should this process be disrupted, the signal transduction would be predicted to be weaker as a result of either less higher order clustering or less initial dimer formation. This could result in a defect like that seen in the Tspan9-deficient platelets. Interestingly, this hypothesis of defective receptor clustering could also offer an explanation for the marked difference in

responses seen between Tspan9-deficient platelets in plasma and washed platelets. In a paper that characterised a GPVI dimer specific antibody in human platelets, Loyau et al. (2012) remarked on an increase of GPVI dimers that occurred on platelets as they progressed through the preparation process, with low levels of GPVI dimer being detected on platelets in whole blood and a 7-fold increase seen on platelets washed and resuspended in buffer. A partial activation of platelets during preparation, causing a pre-clustering of GPVI, could cause the partial rescue of the defect seen between Tspan9-deficient platelet rich plasma and Watson washed platelets. An effect would not necessarily be expected on wildtype platelets as in both conditions GPVI is most likely already clustering at levels at or above the threshold required for efficient responses to ligand. The hypothesis that Tspan9 may be clustering GPVI is not an unlikely scenario as other tetraspanins have been published to be involved in clustering other surface molecules (Doyle et al., 2011, Bailey et al., 2011, Yang et al., 2002). This ability is currently thought to be due to tetraspanins regulating the lateral mobility of their partner proteins in the plasma membrane, thus modulating the nano-scale distribution of individual proteins (Yang et al., 2012a, van Spriel et al., 2012). Additionally, the relatively low copy number of GPVI on the platelet, compared to proteins such as GPIb and αIIbβ3, suggests that regulation may be required to bring these potentially disperse molecules together in an efficient and timely manner.

One question raised by the phenotype of Tspan9-deficient platelets is the normality of the response to collagen, the physiological ligand of GPVI, and the lack of a bleeding defect in these mice. However, it is actually unsurprising in the context of GPVI heterozygote and GPVI knockout mice. GPVI knockout mice only display a

minor bleeding defect and indeed people with a GPVI deficiency due to autoantibodies also only present with mild bleeding (Chu et al., 2006, Cheli et al., 2008b). Furthermore, GPVI heterozygote mouse platelets, with half the number of GPVI molecules, only have a minor defect in response to collagen in aggregation assays and no detectable defect in flow adhesion assays (Snell et al., 2002). Additionally people with naturally occurring polymorphisms in GPVI that result in reduced GPVI surface levels also show normal responses in flow experiments over collagen (Best et al., 2003a). In these scenarios, the collagen-binding integrin α2β1, which does not bind collagen-related peptide, may enable largely normal collagen responses despite reduced GPVI expression or activation.

CHAPTER VI: TSPAN9 REGULATES THE LATERAL DIFFUSION OF GPVI

6.1 Introduction

The work presented in the previous chapter on functional assessments of platelets from the Tspan9 knockout mouse revealed a specific defect in the functioning of GPVI in Tspan9-deficient platelets. This defect manifested in aggregometry experiments as an insensitivity of Tspan9-deficient platelets to the GPVI specific agonist collagen-related peptide. The conclusions of the previous chapter suggested that GPVI, a previously published tetraspanin associated protein (Protty et al., 2009), may be a partner protein for Tspan9 and that Tspan9 may regulate the clustering and/or lateral mobility of GPVI. The aim of the work presented in this chapter was to investigate these hypotheses.

6.2 Results

6.2.1 Tspan9 is expressed on mouse platelets at similar levels as on human platelets, relative to CD9.

The level of Tspan9 relative to CD9 was known for human platelets and suggested that the copy number for Tspan9 in human platelets was around 2800 and that CD9 was around 49000 (Protty et al., 2009). It was important to know the levels of Tspan9 on mouse platelets to understand if it was expressed at high enough levels to be a candidate tetraspanin to partner GPVI (with its human copy number of around 4000) (Senis et al., 2007). Using the western blotting approach described in Protty et al. (2009), lysates of HEK 293T cells that had been transfected with FLAG-tagged Tspan9 and CD9 constructs were first western blotted with an anti-FLAG antibody. The amount of each tetraspanin detected was quantified using the LI-COR Odyssey software (Figure 40 A). These same lysates and three different mouse platelet lysates were then western blotted with an anti-Tspan9 (Figure 40 B) or anti-CD9 antibody (Figure 40 C). The amount of protein detected by these antibodies was also quantified and compared to the FLAG western blot. Using these data, the relative amounts of each protein could be measured. This method revealed that Tspan9 is expressed in mouse platelets at a 1 : 75 ratio to CD9 (Figure 40 D). This level compares to a 1 : 17.5 ratio seen for Tspan9 to CD9 in human platelets (Protty et al., 2009). Even given this difference between human and mouse Tspan9 could still theoretically partner with the majority of GPVI molecules as this conclusion is dependent on the levels of CD9 being similar between human and mouse platelets, which has yet to be determined.

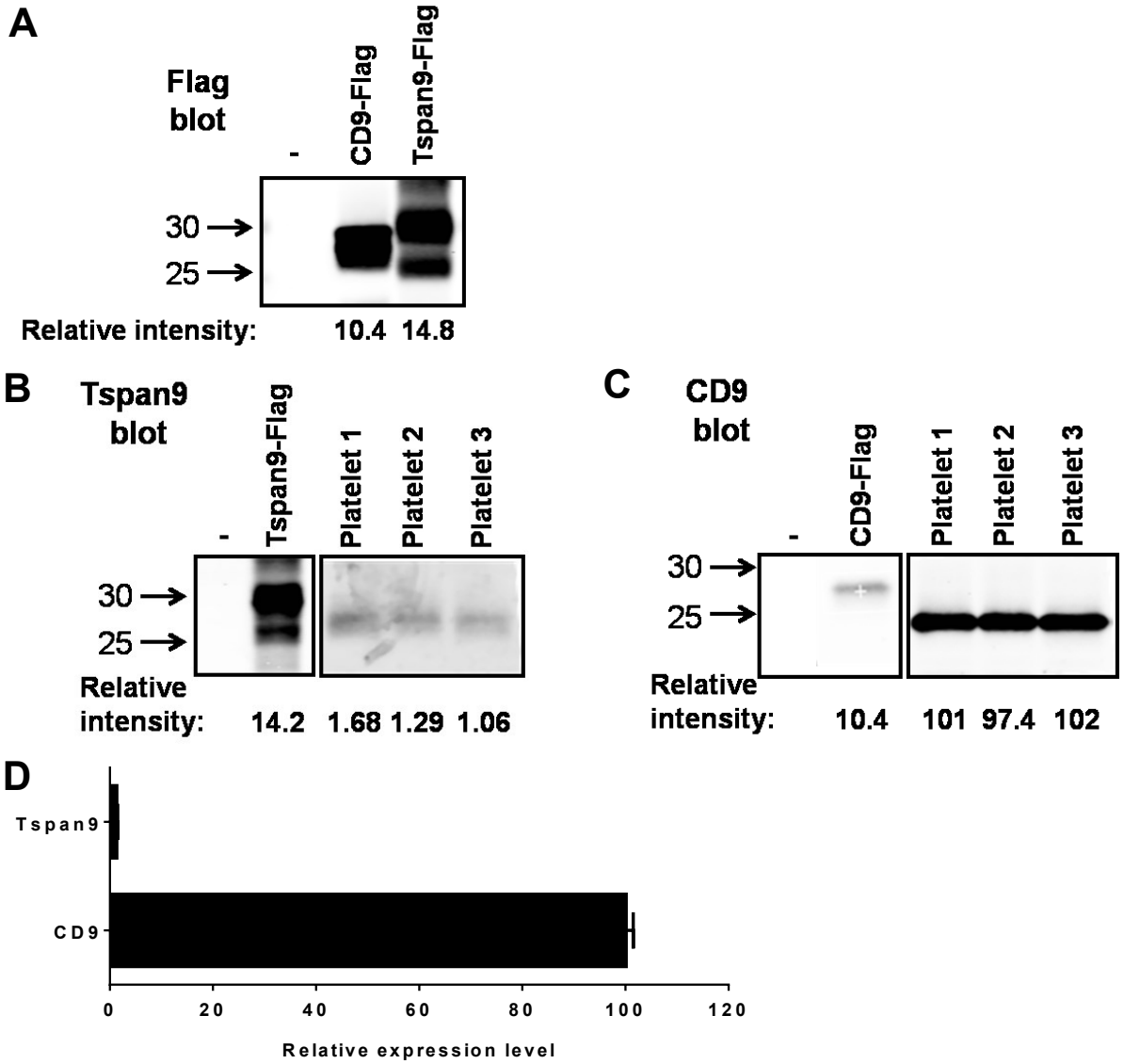

Figure 40. Tspan9 is expressed on mouse platelets at similar levels as on human platelets, relative to CD9.

A western blotting approach was used to discover the relative expression levels of Tspan9 and CD9 on mouse platelets. (A). Lysates of HEK 293T cells transfected with CD9 and Tspan9 FLAG-tagged constructs were western blotted with an anti-FLAG antibody. The intensity of each protein detected was quantified using the LI-COR Odyssey scanning system. These lysates and three different platelet lysates were then western blotted with (B). Tspan9 specific or (C). CD9 specific antibody and the amount of protein detected by these antibodies was related back to the amount detected in the FLAG western blot, and their relative intensities calculated. Both panels in B and C are from the same western blot. The relative intensity of CD9 in platelet lysates was arbitrarily set to 100 (D). The mean relative intensities for Tspan9 and CD9 in three platelet lysates were averaged and presented as relative expression level. Error bars represent standard error. Method originally described in Protty et al. (2009).

6.2.2 GPVI remains associated with tetraspanins in Tspan9-deficient platelets.

If GPVI is the partner protein for Tspan9, and no other platelet tetraspanin, then it would be predicted that GPVI would no longer be associated with tetraspanin microdomains in Tspan9-deficient platelets, as seen for α6 integrin in CD151 deficient cells (Yang et al., 2008). To test this, GPVI was immunoprecipitated from surface biotinylated Tspan9 wildtype and deficient platelets that had been lysed in Brij97, with CD9 and ADAM10 immunoprecipitations for controls and comparison. As previously discussed in the introduction to this thesis, lysis of cells in Brij97 lysis buffer appears to maintain the interactions between tetraspanins thus allowing whole microdomains to be captured by precipitating a tetraspanin microdomain resident protein (Charrin et al., 2003b). The neutravidin western blot for all three conditions in wildtype platelets showed the expected barcode pattern of tetraspanin associatated proteins in addition to the targeted protein (Figure 41). Interestingly, this was also the case in Tspan9-deficient platelets where GPVI immunoprecipitation resulted in the same barcode pattern as seen in the wildtype platelets (Figure 41). This result suggests either that GPVI is not a partner protein for Tspan9 or that another tetraspanin as well as Tspan9 associates with GPVI in platelets.

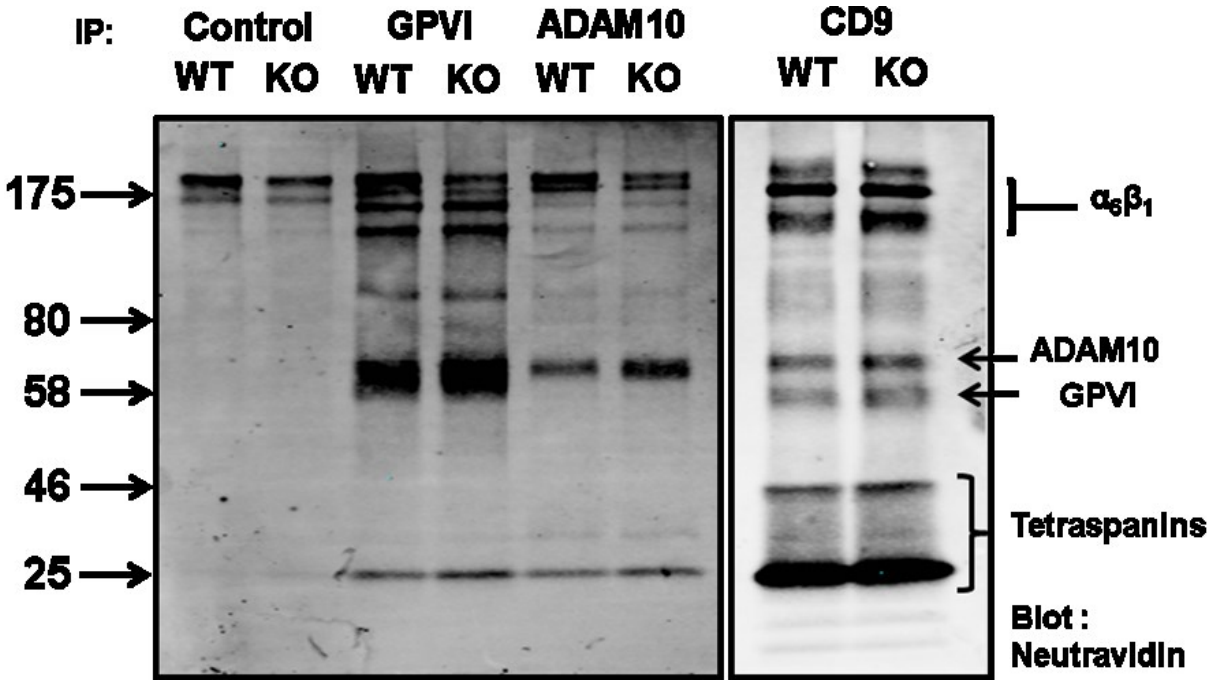

Figure 41. GPVI remains associated with tetraspanins in Tspan9-deficient platelets.

5 x 10^8 washed platelets per i.p. were surface biotinylated using EZ-link sulpho NHS LC Biotin (1 mg/ml) for 30 min. After biotinylation the platelets were lysed in 1 % Brij97 lysis buffer for 1 hour whilst rotating with unconjugated protein G sepharose beads. After this preclear step lysates were incubated with beads that been pre-coupled to either IgG control, anti-CD9, anti-ADAM10 or anti-GPVI antibody for an additional hour. Samples were washed and separated on 4 - 12 % polyacrylamide gradient gels. Separated proteins were western blotted with neutravidin to detect biotinylated proteins from the platelet cell surface. Both panels were from the same blot, but a weaker exposure of the CD9 immunoprecipitations is shown because of their relatively strong signals.

6.2.3 GPVI co-precipitates Tspan9 in Brij97 but not Digitonin.

To look specifically for an interaction between GPVI and Tspan9 (instead of tetraspanin microdomains in general), immunoprecipitations of GPVI from human platelets lysed in Brij97 or Digitonin were the next step in the investigation. Digitonin was used as a separate condition to Brij97 as it is a more stringent detergent that has been used to identify specific tetraspanin binding partners. Examples of this include ADAM10 and the TspanC8 tetraspanins (Haining et al., 2012), CD151 and laminin binding integrins (Serru et al., 1999) and CD9 and CD81 with EWI-2 (Charrin et al., 2003a). To increase the chances of detecting an interaction the amount of starting material used for the immunoprecipitations was increased and as such human platelets were used instead of using several mice for each experiment. In Brij97 lysis conditions GPVI co-precipitated Tspan9 suggesting that there is potential for their interaction in tetraspanin microdomains. However this was not the case in Digitonin lysis conditions where the co-precipitation of Tspan9 was lost (Figure 42). This result suggested either that GPVI is not the partner protein for Tspan9 or that GPVI-Tspan9 interactions are disrupted by Digitonin lysis.

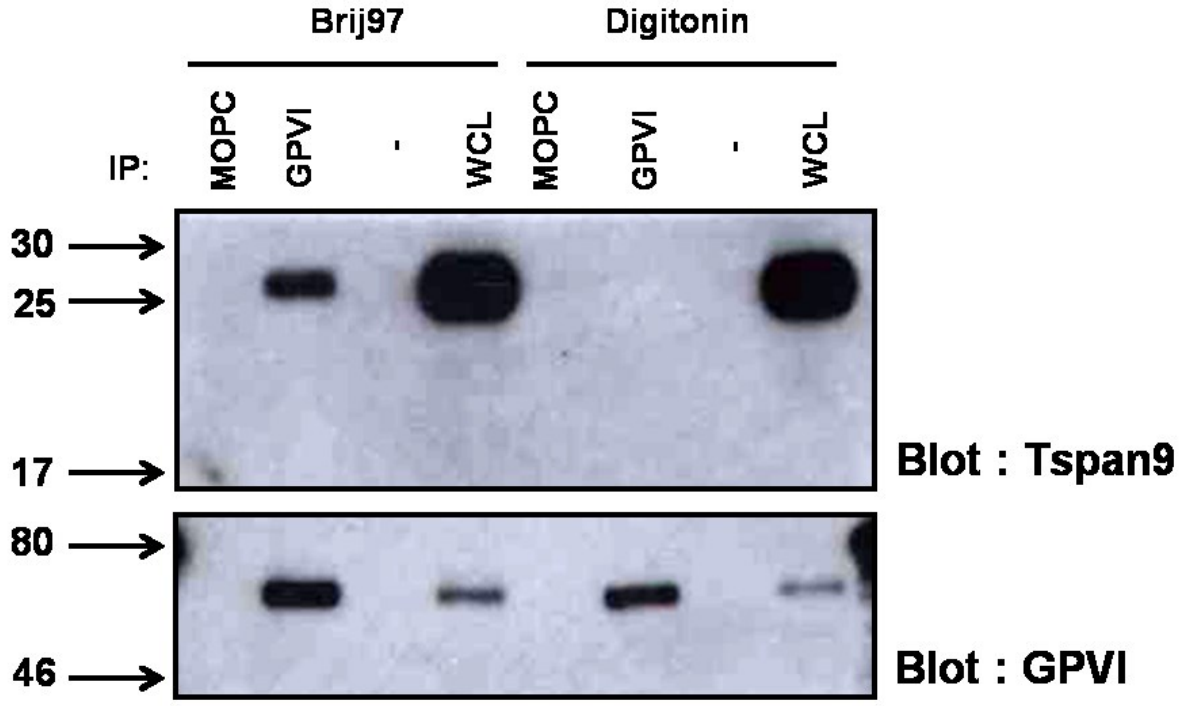

Figure 42. Tspan9 and GPVI co-precipitate in Brij97 but not in Digitonin.

1 x 10^9 washed human platelets per i.p were lysed in either 1 % Brij97 or 1 % Digitonin lysis buffer and pre-cleared with protein G separose beads for 1 hr. Precleared lysates were divided between protein G sepharose beads that had been pre-coupled to either a IgG control (MOPC) or anti-human GPVI polyantibody and rotated for 90 min. Samples were washed and separated on a 12 % acrylamide gel and western blotted for GPVI and Tspan9.

6.2.4 Tspan9 does not appear to promote GPVI dimerisation in a cell line assay.

Despite being unable to provide evidence for a direct interaction between GPVI and Tspan9 by immunoprecipitation, the question remained as to the cause of the phenotype seen in Tspan9-deficient platelets. To begin to investigate the hypothesis that Tspan9 may promote GPVI clustering, GPVI dimer specific antibodies were used to assess the levels of GPVI dimers in conditions with and without Tspan9 by flow cytometry. The antibodies 9E18 (dimer specific) and 3J24 (pan GPVI) were made and characterised by Loyau et al. (2012). These antibodies were raised against human GPVI and as such do not recognise mouse. Therefore this experiment used human GPVI constructs expressed in the HEK 293T cell line, chosen because it expresses neither GPVI nor Tspan9 (Figure 43 A). Using this approach, coexpression of Tspan9 with GPVI was not found to significantly increase the number of GPVI dimers detected by the 9E18 antibody, when compared to GPVI expression alone, or GPVI coexpression with CD9 as a control (Figure 43 B).

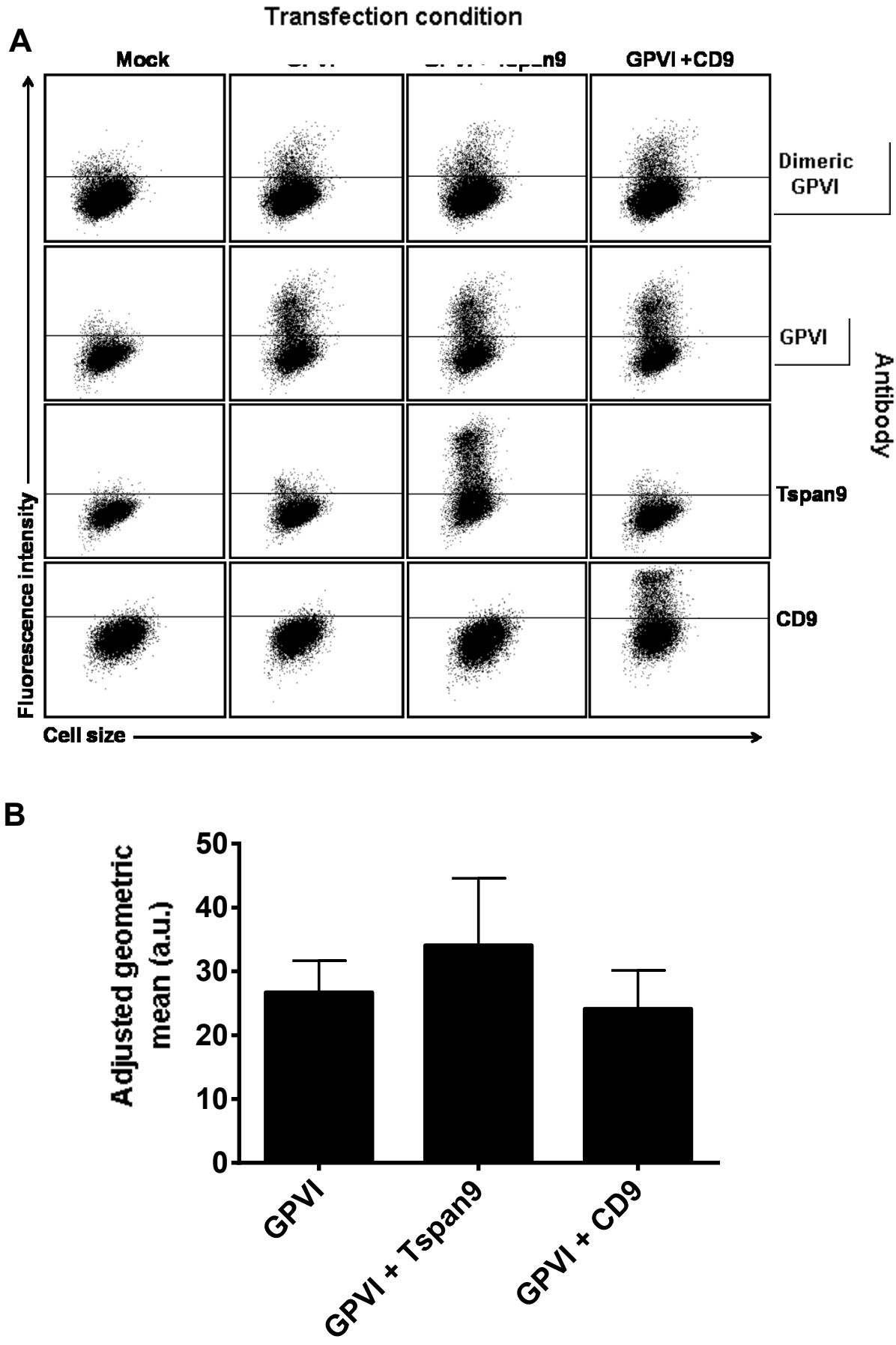
A
Transfection condition
Mock
GPVI +CD9
Dimeric GPVI
GPVI
Tspan9
CD9
Antibody
Fluorescence intensity
Cell size
B
Adjusted geometric mean (a.u.)
50
40
30
20
10
0
GPVI
GPVI + Tspan9
GPVI + CD9

Figure 43

Figure 43. Tspan9 expression does not promote GPVI dimerisation in HEK 293T cells.

HEK 293T cells transfected with GPVI (including the γ-chain) plus either Tspan9 or CD9 were stained with the 9E18 dimer specific antibody, 3J24 pan GPVI antibody or anti-Tspan9 or anti-CD9 as indicated according to the method described in Loyau et al. (2012). (A) Representative flow cytometry dot plots. (B) GPVI dimer levels were corrected for the expression level of GPVI in each condition (assessed by the geometric mean fluorescence intensity of the pan GPVI antibody 3J24) and compared between the different transfection conditions. Error bars represent the standard error from three experiments.

6.2.5 Tspan9 regulates the lateral diffusion of GPVI.

Tetraspanins are emerging as important regulators of the lateral diffusion of other proteins, modulating their movement in the membrane to influence and optimise cell functions (Espenel et al., 2008, Charrin et al., 2009). To test the hypothesis that Tspan9 regulates the lateral diffusion of GPVI, single-particle fluorescence microscopy was employed to directly measure the dynamics of individual GPVI molecules on Tspan9-deficient and wildtype platelets. This technique is well established in many cell types and has been used to assess the dynamics of several different types of transmembrane proteins (Kusumi et al., 2005). However, to our knowledge, this techique has yet to be used in the study of platelets. As such we began by developing a method. To view single molecules in the plasma membrane, total internal reflection microscopy is used to illuminate an area 100 nm from the coverslip, therefore the platelets were required to be spread across the coverslip. No physiological substrate was chosen to promote platelet spreading, instead glass alone was used to activate the platelets. This ensured that there was no ligand for GPVI (as ligand binding could alter dynamics) and no single activatory pathway targeted in this initial assessment of GPVI membrane dynamics. The platelets were spread on the glass for 35 min at 37 °C, then incubated with fluorescent antibody for 10 min, then imaged. The antibodies used were Fab fragments of the monoclonal antibodies JAQ1 (against mouse GPVI) or Nyn.H3 (against mouse CD9, as a control), which had been labelled with a single Atto647N or 565 fluorescent probe, respectively. The antibodies were added to the cells such that only a subpopulation of either protein was labelled in any cell; for these proteins in

platelets the final amount of Fab required fell in the nano-molar range. GPVI-deficient platelets and Fab fragments from control IgG antibodies were used as controls to demonstrate the specificity of the JAQ1 and Nyn.H3 Fab fragments used. The membrane dye $DiOC_6$ was used to visualise the platelet outline and the cells were imaged with 130 ms exposures for 65 s, according to the method set out in Espenel et al. (2008) in which CD9 membrane dynamics in the PC3 prostate cancer cell line were characterised. Stills from the imaging of GPVI and CD9 in wildtype and Tspan9-deficient platelets can be seen in Figure 44 and stills from the imaging of control fab fragments in wildtype platelets and of JAQ1 fab in GPVI deficient platelets can be seen in Figure 45. After imaging videos were analysed using the purpose made software PaTrack (Pierre-Emmanuel Milhiet, Inserm 554, France), which tracked the trajectories of each particle on the imaged platelets. An image of tracked CD9 and GPVI trjectories in wildtype platelets can be seen in Figure 46. After tracking, the PaTrack software also allowed extraction of trajectory motion types and diffusion coefficients for CD9 and GPVI (Figure 47 and Figure 48 respectively).

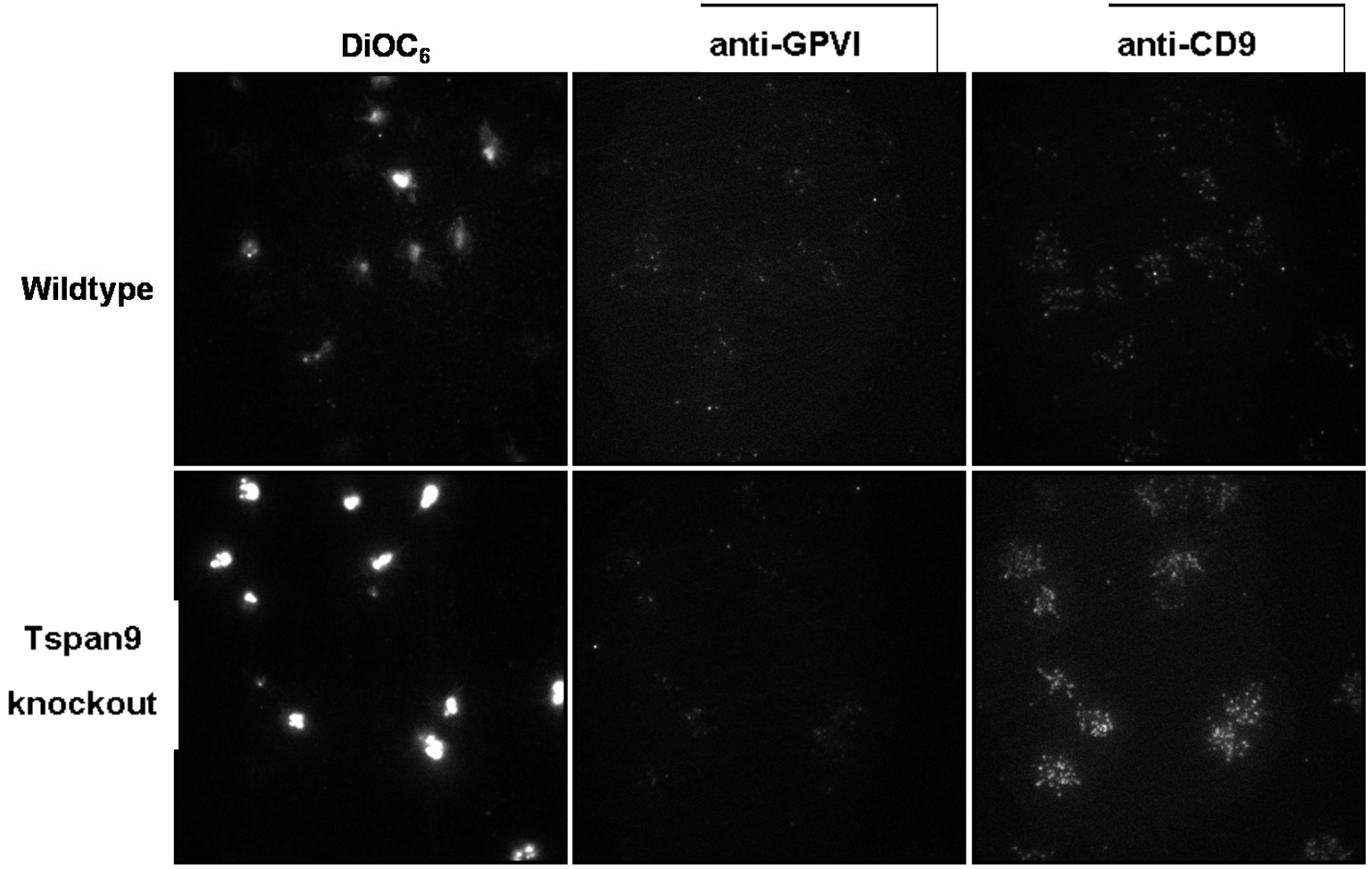

Figure 44. Stills from single particle tracking experiments in wildtype and Tspan9-deficient platelets.

Representative images of wildtype or Tspan9-deficient platelets visualised using $DiOC_6$ membrane dye or single fluor labelled Fab fragments against GPVI or CD9. Fab fragments were added to the cells such that only a subpopulation of proteins were labelled.

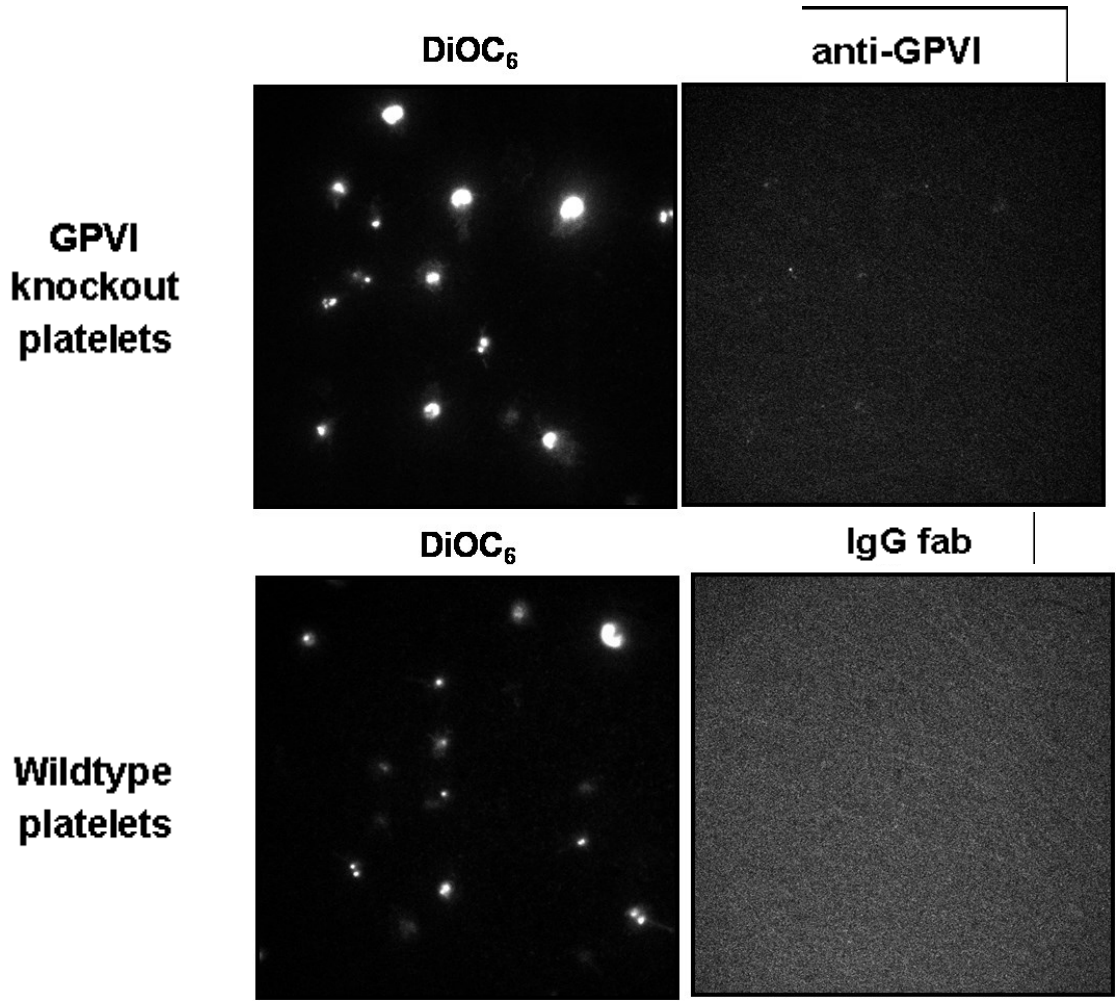

Figure 45. Stills from single particle tracking control experiments in wildtype and GPVI-deficient platelets.

GPVI knockout platelets were labelled with JAQ1 Fab to demonstate the specificity JAQ1 binding to GPVI. Additionally non specfic IgG Fab fragments were used to stain wildtype platelets, again to demonstrate the specificity of the anti-GPVI and CD9 Fab fragments.

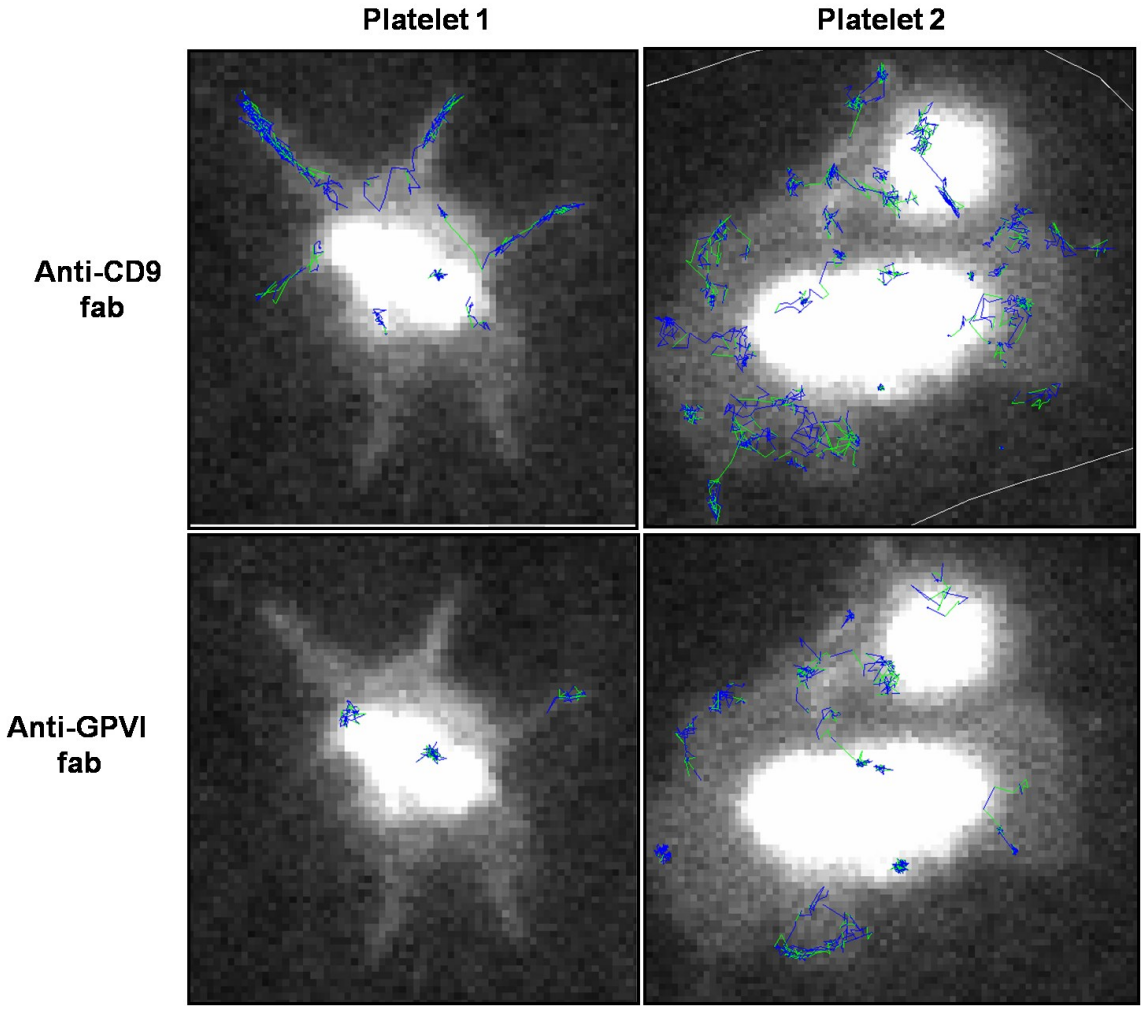

Figure 46. Examples of PaTrack software tracking of CD9 and GPVI proteins

The purpose made software PaTrack was used to analyse the trajectories of JAQ1 labelled GPVI proteins and Nyn.H3 labelled CD9 proteins in wildtype and Tspan-deficient platelets. The trajectories of individual proteins are marked in blue with green stretches in the trajectory representing movements that the software has guessed. These trajectories were used by the software to calculate the mean squared displacement of each individual protein and subsequently motion type and coefficient of diffusion. Images here are of wildtype platelets for demonstration purposes.

In wildtype platelets three different motion types were detected for GPVI trajectories: (1) Brownian diffusion (24 % of total trajectories), characterised by a median diffusion coefficient of 0.079 $\mu m^2/s$, (2) confined or restricted diffusion (59 % of total trajectories) and (3) mixed trajectories with elements of both Brownian and confined diffusion (17 % of total trajectories) (Figure 47 A). In Tspan9-deficient platelets these three motion types were also displayed by GPVI molecules, however the percentage of confined diffusion was significantly increased (69 % of total trajectories). Brownian diffusion accounted for 20 % of total trajectories with a median diffusion coefficient of 0.060 $\mu m^2/s$ and mixed trajectories 11 % of total trajectories, both not significantly different from wildtype. This increase in confined trajectories in Tspan9-deficient platelets resulted in a significantly decreased median diffusion coefficient for the total population from 0.0126 $\mu m^2/s$ to 0.007 $\mu m^2/s$ (Figure 47 B).

To determine whether this GPVI phenotype was shared by another protein in Tspan9-deficient platelets, the diffusion of CD9 was analysed. CD9 was chosen as it is the only mouse platelet tetraspanin for which a good monoclonal antibody is available. CD9 in wildtype and Tspan9-deficient platelets also displayed the three motion types as detected for GPVI (and also as found for CD9 in other cell types (Espenel et al., 2008). In wildtype platelets, Brownian diffusion accounted for 45 % of CD9 trajectories, with a median diffusion coefficient of 0.080 $\mu m^2/s$, confined diffusion 38 % of total trajectories and mixed trajectories 17 % of total trajectories. Interestingly the percentage frequency of CD9 mixed trajectories was significantly increased in Tspan9-deficient platelets to 22 % of total trajectories (Figure 48 A). This increase in mixed trajectories caused a significant increase in the mean diffusion coefficient for the total population and for pure brownian trajectories (Figure 48 B). As the diffusion

of CD9 was not affected in the same way as GPVI, this suggests that the defect seen in GPVI lateral diffusion is not a result of all the proteins in the platelet membrane becoming more confined or slowing down. For easier comparison GPVI and CD9 trajectory data for wildtype and Tspan9-deficient platelets has been complied into Table 11.

Figure 47 - GPVI membrane dynamics

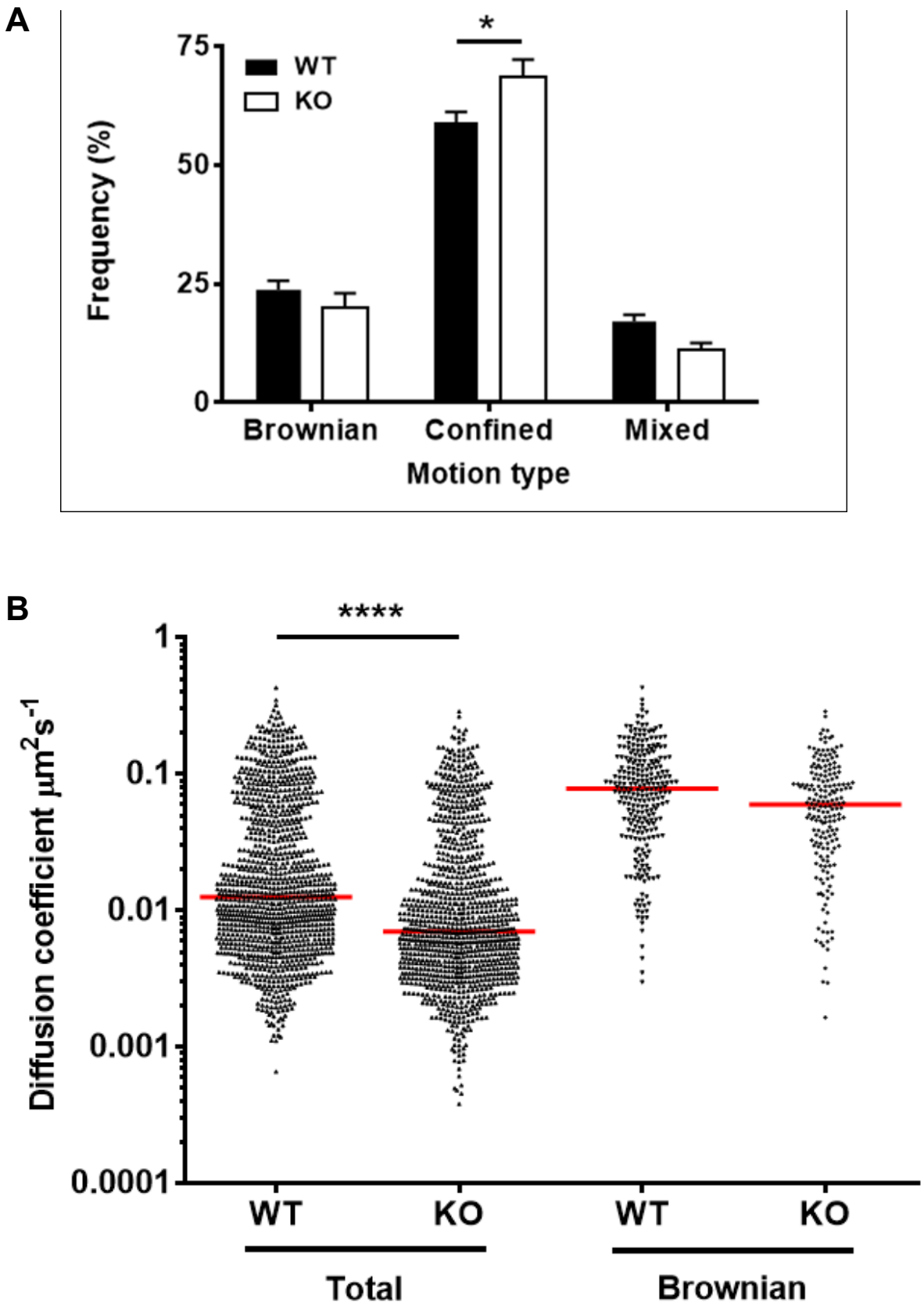

Figure 48 - CD9 membrane dynamics

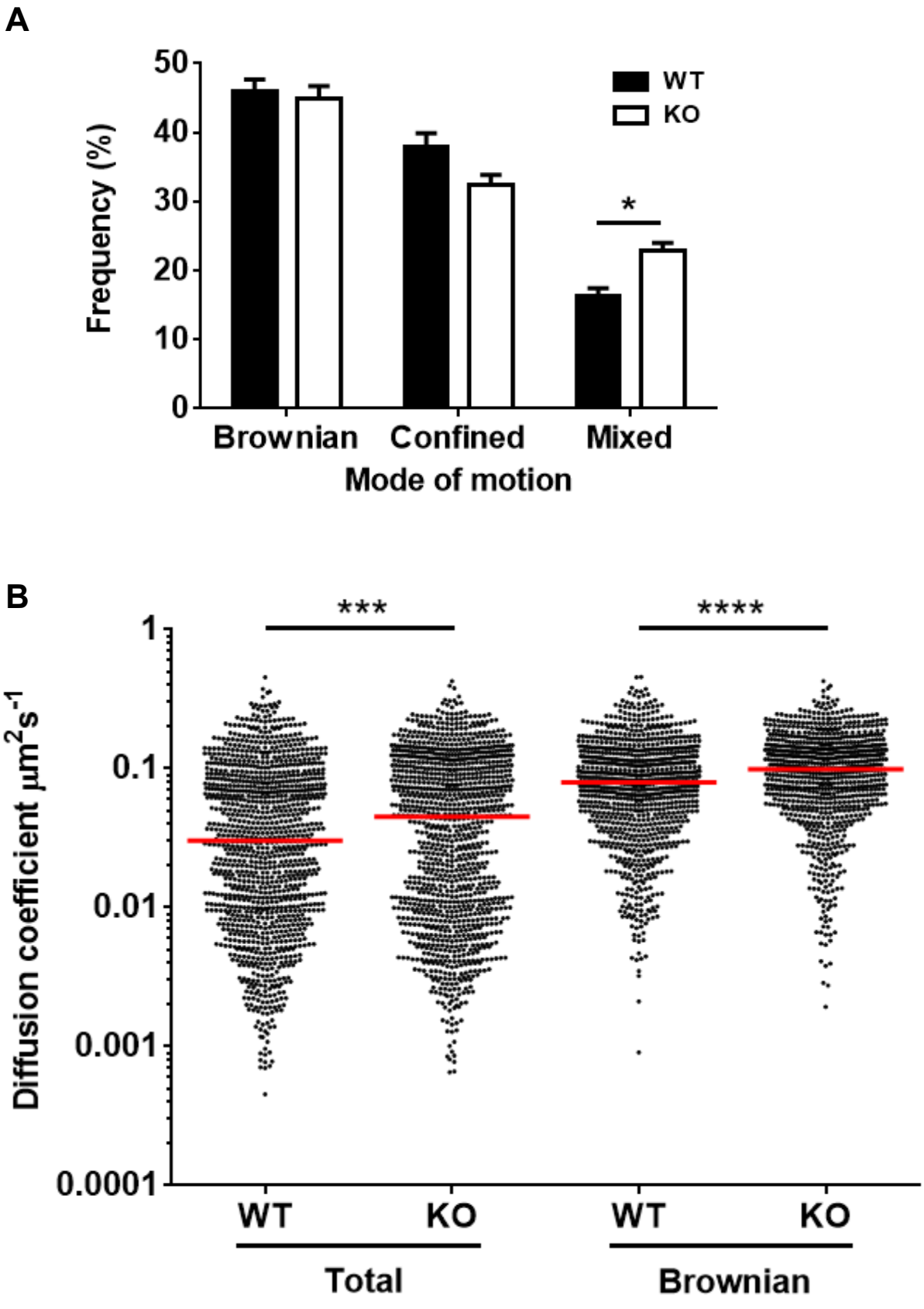

Figure 47. GPVI displays increased confinement in Tspan9-deficient platelets.

A minimum of 100 trajectories from 10 - 15 fields of view per mouse were analysed by the PaTrack software for both wildtype and Tspan9-deficient platelets spread on glass coverslips. The motion type of each trajectory and the associated coefficient of diffusion was extracted from the trajectory mean squared displacement over time. (A) The percentage frequency of each motion type in the total population is shown for wildtype and Tspan9-deficient platelets. 1000 trajectories from n = 3, error bars represent the standard error. (B) Scatter plot of diffusion coefficient for each GPVI molecule in the total population analysed or pure Brownian trajectories only. The median of each group is shown in red.

Figure 48. CD9 displays an increase in mixed motion type in Tspan9-deficient platelets.

A minimum of 100 trajectories from 5 - 10 fields of view per mouse were analysed by the PaTrack software for both wildtype and Tspan9-deficient platelets spread on glass coverslips. The motion type of each trajectory and the associated coefficient of diffusion was extracted from the trajectory mean squared displacement over time. (A) The percentage frequency of each motion type in the total population is shown for wildtype and Tspan9-deficient platelets. 2000 trajectories from n = 3, error bars represent the standard error. (B) Scatter plot of diffusion coefficient for each CD9 molecule in the total population analysed or pure Brownian trajectories. The median of each group is shown in red.

Protein	Tspan9 genotype	D	$D_{Brownian}$	Brownian	Confined	Mixed
		$\mu m^2/s$	$\mu m^2/s$	%	%	%
GPVI	Wildtype	0.0126	0.079	24	59	17
GPVI	Knockout	0.007[a]	0.060	20	69[c]	11
CD9	Wildtype	0.03	0.080	45	38	17
CD9	Knockout	0.045[b]	0.100[a]	44	32	22[c]

Table 11. Diffusion coefficients and modes of motion for GPVI and CD9 in wildtype and Tspan9-deficient platelets.

D is the median coefficient of diffusion for the total population of trajectories analysed. $D_{Brownian}$ is the median coefficient of diffusion for the trajectories that were classified as pure Brownian motion. Percentage frequency for the different types of motion detected are also shown. a represents $p < 0.0001$, b represents $p < 0.001$ and c represents $p < 0.05$. Statistical significance was measured by Kruskal-Wallis followed by a Dunn's multiple comparison test for diffusion coefficients, and by one way ANOVA followed by Sidak's multiple comparison test for (transformed) mode of motion percentage frequencies.

6.2.6 Tspan9 knockout mice heterozygote for GPVI display an aggregation defect in response to collagen

The functional data in the previous chapter, and the single particle tracking in this chapter, suggest that Tspan9 might promote GPVI lateral mobility to facilitate rapid GPVI clustering and signalling upon platelet engagement with collagen. If this were true, it would be predicted that reducing the number of GPVI molecules on the platelet cell surface should result in a more severe aggregation defect in the absence of Tspan9. To test this, a new knockout mouse strain was generated that lacked Tspan9 and was heterozygote for GPVI. This new strain (termed GPVI$^{+/-}$ Tspan9$^{-/-}$) was generated by crossing GPVI knockout mice (Cheli et al., 2008a) with Tspan9 knockout mice to produce mice heterozygous for both proteins. These double heterozygous mice were then crossed with mice either wildtype or knockout for Tspan9 to produce mice heterozygous for GPVI with or without Tspan9, respectively, and controls.

The GPVI$^{+/-}$ Tspan9$^{-/-}$ platelets in plasma were tested in their response to a low dose (1 μg/ml) of collagen in aggregometry assays. These platelets displayed a significant defect in aggregation to 1 μg/ml collagen that manifested as an extension of the shape change phase in aggregometry traces (Figure 49 A). However, GPVI$^{+/-}$ Tspan9$^{+/+}$ platelets aggregated normally to collagen, and quantitation of the data showed this to be similar to GPVI$^{+/+}$ Tspan9$^{+/+}$ and GPVI$^{+/+}$ Tspan9$^{-/-}$ platelets (Figure 49 B). As a control, aggregation to PAR4 peptide by platelets from all four mouse strains tested were normal (Figure 49 A and data not shown). Importantly, GPVI surface levels were reduced by approximately 50% in the GPVI$^{+/-}$ platelets, but other surface antigens tested were normal (Figure 50). Together these data show that the

aggregation defect in the absence of Tspan9 was exacerbated when GPVI levels are halved, since a collagen phenotype was now revealed. This is consistent with the hypothesis that Tspan9 promotes GPVI lateral mobility to promote rapid GPVI clustering and signalling in response to collagen.

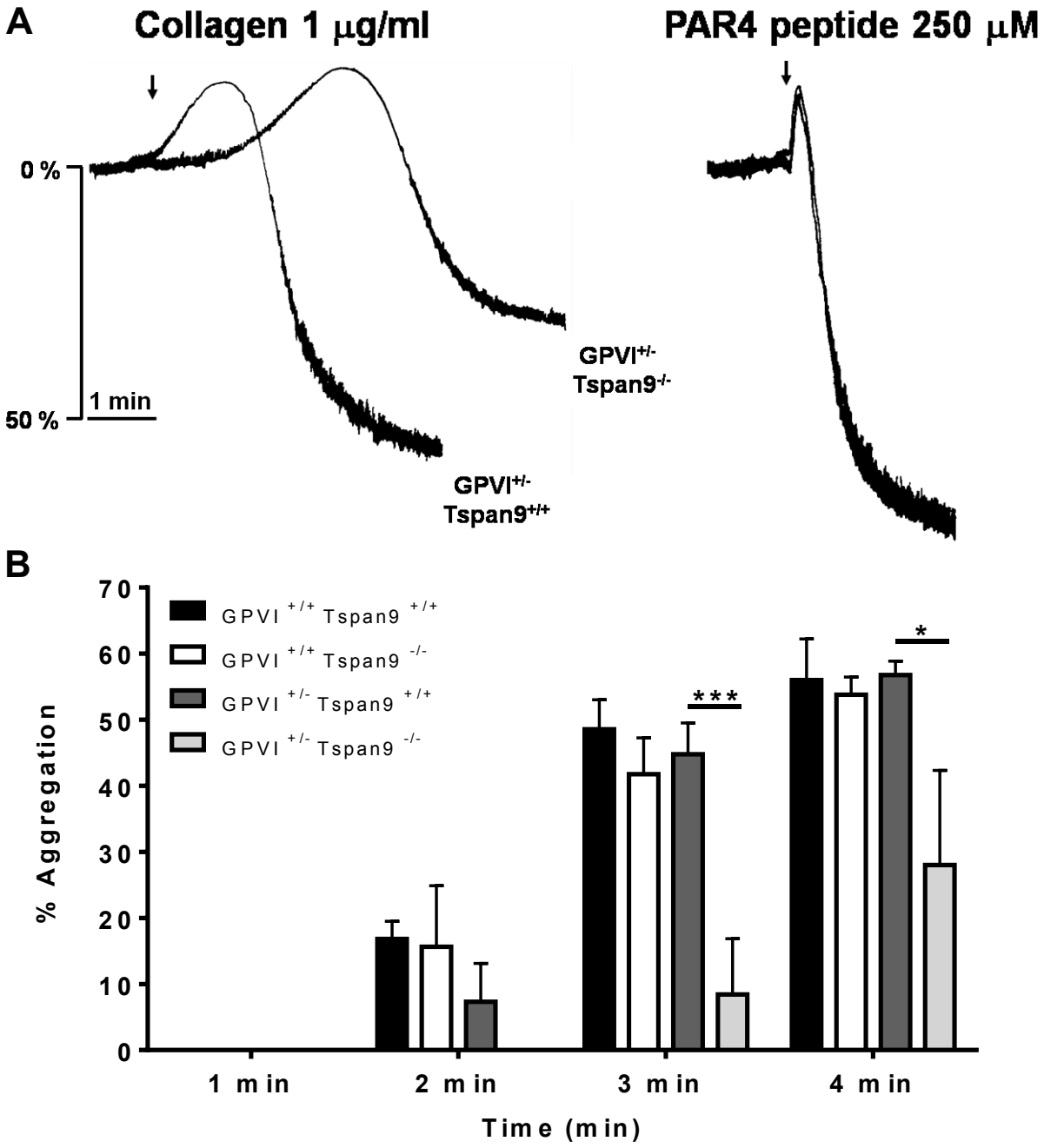

Figure 49. Tspan9-deficient platelets with reduced GPVI levels have an aggregation defect in response to collagen

Platelet rich plasma at 2 x 10^8 platelets/ml from GPVI$^{+/+}$ Tspan9$^{+/+}$, GPVI$^{+/+}$ Tspan9$^{-/-}$, GPVI$^{+/-}$ Tspan9$^{+/+}$ and GPVI$^{+/-}$ Tspan9$^{-/-}$ mice were tested by light transmission aggregometry using 1 μg/ml collagen or 250 μM PAR4 peptide. (A) Representative traces for GPVI$^{+/-}$ Tspan9$^{+/+}$ and GPVI$^{+/-}$ Tspan9$^{-/-}$ responses to 1 μg/ml collagen or 250 μM PAR4 peptide. (B) Aggregation traces were analysed as percentage aggregation over time. n=3-5 error bars represent standard error. Significance was measured by two way ANOVA followed by Bonfferoni post test.

A

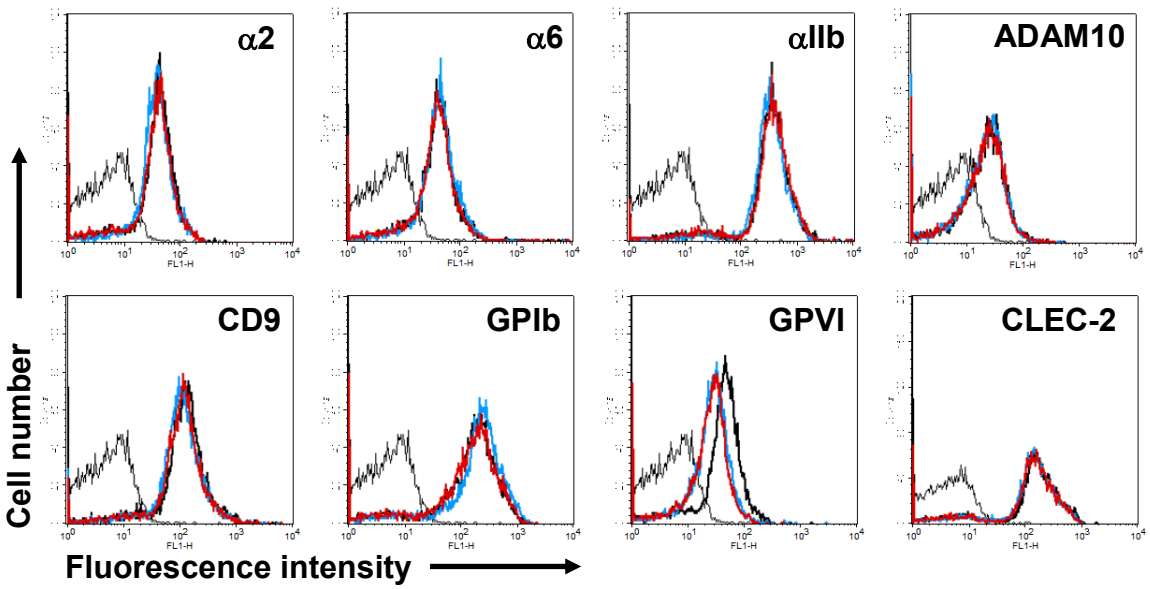

B

Surface protein	GPVI$^{+/+}$ Tspan9$^{+/+}$	GPVI$^{+/-}$ Tspan9$^{+/+}$	GPVI$^{+/-}$ Tspan9$^{-/-}$
Alpha 2	29.49 +/- 1.31	27.67 +/- 2.72	29.40 +/- 2.92
Alpha 6	32.55 +/- 2.22	33.14 +/- 1.50	35.69 +/- 1.60
Alpha IIb	274.48 +/- 8.68	247.75 +/- 10.11	274.31 +/- 33.34
ADAM10	12.86 +/- 1.41	13.32 +/- 1.32	13.98 +/- 1.44
CD9	87.79 +/- 16.67	91.93 +/- 7.19	85.58 +/- 9.62
GPIb	144.17 +/- 43.10	148.47 +/- 13.85	138.84 +/- 35.39
GPVI	36.92 +/- 5.97	20.37 +/- 0.61	19.88 +/- 0.64
CLEC-2	128.26 +/- 25.06	150.22 +/- 22.36	134.93 +/- 27.37

Figure 50. GPVI$^{+/-}$ Tspan9$^{+/+}$ and GPVI$^{+/-}$ Tspan9$^{-/-}$ platelets express normal levels of several surface proteins, except for GPVI.

Whole blood drawn into acid citrate dextrose was incubated with the relevant anti-mouse antibody conjugated to FITC. Platelet specific staining was isolated by gating on platelets by size. A. Representative flow cytometry histogram plots for each indicated protein. GPVI$^{+/+}$ Tspan9$^{+/+}$ in black and GPVI$^{+/-}$ Tspan9$^{+/+}$ in red and GPVI$^{+/-}$ Tspan9$^{+/+}$ in blue. For simplicity only the control trace from wildtype staining is shown. B. Geometric mean intensity used to assess surface receptor levels. n = 3, +/- represents standard deviation around the mean.

6.3 Discussion

Presented here is an investigation into the mechanism by which Tspan9 may regulate GPVI function on platelets. The initial hypothesis was that Tspan9 regulates the clustering and/or the lateral mobility of GPVI. This was based on the results of function testing Tspan9-deficient platelets which revealed a specific defect in responses to the GPVI specific agonist collagen-related peptide, but without any effect on GPVI expression levels. The aim of this investigation was to use an immunoprecipitation and western blotting approach to discover if GPVI was a partner protein for Tspan9, and to use dimer specific antibodies, single-molecule fluorescence microscopy and a Tspan9-deficient mouse on a GPVI heterozygote background to investigate if Tspan9 could regulate GPVI clustering or lateral mobility. The final conclusion of this project was that GPVI may not necessarily be a direct partner protein for Tspan9, however Tspan9 does appear to promote GPVI lateral mobility in the platelet plasma membrane, which could explain the impaired GPVI-induced aggregation in the absence of the tetraspanin.

As the classical approaches to capturing an interaction specifically between GPVI and Tspan9 failed, it could not be concluded that GPVI is a partner protein for Tspan9. A clear example of how a direct partner protein of a tetraspanin behaves in this type of experiment can be seen for α6 integrin, a partner protein of CD151. In CD151 wildtype conditions, immunoprecipitation of tetraspanin microdomains in Brij97 precipitates α6. However, microdomain precipitates from CD151 knockout cells no longer contain α6, as without its partner protein, α6 can no longer interact with tetraspanins (Hemler, 2005). Despite the lack of definitive evidence that GPVI and Tspan9 interact directly with each other, the defect seen in Tspan9-deficient

platelets was specific for GPVI. Furthermore, reducing the number of GPVI molecules on the platelet surface by generating GPVI$^{+/-}$ Tspan9$^{-/-}$ mice exacerbated the Tspan9 phenotype, seen by the development of an aggregation defect to low dose collagen.

Results from single particle tracking experiments suggested that the absence of Tspan9 leads to inefficient diffusion of GPVI in the plasma membrane caused by an increased confinement of GPVI molecules. This change in membrane dynamics causes a decrease in the diffusion speed of the GPVI population in the plasma membrane. This change could cause a dysregulation in GPVI distribution in the membrane, and so potentially clustering on collagen. Whilst this could be the cause of the aggregation defect seen in the Tspan9-deficient platelets, the question remains as to the mechanism by which Tspan9 can influence the type of diffusion GPVI undergoes in the platelet membrane, and this issue will be addressed in the General Discussion.

The membrane dynamics of two other tetraspanins and their partner proteins have been investigated: CD151 and CD37 and their integrin partners α6β1 and α4β1, respectively (van Spriel et al., 2012, Yang et al., 2012b). In both of these studies, knockout of the tetraspanin had an effect on the lateral diffusion of the integrin, as seen here for GPVI. The CD37 study in particular has some interesting similarities to the result found with GPVI. Without CD37, the lateral diffusion of α4β1 was slower than in wildtype conditions (as measured by FRAP), and perhaps more interestingly, the integrin distribution in the plasma membrane was altered resulting in smaller integrin clusters than found in wildtype conditions (as measured by scanning electron microscopy) (van Spriel et al., 2012). Despite not analysing the individual movements

of α4 molecules, as done here for GPVI, the gross effects on the total population offer an appealing precedent when a potential clustering defect in GPVI is considered. Whilst the single particle tracking experiments have clearly demonstrated a change in the behaviour of GPVI molecules, evidence from the study on CD37 and α4β1 suggest that larger scale studies of GPVI membrane diffusion may be more informative as to the overall effect of these changes on GPVI. Such studies may provide a clearer link between GPVI dysregulation and the functional defects seen in Tspan9-deficient platelets.

CHAPTER VII: GENERAL DISCUSSION

The initial aims of this thesis were to investigate the function of the tetraspanins Tspan33 and Tspan9 on platelets, using their respective knockout mice. Experiments with Tspan33-deficient platelets, and evidence from a platelet transcriptomics study by Rowley et al. (2011), led to the conclusion that Tspan33 was not expressed on mouse platelets. However, analyses of Tspan33-deficient red blood cells identified a role for Tspan33 in surface expression of the metalloprotease ADAM10. Further work identified a subgroup of five other tetraspanins that had substantial sequence identity to Tspan33, termed the TspanC8s, and each could interact with ADAM10. This is the first demonstration of redundant functions between three or more tetraspanins. Moreover, it is possible that different TspanC8s target ADAM10 to distinct substrates. Assessments of Tspan9-deficient platelets identified a subtle but specific defect in aggregation induced by the collagen receptor GPVI. Development of single particle tracking, for the first time in platelets, led to the conclusion that Tspan9 may regulate the clustering of the platelet collagen receptor GPVI, most likely by regulating its membrane dynamics.

7.1 Tspan33, and related TspanC8 tetraspanins, regulate ADAM10

Despite being unable to study the function of Tspan33 on platelets, results from this thesis, in combination with other work from the lab and collaborators, demonstrated that Tspan33 is a member of the TspanC8 subfamily of tetraspanins, all of which partner and regulate the metalloprotease ADAM10 (Haining et al., 2012, Dornier et al., 2012, Prox et al., 2012). In terms of ADAM10 biology, finally revealing the tetraspanins with which it associates was exciting as it had been recognised as a tetraspanin associated protein, without an identified tetraspanin partner, since 2006

(André et al., 2006). Additionally, now that its partner tetraspanins have been identified, research assessing the regulation of ADAM10 by tetraspanins can develop and may lead to new approaches in the drug targeting of ADAM10 in human diseases such as Alzheimer's disease and cancer (Saftig and Reiss, 2011). In particular, the existence of six different tetraspanins, with differential expression, that all interact with ADAM10, provides great potential for obtaining increased specificity in the targeting of ADAM10. Work in this thesis, in Dornier et al. (2012) and in Haining et al. (2012), demonstrate that the TspanC8 tetraspanins have differential expression between different cell types and are able, to some extent, to compensate for each other. This may provide a mechanism for overcoming the issues associated with drug targeting the ubiquitously expressed ADAM10 (Saftig and Reiss, 2011).

Several different approaches could harness the therapeutic potential of TspanC8/ADAM10 complexes. Monoclonal antibodies that target a specific TspanC8-ADAM10 complex could potentially disrupt the interaction. This could deregulate ADAM10 substrate targeting, potentially preventing or upregulating the cleavage of a substrate of interest. A different approach would be to design a small molecule inhibitor that would disrupt the interaction between ADAM10 and a TspanC8 tetraspanin in the endoplasmic reticulum or the golgi. This would prevent the cell surface expression of the protein and so potentially prevent the cleavage of several targets on the cell. Finally, TspanC8 tetraspanin mRNA could be introduced into cells using a modified targeted virus. This introduction of a particular TspanC8 tetraspanin could potentially modulate the expression or targeting of ADAM10, although the new TspanC8 would have to compete for ADAM10 with the endogenous TspanC8 expressed in the targeted cell type. Depending on the outcome for ADAM10 function,

all three of these approaches could be useful in diseases such as Alzheimer's, where it is already well established that promoting the cleavage of amyloid precursor protein by ADAM10 is beneficial for prevention of both disease initiation and progression (Vincent and Checler, 2012), or in cancers where ADAM10 is upregulated (Saftig and Reiss, 2011).

The question of why so many tetraspanins associate with ADAM10 is, in itself, a point of interest. Dornier et al. (2012) published a role for TspanC8s Tspan5 and Tspan14, but not Tspan15, in promoting the cleavage of Notch by ADAM10, suggesting that different TspanC8 tetraspanins may facilitate the targeting of ADAM10 to different substrates in different cell types. As many ADAM10 targets do not share an obvious cleavage recognition site, regulation by tetraspanins may address this unclear area of ADAM10 biology. A summary diagram of the regulation of ADAM10 by the TspanC8 tetraspanins can be seen in Figure 51. Some important targets of ADAM10 in the cardiovascular system and a potential TspanC8 tetraspanin that may be involved in their targeting by ADAM10 have also been highlighted in the diagram, although aside from Tspan5 promoting ADAM10 cleavage of Notch, this is speculation included only to demonstrate the possibility of substrate-specific localisation.

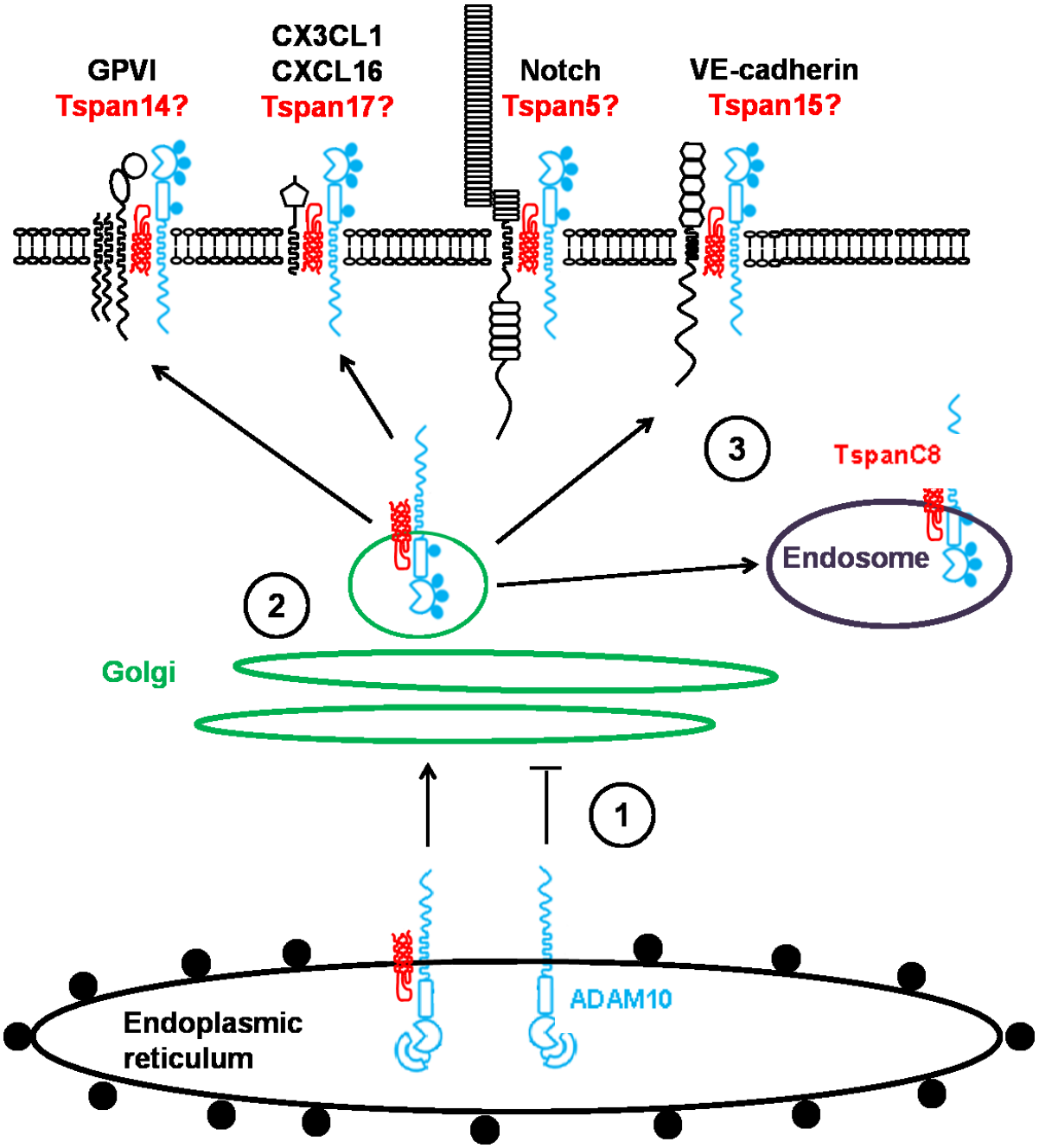

Figure 51. Tetraspanin association regulates ADAM10 egress from the endoplasmic reticulum and may regulate ADAM10 substrate targeting.

1. The TspanC8 tetraspanins associate with ADAM10 in the endoplasmic reticulum. This association is necessary for the egress of ADAM10 from this compartment through an unknown mechanism (Haining et al., 2012, Dornier et al., 2012, Prox et al., 2012). 2. TspanC8 association also promotes the progression of ADAM10 through the golgi where its maturation is completed by furin proteases that remove its prodomain. 3. After leaving the golgi it is hypothesised that different TspanC8 tetraspanins target ADAM10 to different areas of the cell and potentially to different substrates.

Several different experiments could be done to begin investigate the regulation of ADAM10 substrate targeting by tetraspanins. Cleavage of ADAM10 targets in cell lines could be assessed before and after TspanC8 tetraspanin knockdown. Cell types would have to be carefully selected for this experiment and their TspanC8 repertoires determine beforehand by real time PCR. This experiment would have the drawback that ADAM10 surface expression would be affected by TspanC8 knockdown. A different approach could make use of biomolecular fluorescence complementation (BiFC) technology. The two proteins of interest (i.e. ADAM10 and a TspanC8) are expressed with opposite halves of yellow fluorescent protein (YFP). Upon interaction, the two halves of YFP can fold together irreversibly to form a fluorescent YFP molecule. This would allow the ADAM10-TspanC8 dimer to be imaged by fluorescent microscopy, potentially in relation to specific ADAM10 substrates. A more simple and complementary approach would be to look at the sub-cellular location of different fluorescently tagged tetraspanins versus ADAM10 substrates.

Aside from the implications for aiding the understanding of ADAM10 regulation and new insights into its potential as a drug target, the existence of the TspanC8 tetraspanin subfamily makes an important contribution to the study of tetraspanins. It is now clear that when studying the function of one tetraspanin it is important to consider also assessing any closely related tetraspanins. There were already hints to this phenomenon in the tetraspanin literature. In particular, there are several examples of compensation between the two closely related tetraspanins CD9 and CD81, in sharing of the partner proteins EWI-2 and EWI-F (Stipp et al., 2001) and the rescue of CD9-deficient oocyte fusion by CD81 (Takeda et al., 2008, Kaji et al., 2002, Takeda et al., 2003). For investigations into this compensation between TspanC8

tetraspanins, there is a clear need for good antibodies against tetraspanins so that the expression levels of the different family members can be determined on different cell types.

The data mined from Rowley et al. (2011) in the investigation into the function of Tspan33 on platelets highlighted a differential expression of tetraspanins between human and mouse. This is not surprising given that certain other platelet proteins are differentially expressed between these species (e.g. the PAR thrombin receptors). Furthermore, this is unlikely to be a phenomenon restricted to platelets and therefore, despite the difficulty presented by a lack of antibodies to most tetraspanins, their expression should always be assessed when moving studies between species. Finally, the defect reported in erythropoiesis in the Tspan33 knockout mouse (Heikens et al., 2007) suggests that ADAM10 may be important in an aspect of red blood cell differentiation not previously appreciated. Additionally, given that Tspan33 was first identified by its position in a susceptibility locus for myeloid malignancy (Chen et al., 2005), ADAM10 may also be an as yet overlooked protein in the development of these type of cancers.

7.2 Tspan9 and the regulation of GPVI membrane dynamics

Investigations into the functionality of Tspan9-deficient platelets suggested that this tetraspanin was involved in the regulation of the platelet collagen receptor GPVI. The type of defects seen in Tspan9-deficient platelets with GPVI wildtype or heterozygous backgrounds led to the conclusion that Tspan9 may regulate the clustering of the receptor. Single particle tracking experiments suggested that the defect was at the level of GPVI membrane dynamics. Several further experiments, detailed in the following, could develop a better understanding of the phenotype of Tspan9-deficient platelets and so improve upon the current conclusions. Extension of analyses of the Tspan9 knockout mouse by moving to *in vivo* studies of platelet function could lead to a better appreciation of the importance of the contribution of Tspan9 to GPVI regulation. The phenotype displayed in *ex vivo* function tests suggests that platelet function is only mildly affected by the loss of Tspan9 as it is overcome at increasing doses of agonist. However, it cannot be for certain this would follow *in vivo.* One experiment in particular, the transient middle cerebral artery occlusion (tMCAO) model for ischaemic stroke would be particularly informative of the contribution of Tspan9 to GPVI function *in vivo.* This reperfusion injury or thrombo-inflammatory model has (a somewhat unexpected) significant role for GPVI whereas some other models that directly assess thrombosis have a less clear requirement for GPVI expression (Dutting et al., 2012). *In vivo* experiments are currently underway in collaboration with Prof Bernhard Nieswandt, to whom the Tspan9 knockout mice have been sent. Until there is an understanding of the contribution of Tspan9 to GPVI regulation *in vivo* it will be difficult to assess if there is any potential in drug targeting GPVI through its interaction with Tspan9.

Generation of Tspan9-deficient mice on the humanised GPVI background, developed by Mangin et al. (2012), would allow direct assessment of GPVI dimer levels on resting and activated platelets using the human GPVI dimer specific antibodies developed by Loyau et al. (2012) and Jung et al. (2012). This method would be more definitive than the cell line approach used in this thesis which did not find a role for Tspan9 in promoting GPVI dimerisation, despite other experiments indicating that this aspect of GPVI function could be affected. Finally, after the initial assessments of GPVI membrane dynamics presented in this thesis, more detailed analyses of the platelet plasma membrane, with single molecule fluorescent microscopy and FRAP experiments, will further contribute to the understanding of the behaviour of this protein (and others). In particular, assessment of GPVI-GPVI co-diffusion events, the nature, size and components of confinement areas in the platelet membrane, and how behaviour changes upon ligand binding, will be useful in understanding in more detail why GPVI is more confined in Tspan9-deficient platelets.

GPVI initially appeared to be a good candidate partner protein for Tspan9 as it appeared specifically affected by Tspan9 deficiency and was already a known tetraspanin associated protein (Protty et al., 2009). However, GPVI still appeared associated with tetraspanin microdomains in Tspan9-deficient platelets. Given the results from the study of Tspan33 and the TspanC8 tetraspanins, one possible explanation for this is that the loss of Tspan9 is compensated for by another tetraspanin. According to the dendrogram of mammalian tetraspanins (Haining et al., 2012), the most closely related tetraspanin to Tspan9 is Tspan4, which shares 56% amino acid sequence identity; all other tetraspanins are less than 40% identical to Tspan9. Tspan4 is relatively uncharacterised and is yet to be studied on platelets and

was not studied in this thesis, and so is an important topic for further study in the continuation of this project. The various human and mouse platelet proteomic and transcriptomics studies suggest that Tspan4 may be expressed on both human and mouse platelets, albeit at low levels (Senis et al., 2007, Lewandrowski et al., 2009a, Rowley et al., 2011). Tspan4 is one of the few tetraspanins for which a good antibody exists and so confirmation of its expression in platelets would be the first experiment in investigations into its function and potential compensation for Tspan9 on platelets. Other possibilities that could explain the association of GPVI with Tspan9-deficient tetraspanin microdomains include that Tspan9 does not associate directly with GPVI. Another unidentified tetraspanin could be a bridge between Tspan9 and GPVI or indeed the γ-chain. Another receptor that associates with the γ-chain is the high affinity receptor for IgE, FcεRI, which was found to be associated with CD9 and CD81 on antigen presenting cells (Peng et al., 2011). This suggests that an association between the γ-chain and a tetraspanin on platelets is possible. To investigate the possibility of the γ-chain bridging between tetraspanins and GPVI, the γ-chain could be immunoprecipitated from GPVI deficient platelets in Brij97 to assess if it is tetraspanin associated without GPVI. An alternative method for discovering the partner protein for Tspan9, which is less directed toward GPVI, would be to immunoprecipitate tetraspanin microdomains in Brij97 from Tspan9-deficient platelets, and use mass spectrometry to look for a platelet protein that is missing when compared to tetraspanin microdomains from wildtype platelets.

Despite the partner protein for Tspan9 remaining unknown it is clear that removing it from the platelet cell surface has an effect on GPVI membrane dynamics, as shown by the single particle tracking experiments. There are no published mechanisms,

even for well established tetraspanin-partner protein pairs (Yang et al., 2012a, van Spriel et al., 2012), for exactly how tetraspanins exert their effects on partner protein lateral diffusion. It is therefore not straightforward to determine how Tspan9, which may not directly associate with GPVI, contributes to GPVI membrane dynamics. Three possible mechanisms are discussed in the following, along with experiments that could be used to test each hypothesis.

The first mechanism suggests that Tspan9 and GPVI do interact in the platelet membrane and that through an interaction between the cytoplasmic tails of GPVI, or γ-chains, and Tspan9, the tail of GPVI folds up toward the underside of the cell membrane. This would reduce the number of interactions the GPVI tail was available for and so potentially limit the dwell time of GPVI in confined areas of the membrane, where it has been shown that interactions with intracellular scaffold proteins are promoted (Triller and Choquet, 2003). A diagram of this mechanism can be seen in Figure 52. There is some potential for an interaction between the tails of GPVI and Tspan9 as this area of Tspan9 contains several charged residues that could facilitate such an interaction (Seigneuret, 2006). There is currently no published interaction of this kind between a transmembrane partner protein and a tetraspanin, however the intracellular tails of tetraspanins have been demonstrated as important for their function in several studies (Wang et al., 2011, Harris et al., 2013, Latysheva et al., 2006). To investigate this hypothesis, first the dwell time of GPVI molecules in confined areas of the membrane could be measured using the single molecule fluorescence microscopy approach described in Chapter 6. This could be compared between wildtype and Tspan9-deficient platelets to investigate if this is the cause of the observed increased confinement of GPVI in Tspan9-deficient platelets. Should

this be the case, the membrane dynamics of GPVI mutants that lack intracellular tail segments, or Tspan9 chimera constructs that contain another tetraspanin's intracellular tails, could be assessed in transfected cells and compared to wildtype constructs to assess the contribution of the tails of these proteins to GPVI membrane dynamics.

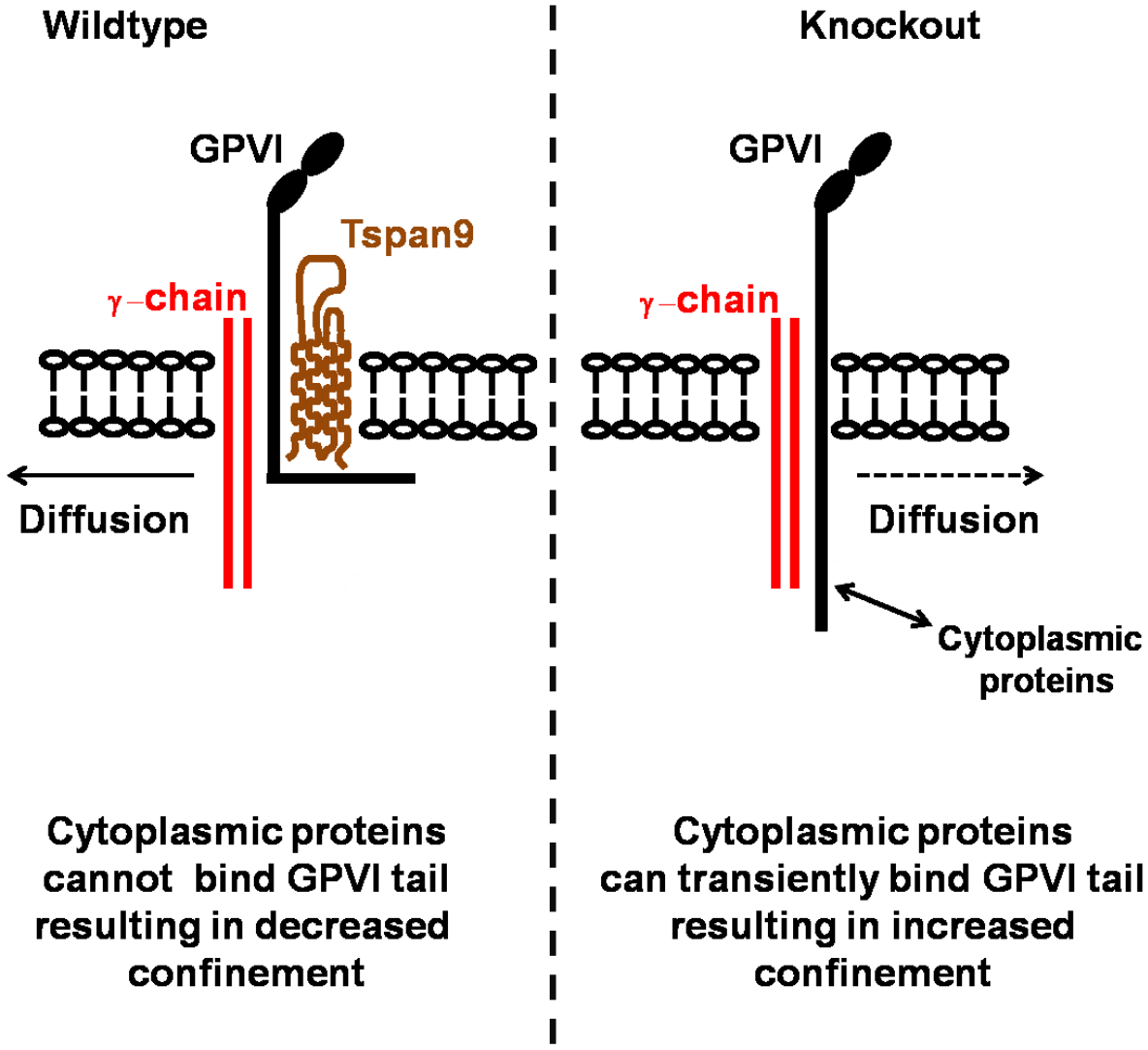

Figure 52. The intracellular tails of Tspan9 may associate with the intracellular tails of GPVI causing it to fold up to the membrane

An interaction between the intracellular tails of GPVI and Tspan9 causes the tail of GPVI to fold toward the membrane. This folding masks potential binding sites for cytosolic proteins which are thought to be abundant underneath membrane confinement areas. This folding would reduce these cytosolic proteins from binding the tail and causing overly long GPVI dwell times in confinement. In Tspan9-deficient platelets this folding would not occur, leading to cytosolic proteins binding the tail of GPVI, causing an increase in confinement of the protein.

An alternative mechanism that could also explain the increased confinement of GPVI in Tspan9-deficient platelets is that Tspan9 associates not with GPVI but another platelet membrane protein. This protein, without its tetraspanin partner, could become immobile in confined areas in the membrane. This unknown protein could then act as a barrier to GPVI molecules leaving these confined areas, thus increasing GPVI dwell times. A diagram of this mechanism can be seen in Figure 53. The idea that immobile proteins form a barrier around areas of confinement in the membrane is described by Kusumi et al. (2005) and forms part of the picket fence model of plasma membrane compartmentalisation. To investigate this hypothesis, single molecule fluorescence microscopy could be used to assess the dwell times of GPVI molecules between Tspan9 wildtype and deficient platelets, as previously mentioned, and additionally the sizes of the regions of GPVI confinement can be measured. This would distinguish between GPVI molecules being more confined due to larger confinement areas, as opposed to increased confinement area fencing. Assessment of the dynamics of other known tetraspanin associated proteins, such as ADAM10 (Haining et al., 2012), could also be informative as other proteins should also encounter the same barrier, should it exist, causing a similar increase in confined area dwell time and general confined diffusion.

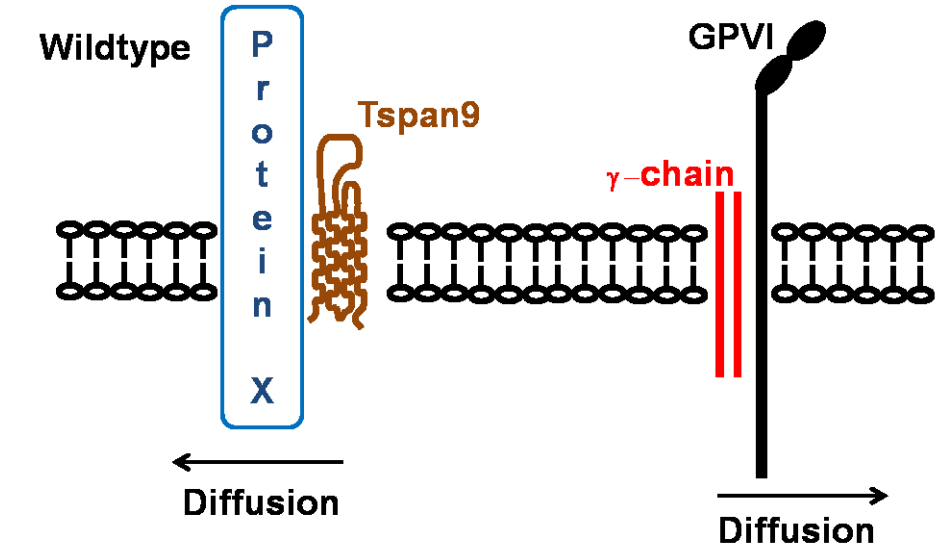

Unknown Tspan9 partner protein is able to diffuse in the membrane.
GPVI diffusion unaffected

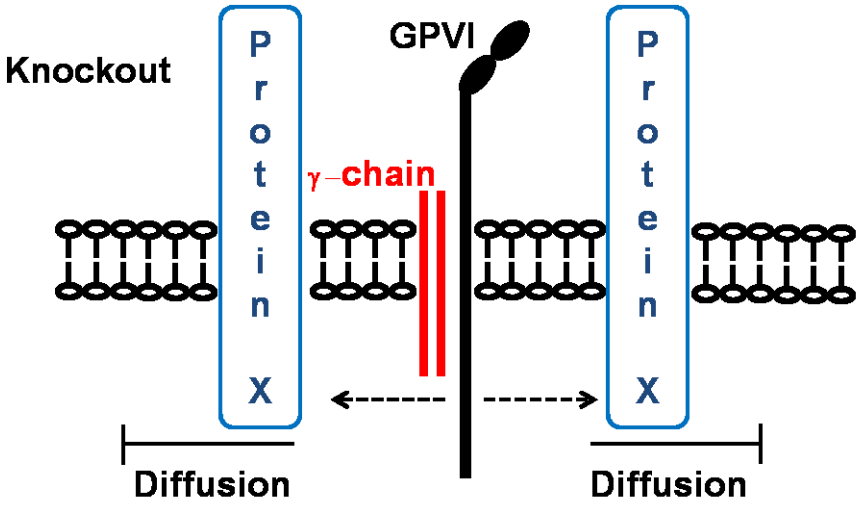

Unknown Tspan9 partner protein is unable to diffuse in the membrane.
GPVI becomes more confined

Figure 53.

Figure 53. Tspan9 may regulate the lateral diffusion of another partner protein, which without Tspan9 causes increased confinement of GPVI.

Tspan9 may not associate with GPVI and instead partner another protein, depicted in this diagram as Protein X. The association of Tspan9 with Protein X regulates the lateral diffusion of this protein, promoting Brownian modes of motion. In Tspan9-deficient platelets, Protein X becomes more confined without Tspan9, augmenting the picket fence barrier around confinement areas. This increase in confined domain barriers prevents GPVI from leaving confined domains as easily, causing its increased confinement in Tspan9-deficient cells.

The final hypothesis suggests that Tspan9 associates with GPVI and that this interaction promotes the association of specific lipids with the tetraspanin-receptor complex (Figure 54). The association of lipids such as cholesterol is thought to promote protein lateral diffusion (Mayor and Rao, 2004, Dietrich et al., 2002) and may aid GPVI in overcoming the expected decrease in diffusion speed when it dimerises. Overcoming this limiting step in higher order clustering would potentially allow the formation of GPVI dimer clusters at rates comparable to initial dimer formation itself. As receptor clustering is thought to increase signalling strength into the platelet (Nieswandt and Watson, 2003), a reduction in dimer diffusion speed could result in the collagen-related peptide insensitivity seen in Tspan9-deficient platelets. To investigate this hypothesis, the association of GPVI with lipid could be assessed using fractionation of wildtype and Tspan9-deficient platelet membranes over sucrose gradients, predicting that GPVI would appear in increased density fractions in Tspan9-deficient conditions. Alternatively, a lipidomics approach could be adopted, in which GPVI could be immunoprecipitated from wildtype or Tspan9-deficient platelets and any associated lipid analysed and compared using mass spectrometry. A similar approach was taken to determine the composition of T-cell receptor activation domains (Zech et al., 2009). Additionally, single particle fluorescence microscopy could be used to capture instances of co-diffusion between GPVI molecules and measure the speed at which they diffuse before and after dimerisation. A similar analysis for CD9 molecules demonstrated a continuation of the same diffusion speed of CD9 molecules before and during co-diffusion, and a similar hypothesis regarding diffusion with a platform of associated lipid was proposed to explain this phenomenon (Espenel et al., 2008). Important to the

discussion, in the context of this hypothesis, is the potential association of GPVI with lipid rafts. Whilst it has been reported that GPVI is associated with lipid rafts, this subject remains a controversial area in GPVI biology, with two labs reporting GPVI association under basal conditions (Wonerow et al., 2002, Ezumi et al., 2002) and another suggesting the translocation of GPVI to rafts upon dimerisation (Locke et al., 2002). In the light of this controversy it is difficult to assess the contribution of lipid rafts to the regulation of GPVI dimerisation and clustering. Should this hypothesis of tetraspanins bringing associated lipid to GPVI be correct, then the lipid rafts in which GPVI has been captured could be tetraspanin microdomains mistaken for lipid rafts. As discussed in the introduction to this thesis, tetraspanin microdomains can occasionally be found in the light fractions of sucrose gradients if the cells have been lysed in low stringency conditions. The difference in lipid raft preparation between labs could mean that in some cases tetraspanin microdomains are captured and in some cases not, perhaps explaining the difference seen between the two conflicting studies.

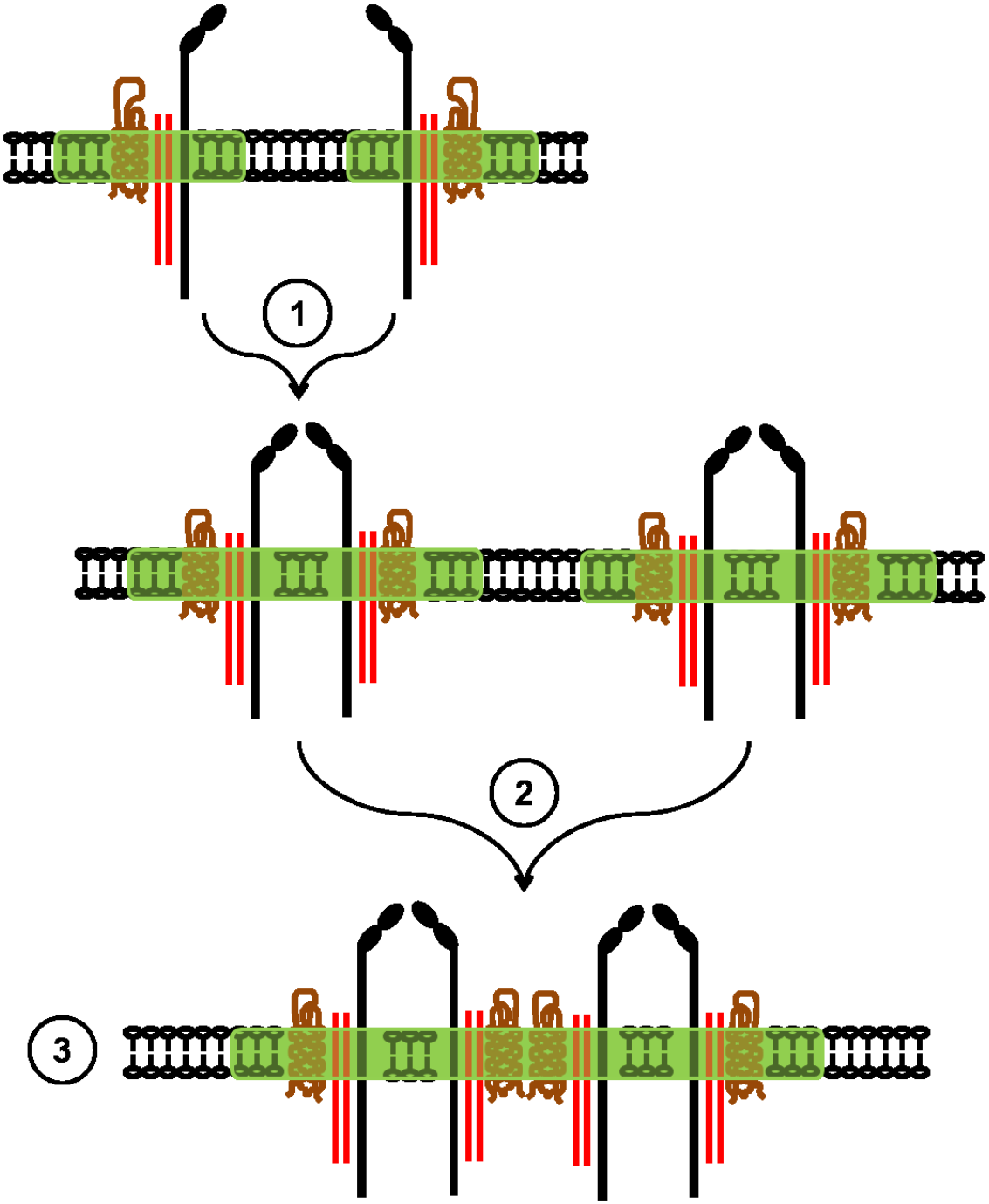

Figure 54.

Figure 54. Tspan9 association with GPVI brings tetraspanin associated lipids to GPVI which promotes efficient GPVI multimerisation.

1. Tspan9 associates with GPVI, which in turn leads to association of tetraspanin associated membrane lipids with GPVI. As such, GPVI diffuses through the platelet membrane in its own tiny microdomain.

2. GPVI association with Tspan9 leads to its association with the tetraspanin web. This series of interactions organises the GPVI population such that dimerisation occurs efficiently.

3. GPVI dimers, associated with their mini microdomains, cluster as efficiently as GPVI monomers dimerise, due to their association with membrane lipid through Tspan9. This lipid association overcomes a limiting step in GPVI dimer diffusion that would be caused by the increase in size from GPVI monomer to dimer, thus allowing rapid multimerisation of GPVI.

Taking a step back from speculation on the mechanism of how Tspan9 influences the membrane dynamics of GPVI, a more general mechanism of tetraspanin regulation of GPVI can be considered. Through its association with a tetraspanin, GPVI would be expected to undergo a series of interactions with tetraspanin microdomains during its diffusion through the platelet membrane. Interacting with the tetraspanin web in this way could modulate the distribution of GPVI in the membrane such that the population is optimised to ensure an appropriate pool of GPVI dimers is maintained, resulting in efficient responses to ligand. This organisation of partner protein distribution by interaction with the tetraspanin web is seen in the regulation of α4β1 integrin by CD37 on B cells (van Spriel et al., 2012). Additionally, GPVI association with tetraspanins would, upon clustering, promote the interaction of other tetraspanins and their partners with GPVI clusters. Of particular interest in this scenario is the recruitment of ADAM10, a sheddase for GPVI, to GPVI clusters. Occuring through the interactions of Tspan14 and GPVI-associated tetraspanins this could be a mechanism to ensure efficient receptor shedding. To investigate this hypothesis, confocal microscopy or scanning electron microscopy could be used to assess and compare the distribution of GPVI in wildtype and Tspan9-deficient platelets.

7.3 The role of Tspan9 on cell types other than platelets.

As the aim of this thesis was to investigate the function of Tspan9 on platelets, no other cell types have been a focus of investigation. Despite being most highly expressed on platelets and, compared to other tetraspanins, relatively platelet specific, Tspan9 has been shown to be clearly expressed in mouse brain, heart, kidney, lung and liver by western blot (Protty et al., 2009). Closer inspection of tissue

sections from these organs, stained with Tspan9 antibody (Appendix Figure 2), revealed the expression of Tspan9 to be mainly on the endothelial and epithelial cells of these tissues. As GPVI expression is restricted to platelets, the work in this thesis cannot provide substantial insights into the function of Tspan9 in endothelial or epithelial cells. One approach to attempt to discover partner proteins for Tspan9 could be the proteomics approach previously discussed, where tetraspanin microdomains are immunoprecipitated from a particular tissue, taken from Tspan9 wildtype or knockout mice, and mass spectrometry used to analyse the resident proteins. Any protein missing in the knockout microdomains would be a likely candidate partner protein for Tspan9. As Tspan9 is most highly expressed in lung, compared to other organs (Protty et al., 2009), this would be a good tissue to use for this type of experiment.

7.4 Contribution and context of this thesis to wider research on tetraspanins, platelets and ADAM10

Despite being unable to arrive at a firm conclusion as to the function of Tspan9 on platelets, the work in this thesis on the function of the tetraspanins Tspan9 and Tspan33 has contributed novel findings to the fields of platelet, red blood cell, tetraspanin and ADAM10 research.

Aside from the previously discussed contribution to ADAM10 biology, investigations into Tspan33 and the TspanC8 tetraspanins has led to the identification of Tspan14 as a promising avenue of research into the function of ADAM10 and tetraspanins on mouse platelets. Additionally ADAM10 has also been identified as having possible roles in erythropoiesis, and its dysregulation or mutation as having possible roles in the development of myeloid malignancies as previously discussed. Studies into the function of Tspan9 have added to the growing evidence that tetraspanins can regulate the membrane dynamics of their partner proteins and has highlighted potentially the first definitive mechanism of action for a tetraspanin on platelets. The single particle tracking studies are the first of their kind in platelets. Subsequent development of the technique could lead to a new avenue of research into platelets and megakaryocytes, presenting the opportunity to investigate and characterise the organisation of the platelet cell membrane and address long standing questions such as the mechanisms regulating receptor multimerisation. Additionally, prior to the results presented in this thesis, the function of Tspan9 was unknown in any cell type and as such lends a starting point for the study of this protein in other cell types in the cardiovascular system and beyond.

APPENDIX

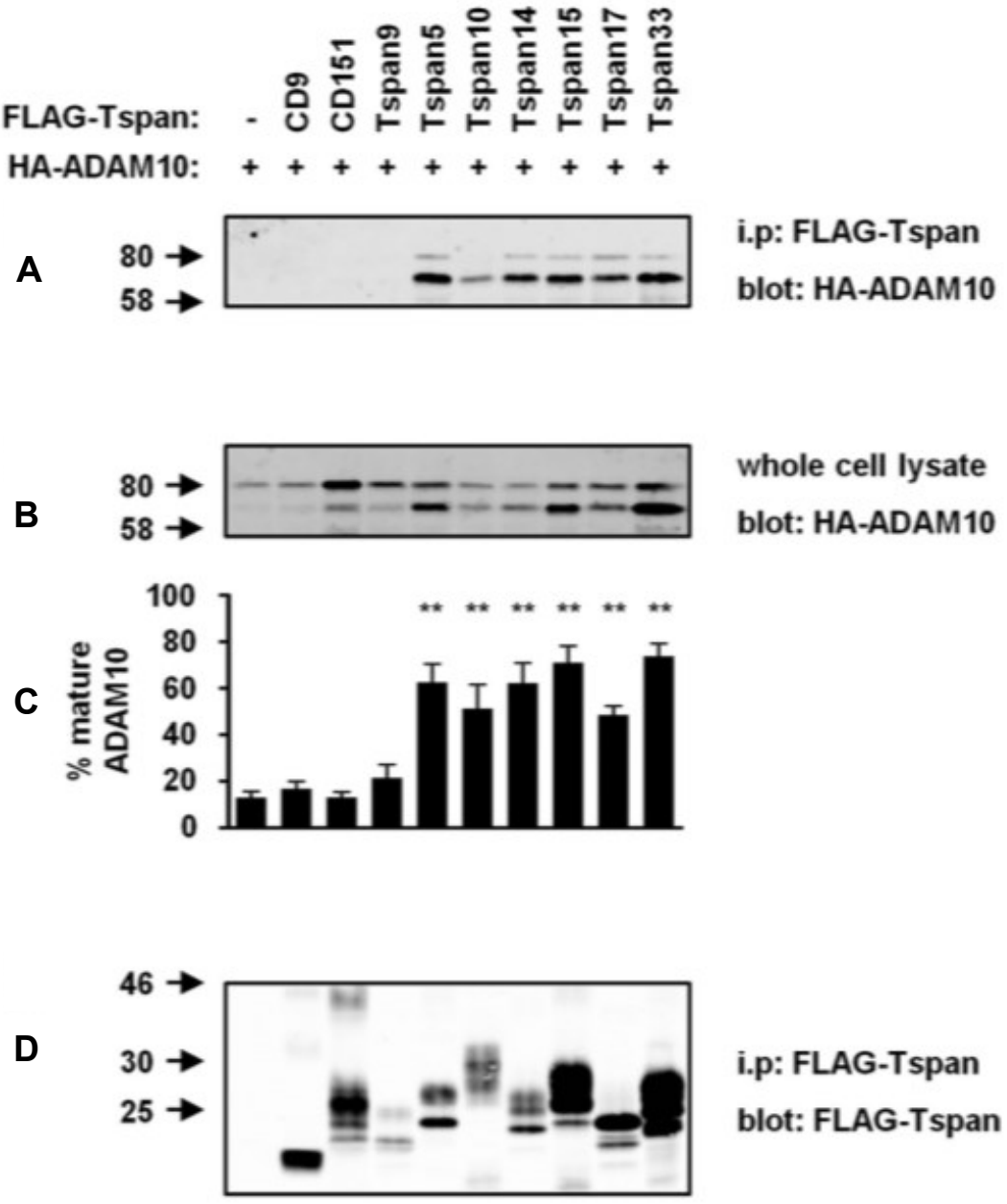

Figure 1.

Figure 1. All TspanC8 tetraspanins associate with ADAM10 and promote its maturation.

HEK 293T cells were co-transfected with HA tagged ADAM10 and a FLAG tagged tetraspanin from the TspanC8 subfamily or CD9, CD151 or Tspan9 as a control. Cells were lysed in 1 % Digitonin lysis buffer and FLAG immunoprecipitated. (A) FLAG immunoprecipitates were western blotted with an anti HA antibody to detect ADAM10 co-precipitation. (B) Whole cell lysates from each condition were western blotted for ADAM10 and revealed an increase in mature ADAM10 (lower band) in TspanC8 transfected cells. (C) The effect on ADAM10 maturation was quantified as % of total ADAM10 detected using the Odyssey LI-COR infra red imaging system. Only in TspanC8 transfected cells was the % of mature ADAM10 significantly increased over basal (ADAM10 transfection alone). n = 3 error bars represent standard error. Significance determined by one way ANOVA followed by Dunn's multiple comparison post test (D) Immunoprecipitates were western blotted with an anti FLAG antibody to detected the precipitated tetraspanin in each condition. This work was done by Dr. Jing Yang from our lab and quantitated by Elizabeth Haining. Figure modified from Haining et al. (2012)

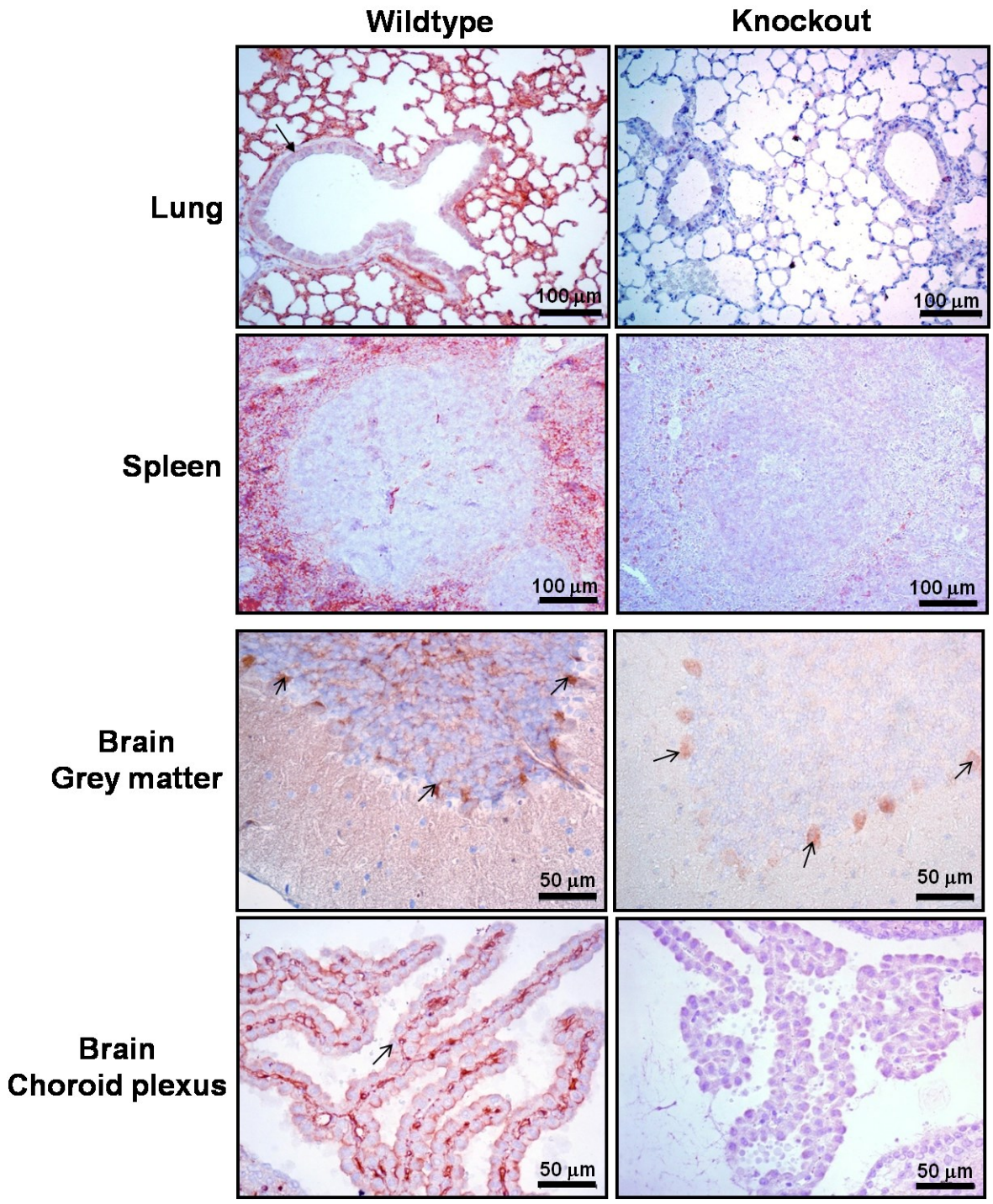
Wildtype
Knockout
Lung
Spleen
Brain
Grey matter
Brain
Choroid plexus
100 µm
100 µm
100 µm
100 µm
50 µm
50 µm
50 µm
50 µm

Figure 2

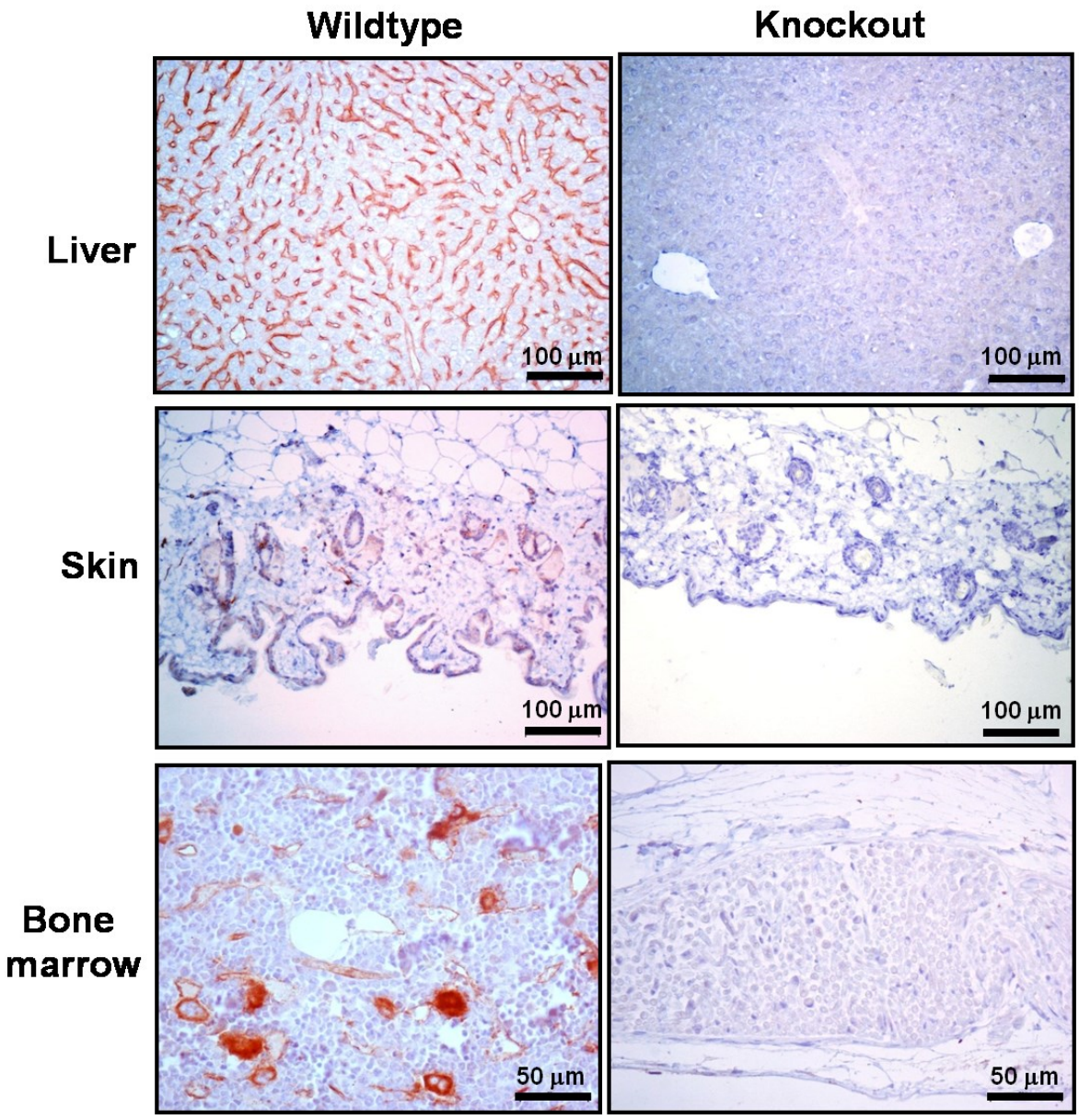

Figure 2. Tspan9 antibody stained tissue sections from Tspan9 wildtype and knockout mice.

Paraformaldehyde fixed whole tissues from Tspan9 wildtype and knockout mice were sectioned and stained with the anti Tspan9 antibody. Sectioning, staining and imaging done by Hanna Romanska.

List of references

ANDRÉ, M., LE CAER, J. P., GRECO, C., PLANCHON, S., EL NEMER, W., BOUCHEIX, C., RUBINSTEIN, E., CHAMOT-ROOKE, J. & LE NAOUR, F. 2006. Proteomic analysis of the tetraspanin web using LC-ESI-MS/MS and MALDI-FTICR-MS. *Proteomics,* 6**,** 1437-49.

ARTHUR, J. F., DUNKLEY, S. & ANDREWS, R. K. 2007. Platelet glycoprotein VI-related clinical defects. *Br J Haematol,* 139**,** 363-72.

ASLAN, J. E. & MCCARTY, O. J. 2013. Rho GTPases in platelet function. *J Thromb Haemost,* 11**,** 35-46.

AUGER, J. M., KUIJPERS, M. J., SENIS, Y. A., WATSON, S. P. & HEEMSKERK, J. W. 2005. Adhesion of human and mouse platelets to collagen under shear: a unifying model. *FASEB J,* 19**,** 825-7.

BAILEY, R. L., HERBERT, J. M., KHAN, K., HEATH, V. L., BICKNELL, R. & TOMLINSON, M. G. 2011. The emerging role of tetraspanin microdomains on endothelial cells. *Biochem Soc Trans,* 39**,** 1667-73.

BARREIRO, O., ZAMAI, M., YÁÑEZ-MÓ, M., TEJERA, E., LÓPEZ-ROMERO, P., MONK, P. N., GRATTON, E., CAIOLFA, V. R. & SÁNCHEZ-MADRID, F. 2008. Endothelial adhesion receptors are recruited to adherent leukocytes by inclusion in preformed tetraspanin nanoplatforms. *J Cell Biol,* 183**,** 527-42.

BASSANI, S., CINGOLANI, L. A., VALNEGRI, P., FOLCI, A., ZAPATA, J., GIANFELICE, A., SALA, C., GODA, Y. & PASSAFARO, M. 2012. The X-linked intellectual disability protein TSPAN7 regulates excitatory synapse development and AMPAR trafficking. *Neuron,* 73**,** 1143-58.

BENDER, M., HAGEDORN, I. & NIESWANDT, B. 2011. Genetic and antibody-induced glycoprotein VI deficiency equally protects mice from mechanically and FeCl(3) -induced thrombosis. *J Thromb Haemost,* 9**,** 1423-6.

BENDER, M., HOFMANN, S., STEGNER, D., CHALARIS, A., BÖSL, M., BRAUN, A., SCHELLER, J., ROSE-JOHN, S. & NIESWANDT, B. 2010. Differentially regulated GPVI ectodomain shedding by multiple platelet-expressed proteinases. *Blood,* 116**,** 3347-55.

BENDER, M., MAY, F., LORENZ, V., THIELMANN, I., HAGEDORN, I., FINNEY, B. A., VOGTLE, T., REMER, K., BRAUN, A., BOSL, M., WATSON, S. P. & NIESWANDT, B. 2013. Combined in vivo depletion of glycoprotein VI and C-type lectin-like receptor 2 severely compromises hemostasis and abrogates arterial thrombosis in mice. *Arterioscler Thromb Vasc Biol,* 33**,** 926-34.

BERDITCHEVSKI, F. & ODINTSOVA, E. 2007. Tetraspanins as regulators of protein trafficking. *Traffic,* 8**,** 89-96.

BERDITCHEVSKI, F., ODINTSOVA, E., SAWADA, S. & GILBERT, E. 2002. Expression of the palmitoylation-deficient CD151 weakens the association of alpha 3 beta 1 integrin with the tetraspanin-enriched microdomains and affects integrin-dependent signaling. *J Biol Chem,* 277**,** 36991-7000.

BEST, D., SENIS, Y. A., JARVIS, G. E., EAGLETON, H. J., ROBERTS, D. J., SAITO, T., JUNG, S. M., MOROI, M., HARRISON, P., GREEN, F. R. & WATSON, S. P. 2003a. GPVI levels in platelets: relationship to platelet function at high shear. *Blood,* 102**,** 2811-8.

BEST, D., SENIS, Y. A., JARVIS, G. E., EAGLETON, H. J., ROBERTS, D. J., SAITO, T., JUNG, S. M., MOROI, M., HARRISON, P., GREEN, F. R. & WATSON, S.

P. 2003b. GPVI levels in platelets: relationship to platelet function at high shear. *Blood,* 102**,** 2811-8.

BOESZE-BATTAGLIA, K., STEFANO, F. P., FITZGERALD, C. & MULLER-WEEKS, S. 2007. ROM-1 potentiates photoreceptor specific membrane fusion processes. *Exp Eye Res,* 84**,** 22-31.

BOULAFTALI, Y., HESS, P. R., GETZ, T. M., CHOLKA, A., STOLLA, M., MACKMAN, N., OWENS, A. P., 3RD, WARE, J., KAHN, M. L. & BERGMEIER, W. 2013. Platelet ITAM signaling is critical for vascular integrity in inflammation. *J Clin Invest,* 123**,** 908-16.

BUSSE, R. & MULSCH, A. 1990. Calcium-dependent nitric oxide synthesis in endothelial cytosol is mediated by calmodulin. *FEBS Lett,* 265**,** 133-6.

CHARRIN, S., LE NAOUR, F., LABAS, V., BILLARD, M., LE CAER, J. P., EMILE, J. F., PETIT, M. A., BOUCHEIX, C. & RUBINSTEIN, E. 2003a. EWI-2 is a new component of the tetraspanin web in hepatocytes and lymphoid cells. *Biochem J,* 373**,** 409-21.

CHARRIN, S., LE NAOUR, F., SILVIE, O., MILHIET, P. E., BOUCHEIX, C. & RUBINSTEIN, E. 2009. Lateral organization of membrane proteins: tetraspanins spin their web. *Biochem J,* 420**,** 133-54.

CHARRIN, S., MANIÉ, S., BILLARD, M., ASHMAN, L., GERLIER, D., BOUCHEIX, C. & RUBINSTEIN, E. 2003b. Multiple levels of interactions within the tetraspanin web. *Biochem Biophys Res Commun,* 304**,** 107-12.

CHARRIN, S., MANIÉ, S., OUALID, M., BILLARD, M., BOUCHEIX, C. & RUBINSTEIN, E. 2002. Differential stability of tetraspanin/tetraspanin interactions: role of palmitoylation. *FEBS Lett,* 516**,** 139-44.

CHARRIN, S., MANIÉ, S., THIELE, C., BILLARD, M., GERLIER, D., BOUCHEIX, C. & RUBINSTEIN, E. 2003c. A physical and functional link between cholesterol and tetraspanins. *Eur J Immunol,* 33**,** 2479-89.

CHASIS, J. A. & MOHANDAS, N. 2008. Erythroblastic islands: niches for erythropoiesis. *Blood,* 112**,** 470-8.

CHELI, Y., JENSEN, D., MARCHESE, P., HABART, D., WILTSHIRE, T., COOKE, M., FERNANDEZ, J. A., WARE, J., RUGGERI, Z. M. & KUNICKI, T. J. 2008a. The Modifier of hemostasis (Mh) locus on chromosome 4 controls in vivo hemostasis of Gp6-/- mice. *Blood,* 111**,** 1266-73.

CHELI, Y., JENSEN, D., MARCHESE, P., HABART, D., WILTSHIRE, T., COOKE, M., FERNANDEZ, J. A., WARE, J., RUGGERI, Z. M. & KUNICKI, T. J. 2008b. The Modifier of hemostasis (Mh) locus on chromosome 4 controls in vivo hemostasis of Gp6-/- mice. *Blood,* 111**,** 1266-73.

CHEN, Z., PASQUINI, M., HONG, B., DEHART, S., HEIKENS, M. & TSAI, S. 2005. The human Penumbra gene is mapped to a region on chromosome 7 frequently deleted in myeloid malignancies. *Cancer Genet Cytogenet,* 162**,** 95-8.

CHIU, W. H., CHANDLER, J., CNOPS, G., VAN LIJSEBETTENS, M. & WERR, W. 2007. Mutations in the TORNADO2 gene affect cellular decisions in the peripheral zone of the shoot apical meristem of Arabidopsis thaliana. *Plant Mol Biol,* 63**,** 731-44.

CHU, X., HOU, M., PENG, J., ZHU, Y., ZHANG, F., JI, X., WANG, L. & MA, D. 2006. Identification of human platelet glycoprotein VI-specific IgG autoantibody and its fragments. *Blood Coagul Fibrinolysis,* 17**,** 403-7.

CLAAS, C., STIPP, C. S. & HEMLER, M. E. 2001. Evaluation of prototype transmembrane 4 superfamily protein complexes and their relation to lipid rafts. *J Biol Chem,* 276**,** 7974-84.

CLEMETSON, K. J. 2012. Platelets and primary haemostasis. *Thromb Res,* 129**,** 220-4.

CNOPS, G., NEYT, P., RAES, J., PETRARULO, M., NELISSEN, H., MALENICA, N., LUSCHNIG, C., TIETZ, O., DITENGOU, F., PALME, K., AZMI, A., PRINSEN, E. & VAN LIJSEBETTENS, M. 2006. The TORNADO1 and TORNADO2 genes function in several patterning processes during early leaf development in Arabidopsis thaliana. *Plant Cell,* 18**,** 852-66.

CODINA, J., LI, J. & DUBOSE, T. D., JR. 2005. CD63 interacts with the carboxy terminus of the colonic H+-K+-ATPase to decrease [corrected] plasma membrane localization and 86Rb+ uptake. *Am J Physiol Cell Physiol,* 288**,** C1279-86.

CONLEY, S. M., STUCK, M. W. & NAASH, M. I. 2012. Structural and functional relationships between photoreceptor tetraspanins and other superfamily members. *Cell Mol Life Sci,* 69**,** 1035-47.

CRAWFORD, H. C., DEMPSEY, P. J., BROWN, G., ADAM, L. & MOSS, M. L. 2009. ADAM10 as a therapeutic target for cancer and inflammation. *Curr Pharm Des,* 15**,** 2288-99.

CUNNINGHAM, M. R., NISAR, S. P. & MUNDELL, S. J. 2013. Molecular mechanisms of platelet P2Y(12) receptor regulation. *Biochem Soc Trans,* 41**,** 225-30.

CURTI, E., KWITYN, C., ZHAN, B., GILLESPIE, P., BRELSFORD, J., DEUMIC, V., PLIESKATT, J., REZENDE, W. C., TSAO, E., KALAMPANAYIL, B., HOTEZ, P. J. & BOTTAZZI, M. E. 2013. Expression at a 20L scale and purification of the extracellular domain of the Schistosoma mansoni TSP-2 recombinant protein: A vaccine candidate for human intestinal schistosomiasis. *Hum Vaccin Immunother,* 9.

DAWOOD, B. B., WILDE, J. & WATSON, S. P. 2007. Reference curves for aggregation and ATP secretion to aid diagnose of platelet-based bleeding disorders: effect of inhibition of ADP and thromboxane A(2) pathways. *Platelets,* 18**,** 329-45.

DELAGUILLAUMIE, A., HARRIAGUE, J., KOHANNA, S., BISMUTH, G., RUBINSTEIN, E., SEIGNEURET, M. & CONJEAUD, H. 2004. Tetraspanin CD82 controls the association of cholesterol-dependent microdomains with the actin cytoskeleton in T lymphocytes: relevance to co-stimulation. *J Cell Sci,* 117**,** 5269-82.

DESALLE, R., MARES, R. & GARCIA-ESPAÑA, A. 2010. Evolution of cysteine patterns in the large extracellular loop of tetraspanins from animals, fungi, plants and single-celled eukaryotes. *Mol Phylogenet Evol,* 56**,** 486-91.

DEUSS, M., REISS, K. & HARTMANN, D. 2008. Part-time alpha-secretases: the functional biology of ADAM 9, 10 and 17. *Curr Alzheimer Res,* 5**,** 187-201.

DIETRICH, C., YANG, B., FUJIWARA, T., KUSUMI, A. & JACOBSON, K. 2002. Relationship of lipid rafts to transient confinement zones detected by single particle tracking. *Biophys J,* 82**,** 274-84.

DOLZNIG, H., BOULME, F., STANGL, K., DEINER, E. M., MIKULITS, W., BEUG, H. & MULLNER, E. W. 2001. Establishment of normal, terminally differentiating

mouse erythroid progenitors: molecular characterization by cDNA arrays. *Faseb j,* 15**,** 1442-4.

DORNIER, E., COUMAILLEAU, F., OTTAVI, J. F., MORETTI, J., BOUCHEIX, C., MAUDUIT, P., SCHWEISGUTH, F. & RUBINSTEIN, E. 2012. TspanC8 tetraspanins regulate ADAM10/Kuzbanian trafficking and promote Notch activation in flies and mammals. *J Cell Biol,* 199**,** 481-96.

DOYLE, E. L., RIDGER, V., FERRARO, F., TURMAINE, M., SAFTIG, P. & CUTLER, D. F. 2011. CD63 is an essential cofactor to leukocyte recruitment by endothelial P-selectin. *Blood,* 118**,** 4265-73.

DUFFIELD, A., KAMSTEEG, E. J., BROWN, A. N., PAGEL, P. & CAPLAN, M. J. 2003. The tetraspanin CD63 enhances the internalization of the H,K-ATPase beta-subunit. *Proc Natl Acad Sci U S A,* 100**,** 15560-5.

DUMON, S., HEATH, V. L., TOMLINSON, M. G., GOTTGENS, B. & FRAMPTON, J. 2006. Differentiation of murine committed megakaryocytic progenitors isolated by a novel strategy reveals the complexity of GATA and Ets factor involvement in megakaryocytopoiesis and an unexpected potential role for GATA-6. *Exp Hematol,* 34**,** 654-63.

DUMONT, B., LASNE, D., ROTHSCHILD, C., BOUABDELLI, M., OLLIVIER, V., OUDIN, C., AJZENBERG, N., GRANDCHAMP, B. & JANDROT-PERRUS, M. 2009. Absence of collagen-induced platelet activation caused by compound heterozygous GPVI mutations. *Blood,* 114**,** 1900-3.

DUNN, C. D., SULIS, M. L., FERRANDO, A. A. & GREENWALD, I. 2010. A conserved tetraspanin subfamily promotes Notch signaling in Caenorhabditis elegans and in human cells. *Proc Natl Acad Sci U S A,* 107**,** 5907-12.

DUTTING, S., BENDER, M. & NIESWANDT, B. 2012. Platelet GPVI: a target for antithrombotic therapy?! *Trends Pharmacol Sci,* 33**,** 583-90.

ECHTLER, K., STARK, K., LORENZ, M., KERSTAN, S., WALCH, A., JENNEN, L., RUDELIUS, M., SEIDL, S., KREMMER, E., EMAMBOKUS, N. R., VON BRUEHL, M. L., FRAMPTON, J., ISERMANN, B., GENZEL-BOROVICZENY, O., SCHREIBER, C., MEHILLI, J., KASTRATI, A., SCHWAIGER, M., SHIVDASANI, R. A. & MASSBERG, S. 2010. Platelets contribute to postnatal occlusion of the ductus arteriosus. *Nat Med,* 16**,** 75-82.

EHRHARDT, C., SCHMOLKE, M., MATZKE, A., KNOBLAUCH, A., WILL, C., WIXLER, V. & LUDWIG, S. 2006. Polyethylenimine, a cost-effective transfection reagent

Signal Transduction Volume 6, Issue 3. *Signal Transduction* [Online], 6. Available: http://onlinelibrary.wiley.com/doi/10.1002/sita.200500073/abstract [Accessed 01].

ELLISON, S., MORI, J., BARR, A. J. & SENIS, Y. A. 2010. CD148 enhances platelet responsiveness to collagen by maintaining a pool of active Src family kinases. *J Thromb Haemost,* 8**,** 1575-83.

ENDRES, K. & FAHRENHOLZ, F. 2010. Upregulation of the alpha-secretase ADAM10--risk or reason for hope? *FEBS J,* 277**,** 1585-96.

ESPENEL, C., MARGEAT, E., DOSSET, P., ARDUISE, C., LE GRIMELLEC, C., ROYER, C. A., BOUCHEIX, C., RUBINSTEIN, E. & MILHIET, P. E. 2008. Single-molecule analysis of CD9 dynamics and partitioning reveals multiple modes of interaction in the tetraspanin web. *J Cell Biol,* 182**,** 765-76.

EZUMI, Y., KODAMA, K., UCHIYAMA, T. & TAKAYAMA, H. 2002. Constitutive and functional association of the platelet collagen receptor glycoprotein VI-Fc receptor gamma-chain complex with membrane rafts. *Blood,* 99**,** 3250-5.

FORRAI, A. & ROBB, L. 2005. The gene trap resource: a treasure trove for hemopoiesis research. *Exp Hematol,* 33**,** 845-56.

FRADKIN, L. G., KAMPHORST, J. T., DIANTONIO, A., GOODMAN, C. S. & NOORDERMEER, J. N. 2002. Genomewide analysis of the Drosophila tetraspanins reveals a subset with similar function in the formation of the embryonic synapse. *Proc Natl Acad Sci U S A,* 99**,** 13663-8.

FRIEDRICH, G. & SORIANO, P. 1991. Promoter traps in embryonic stem cells: a genetic screen to identify and mutate developmental genes in mice. *Genes Dev,* 5**,** 1513-23.

FUCHS, T. A., BRILL, A. & WAGNER, D. D. 2012. Neutrophil Extracellular Trap Impact on Deep Vein Thrombosis. *Arterioscler Thromb Vasc Biol*.

FUENTES Q, E., FUENTES Q, F., ANDRÉS, V., PELLO, O. M., DE MORA, J. F. & PALOMO G, I. 2012. Role of platelets as mediators that link inflammation and thrombosis in atherosclerosis. *Platelets*.

FURIE, B. C. & FURIE, B. 2006. Tissue factor pathway vs. collagen pathway for in vivo platelet activation. *Blood Cells Mol Dis,* 36**,** 135-8.

GARDINER, E. E., KARUNAKARAN, D., SHEN, Y., ARTHUR, J. F., ANDREWS, R. K. & BERNDT, M. C. 2007. Controlled shedding of platelet glycoprotein (GP)VI and GPIb-IX-V by ADAM family metalloproteinases. *J Thromb Haemost,* 5**,** 1530-7.

GNANASEKAR, M., ANAND, S. B. & RAMASWAMY, K. 2008. Identification and cloning of a novel tetraspanin (TSP) homologue from Brugia malayi. *DNA Seq,* 19**,** 151-6.

GOLDBERG, A. F. 2006. Role of peripherin/rds in vertebrate photoreceptor architecture and inherited retinal degenerations. *Int Rev Cytol,* 253**,** 131-75.

GOLDBERG, A. F., RITTER, L. M., KHATTREE, N., PEACHEY, N. S., FARISS, R. N., DANG, L., YU, M. & BOTTRELL, A. R. 2007. An intramembrane glutamic acid governs peripherin/rds function for photoreceptor disk morphogenesis. *Invest Ophthalmol Vis Sci,* 48**,** 2975-86.

GORDÓN-ALONSO, M., YAÑEZ-MÓ, M., BARREIRO, O., ALVAREZ, S., MUÑOZ-FERNÁNDEZ, M. A., VALENZUELA-FERNÁNDEZ, A. & SÁNCHEZ-MADRID, F. 2006. Tetraspanins CD9 and CD81 modulate HIV-1-induced membrane fusion. *J Immunol,* 177**,** 5129-37.

GOSCHNICK, M. W., LAU, L. M., WEE, J. L., LIU, Y. S., HOGARTH, P. M., ROBB, L. M., HICKEY, M. J., WRIGHT, M. D. & JACKSON, D. E. 2006. Impaired "outside-in" integrin alphaIIbbeta3 signaling and thrombus stability in TSSC6-deficient mice. *Blood,* 108**,** 1911-8.

GRANSETH, E., VON HEIJNE, G. & ELOFSSON, A. 2005. A study of the membrane-water interface region of membrane proteins. *J Mol Biol,* 346**,** 377-85.

GREENBAUM, D., COLANGELO, C., WILLIAMS, K. & GERSTEIN, M. 2003. Comparing protein abundance and mRNA expression levels on a genomic scale. *Genome Biol,* 4**,** 117.

GREENE, T. K., SCHIVIZ, A., HOELLRIEGL, W., PONCZ, M., MUCHITSCH, E. M. & ISTH, A. M. S. O. T. S. A. S. C. O. T. 2010. Towards a standardization of the murine tail bleeding model. *J Thromb Haemost,* 8**,** 2820-2.

GREENWALD, I. & KOVALL, R. 2013. Notch signaling: genetics and structure. *WormBook***,** 1-28.

GRESELE, P., MOMI, S. & FALCINELLI, E. 2011. Anti-platelet therapy: phosphodiesterase inhibitors. *Br J Clin Pharmacol,* 72**,** 634-46.

HAEUW, J. F., GOETSCH, L., BAILLY, C. & CORVAIA, N. 2011. Tetraspanin CD151 as a target for antibody-based cancer immunotherapy. *Biochem Soc Trans,* 39**,** 553-8.

HAINING, E. J., YANG, J., BAILEY, R. L., KHAN, K., COLLIER, R., TSAI, S., WATSON, S. P., FRAMPTON, J., GARCIA, P. & TOMLINSON, M. G. 2012. The TspanC8 subgroup of tetraspanins interacts with A disintegrin and metalloprotease 10 (ADAM10) and regulates its maturation and cell surface expression. *J Biol Chem,* 287**,** 39753-65.

HARRIS, H. J., CLERTE, C., FARQUHAR, M. J., GOODALL, M., HU, K., RASSAM, P., DOSSET, P., WILSON, G. K., BALFE, P., IJZENDOORN, S. C., MILHIET, P. E. & MCKEATING, J. A. 2013. Hepatoma polarization limits CD81 and hepatitis C virus dynamics. *Cell Microbiol,* 15**,** 430-45.

HARTMANN, D., DE STROOPER, B., SERNEELS, L., CRAESSAERTS, K., HERREMAN, A., ANNAERT, W., UMANS, L., LÜBKE, T., LENA ILLERT, A., VON FIGURA, K. & SAFTIG, P. 2002. The disintegrin/metalloprotease ADAM 10 is essential for Notch signalling but not for alpha-secretase activity in fibroblasts. *Hum Mol Genet,* 11**,** 2615-24.

HE, Z. Y., GUPTA, S., MYLES, D. & PRIMAKOFF, P. 2009. Loss of surface EWI-2 on CD9 null oocytes. *Mol Reprod Dev,* 76**,** 629-36.

HEIKENS, M. J., CAO, T. M., MORITA, C., DEHART, S. L. & TSAI, S. 2007. Penumbra encodes a novel tetraspanin that is highly expressed in erythroid progenitors and promotes effective erythropoiesis. *Blood,* 109**,** 3244-52.

HEMLER, M. E. 2001. Specific tetraspanin functions. *J Cell Biol,* 155**,** 1103-7.

HEMLER, M. E. 2005. Tetraspanin functions and associated microdomains. *Nat Rev Mol Cell Biol,* 6**,** 801-11.

HERMANS, C., WITTEVRONGEL, C., THYS, C., SMETHURST, P. A., VAN GEET, C. & FRESON, K. 2009. A compound heterozygous mutation in glycoprotein VI in a patient with a bleeding disorder. *J Thromb Haemost,* 7**,** 1356-63.

HIGGINBOTTOM, A., WILKINSON, I., MCCULLOUGH, B., LANZA, F., AZORSA, D. O., PARTRIDGE, L. J. & MONK, P. N. 2000. Antibody cross-linking of human CD9 and the high-affinity immunoglobulin E receptor stimulates secretion from transfected rat basophilic leukaemia cells. *Immunology,* 99**,** 546-52.

HIRANO, C., NAGATA, M., NOMAN, A. A., KITAMURA, N., OHNISHI, M., OHYAMA, T., KOBAYASHI, T., SUZUKI, K., YOSHIZAWA, M., IZUMI, N., FUJITA, H. & TAKAGI, R. 2009. Tetraspanin gene expression levels as potential biomarkers for malignancy of gingival squamous cell carcinoma. *Int J Cancer,* 124**,** 2911-6.

HOFFMEISTER, K. M. 2011. The role of lectins and glycans in platelet clearance. *J Thromb Haemost,* 9 Suppl 1**,** 35-43.

HU, C. C., LIANG, F. X., ZHOU, G., TU, L., TANG, C. H., ZHOU, J., KREIBICH, G. & SUN, T. T. 2005. Assembly of urothelial plaques: tetraspanin function in membrane protein trafficking. *Mol Biol Cell,* 16**,** 3937-50.

HUGHES, C. E., AUGER, J. M., MCGLADE, J., EBLE, J. A., PEARCE, A. C. & WATSON, S. P. 2008. Differential roles for the adapters Gads and LAT in platelet activation by GPVI and CLEC-2. *J Thromb Haemost,* 6**,** 2152-9.

HUX, B. D. & MARTIN, L. G. 2012. Platelet transfusions: treatment options for hemorrhage secondary to thrombocytopenia. *J Vet Emerg Crit Care (San Antonio),* 22**,** 73-80.

IWASAKI, T., TAKEDA, Y., MARUYAMA, K., YOKOSAKI, Y., TSUJINO, K., TETSUMOTO, S., KUHARA, H., NAKANISHI, K., OTANI, Y., JIN, Y., KOHMO, S., HIRATA, H., TAKAHASHI, R., SUZUKI, M., INOUE, K., NAGATOMO, I., GOYA, S., KIJIMA, T., KUMAGAI, T., TACHIBANA, I., KAWASE, I. & KUMANOGOH, A. 2013. Deletion of tetraspanin CD9 diminishes lymphangiogenesis in vivo and in vitro. *J Biol Chem,* 288**,** 2118-31.

JACKSON, S. P., NESBITT, W. S. & KULKARNI, S. 2003. Signaling events underlying thrombus formation. *J Thromb Haemost,* 1**,** 1602-12.

JENNINGS, L. K. 2009. Role of Platelets in Atherothrombosis. *American Journal of Cardiology,* 103**,** 4A-10A.

JUNG, S. M., MOROI, M., SOEJIMA, K., NAKAGAKI, T., MIURA, Y., BERNDT, M. C., GARDINER, E. E., HOWES, J. M., PUGH, N., BIHAN, D., WATSON, S. P. & FARNDALE, R. W. 2012. Constitutive dimerization of glycoprotein VI (GPVI) in resting platelets is essential for binding to collagen and activation in flowing blood. *J Biol Chem,* 287**,** 30000-13.

JUNGE, H. J., YANG, S., BURTON, J. B., PAES, K., SHU, X., FRENCH, D. M., COSTA, M., RICE, D. S. & YE, W. 2009. TSPAN12 regulates retinal vascular development by promoting Norrin- but not Wnt-induced FZD4/beta-catenin signaling. *Cell,* 139**,** 299-311.

KAHN, M. L., ZHENG, Y. W., HUANG, W., BIGORNIA, V., ZENG, D., MOFF, S., FARESE, R. V., JR., TAM, C. & COUGHLIN, S. R. 1998. A dual thrombin receptor system for platelet activation. *Nature,* 394**,** 690-4.

KAJI, K., ODA, S., MIYAZAKI, S. & KUDO, A. 2002. Infertility of CD9-deficient mouse eggs is reversed by mouse CD9, human CD9, or mouse CD81; polyadenylated mRNA injection developed for molecular analysis of sperm-egg fusion. *Dev Biol,* 247**,** 327-34.

KARAMATIC CREW, V., BURTON, N., KAGAN, A., GREEN, C. A., LEVENE, C., FLINTER, F., BRADY, R. L., DANIELS, G. & ANSTEE, D. J. 2004. CD151, the first member of the tetraspanin (TM4) superfamily detected on erythrocytes, is essential for the correct assembly of human basement membranes in kidney and skin. *Blood,* 104**,** 2217-23.

KATO, K., KANAJI, T., RUSSELL, S., KUNICKI, T. J., FURIHATA, K., KANAJI, S., MARCHESE, P., REININGER, A., RUGGERI, Z. M. & WARE, J. 2003. The contribution of glycoprotein VI to stable platelet adhesion and thrombus formation illustrated by targeted gene deletion. *Blood,* 102**,** 1701-7.

KAWAKAMI, Y., KAWAKAMI, K., STEELANT, W. F., ONO, M., BAEK, R. C., HANDA, K., WITHERS, D. A. & HAKOMORI, S. 2002. Tetraspanin CD9 is a "proteolipid," and its interaction with alpha 3 integrin in microdomain is

promoted by GM3 ganglioside, leading to inhibition of laminin-5-dependent cell motility. *J Biol Chem,* 277**,** 34349-58.
KAZAROV, A. R., YANG, X., STIPP, C. S., SEHGAL, B. & HEMLER, M. E. 2002. An extracellular site on tetraspanin CD151 determines alpha 3 and alpha 6 integrin-dependent cellular morphology. *J Cell Biol,* 158**,** 1299-309.
KHANDELWAL, S. & ROCHE, P. A. 2010. Distinct MHC class II molecules are associated on the dendritic cell surface in cholesterol-dependent membrane microdomains. *J Biol Chem,* 285**,** 35303-10.
KITADOKORO, K., BORDO, D., GALLI, G., PETRACCA, R., FALUGI, F., ABRIGNANI, S., GRANDI, G. & BOLOGNESI, M. 2001a. CD81 extracellular domain 3D structure: insight into the tetraspanin superfamily structural motifs. *EMBO J,* 20**,** 12-8.
KITADOKORO, K., GALLI, G., PETRACCA, R., FALUGI, F., GRANDI, G. & BOLOGNESI, M. 2001b. Crystallization and preliminary crystallographic studies on the large extracellular domain of human CD81, a tetraspanin receptor for hepatitis C virus. *Acta Crystallogr D Biol Crystallogr,* 57**,** 156-8.
KLEINSCHNITZ, C., POZGAJOVA, M., PHAM, M., BENDSZUS, M., NIESWANDT, B. & STOLL, G. 2007. Targeting platelets in acute experimental stroke: impact of glycoprotein Ib, VI, and IIb/IIIa blockade on infarct size, functional outcome, and intracranial bleeding. *Circulation,* 115**,** 2323-30.
KOBAYASHI, T., VISCHER, U. M., ROSNOBLET, C., LEBRAND, C., LINDSAY, M., PARTON, R. G., KRUITHOF, E. K. & GRUENBERG, J. 2000. The tetraspanin CD63/lamp3 cycles between endocytic and secretory compartments in human endothelial cells. *Mol Biol Cell,* 11**,** 1829-43.
KOPCZYNSKI, C. C., DAVIS, G. W. & GOODMAN, C. S. 1996. A neural tetraspanin, encoded by late bloomer, that facilitates synapse formation. *Science,* 271**,** 1867-70.
KOVALENKO, O. V., METCALF, D. G., DEGRADO, W. F. & HEMLER, M. E. 2005. Structural organization and interactions of transmembrane domains in tetraspanin proteins. *BMC Struct Biol,* 5**,** 11.
KUSUMI, A., NAKADA, C., RITCHIE, K., MURASE, K., SUZUKI, K., MURAKOSHI, H., KASAI, R. S., KONDO, J. & FUJIWARA, T. 2005. Paradigm shift of the plasma membrane concept from the two-dimensional continuum fluid to the partitioned fluid: high-speed single-molecule tracking of membrane molecules. *Annu Rev Biophys Biomol Struct,* 34**,** 351-78.
KWON, M. J., PARK, S., CHOI, J. Y., OH, E., KIM, Y. J., PARK, Y. H., CHO, E. Y., NAM, S. J., IM, Y. H., SHIN, Y. K. & CHOI, Y. L. 2012. Clinical significance of CD151 overexpression in subtypes of invasive breast cancer. *Br J Cancer,* 106**,** 923-30.
LAMBOU, K., THARREAU, D., KOHLER, A., SIRVEN, C., MARGUERETTAZ, M., BARBISAN, C., SEXTON, A. C., KELLNER, E. M., MARTIN, F., HOWLETT, B. J., ORBACH, M. J. & LEBRUN, M. H. 2008. Fungi have three tetraspanin families with distinct functions. *BMC Genomics,* 9**,** 63.
LAMMERDING, J., KAZAROV, A. R., HUANG, H., LEE, R. T. & HEMLER, M. E. 2003. Tetraspanin CD151 regulates alpha6beta1 integrin adhesion strengthening. *Proc Natl Acad Sci U S A,* 100**,** 7616-21.
LATYSHEVA, N., MURATOV, G., RAJESH, S., PADGETT, M., HOTCHIN, N. A., OVERDUIN, M. & BERDITCHEVSKI, F. 2006. Syntenin-1 is a new component

of tetraspanin-enriched microdomains: mechanisms and consequences of the interaction of syntenin-1 with CD63. *Mol Cell Biol,* 26**,** 7707-18.

LAU, L. M., WEE, J. L., WRIGHT, M. D., MOSELEY, G. W., HOGARTH, P. M., ASHMAN, L. K. & JACKSON, D. E. 2004. The tetraspanin superfamily member CD151 regulates outside-in integrin alphaIIbbeta3 signaling and platelet function. *Blood,* 104**,** 2368-75.

LEVIN, J. & BESSMAN, J. D. 1983. The inverse relation between platelet volume and platelet number. Abnormalities in hematologic disease and evidence that platelet size does not correlate with platelet age. *J Lab Clin Med,* 101**,** 295-307.

LEVY, S., TODD, S. C. & MAECKER, H. T. 1998. CD81 (TAPA-1): a molecule involved in signal transduction and cell adhesion in the immune system. *Annu Rev Immunol,* 16**,** 89-109.

LEWANDROWSKI, U., WORTELKAMP, S., LOHRIG, K., ZAHEDI, R. P., WOLTERS, D. A., WALTER, U. & SICKMANN, A. 2009a. Platelet membrane proteomics: a novel repository for functional research. *Blood,* 114**,** e10-9.

LEWANDROWSKI, U., WORTELKAMP, S., LOHRIG, K., ZAHEDI, R. P., WOLTERS, D. A., WALTER, U. & SICKMANN, A. 2009b. Platelet membrane proteomics: a novel repository for functional research. *Blood,* 114**,** E10-E19.

LI, R. & EMSLEY, J. 2013. The organizing principle of the platelet glycoprotein Ib-IX-V complex. *J Thromb Haemost,* 11**,** 605-14.

LICHTENTHALER, S. F. 2011. Alpha-secretase in Alzheimer's disease: molecular identity, regulation and therapeutic potential. *J Neurochem,* 116**,** 10-21.

LIU, L., HE, B., LIU, W. M., ZHOU, D., COX, J. V. & ZHANG, X. A. 2007a. Tetraspanin CD151 promotes cell migration by regulating integrin trafficking. *J Biol Chem,* 282**,** 31631-42.

LIU, L., HE, B., LIU, W. M., ZHOU, D., COX, J. V. & ZHANG, X. A. 2007b. Tetraspanin CD151 promotes cell migration by regulating integrin trafficking. *J Biol Chem,* 282**,** 31631-42.

LOCKE, D., CHEN, H., LIU, Y., LIU, C. & KAHN, M. L. 2002. Lipid rafts orchestrate signaling by the platelet receptor glycoprotein VI. *J Biol Chem,* 277**,** 18801-9.

LOCKYER, S., OKUYAMA, K., BEGUM, S., LE, S., SUN, B., WATANABE, T., MATSUMOTO, Y., YOSHITAKE, M., KAMBAYASHI, J. & TANDON, N. N. 2006. GPVI-deficient mice lack collagen responses and are protected against experimentally induced pulmonary thromboembolism. *Thromb Res,* 118**,** 371-80.

LOEWEN, C. J., MORITZ, O. L., TAM, B. M., PAPERMASTER, D. S. & MOLDAY, R. S. 2003. The role of subunit assembly in peripherin-2 targeting to rod photoreceptor disk membranes and retinitis pigmentosa. *Mol Biol Cell,* 14**,** 3400-13.

LORDKIPANIDZE, M., PHARAND, C., SCHAMPAERT, E., PALISAITIS, D. A. & DIODATI, J. G. 2009. Evaluation of the platelet count drop method for assessment of platelet function in comparison with "gold standard" light transmission aggregometry. *Thromb Res,* 124**,** 418-22.

LOWE, K. L., NAVARRO-NUNEZ, L. & WATSON, S. P. 2012. PL-06 Platelet CLEC-2 and podoplanin in cancer metastasis. *Thromb Res,* 129 Suppl 1**,** S30-7.

LOYAU, S., DUMONT, B., OLLIVIER, V., BOULAFTALI, Y., FELDMAN, L., AJZENBERG, N. & JANDROT-PERRUS, M. 2012. Platelet glycoprotein VI

dimerization, an active process inducing receptor competence, is an indicator of platelet reactivity. *Arterioscler Thromb Vasc Biol,* 32**,** 778-85.

LUNARDI, C., BASON, C., NAVONE, R., MILLO, E., DAMONTE, G., CORROCHER, R. & PUCCETTI, A. 2000. Systemic sclerosis immunoglobulin G autoantibodies bind the human cytomegalovirus late protein UL94 and induce apoptosis in human endothelial cells. *Nat Med,* 6**,** 1183-6.

MAECKER, H. T., DO, M. S. & LEVY, S. 1998. CD81 on B cells promotes interleukin 4 secretion and antibody production during T helper type 2 immune responses. *Proc Natl Acad Sci U S A,* 95**,** 2458-62.

MANGIN, P. H., KLEITZ, L., BOUCHEIX, C., GACHET, C. & LANZA, F. 2009. CD9 negatively regulates integrin alpha(IIb)beta(3) activation and could thus prevent excessive platelet recruitment at sites of vascular injury. *Journal of Thrombosis and Haemostasis,* 7**,** 900-902.

MANGIN, P. H., TANG, C., BOURDON, C., LOYAU, S., FREUND, M., HECHLER, B., GACHET, C. & JANDROT-PERRUS, M. 2012. A humanized glycoprotein VI (GPVI) mouse model to assess the antithrombotic efficacies of anti-GPVI agents. *J Pharmacol Exp Ther,* 341**,** 156-63.

MANNE, B. K., GETZ, T. M., HUGHES, C. E., ALSHEHRI, O., DANGELMAIER, C., NAIK, U. P., WATSON, S. P. & KUNAPULI, S. P. 2013. Fucoidan is a novel platelet agonist for the C-type lectin-like receptor 2 (CLEC-2). *J Biol Chem,* 288**,** 7717-26.

MARSHALL, P. W., WILLIAMS, A. J., DIXON, R. M., GROWCOTT, J. W., WARBURTON, S., ARMSTRONG, J. & MOORES, J. 1997. A comparison of the effects of aspirin on bleeding time measured using the Simplate method and closure time measured using the PFA-100, in healthy volunteers. *Br J Clin Pharmacol,* 44**,** 151-5.

MARUOKA, T., NAGATA, T. & KASAHARA, M. 2004. Identification of the rat IgA Fc receptor encoded in the leukocyte receptor complex. *Immunogenetics,* 55**,** 712-6.

MASSBERG, S., GAWAZ, M., GRÜNER, S., SCHULTE, V., KONRAD, I., ZOHLNHÖFER, D., HEINZMANN, U. & NIESWANDT, B. 2003. A crucial role of glycoprotein VI for platelet recruitment to the injured arterial wall in vivo. *J Exp Med,* 197**,** 41-9.

MAYOR, S. & RAO, M. 2004. Rafts: scale-dependent, active lipid organization at the cell surface. *Traffic,* 5**,** 231-40.

MAZHARIAN, A., WANG, Y. J., MORI, J., BEM, D., FINNEY, B., HEISING, S., GISSEN, P., WHITE, J. G., BERNDT, M. C., GARDINER, E. E., NIESWANDT, B., DOUGLAS, M. R., CAMPBELL, R. D., WATSON, S. P. & SENIS, Y. A. 2012. Mice lacking the ITIM-containing receptor G6b-B exhibit macrothrombocytopenia and aberrant platelet function. *Sci Signal,* 5**,** ra78.

MCCARTY, O. J., CALAMINUS, S. D., BERNDT, M. C., MACHESKY, L. M. & WATSON, S. P. 2006. von Willebrand factor mediates platelet spreading through glycoprotein Ib and alpha(IIb)beta3 in the presence of botrocetin and ristocetin, respectively. *J Thromb Haemost,* 4**,** 1367-78.

MIAO, W. M., VASILE, E., LANE, W. S. & LAWLER, J. 2001. CD36 associates with CD9 and integrins on human blood platelets. *Blood,* 97**,** 1689-96.

MIN, G., WANG, H., SUN, T. T. & KONG, X. P. 2006. Structural basis for tetraspanin functions as revealed by the cryo-EM structure of uroplakin complexes at 6-A resolution. *J Cell Biol,* 173**,** 975-83.

MITSUZUKA, K., HANDA, K., SATOH, M., ARAI, Y. & HAKOMORI, S. 2005. A specific microdomain ("glycosynapse 3") controls phenotypic conversion and reversion of bladder cancer cells through GM3-mediated interaction of alpha3beta1 integrin with CD9. *J Biol Chem,* 280**,** 35545-53.

MONTPELLIER, C., TEWS, B. A., POITRIMOLE, J., ROCHA-PERUGINI, V., D'ARIENZO, V., POTEL, J., ZHANG, X. A., RUBINSTEIN, E., DUBUISSON, J. & COCQUEREL, L. 2011. Interacting regions of CD81 and two of its partners, EWI-2 and EWI-2wint, and their effect on hepatitis C virus infection. *J Biol Chem,* 286**,** 13954-65.

MORIBE, H., KONAKAWA, R., KOGA, D., USHIKI, T., NAKAMURA, K. & MEKADA, E. 2012. Tetraspanin is required for generation of reactive oxygen species by the dual oxidase system in Caenorhabditis elegans. *PLoS Genet,* 8**,** e1002957.

MORIBE, H., YOCHEM, J., YAMADA, H., TABUSE, Y., FUJIMOTO, T. & MEKADA, E. 2004. Tetraspanin protein (TSP-15) is required for epidermal integrity in Caenorhabditis elegans. *J Cell Sci,* 117**,** 5209-20.

MOROI, M., JUNG, S. M., SHINMYOZU, K., TOMIYAMA, Y., ORDINAS, A. & DIAZ-RICART, M. 1996. Analysis of platelet adhesion to a collagen-coated surface under flow conditions: the involvement of glycoprotein VI in the platelet adhesion. *Blood,* 88**,** 2081-92.

NABOKINA, S. M., SENTHILKUMAR, S. R. & SAID, H. M. 2011. Tspan-1 interacts with the thiamine transporter-1 in human intestinal epithelial cells and modulates its stability. *Am J Physiol Gastrointest Liver Physiol,* 301**,** G808-13.

NIESWANDT, B., BERGMEIER, W., SCHULTE, V., RACKEBRANDT, K., GESSNER, J. E. & ZIRNGIBL, H. 2000. Expression and function of the mouse collagen receptor glycoprotein VI is strictly dependent on its association with the FcRgamma chain. *J Biol Chem,* 275**,** 23998-4002.

NIESWANDT, B., KLEINSCHNITZ, C. & STOLL, G. 2011a. Ischaemic stroke: a thrombo-inflammatory disease? *J Physiol,* 589**,** 4115-23.

NIESWANDT, B., PLEINES, I. & BENDER, M. 2011b. Platelet adhesion and activation mechanisms in arterial thrombosis and ischaemic stroke. *J Thromb Haemost,* 9 Suppl 1**,** 92-104.

NIESWANDT, B., SCHULTE, V., BERGMEIER, W., MOKHTARI-NEJAD, R., RACKEBRANDT, K., CAZENAVE, J. P., OHLMANN, P., GACHET, C. & ZIRNGIBL, H. 2001. Long-term antithrombotic protection by in vivo depletion of platelet glycoprotein VI in mice. *J Exp Med,* 193**,** 459-69.

NIESWANDT, B. & WATSON, S. P. 2003. Platelet-collagen interaction: is GPVI the central receptor? *Blood,* 102**,** 449-61.

NURDEN, A. T. 2011. Platelets, inflammation and tissue regeneration. *Thromb Haemost,* 105 Suppl 1**,** S13-33.

NYDEGGER, S., KHURANA, S., KREMENTSOV, D. N., FOTI, M. & THALI, M. 2006. Mapping of tetraspanin-enriched microdomains that can function as gateways for HIV-1. *J Cell Biol,* 173**,** 795-807.

ODINTSOVA, E., BUTTERS, T. D., MONTI, E., SPRONG, H., VAN MEER, G. & BERDITCHEVSKI, F. 2006. Gangliosides play an important role in the organization of CD82-enriched microdomains. *Biochem J,* 400**,** 315-25.

ODINTSOVA, E., SUGIURA, T. & BERDITCHEVSKI, F. 2000. Attenuation of EGF receptor signaling by a metastasis suppressor, the tetraspanin CD82/KAI-1. *Curr Biol,* 10**,** 1009-12.

OFFERMANNS, S. 2006. Activation of platelet function through G protein-coupled receptors. *Circ Res,* 99**,** 1293-304.

OLMOS, E., REISS, B. & DEKKER, K. 2003. The ekeko mutant demonstrates a role for tetraspanin-like protein in plant development. *Biochem Biophys Res Commun,* 310**,** 1054-61.

ORLOWSKI, E., CHAND, R., YIP, J., WONG, C., GOSCHNICK, M. W., WRIGHT, M. D., ASHMAN, L. K. & JACKSON, D. E. 2009. A platelet tetraspanin superfamily member, CD151, is required for regulation of thrombus growth and stability in vivo. *J Thromb Haemost,* 7**,** 2074-84.

PAN, Y., BROWN, C., WANG, X. & GEISERT, E. E. 2007. The developmental regulation of CD81 in the rat retina. *Mol Vis,* 13**,** 181-9.

PATEL, S. R., HARTWIG, J. H. & ITALIANO, J. E., JR. 2005. The biogenesis of platelets from megakaryocyte proplatelets. *J Clin Invest,* 115**,** 3348-54.

PEARSON, M. S., PICKERING, D. A., MCSORLEY, H. J., BETHONY, J. M., TRIBOLET, L., DOUGALL, A. M., HOTEZ, P. J. & LOUKAS, A. 2012. Enhanced protective efficacy of a chimeric form of the schistosomiasis vaccine antigen Sm-TSP-2. *PLoS Negl Trop Dis,* 6**,** e1564.

PENG, W. M., YU, C. F., KOLANUS, W., MAZZOCCA, A., BIEBER, T., KRAFT, S. & NOVAK, N. 2011. Tetraspanins CD9 and CD81 are molecular partners of trimeric FcεRI on human antigen-presenting cells. *Allergy,* 66**,** 605-11.

PILERI, P., UEMATSU, Y., CAMPAGNOLI, S., GALLI, G., FALUGI, F., PETRACCA, R., WEINER, A. J., HOUGHTON, M., ROSA, D., GRANDI, G. & ABRIGNANI, S. 1998. Binding of hepatitis C virus to CD81. *Science,* 282**,** 938-41.

PITCHFORD, S. C., LODIE, T. & RANKIN, S. M. 2012. VEGFR1 stimulates a CXCR4-dependent translocation of megakaryocytes to the vascular niche, enhancing platelet production in mice. *Blood*.

POSTINA, R., SCHROEDER, A., DEWACHTER, I., BOHL, J., SCHMITT, U., KOJRO, E., PRINZEN, C., ENDRES, K., HIEMKE, C., BLESSING, M., FLAMEZ, P., DEQUENNE, A., GODAUX, E., VAN LEUVEN, F. & FAHRENHOLZ, F. 2004. A disintegrin-metalloproteinase prevents amyloid plaque formation and hippocampal defects in an Alzheimer disease mouse model. *J Clin Invest,* 113**,** 1456-64.

PROTTY, M. B., WATKINS, N. A., COLOMBO, D., THOMAS, S. G., HEATH, V. L., HERBERT, J. M., BICKNELL, R., SENIS, Y. A., ASHMAN, L. K., BERDITCHEVSKI, F., OUWEHAND, W. H., WATSON, S. P. & TOMLINSON, M. G. 2009. Identification of Tspan9 as a novel platelet tetraspanin and the collagen receptor GPVI as a component of tetraspanin microdomains. *Biochem J,* 417**,** 391-400.

PROX, J., WILLENBROCK, M., WEBER, S., LEHMANN, T., SCHMIDT-ARRAS, D., SCHWANBECK, R., SAFTIG, P. & SCHWAKE, M. 2012. Tetraspanin15 regulates cellular trafficking and activity of the ectodomain sheddase ADAM10. *Cell Mol Life Sci*.

RAJESH, S., SRIDHAR, P., TEWS, B. A., FENEANT, L., COCQUEREL, L., WARD, D. G., BERDITCHEVSKI, F. & OVERDUIN, M. 2012. Structural basis of ligand interactions of the large extracellular domain of tetraspanin CD81. *J Virol,* 86**,** 9606-16.

RANA, S. & ZÖLLER, M. 2011. Exosome target cell selection and the importance of exosomal tetraspanins: a hypothesis. *Biochem Soc Trans,* 39**,** 559-62.

RAPOSO, G. & STOORVOGEL, W. 2013. Extracellular vesicles: exosomes, microvesicles, and friends. *J Cell Biol,* 200**,** 373-83.

REYNOLDS, G. M., HARRIS, H. J., JENNINGS, A., HU, K., GROVE, J., LALOR, P. F., ADAMS, D. H., BALFE, P., HÜBSCHER, S. G. & MCKEATING, J. A. 2008. Hepatitis C virus receptor expression in normal and diseased liver tissue. *Hepatology,* 47**,** 418-27.

ROBAK, T., ROBAK, P. & SMOLEWSKI, P. 2009. TRU-016, a humanized anti-CD37 IgG fusion protein for the potential treatment of B-cell malignancies. *Curr Opin Investig Drugs,* 10**,** 1383-90.

ROWLEY, J. W., OLER, A. J., TOLLEY, N. D., HUNTER, B. N., LOW, E. N., NIX, D. A., YOST, C. C., ZIMMERMAN, G. A. & WEYRICH, A. S. 2011. Genome-wide RNA-seq analysis of human and mouse platelet transcriptomes. *Blood,* 118**,** e101-11.

SACHS, N., KREFT, M., VAN DEN BERGH WEERMAN, M. A., BEYNON, A. J., PETERS, T. A., WEENING, J. J. & SONNENBERG, A. 2006. Kidney failure in mice lacking the tetraspanin CD151. *J Cell Biol,* 175**,** 33-9.

SAFTIG, P. & REISS, K. 2011. The "A Disintegrin And Metalloproteases" ADAM10 and ADAM17: novel drug targets with therapeutic potential? *Eur J Cell Biol,* 90**,** 527-35.

SALA-VALDÉS, M., URSA, A., CHARRIN, S., RUBINSTEIN, E., HEMLER, M. E., SÁNCHEZ-MADRID, F. & YÁÑEZ-MÓ, M. 2006. EWI-2 and EWI-F link the tetraspanin web to the actin cytoskeleton through their direct association with ezrin-radixin-moesin proteins. *J Biol Chem,* 281**,** 19665-75.

SCHEFFER, K. D., GAWLITZA, A., SPODEN, G. A., ZHANG, X. A., LAMBERT, C., BERDITCHEVSKI, F. & FLORIN, L. 2013. Tetraspanin CD151 mediates papillomavirus type 16 endocytosis. *J Virol,* 87**,** 3435-46.

SCHOLZ, C. J., SAUER, G. & DEISSLER, H. 2009a. Glycosylation of tetraspanin Tspan-1 at four distinct sites promotes its transition through the endoplasmic reticulum. *Protein Pept Lett,* 16**,** 1244-8.

SCHOLZ, C. J., SAUER, G. & DEISSLER, H. 2009b. Glycosylation of tetraspanin Tspan-1 at four distinct sites promotes its transition through the endoplasmic reticulum. *Protein Pept Lett,* 16**,** 1244-8.

SCHRÖDER, J., LÜLLMANN-RAUCH, R., HIMMERKUS, N., PLEINES, I., NIESWANDT, B., ORINSKA, Z., KOCH-NOLTE, F., SCHRÖDER, B., BLEICH, M. & SAFTIG, P. 2009. Deficiency of the tetraspanin CD63 associated with kidney pathology but normal lysosomal function. *Mol Cell Biol,* 29**,** 1083-94.

SEIGNEURET, M. 2006. Complete predicted three-dimensional structure of the facilitator transmembrane protein and hepatitis C virus receptor CD81: conserved and variable structural domains in the tetraspanin superfamily. *Biophys J,* 90**,** 212-27.

SEIGNEURET, M., DELAGUILLAUMIE, A., LAGAUDRIÈRE-GESBERT, C. & CONJEAUD, H. 2001. Structure of the tetraspanin main extracellular domain.

A partially conserved fold with a structurally variable domain insertion. *J Biol Chem,* 276**,** 40055-64.

SENIS, Y. A., TOMLINSON, M. G., ELLISON, S., MAZHARIAN, A., LIM, J., ZHAO, Y., KORNERUP, K. N., AUGER, J. M., THOMAS, S. G., DHANJAL, T., KALIA, N., ZHU, J. W., WEISS, A. & WATSON, S. P. 2009. The tyrosine phosphatase CD148 is an essential positive regulator of platelet activation and thrombosis. *Blood,* 113**,** 4942-54.

SENIS, Y. A., TOMLINSON, M. G., GARCÍA, A., DUMON, S., HEATH, V. L., HERBERT, J., COBBOLD, S. P., SPALTON, J. C., AYMAN, S., ANTROBUS, R., ZITZMANN, N., BICKNELL, R., FRAMPTON, J., AUTHI, K. S., MARTIN, A., WAKELAM, M. J. & WATSON, S. P. 2007. A comprehensive proteomics and genomics analysis reveals novel transmembrane proteins in human platelets and mouse megakaryocytes including G6b-B, a novel immunoreceptor tyrosine-based inhibitory motif protein. *Mol Cell Proteomics,* 6**,** 548-64.

SERRU, V., LE NAOUR, F., BILLARD, M., AZORSA, D. O., LANZA, F., BOUCHEIX, C. & RUBINSTEIN, E. 1999. Selective tetraspan-integrin complexes (CD81/alpha4beta1, CD151/alpha3beta1, CD151/alpha6beta1) under conditions disrupting tetraspan interactions. *Biochem J,* 340 (Pt 1)**,** 103-11.

SHIVDASANI, R. A. & SCHULZE, H. 2005. **Culture, Expansion, and Differentiation of Murine Megakaryocytes**.

SHOHAM, T., RAJAPAKSA, R., BOUCHEIX, C., RUBINSTEIN, E., POE, J. C., TEDDER, T. F. & LEVY, S. 2003. The tetraspanin CD81 regulates the expression of CD19 during B cell development in a postendoplasmic reticulum compartment. *J Immunol,* 171**,** 4062-72.

SILVIE, O., RUBINSTEIN, E., FRANETICH, J. F., PRENANT, M., BELNOUE, E., RÉNIA, L., HANNOUN, L., ELING, W., LEVY, S., BOUCHEIX, C. & MAZIER, D. 2003. Hepatocyte CD81 is required for Plasmodium falciparum and Plasmodium yoelii sporozoite infectivity. *Nat Med,* 9**,** 93-6.

SIMONS, K. & GERL, M. J. 2010. Revitalizing membrane rafts: new tools and insights. *Nat Rev Mol Cell Biol,* 11**,** 688-99.

SINENKO, S. A. & MATHEY-PREVOT, B. 2004. Increased expression of Drosophila tetraspanin, Tsp68C, suppresses the abnormal proliferation of ytr-deficient and Ras/Raf-activated hemocytes. *Oncogene,* 23**,** 9120-8.

SKARNES, W. C. 2000. Gene trapping methods for the identification and functional analysis of cell surface proteins in mice. *Methods Enzymol,* 328**,** 592-615.

SMOLENSKI, A. 2012. Novel roles of cAMP/cGMP-dependent signaling in platelets. *J Thromb Haemost,* 10**,** 167-76.

SNELL, D. C., SCHULTE, V., JARVIS, G. E., ARASE, K., SAKURAI, D., SAITO, T., WATSON, S. P. & NIESWANDT, B. 2002. Differential effects of reduced glycoprotein VI levels on activation of murine platelets by glycoprotein VI ligands. *Biochem J,* 368**,** 293-300.

STEGNER, D. & NIESWANDT, B. 2011. Platelet receptor signaling in thrombus formation. *J Mol Med (Berl),* 89**,** 109-21.

STIPP, C. S., KOLESNIKOVA, T. V. & HEMLER, M. E. 2001. EWI-2 is a major CD9 and CD81 partner and member of a novel Ig protein subfamily. *J Biol Chem,* 276**,** 40545-54.

STIPP, C. S., KOLESNIKOVA, T. V. & HEMLER, M. E. 2003. Functional domains in tetraspanin proteins. *Trends Biochem Sci,* 28**,** 106-12.

SUZUKI-INOUE, K., INOUE, O., FRAMPTON, J. & WATSON, S. P. 2003. Murine GPVI stimulates weak integrin activation in PLCgamma2-/- platelets: involvement of PLCgamma1 and PI3-kinase. *Blood,* 102**,** 1367-73.

SUZUKI-INOUE, K., INOUE, O. & OZAKI, Y. 2011. Novel platelet activation receptor CLEC-2: from discovery to prospects. *J Thromb Haemost,* 9 Suppl 1**,** 44-55.

SÉVERIN, S., NASH, C. A., MORI, J., ZHAO, Y., ABRAM, C., LOWELL, C. A., SENIS, Y. A. & WATSON, S. P. 2012. Distinct and overlapping functional roles of Src family kinases in mouse platelets. *J Thromb Haemost*.

TACHIBANA, I., BODOROVA, J., BERDITCHEVSKI, F., ZUTTER, M. M. & HEMLER, M. E. 1997. NAG-2, a novel transmembrane-4 superfamily (TM4SF) protein that complexes with integrins and other TM4SF proteins. *J Biol Chem,* 272**,** 29181-9.

TAKEDA, Y., HE, P., TACHIBANA, I., ZHOU, B., MIYADO, K., KANEKO, H., SUZUKI, M., MINAMI, S., IWASAKI, T., GOYA, S., KIJIMA, T., KUMAGAI, T., YOSHIDA, M., OSAKI, T., KOMORI, T., MEKADA, E. & KAWASE, I. 2008. Double deficiency of tetraspanins CD9 and CD81 alters cell motility and protease production of macrophages and causes chronic obstructive pulmonary disease-like phenotype in mice. *J Biol Chem,* 283**,** 26089-97.

TAKEDA, Y., TACHIBANA, I., MIYADO, K., KOBAYASHI, M., MIYAZAKI, T., FUNAKOSHI, T., KIMURA, H., YAMANE, H., SAITO, Y., GOTO, H., YONEDA, T., YOSHIDA, M., KUMAGAI, T., OSAKI, T., HAYASHI, S., KAWASE, I. & MEKADA, E. 2003. Tetraspanins CD9 and CD81 function to prevent the fusion of mononuclear phagocytes. *J Cell Biol,* 161**,** 945-56.

TEJERA, E., ROCHA-PERUGINI, V., LOPEZ-MARTIN, S., PEREZ-HERNANDEZ, D., BACHIR, A. I., HORWITZ, A. R., VAZQUEZ, J., SANCHEZ-MADRID, F. & YANEZ-MO, M. 2013. CD81 regulates cell migration through its association with Rac GTPase. *Mol Biol Cell,* 24**,** 261-73.

TESTA, U. 2004. Apoptotic mechanisms in the control of erythropoiesis. *Leukemia,* 18**,** 1176-99.

THALI, M. 2011. Tetraspanin functions during HIV-1 and influenza virus replication. *Biochem Soc Trans,* 39**,** 529-31.

TRAGGIAI, E., LUNARDI, C., BASON, C., DOLCINO, M., TINAZZI, E., CORROCHER, R. & PUCCETTI, A. 2010. Generation of anti-NAG-2 mAb from patients' memory B cells: implications for a novel therapeutic strategy in systemic sclerosis. *Int Immunol,* 22**,** 367-74.

TRAN, M. H., FREITAS, T. C., COOPER, L., GAZE, S., GATTON, M. L., JONES, M. K., LOVAS, E., PEARCE, E. J. & LOUKAS, A. 2010. Suppression of mRNAs encoding tegument tetraspanins from Schistosoma mansoni results in impaired tegument turnover. *PLoS Pathog,* 6**,** e1000840.

TRAN, M. H., PEARSON, M. S., BETHONY, J. M., SMYTH, D. J., JONES, M. K., DUKE, M., DON, T. A., MCMANUS, D. P., CORREA-OLIVEIRA, R. & LOUKAS, A. 2006. Tetraspanins on the surface of Schistosoma mansoni are protective antigens against schistosomiasis. *Nat Med,* 12**,** 835-40.

TRILLER, A. & CHOQUET, D. 2003. Synaptic structure and diffusion dynamics of synaptic receptors. *Biol Cell,* 95**,** 465-76.

TSAI, Y. C. & WEISSMAN, A. M. 2011. Dissecting the diverse functions of the metastasis suppressor CD82/KAI1. *FEBS Lett,* 585**,** 3166-73.

TSITSIKOV, E. N., GUTIERREZ-RAMOS, J. C. & GEHA, R. S. 1997. Impaired CD19 expression and signaling, enhanced antibody response to type II T independent antigen and reduction of B-1 cells in CD81-deficient mice. *Proc Natl Acad Sci U S A,* 94**,** 10844-9.

TU, L., KONG, X. P., SUN, T. T. & KREIBICH, G. 2006. Integrity of all four transmembrane domains of the tetraspanin uroplakin Ib is required for its exit from the ER. *J Cell Sci,* 119**,** 5077-86.

UHRIN, P., ZAUJEC, J., BREUSS, J. M., OLCAYDU, D., CHRENEK, P., STOCKINGER, H., FUERTBAUER, E., MOSER, M., HAIKO, P., FAESSLER, R., ALITALO, K., BINDER, B. R. & KERJASCHKI, D. 2010. Novel function for blood platelets and podoplanin in developmental separation of blood and lymphatic circulation. *Blood,* 115**,** 3997-4005.

VAN SPRIEL, A. B., DE KEIJZER, S., VAN DER SCHAAF, A., GARTLAN, K. H., SOFI, M., LIGHT, A., LINSSEN, P. C., BOEZEMAN, J. B., ZUIDSCHERWOUDE, M., REINIEREN-BEEREN, I., CAMBI, A., MACKAY, F., TARLINTON, D. M., FIGDOR, C. G. & WRIGHT, M. D. 2012. The tetraspanin CD37 orchestrates the alpha(4)beta(1) integrin-Akt signaling axis and supports long-lived plasma cell survival. *Sci Signal,* 5**,** ra82.

VAN ZELM, M. C., SMET, J., ADAMS, B., MASCART, F., SCHANDENE, L., JANSSEN, F., FERSTER, A., KUO, C.-C., LEVY, S., VAN DONGEN, J. J. M. & VAN DER BURG, M. 2010. CD81 gene defect in humans disrupts CD19 complex formation and leads to antibody deficiency. *Journal of Clinical Investigation,* 120**,** 1265-1274.

VEGIOPOULOS, A., GARCIA, P., EMAMBOKUS, N. & FRAMPTON, J. 2006. Coordination of erythropoiesis by the transcription factor c-Myb. *Blood,* 107**,** 4703-10.

VERSTEEG, H. H., HEEMSKERK, J. W., LEVI, M. & REITSMA, P. H. 2013. New fundamentals in hemostasis. *Physiol Rev,* 93**,** 327-58.

VINCENT, B. & CHECLER, F. 2012. α-Secretase in Alzheimer's disease and beyond: mechanistic, regulation and function in the shedding of membrane proteins. *Curr Alzheimer Res,* 9**,** 140-56.

VINCENT, B. & GOVITRAPONG, P. 2011. Activation of the α-secretase processing of AβPP as a therapeutic approach in Alzheimer's disease. *J Alzheimers Dis,* 24 Suppl 2**,** 75-94.

VON HUNDELSHAUSEN, P. & WEBER, C. 2007. Platelets as immune cells - Bridging inflammation and cardiovascular disease. *Circulation Research,* 100**,** 27-40.

WANG, H., RANA, S., GIESE, N., BUCHLER, M. W. & ZOLLER, M. 2013. Tspan8, CD44v6 and alpha6beta4 are biomarkers of migrating pancreatic cancer-initiating cells. *Int J Cancer,* 133**,** 416-26.

WANG, H. X., KOLESNIKOVA, T. V., DENISON, C., GYGI, S. P. & HEMLER, M. E. 2011. The C-terminal tail of tetraspanin protein CD9 contributes to its function and molecular organization. *J Cell Sci,* 124**,** 2702-10.

WANG, L., LIU, L., CHE, Y., JIANG, L., DONG, C., ZHANG, Y. & LI, Q. 2010. Egress of HSV-1 capsid requires the interaction of VP26 and a cellular tetraspanin membrane protein. *Virol J,* 7**,** 156.

WATSON, S. P., ASAZUMA, N., ATKINSON, B., BERLANGA, O., BEST, D., BOBE, R., JARVIS, G., MARSHALL, S., SNELL, D., STAFFORD, M., TULASNE, D., WILDE, J., WONEROW, P. & FRAMPTON, J. 2001. The role of ITAM- and ITIM-coupled receptors in platelet activation by collagen. *Thromb Haemost,* 86**,** 276-88.

WATTS, T., BARIGOU, M. & NASH, G. B. 2013. Comparative rheology of the adhesion of platelets and leukocytes from flowing blood: why are platelets so small? *Am J Physiol Heart Circ Physiol,* 304**,** H1483-94.

WILES, M. V., VAUTI, F., OTTE, J., FUCHTBAUER, E. M., RUIZ, P., FUCHTBAUER, A., ARNOLD, H. H., LEHRACH, H., METZ, T., VON MELCHNER, H. & WURST, W. 2000. Establishment of a gene-trap sequence tag library to generate mutant mice from embryonic stem cells. *Nat Genet,* 24**,** 13-4.

WONEROW, P., OBERGFELL, A., WILDE, J. I., BOBE, R., ASAZUMA, N., BRDICKA, T., LEO, A., SCHRAVEN, B., HOREJSI, V., SHATTIL, S. J. & WATSON, S. P. 2002. Differential role of glycolipid-enriched membrane domains in glycoprotein VI- and integrin-mediated phospholipase Cgamma2 regulation in platelets. *Biochem J,* 364**,** 755-65.

WRIGHT, M. D., GEARY, S. M., FITTER, S., MOSELEY, G. W., LAU, L. M., SHENG, K. C., APOSTOLOPOULOS, V., STANLEY, E. G., JACKSON, D. E. & ASHMAN, L. K. 2004. Characterization of mice lacking the tetraspanin superfamily member CD151. *Mol Cell Biol,* 24**,** 5978-88.

WU, H., LI, J., PENG, L., LIU, H., WU, W., ZHOU, Y., HOU, Q. & KONG, D. 2001. Anti-human platelet tetraspanin (CD9) monoclonal antibodies induce platelet integrin alpha IIb beta 3 activation in a Fc receptor-independent fashion. *Chin Med J (Engl),* 114**,** 14-8.

XU, D., SHARMA, C. & HEMLER, M. E. 2009. Tetraspanin12 regulates ADAM10-dependent cleavage of amyloid precursor protein. *FASEB J,* 23**,** 3674-81.

XU, H., LEE, S. J., SUZUKI, E., DUGAN, K. D., STODDARD, A., LI, H. S., CHODOSH, L. A. & MONTELL, C. 2004. A lysosomal tetraspanin associated with retinal degeneration identified via a genome-wide screen. *EMBO J,* 23**,** 811-22.

YANG, H., XIAO, X., LI, S., MAI, G. & ZHANG, Q. 2011. Novel TSPAN12 mutations in patients with familial exudative vitreoretinopathy and their associated phenotypes. *Mol Vis,* 17**,** 1128-35.

YANG, X., CLAAS, C., KRAEFT, S. K., CHEN, L. B., WANG, Z., KREIDBERG, J. A. & HEMLER, M. E. 2002. Palmitoylation of tetraspanin proteins: modulation of CD151 lateral interactions, subcellular distribution, and integrin-dependent cell morphology. *Mol Biol Cell,* 13**,** 767-81.

YANG, X. H., MIRCHEV, R., DENG, X., YACONO, P., YANG, H. L., GOLAN, D. E. & HEMLER, M. E. 2012a. CD151 restricts the alpha6 integrin diffusion mode. *J Cell Sci,* 125**,** 1478-87.

YANG, X. H., MIRCHEV, R., DENG, X., YACONO, P., YANG, H. L., GOLAN, D. E. & HEMLER, M. E. 2012b. CD151 restricts the α6 integrin diffusion mode. *J Cell Sci,* 125**,** 1478-87.

YANG, X. H., RICHARDSON, A. L., TORRES-ARZAYUS, M. I., ZHOU, P., SHARMA, C., KAZAROV, A. R., ANDZELM, M. M., STROMINGER, J. L., BROWN, M. & HEMLER, M. E. 2008. CD151 accelerates breast cancer by regulating alpha 6

integrin function, signaling, and molecular organization. *Cancer Res,* 68**,** 3204-13.

YAUCH, R. L. & HEMLER, M. E. 2000. Specific interactions among transmembrane 4 superfamily (TM4SF) proteins and phosphoinositide 4-kinase. *Biochem J,* 351 Pt 3**,** 629-37.

YOSHIDA, T., KAWANO, Y., SATO, K., ANDO, Y., AOKI, J., MIURA, Y., KOMANO, J., TANAKA, Y. & KOYANAGI, Y. 2008. A CD63 mutant inhibits T-cell tropic human immunodeficiency virus type 1 entry by disrupting CXCR4 trafficking to the plasma membrane. *Traffic,* 9**,** 540-58.

YU, M. & CANTOR, A. B. 2012. Megakaryopoiesis and thrombopoiesis: an update on cytokines and lineage surface markers. *Methods Mol Biol,* 788**,** 291-303.

YÁÑEZ-MÓ, M., BARREIRO, O., GORDON-ALONSO, M., SALA-VALDÉS, M. & SÁNCHEZ-MADRID, F. 2009. Tetraspanin-enriched microdomains: a functional unit in cell plasma membranes. *Trends Cell Biol,* 19**,** 434-46.

ZECH, T., EJSING, C. S., GAUS, K., DE WET, B., SHEVCHENKO, A., SIMONS, K. & HARDER, T. 2009. Accumulation of raft lipids in T-cell plasma membrane domains engaged in TCR signalling. *Embo j,* 28**,** 466-76.

ZEMNI, R., BIENVENU, T., VINET, M. C., SEFIANI, A., CARRIE, A., BILLUART, P., MCDONELL, N., COUVERT, P., FRANCIS, F., CHAFEY, P., FAUCHEREAU, F., FRIOCOURT, G., DES PORTES, V., CARDONA, A., FRINTS, S., MEINDL, A., BRANDAU, O., RONCE, N., MORAINE, C., VAN BOKHOVEN, H., ROPERS, H. H., SUDBRAK, R., KAHN, A., FRYNS, J. P., BELDJORD, C. & CHELLY, J. 2000. A new gene involved in X-linked mental retardation identified by analysis of an X;2 balanced translocation. *Nat Genet,* 24**,** 167-70.

ZHANG, X. A., BONTRAGER, A. L. & HEMLER, M. E. 2001. Transmembrane-4 superfamily proteins associate with activated protein kinase C (PKC) and link PKC to specific beta(1) integrins. *J Biol Chem,* 276**,** 25005-13.

ZHI, H., RAUOVA, L., HAYES, V., GAO, C., BOYLAN, B., NEWMAN, D. K., MCKENZIE, S. E., COOLEY, B. C., PONCZ, M. & NEWMAN, P. J. 2013. Cooperative integrin/ITAM signaling in platelets enhances thrombus formation in vitro and in vivo. *Blood,* 121**,** 1858-67.

ZHOU, G., MO, W. J., SEBBEL, P., MIN, G., NEUBERT, T. A., GLOCKSHUBER, R., WU, X. R., SUN, T. T. & KONG, X. P. 2001. Uroplakin Ia is the urothelial receptor for uropathogenic Escherichia coli: evidence from in vitro FimH binding. *J Cell Sci,* 114**,** 4095-103.

ZOLLER, M. 2009. Tetraspanins: push and pull in suppressing and promoting metastasis. *Nat Rev Cancer,* 9**,** 40-55.